RUI TWOHIG HUGMAN

Numerical Approaches to Simulate Groundwater Flow and Transport in Coastal Aquifers – From Regional Scale Management to Submarine Groundwater Discharge

UNIVERSIDADE DO ALGARVE

Faculdade de Ciências e Tecnologia

2016

RUI TWOHIG HUGMAN

Numerical Approaches to Simulate Groundwater Flow and Transport in Coastal Aquifers – From Regional Scale Management to Submarine Groundwater Discharge

Doutoramento em

Ciências do Mar, da Terra e do Ambiente

ramo Geociências, especialidade em Hidrogeologia

Trabalho efetuado sob a coorientação de:

Prof. Doutor José Paulo Monteiro

Prof. Doutor Tibor Stigter

UNIVERSIDADE DO ALGARVE

Faculdade de Ciências e Tecnologia

2016

Numerical Approaches to Simulate Groundwater Flow and Transport in Coastal Aquifers – From Regional Scale Management to Submarine Groundwater Discharge

Declaração de autoria de trabalho

Declaro ser o autor deste trabalho, que é original e inédito. Autores e trabalhos consultados estão devidamente citados no texto e constam da listagem de referências incluída.

Rui Twohig Hugman

_____

(assinatura)

Acknowledgments

I wish to thank all those that have contributed to the development of this body of work, as well as all my friends and colleagues that have in some way had an impact on these last four years of my life. In particular, I wish to express my gratitude and thanks to:

My supervisors for providing the encouragement, guidance, support and friendship to get me to this point. José Paulo for introducing me to the world of hydrogeology with such catching enthusiasm and doing everything to help during these early stages of my career. Tibor for your infinite patience in catching all the mistakes in my work and for teaching me to think, write and publish! If it were not for you, I would not be writing this today.

My parents for supporting and encouraging me during the last thirty years. Thank you for getting me here. You have both been role models that I look up to. I hope not to be too much of a disappointment!

To Vanessa for putting up with me during these tough years. Thank you for the good as well as the bad times.

Luis and Nuria for their company during the long office hours as well for listening and providing feedback in solving many problems.

Alain Frances and Judite Fernandes for their help and support during the FREEZE project and in the research on the *Albufeira-Rib.Quarteira* aquifer.

Finally, I wish to acknowledge the Fundação para a Ciência e Tecnologia (FCT) for the PhD grant SFRH/BD/80149/2011, as well as DHI for supplying a student license of the FEFLOW software.

The research leading to these results has also received support from the CLIMWAT project funded under the CIRCLE-MED network of the CIRCLE-2 ERA-Net, the FREEZE project (PTDC/MAR/102030/2008), financed by the Fundação para a Ciência e a Tecnologia (FCT) as well as the MARSOL project financed by the European Union Seventh Framework Programme (FP7/2007‐2013) under grant agreement No. 619120.

Abstract

Numerical models of varying scales and degree of complexity are developed to study issues, directly or indirectly, related to coastal aquifer management in the Algarve (south Portugal). Three areas are used as case studies which cover a range of issues from saltwater intrusion, submarine groundwater discharge and groundwater transport of pollutants to coastal waters. Theoretical questions related to maximizing sustainable yield taking into account spatiotemporal heterogeneity, variability and scales are analyzed. Results highlight that aquifer properties have an important role in determining the resilience of an aquifer and therefore to which degree it is dependent on the spatial and temporal distribution of abstraction and recharge. Furthermore, reducing the time scale for which sustainable yield is defined allows for an increase in withdrawal volumes whilst maintaining the sustainability of the system. In fact, not reducing the temporal scale leads to an irretrievable loss of freshwater during recharge periods which will increase with the expected changes in climate. Simulated effects of climate change show that SWI will be a cause for concern in the long-term if current water use and practices are maintained. Changes in seasonal rainfall patterns will affect freshwater discharge rates within the short-term, however the impacts on seawater intrusion will require longer to take effect. Several management and technical solutions are feasible and simulations show that they do contribute to reducing negative impacts. Insights into the hydrogeological dynamics of several of the studied systems are also provided, which contribute to groundwater resource management by (1) supplying estimates of sustainable yield, (2) re-enforcing existing or providing new conceptual models of system behaviour, and (3) providing insight into seawater intrusion mechanisms and guidance on further data needs.

keywords: coastal aquifer, sustainable yield, numerical modelling, variable density flow, water resource management, submarine groundwater discharge

Resumo

Desenvolveram-se modelos numéricos com diferentes escalas e graus de complexidade para investigar problemas de gestão de aquíferos costeiros, utilizando para o efeito dados de três casos de estudo na costa Sul de Portugal (Algarve), através dos quais se abordam questões específicas deste tipo de aquíferos que vão da descarga submarina de água subterrânea à intrusão salina, passando pelo transporte de poluentes para as águas costeiras. No entanto, a necessidade de abordar problemas em casos de estudo concretos facultou igualmente a possibilidade de tratamento de aspectos relacionados com a gestão de aquíferos que, não sendo específicos de aquíferos costeiros, se colocam igualmente nestes casos e afectam a evolução espácio-temporal da interface mar-aquífero. Neste campo abordou-se a problemática da maximização da exploração sustentável das águas subterrâneas, tendo em conta aspectos teóricos relacionados com a variabilidade temporal e heterogeneidade espacial das variáveis de estado e parâmetros hidráulicos envolvidos. Os resultados obtidos põem em evidência o facto das propriedades especifícas de cada aquífero controlarem, de forma preponderante, o seu grau de dependência da evolução temporal e variação espacial do seu regime de exploração e recarga e, por consequência, a sua resiliência à degradação quantitativa e qualitativa dos recursos hídricos subterrâneos.

Os resultados obtidos permitiram constatar que a redução de escala temporal para a qual o conceito de exploração sustentável é operacionalizado, permite o aumento do volume extraído de águas subterrâneas para o qual se evita a degradação dos recursos. Com efeito, não reduzir a habitual escala temporal da gestão de aquíferos costeiros, normalmente baseada em balanços anuais médios, conduz inevitavelmente a uma perda de água doce durante os períodos de recarga. Por outro lado, os resultados obtidos a partir da simulação do efeito de alterações climáticas mostram que a intrusão de água salgada será motivo de efeitos negativos, a longo termo, se as práticas de gestão actuais se mantiverem. As mudanças nos padrões sazonais de recarga afectarão as descargas de água a curto prazo. No entanto, os impactos na intrusão salina só se farão sentir a mais longo prazo.

O trabalho realizado permite comprovar que existem actualmente soluções técnicas e científicas viáveis para contribuir para a redução dos impactos negativos decorrentes dos modelos de gestão da água actualmente em uso. De forma mais específica, mostra-se que, recorrendo à caracterização hidrodinâmica apresentada para os sistemas aquíferos

estudados, foi possível definir medidas conducentes à previsível redução da degradação quantitativa e qualitativa dos seus recursos hídricos, nomeadamente através de: (1) apresentação de estimativas de exploração sustentáveis; (2) aprofundamento de modelos conceptuais pré-existentes ou proposta de novos modelos conceptuais, respeitantes ao funcionamento dos sistemas aquíferos em estudo e (3) proposta de uma visão dos mecanismos que controlam a intrusão salina e definição dos aspectos a ter em conta das necessidades de monitorização das variáveis relevantes para gestão.

Sob o ponto de vista prático da utilidade que este trabalho possa vir a despertar, considera-se ainda útil fazer referência ao facto das metodologias actualmente disponíveis para a modelação numérica de aquíferos costeiros serem viáveis em contextos de aplicação de metodologias com graus de exigência muito diferentes. A leitura desta tese permite constatar que a utilização de modelos em que seja efectuada a caracterização dos modelos de fluxo e transporte que têm em conta o problema da influência da variação de densidade da água doce e salgada são extremamente onerosos, quer no que respeita ao tempo de computação empregue, quer à complexidade envolvida no manuseamento das ferramentas informáticas mais avançadas existentes na actualidade para este fim. Apesar disso, existem processos naturais cuja análise só pode ser efectuada recorrendo a este tipo de conceitos e metodologias. Por outro lado, na prática de projectos de hidrologia aplicada, pode considerar-se que podem ser encontradas soluções adequadas para a resolução de problemas comuns de gestão de recursos hídricos de zonas costeiras para os quais podem encontrar-se soluções muito mais económicas, quer em termos computacionais, quer em termos das exigências do grau de especialização dos profissionais envolvidos na prática da modelação hidrogeológica.

termos chave: aquíferos costeiros, exploração sustentável, modelação numérica, fluxo com densidade variável, gestão de recursos hídricos, descargas de água submarina

Index

List of Figures

List of Tables

1. Introduction

1.1. Coastal Groundwater: Seawater Intrusion & Coastal Groundwater Discharge

The interaction between fresh and saltwater presents unique issues with respect to the sustainable management of groundwater in coastal regions. These issues are primarily those of seawater intrusion (SWI) and changes in the amount and quality of groundwater discharge to coastal ecosystems (Barlow 2003).

Freshwater in coastal aquifers usually flows from recharge areas in-land to coastal discharge areas where groundwater levels are lowest. At the coast, fresh groundwater comes into contact with higher density saline groundwater. This density difference is enough for freshwater to remain above saltwater, separated by a transition zone where some mixing occurs, usually referred to as the fresh-saltwater interface. The location of this interface is controlled by the amount of freshwater flowing through the aquifer, the thickness and hydraulic properties of the aquifer and adjacent confining units, and the relative densities of seawater and freshwater (Barlow 2003). Any changes in groundwater flow or levels affect the equilibrium between fresh and saltwater pressures, causing the interface to move. Changes can be influenced by both anthropogenic (e.g. abstraction or land-use change) or environmental (e.g. variation in climate or sea-level fluctuations) causes (Werner et al 2012). SWI in hydrogeology is defined as the landward movement of the interface (Bear et al 1999), and is usually associated to reduced freshwater discharge.

Approximately half of the global human population lives in coastal areas (Oude Essink 2001b). Of the population in Mediterranean countries, about 37% live near the coast, and the situation is reinforced by a seasonal, tourist and migratory flow of more than 100 million people (MED-EUWI 2007). As in many parts of the world, freshwater availability in the Mediterranean region is under increasing pressures from water consuming and contaminating activities, which threaten drinking water and irrigation supplies (Stigter et al 2013a). Current predictions indicate that climate change will contribute to aggravate these pressures, with decreasing rainfall and longer and more frequent drought periods (Giorgi 2006). Managing these freshwater reserves is an increasingly important issue, in particular

for coastal areas where a large percentage of the population is concentrated. Freshwater stored in coastal aquifers is under the added threat of contamination due to SWI (Custodio 2002). On the other hand, these aquifers can represent a significant portion of the freshwater discharge to the sea, as well as being an important pathway for nutrient and contaminant transport to coastal marine areas (Burnett et al 2006). Increasingly, submarine groundwater discharge (SGD) is being recognized as a significant, but still poorly quantified, source of nutrients and other dissolved elements to coastal marine environments (Taniguchi et al 2002).

Water resource related issues, focusing on SWI, have usually motivated most research on coastal aquifers. Since Ghyben (1889) and Herzberg (1901) both independently first studied this phenomena, numerous efforts to simulate and study this process have been carried out. There is mounting evidence that SGD can have a significant impact on the coastal marine environment (e.g. Johannes (1980), Taniguchi et al. (2002), Price et al. (2006), Andersen et al. (2007)). Recent research in the South of Portugal has demonstrated the role of SGD in nutrient transport to a coastal lagoon (Leote et al 2008; Kontar and Newton 2009; Ibánhez et al 2011) and to increased ecosystem diversity near submarine springs in the region (Encarnação et al 2013). Understanding SGD is also important form a water resource management perspective, as SWI and SGD are effectively two components of the same process, which directly affect each other. The extent of SWI or SGD at a given location is essentially an issue of balance between fresh and seawater pressures (Taniguchi et al 2002). The amount of flow to the sea controls seawater encroachment in some conditions, and on the other hand, the rate of SWI and related processes, such as upward movement of saline waters due to over pumping, may affect SGD rates. Finally, managers of coastal aquifers require knowledge of SGD to assess the volume of fresh water lost to the sea, and therefore unavailable for human use. Thus, it makes sense to consider and quantify both these components when discussing either the management of coastal groundwater reserves or the spatial and temporal distribution of SGD.

1.2. Coastal Groundwater Models

A method common to both SGD and SWI studies are numerical models. In part due to the inherent difficulty in measuring both phenomena at large scales, models are the most widely applied when studying these phenomena at regional scales. The distinguishing feature of SWI models, relative to common groundwater flow models, is the variation of density caused by the variation in salinity. Although the seawater density is only 2.5% larger than that of freshwater, the difference has a major impact. There are currently three main approaches to deal with the SWI when developing models of coastal aquifers: (1) ignoring it, (2) sharp-interface models and (3) variable density models (Dausman et al 2010). In sharp-interface models, the freshwater and saltwater are treated as two immiscible fluids separated by an interface, along which freshwater and saltwater pressures are continuous. In variable density models, the transition zone between freshwater and saltwater has a finite thickness and the density of the water varies continuously. Analytical solutions for SWI are predominantly based on the sharp-interface assumption, whereas variable density models are mainly resolved using numerical solutions. Only variable density models provide salinity predictions that can then be compared to field salinity measurements.

The limited number of analytical solutions for variable density flow problems creates a heavy dependence on computer codes for simulating SWI processes (Simmons et al 2010). The combination of the improved understanding of physical and chemical processes with advances in software as well as processing capacity during the last couple of decades, have led to an increased growth and application of codes capable of simulating SWI in real-world coastal aquifers (Simmons 2005). Thus, numerical models have become irreplaceable tools in dealing with SWI issues ranging from understanding groundwater systems at local or regional scales to testing scenarios for resource management purposes.

1.3. Numerical Models: where do they fit in coastal aquifer management?

The common preconception is that the purpose of numerical models is to provide a realistic representation of a known system, which can be used to analyze hypothetical scenarios such as environmental changes or evaluate management alternatives. Although this is usually the

goal for most modelling studies, the role of numerical models within the study of coastal aquifer begins much earlier.

Figure 1.1 presents the planning approach to coastal aquifer management, as recommended in Maimone et al (2003). These authors highlight the unusual placement of groundwater modelling prior to field studies. Compiling and visualizing available information during the modelling process can often help the planning team to develop a better understanding of the data and the SWI mechanisms. In a similar manner, simple simulations can often highlight issues with a proposed conceptual model, that allow the team to imediately discard incorrect ideas or become aware of previously unconsidered ones. Preliminary modelling has been shown to significantly minimize the costs associated with extensive field studies by focusing them in the areas most likely to yield important data (Maimone et al 2003). Given that coastal aquifer studies must often cover large areas, employing expensive methods that can provide information on lateral variation (e.g. two- and three-dimensional geo-electrical, airborne electromagnetic and seismic methods) cost can easily become a limiting factor (Post 2005).

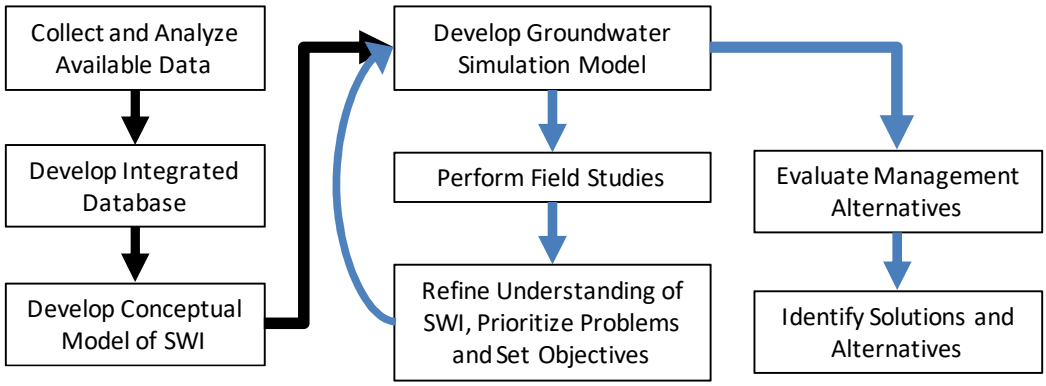

Figure 1.1 Study approach for coastal aquifer management (adapted from Maimone et al (2003)).

Once adequate data has been collected, numerical models can be updated and refined to take into account the updated conceptual models of the system. After validation against field observations, these can then be used in the assessment of management alternatives and prediction of impacts of environmental changes.

Management and modelling of SWI processes in the Algarve is at the third and fourth steps of the study approach shown in Figure 1.1. Extensive historical groundwater level and quality records as well as continuous monitoring networks provide a large body of existing data, most of which is integrated in a publicly available online database. Although some studies focused on identifying SWI processes during the 1980's (e.g. Silva et al 1986; Almeida and Silva 1990; Lourenço 1992), very few since then provide adequate information on the interaction between salt and fresh groundwater. During the last decade several numerical flow models of coastal aquifers in the region have been developed and subsequently applied for management purposes (e.g. Monteiro et al 2002; Vieira and Monteiro 2003; Monteiro and Costa 2004; Monteiro et al 2006; Monteiro et al 2007a; Monteiro et al 2007b). However, so far these have usually been focused on simulating regional water budgets and flow patterns and not considering SWI processes. Recent developments in available groundwater modelling software and computational capacity, now allow for the development of more complex models, taking into account the density-coupled flow and transport processes associated with the interaction between fresh and salt groundwater. As such, a portion of the following body of work revolves around the fourth stage in Figure 1.1, developing preliminary models that shall contribute to guide future work in refining our understanding of these coastal aquifer systems.

1.4. Coastal Aquifer Management Policy in the Algarve (south Portugal)

The occurrence of SWI in the Algarve region first became an issue for concern during the 1980’s. The introduction of drilling technology during the 1960's led to an rapid increase in groundwater use, with the construction of thousands of boreholes (Monteiro and Costa 2004). For several decades, these were the main source for public water supply and irrigation with little to no regional planning. Several studies during this period identified the occurrence of seawater intrusion in the region (e.g. Almeida 1985; Almeida and Silva 1990; Lourenço 1992), and in the beginning of the 1990’s, growing concern over deteriorating groundwater quality lead the regional water regulatory agency to designate a blanket area along the coast as ‘critical’, where the drilling of new boreholes was forbidden as a preventative measure (Figure 1.2).

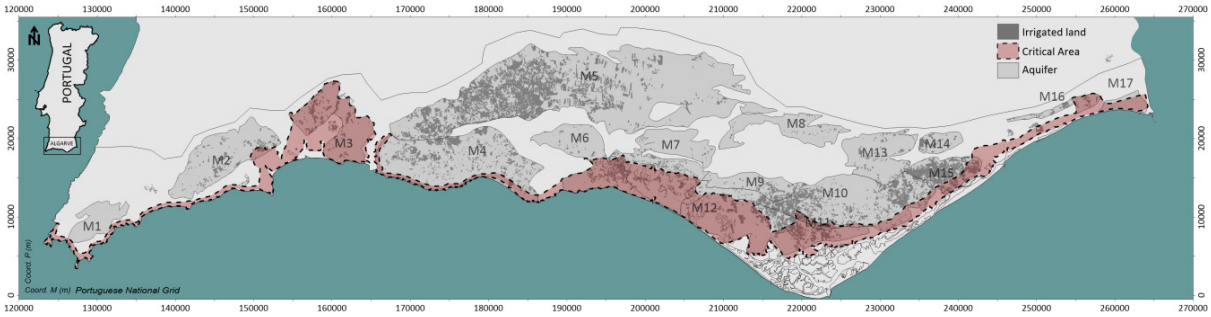

Figure 1.2 - Main aquifer systems of the Algarve and extent of the "*critical area*".

At the end of the 1990's, a regional scale public water supply system based on surface water dams was put into practice, which led to a significant decrease in groundwater use and an evident recovery in groundwater levels and water quality over the last decade. Currently almost all public water supply is from large surface water reservoirs, with groundwater being maintained as a strategic reserve and mostly used to supply irrigation needs (Monteiro and Costa 2004). As a result of the combination of reduced groundwater extraction and the preventative measures, almost all groundwater bodies in the Algarve do not show signs of SWI or of being overexploited (Bettencourt et al 2013).

However, the current regulatory agency (the *Agência Portuguesa do Ambiente* - APA) is under growing pressure from end users to emit groundwater use permits within the critical area – mainly for small agricultural plots within the national agricultural reserve that do not have access to other sources of water (Reis and Gago 2013). At the same time, current climate change predictions point towards a decrease in recharge, increase in extreme weather events and rise in sea level - all of which may have significant impacts on freshwater availability in coastal areas (Santos and Miranda 2006).

During the most recent generation of River Basin Management Plans, one of the measures suggested to guarantee the continued good groundwater quantity and quality status was the development of a plan to prevent seawater intrusion that should include the review of rules governing groundwater use within the critical area as well as detailed study of the effect on SWI of predicted changes in climate and water use (Bettencourt et al 2013).

Accordingly, the Algarve regional branch of APA is currently developing a Specific Water Management Plan (SWMP) for the coastal zone, in which the extent of the critical area, as

well as the restrictions to groundwater use and licensing are being reviewed. However, the currently available data on SWI and the effects of predicted changes in groundwater use, climate and sea level in the region is still limited. The following chapters aim to contribute to the discussion on how to sustainably manage these coastal groundwater bodies, providing conceptual insight on the impact of spatial and temporal variability as well as practical assessments of specific groundwater bodies.

1.5. Thesis Objectives and Outline

The following body of work addresses issues of coastal aquifer management and assessment for several hydrogeological systems in the Algarve, through the use of numerical models of varying scales and degrees of complexity. The overall goal is to provide insights into the factors influencing sustainable use, and support managers and policy makers with the necessary information for adequate coastal aquifer management.

After the introduction and outline presented in the current chapter, **chapter 2** presents the set of equations that describe groundwater flow and transport in porous media under variable density conditions. Some general remarks are made on the numerical solution of the advective-dispersive transport equation and the impact on practical issues of model development.

The subsequent chapters discuss the development of numerical models for several aquifer systems of the central and eastern Algarve, focusing on problems ranging from defining sustainable yields to improving the conceptual understanding of the hydrogeological systems and processes controlling SWI and SGD. These are organised by case study, in which **chapters 3**, **4** and **5** centre on the *Querença-Silves* (QS), **chapter 6** and **7** focus on the *Albufeira-Ribeira de Quarteira* (ARQ) and *Quarteira* (QRT) aquifer systems, **chapter 8** focuses on the group of aquifers that discharge into the Ria Formosa and **chapter 9** highlights the *Campina de Faro* (CF). In general, for each study area a large scale flow model is first applied to assess regional processes and provide an overview of temporal and spatial distribution of SGD, followed by a smaller scale density-coupled flow and transport model to assess SWI or

analyze issues specific to variable density problems. A summary of the case studies and respective models is presented in Table 1.1.

Table 1.1 Summary of aquifer systems and the respective models and issues assesed.

Aquifer system	Models	Issues
Querença-Silves (M5)	2D plane flow	• Theoretical assessment of factors affecting sustainable yield; • Impact of spatiotemporal variability of abstraction and recharge on sustainable yield; • Impact of abstraction on fresh groundwater discharge;
	2D cross-section density-coupled flow & transport	• Impact of abstraction, climate change and mitigation measures on seawater intrusion;
Albufeira-RibQuarteira (M6) & Quarteira (M7)	2D plane flow	• Spatiotemporal variability of abstraction and recharge on sustainable yield; • Influence of uncertainty in surface/groundwater interaction on sustainable yield;
	2D cross-section density-coupled flow & transport	• Assessment of the feasibility for offshore freshwater continuation under local conditions;
Almancil-Medronhal, S.Joao da Venda-Quelfes, Chão de Cevada-Quinta João de Ourém, Campina de Faro, Peral-Moncarapacho & Luz-Tavira (M9-M13 & M15)	2D plane flow & transport	• Simulation of groundwater contribution of nitrogen to the Ria Formosa coastal lagoon;
Campina de Faro (M12)	3D cross-section density-coupled flow & transport	• Simulation of SWI processes and estimate of lateral inflow to the CF;

Chapter 3 contributes to understanding the importance of four factors on the determination of sustainable yields: i) aquifer properties, ii) temporal distribution of recharge, iii) temporal distribution of groundwater pumping and iv) spatial distribution of pumping wells. It is important to understand how the present-day and future vulnerability of groundwater systems and associated groundwater dependent ecosystems (GDEs) to pumping activities depend on these critical factors and what the risks are of considering sustainable yield as a fixed percentage of mean annual recharge. The individual and joint effects of the four referred aspects are analyzed by calibrating and validating a numerical finite element groundwater flow model and then running a number of scenarios where the effect of the

dynamic nature of recharge and abstraction, as well as that of aquifer properties and well location, are simulated. The model is subsequently used to determine sustainable pumping rates as a function of the indicated factors.

In **chapter 4**, the model described in **chapter 3** is used to run a number of scenarios where the abstraction rates for public water supply are determined for various time-scales (ranging from daily to annual) as a fixed percentage of the recharge during the previous time-period. The purpose is to understand the effects and feasibility of defining groundwater abstraction rates at various time scales in integrated water supply systems to maximize sustainable yield and minimize freshwater losses. Maximising the amount of an available freshwater resource is fundamental in regions where this resource is scarce, including Mediterranean regions such as Southern Portugal. Current climate change studies are predicting short-term shifts in seasonal distribution and an increase in inter-annual variability of rainfall in Mediterranean regions (Giorgi 2006; Santos and Miranda 2006; Stigter et al 2014). More specifically, rainfall is predicted to be concentrated in the winter, with significant reductions in spring and autumn. On an inter-annual basis, extreme events (high rainfall and droughts) will be more frequent. All of which are shown in **chapter 3** to lead to larger freshwater loss during the wet season, in particular if groundwater abstraction is largely concentrated during the dry months, which is often the case.

In **chapters 3** and **4** a simple flow model is applied to address issues of sustainable yield merely taking into account impacts of abstraction on SGD rates. In **chapter 5** a density-coupled flow and transport model is applied to assesses the potential for SWI in the QS aquifer system for a range of climate change and groundwater use and adaptation scenarios. The impact of seasonal variability on the extent of SWI is also addressed. An ensemble of climate scenarios previously developed by Stigter et al (2014) are applied to a local-scale cross-sectional density-coupled flow and transport model. Results incorporate uncertainty from climate modelling by including input from three climate models, two downscaling methods and two soil water budget methods to determine monthly recharge rates and crop water demand. Innovative aspects include the simulation of seasonal and inter-annual variation and assessment of the impact of changes in recharge regimes on SWI. Identified

adaptation measures are subsequently simulated for the worst case climate scenario to determine their relative effectiveness in reducing SWI.

Chapter 6 characterizes epistemic uncertainty with regard to the parameterization and the definition of boundary conditions while developing a groundwater flow model to provide estimates of the spatial and temporal distribution of freshwater discharge along the coastline. This is done for the ARQ and QRT coastal aquifer systems, for which preferential continental discharge and near-shore SGD has been observed at certain locations. The model is further used to simulate different past and present scenarios of groundwater pumping, to provide an estimate of sustainable yields based on predefined criteria, and to analyze the importance of well location on these yields.

During the course of this PhD research, the multidisciplinary research project FREEZE (PTDC/MAR/102030/2008) identified signs of SGD several kilometres from the shoreline of the ARQ (Francés et al 2014; Sousa et al 2014; Fernandes et al 2015). Along with new data from on-shore geophysical and offshore seismic surveys, a new conceptual model of the ARQ aquifer system was proposed (Francés et al 2015). In **chapter 7**, numerical models were applied to test the possibility of an offshore continuation of fresh groundwater over several kilometres under local conditions and test the feasibility of the conceptual model. Due to the high computational demand of variable density modelling, in an initial phase simplified two-dimensional cross section models were used to test the conceptual model and reduce uncertainty in regards to model parameters for future work. This represents the initial step in developing and calibrating a three-dimensional regional scale model of the system, which aims to supply an estimate of the spatial distribution of SGD as well as serve as a decision support tool for the local water resources management agency.

Despite improved agricultural practices and significant reductions in groundwater use, the group of aquifers that drain in to the Ria Formosa coastal lagoon still suffer from high values of nitrate concentrations and overexploitation in some areas. In fact, the only two nitrate vulnerable zones (NVZ) designated according to the EU's Nitrate Directive in the Algarve are within this area. **Chapter 8** describes the development and application of a two-dimensional flow and mass transport model (ignoring density effects) for a selected group of aquifer

systems that discharge directly to the Ria Formosa. Processes that contribute to elevated nitrate concentrations are assessed and the effect of irrigation return flow on nitrate concentration levels is analyzed. Subsequently the relative effect of potential mitigation measures are compared. The same model is applied to assess the long-term impacts of changes in groundwater use and climate on the potential extent of SWI.

Results from **chapter 8** highlighted the significant risk of SWI for the CF aquifer system under current groundwater use. However, despite low groundwater levels in this system during the last several decades, only recently has there been any indication of seawater encroachment. In **chapter 9**, a three-dimensional density-coupled flow and transport model is developed to improve the conceptual understanding of this multi-layer aquifer system and assess the impact of current groundwater use on SWI.

Finally, **chapter 10** provides a summary of the conclusions and results of each chapter as well as some general insights and remarks on numerical modelling of coastal aquifer systems for practical real-world problems.

2. Theoretical Background and Governing Equations

The following chapter provides an overview of the set of equations to describe flow and transport taking into account variation in fluid density, as well as some general remarks on practical issues of model development.

2.1. The fresh-saltwater interface in coastal aquifers

In coastal aquifers, freshwater discharges into the sea along seepage faces along the shoreline and into shallow water at the sea floor. The interface between fresh and salt water is a narrow mixing zone that results from molecular diffusion along with mixing caused by fluctuating head and other mechanical dispersion processes (Fitts, 2002).

A simple and useful method for estimating the depth of the fresh-saltwater interface, developed independently by two scientists around 1900, is known as the Ghyben-Herzberg relation. It is based on the assumptions that (1) the interface is sharp, with no mixing, (2) there is no resistance to vertical flow and (3) at the shoreline freshwater head equals sea elevation. Thus, a point at depth z_s below sea level, pressure in saltwater is:

$$p_s = \rho_s g z_s \tag{2.1}$$

where ρ_s is saltwater density [ML^{-3}] and g is acceleration due to gravity [LT^{-2}]. The pressure in fresh water at the same point, is given by:

$$p_f = \rho_f g(z_s + h) \tag{2.2}$$

in which ρ_f is freshwater density [ML^{-3}] and h is hydraulic head [L] in the fresh water measured from the datum. As we are assuming hydrostatic conditions $p_s = p_f$, and therefore resolving for z_s yields the Ghyben-Herzberg relation:

$$z_s = \frac{\rho_f}{\rho_s - \rho_f} \tag{2.3}$$

For ρ_s=1025 g.cm^{-3} (typical ocean densities) and ρ_f=1000 g.cm^{-3} the above equation reduces to the simple relation:

$$z_s = 40h \qquad 2.4$$

2.2. Variable-density groundwater flow

2.2.1. General form of Darcy's law

According to the standard definition of Darcy's law, specific discharge (q) can be expressed in three dimensions as follows:

$$\begin{aligned} q_x &= -K_x \frac{\partial h}{\partial x} \\ q_y &= -K_y \frac{\partial h}{\partial y} \\ q_z &= -K_z \frac{\partial h}{\partial z} \end{aligned} \qquad 2.5$$

where K_x, K_y and K_z are values of hydraulic conductivity [LT^{-1}] along the x, y and z Cartesian axes and assuming these coincide with the principle axes of hydraulic conductivity, and h is hydraulic head [L]. This can be expressed in more compact manner, applying the gradient operator ∇[1]:

[1]the *nabla* operator ∇ is used to express the space derivatives in more than one dimension (Holzbecher, 1998). For three dimensions, the ∇-operator is defined by the following vector:

$$\nabla = \begin{bmatrix} \frac{\partial}{\partial x} \\ \frac{\partial}{\partial y} \\ \frac{\partial}{\partial z} \end{bmatrix}$$

$$\boldsymbol{q} = -\boldsymbol{K} \cdot \nabla h \tag{2.6}$$

where ***K*** is the hydraulic conductivity tensor [LT^{-1}], and ***q*** is the specific discharge vector [LT^{-1}], Hydraulic conductivity is expressed by:

$$K = \frac{\rho g k}{\mu} \tag{2.7}$$

where, ρ is the density of the fluid [ML^{-3}], g is acceleration due to gravity [LT^{-2}], k is intrinsic permeability [L^2], μ represents dynamic viscosity [$ML^{-1}T^{-1}$].

2.2.2. Darcy's law for variable-density groundwater flow

When fluid density variations are significant, they must be taken into account in the analysis of groundwater flow. In which case the standard definition of Darcy's law must be adapted to include water density as a variable. Assuming that the principal directions of intrinsic permeability align with *x*, *y* and *z* Cartesian axes, then Darcy's law for variable density is written (Bear, 1972):

$$\begin{aligned} q_x &= -\frac{k_x}{\mu}\frac{\partial p}{\partial x} \\ q_y &= -\frac{k_y}{\mu}\frac{\partial p}{\partial y} \\ q_z &= -\frac{k_z}{\mu}\left(\frac{\partial p}{\partial z} + \rho g\right) \end{aligned} \tag{2.8}$$

where *p* is pressure [ML^{-1}]. And which can be reduced to:

$$\boldsymbol{q} = -\frac{\mathbf{k}}{\mu}(\nabla \mathrm{p} - \rho \mathrm{g}) \tag{2.9}$$

where $\mathbf{k}$ is the permeability tensor [L^2].

2.3. Governing equation for flow and transport

Based on the principle of mass conservation for fluid and solute, the rate of accumulation of mass stored in a representative elementary volume is equal to the sum of mass fluxes across

the face of the element and the mass exchange from sinks or sources. The mathematical expression for the conservation of mass is thus:

$$\frac{\partial(\rho\theta)}{\partial t} = -\nabla \cdot (\rho \boldsymbol{q}) + \bar{\rho} q_s \qquad 2.10$$

where $\bar{\rho}$ is the density of water entering/leaving from a sink/source [ML^{-3}], q_s is the volumetric flow rate per unit volume of aquifer representing sources and sinks [T^{-1}], θ is porosity [-] and t is time [T]. The first section of the right hand side is the net flux of mass into the medium, the second part of the mass which enters/exists through sources and sinks. The left hand is the time rate of change in the mass stored.

If $\boldsymbol{q}$ in equation (2.10) is replaced with equation (2.9), then one equation results:

$$\frac{\partial(\rho\theta)}{\partial t} = -\nabla \cdot (\rho \frac{\mathbf{k}}{\mu}(\nabla \mathrm{p} - \rho \mathrm{g})) + \bar{\rho} q_s \qquad 2.11$$

For saturated soil water conditions, the left hand side of equation (2.11) can be further expanded to obtain the general form of the partial differential equation for variable-density groundwater flow in saturated porous media:

$$\rho S_p \frac{\partial p}{\partial t} + \theta \frac{\partial \rho}{\partial c}\frac{\partial c}{\partial t} = -\nabla \cdot (\rho \frac{\mathbf{k}}{\mu}(\nabla \mathrm{p} - \rho \mathrm{g})) + \bar{\rho} q_s \qquad 2.12$$

where p is pore pressure [$ML^{-1}T^{-2}$] , c is solute concentration [ML^{-3}], in which S_p is the specific storage in terms of pressure [$M^{-1}LT^{-2}$]. On the left the first term is rate of fluid mass accumulation due to pore pressure change and the second term is rate of fluid mass accumulation due to the change in solute concentration. If density is constant this last term cancels.

Groundwater flow is often simulated using equation (2.12) and assuming that density, viscosity, porosity and permeability are constant, in which case it is a differential equation for p and can be solved numerically if certain boundary and initial conditions are specified (Holzbecher, 1998).

Excluding exceptional cases, characteristics of the porous medium are usually not influenced by the flow (e.g. porosity may change under higher pressure or dissolution processes), making the above assumption valid. However, viscosity and density are affected by changes salinity or temperature gradients. Thus, for cases in which these are variable, the solution of Equation (2.12) requires equations of state linking density and viscosity to solute concentration:

$$\rho(c,T,p) \qquad\qquad \mu(c,T,p) \tag{2.13}$$

As the focus of the current document is on the effect of salinity, the solution for temperature will not be presented. Readers are advised to consult Holzbecher (1998) or similar texts for further reading regarding formulation for temperature and some of the formulations for equations of state. For seawater, the relationship between concentration and density can be expressed by a linear empirical relationship, such as:

$$\rho = \rho_s \left(1 + \left(\frac{\rho_s - \rho_f}{\rho_f}\right)\frac{c}{c_s}\right) \tag{2.14}$$

where ρ_s and c_s are the density and concentration of the reference seawater. The change in solute concentration between freshwater and seawater is insufficient to cause significant effects on viscosity, which is therefore usually ignored for such problems.

Solute mass is transported in porous media by groundwater flow (advection), molecular diffusion and mechanical dispersion and is described by the following partial differential equation (Zheng and Bennett, 1995):

$$\frac{\partial}{\partial t}(\theta R \rho c) = \nabla \cdot \left(\rho(-\boldsymbol{q}c + \theta \boldsymbol{D}\nabla \mathrm{c})\right) + q_c \tag{2.15}$$

where R is the retardation factor [-] and $\boldsymbol{D}$ is the general dispersion tensor [L^2T^{-1}]. The left side describes temporal change of mass, in which the *retardation factor,* R, can usually be omitted in salt transport problems as the main components interact only slightly with the solid matrix (thus $R \approx 1$). On the right side, the first term describes *advection*, the second stands for *diffusion* and *dispersion* and the final term accounts for sources and sinks.

The hydrodynamic dispersion coefficient tensor includes the processes of molecular diffusion, longitudinal and transversal dispersion and is defined by (Bear, 1976):

$$\boldsymbol{D} = \left(D_{ij}\right) = \left((D + \alpha_T u)\delta_{ij} + (\alpha_L - \alpha_T)\frac{u_i u_j}{u}\right) \quad 2.16$$

D is diffusivity [L^2T^{-1}], α_L and α_T longitudinal and transversal dispersivity [L], u_i and u_j are velocity in i and $j$direction [L^2T^{-1}], u is the flow velocity [L^2T^{-1}].

The coupled solution of equations (2.12) and (2.15) describes variable density fluid flow and solute transport. The entire set is difficult to solve and most modellers use simplifications suitable for their specific problems (Holzbecher, 1998).

2.3.1. The Oberbeck-Boussinesq assumption

The differential equations can be simplified significantly with the Oberbeck-Boussinesq assumption. The most simple formulation states that changes in density can be neglected except for the buoyancy term in Darcy's Law. Thus, equations (2.11) and (2.15) can be simplified to:

$$\frac{\partial(\theta)}{\partial t} = -\nabla \cdot (\rho \frac{\mathbf{k}}{\mu}(\nabla \mathrm{p} - \rho \mathrm{g})) + q_s \quad 2.17$$

and

$$\frac{\partial}{\partial t}(\theta R c) = \nabla(\theta \boldsymbol{D} \nabla \mathrm{c}) - \boldsymbol{q}\nabla c + q_c \quad 2.18$$

This is only valid for cases in which the density variations throughout the system remain relatively small in comparison to the reference density, and as such is not valid for high concentration brines but is applicable to modelling interactions between fresh and seawater in coastal aquifers.

2.1. Remarks on the numerical solution of the advective-dispersive transport equation

The solution of the advective-dispersive transport equation is numerically more difficult than the flow equation, in particular when the advective component dominates over dispersion

(Huyakorn and Pinder 1983). Numerical approximations of the derivatives of the transport equation introduce truncation and oscillation errors (Oude Essink and Boekelman 1996). Although, in general, representation of the dispersion by the finite element method is accurate if numerical dispersion is small with respect to the hydrodynamic dispersion (Bear and Verruijt 1987). Truncation error acts as an additional dispersion term, usually referred to as numerical dispersion, which may affect the accuracy of the solution. Oscillation errors occur due to overshoot and undershoot of the solution, usually near the concentration front, with erroneously high values upstream of the moving front (overshoot) and low values downstream of the front (undershoot) (Huyakorn and Pinder 1983).

Pinder and Gray (2008) have shown that the numerical difficulty is due to the inability of the numerical approximation to propagate short wavelength harmonics. When the value of the physical dispersion coefficient is decreased, these short wavelength harmonics become more important for the accurate description of the concentration front (Huyakorn and Pinder 1983). According to Huyakorn and Pinder (1983), numerical oscillations on the solution of the finite element solution can be effectively eliminated if the element size is selected so that grid Peclet number (P_e) does not exceed two for linear basic functions (and four for quadratic basic functions):

$$P_e = \frac{v\Delta x}{D} \leq 2 \qquad 2.19$$

where Δx is the dimension of the element [L], D is the hydrodynamic dispersion [L^2T^{-1}] and v is the effective velocity [LT^{-1}]. In advective dominated solute transport, mechanical dispersion dominates over molecular diffusion, with $D \approx \alpha_L v$. Thus, equation (2.19) becomes:

$$P_e = \frac{\Delta x}{\alpha_L} \leq 2 \qquad 2.20$$

Solving equation (2.20) for Δx shows that numerical accuracy requires element dimensions to be:

$$\Delta x \leq 2\alpha_L \quad (2.21)$$

Thus, to minimize errors, the model mesh or grid should be designed so that element or cell size takes into account the magnitude of the physical parameter dispersivity, although acceptable solutions have been obtained for P_e as high as ten (Huyakorn and Pinder 1983; Wang and Anderson 1995). In their review of data on field-scale dispersion, Gelhar et al (1992) found that values for longitudinal dispersivity range between 10^{-2} m and 10^{4} m, depending on aquifer characteristics and scale effects. These same authors suggested that, in general, lower longitudinal dispersivity is more likely to be realistic for field applications. In practice, this means that the mesh or grid for transport models requires element or cells with dimensions in the order of centimetres or meters to properly represent the physical characteristics of a given system. For real world applications, in which study areas can be in the order of 10's to 100's of square kilometres, this requirement leads to exceedingly large numbers of cells or elements. When dealing with local scale transport problems, this issue can be reduced using larger cell/element dimensions in areas where no transport occurs and local refinements in the remainder. However, as SWI processes in coastal aquifers usually occur over a significant portion of the model domain, local refinements do not provide significant reductions in the amount of cells/elements. Thus the simulation of large-scale three-dimensional coastal aquifer systems, apart from being numerically complex, is also computationally expensive due to the large number of cells/elements required to guarantee numerical stability.

3. Importance of spatio-temporal distribution of recharge, abstraction and aquifer properties for sustainable groundwater exploitation – the case of the *Querença-Silves* aquifer[2]

The following chapter discusses the effect of four factors when defining the sustainable yield of an aquifer: i) aquifer properties, ii) temporal distribution of recharge, iii) temporal distribution of groundwater pumping and iv) spatial distribution of pumping wells. A theoretical analysis is applied using a numerical groundwater flow model of the Querença-Silves coastal aquifer, focusing on the impact of groundwater use on natural discharge rates. The model is subsequently used to determine sustainable pumping rates as a function of the indicated factors.

3.1. Introduction: Sustainable Yield

Many aquifers in the world possess high storage capacity and water quality, allowing them to constitute a prime source of water for human consumption and agriculture, even in dry seasonal periods when rainfall is scarce and surface water is fast depleted (Van Camp et al 2010). Groundwater depletion is the inevitable and natural outcome of withdrawing significant amounts of water from an aquifer (Sophocleous 1997; Bredehoeft 1997; Konikow and Kendy 2005; Bekesi et al 2009). The abstracted water is initially removed from groundwater storage, but over time may be increasingly derived from decreased discharge and increased recharge (Bredehoeft 1997; Konikow and Kendy 2005; Bekesi et al 2009). This is defined as capture by Lohman et al (1970) and can be the cause of negative impacts such as depletion of stream flows, drying of springs, and loss of riparian ecosystems and wetlands. The introduction of safe yield intends to avoid these negative impacts.

[2] The following chapter is adapted from **Hugman** R, Stigter TY, Monteiro JP, Nunes L (2012) Influence of aquifer properties and the spatial and temporal distribution of recharge and abstraction on sustainable yields in semi-arid regions. Hydrol Process 26:2791–2801. doi: 10.1002/hyp.8353

The concept of safe yield has been recognized since the beginning of the last century (Lee 1915; Theis 1940). It has since been defined by Sophocleous (1997) as the attainment and maintenance of a long-term balance between the amount of groundwater withdrawn annually and the annual amount of recharge. But the concept was not matched with appropriate methods to determine the safe yield and to assess the impacts (Zhou 2009). In practice, safe yield is often calculated as a percentage of the natural recharge. A misperception is that the development of groundwater is considered to be safe if the rate of groundwater withdrawal does not exceed the rate of natural recharge. The natural recharge alone cannot determine the safe yield; the impacts of dynamic development of the capture on society, economy, and the natural environment must be assessed (Zhou 2009).

The concept of sustainability appeared in the early 1980s, and is centred on the idea of managing rates of resource use so as to meet the needs of the present generation without compromising the needs of future generations to meet their needs (Alley and Leake 2004). This lead to a shift in focus from safe yield to sustainable yield, which is defined as the development and use of groundwater resource in a manner that can be maintained for an indefinite time without causing unacceptable environmental, economic, or social consequences (Alley et al 1999; Sophocleous 2000; Custodio 2002).

Kalf and Woolley (2005) give a review of the evolution of the concept of safe to sustainable yield and discuss methodology of determining sustainable yield based on principles of conservation of mass at the water basin scale. However, Zhou (2009) suggests that this method is still insufficient as it defines the sustainable yield as the sustainable pumping rate which can be sustained by natural and induced recharge and does not take into account if the pumping causes unacceptable environmental, economic, or social consequences. Zhou (2009) goes on to suggest that the sustainable yield cannot be simply calculated as a single value using the water balance; it requires assessing the dynamic response of the groundwater to the introduced pumping regime, which is rarely performed.

This paper aims to contribute to understanding the importance of four factors on the determination of sustainable yields: i) aquifer properties, ii) temporal distribution of recharge, iii) temporal distribution of groundwater pumping and iv) spatial distribution of

pumping wells. It is important to understand how the present-day and future vulnerability of groundwater systems and associated groundwater dependent ecosystems (GDEs) to pumping activities depend on these critical factors and what the risks are of considering sustainable yield as a fixed percentage of mean annual recharge.

The hydraulic properties of an aquifer reflect its transmissivity and storage capacity, and hence its resilience, particularly its response to extreme events such as droughts. Regarding the temporal distribution of rainfall and recharge, climate change studies are showing that in Mediterranean regions significant shifts in seasonal distribution and inter-annual variability are predicted (Stigter et al 2011a). More specifically, rainfall events are expected to be concentrated in the winter, with large reductions in spring and autumn. On an inter-annual basis, extreme events (high rainfall and droughts) will be more frequent. Therefore, groundwater storage will gain more importance. In the long-term, i.e. 2070-2100, mean annual recharge will drop significantly (Stigter et al 2011a). When aquifer recharge is reduced, developing long-term sustainable exploitation strategies may be a difficult challenge (Van Camp et al 2010). By studying the influence of the spatial and temporal distribution of groundwater pumping on sustainable yields, these can be optimized to a certain extent by water management agencies.

The individual and joint effects of the four referred aspects are analyzed by calibrating and validating a numerical finite element groundwater flow model for a case study in the south of Portugal and then running a number of so-called transient cyclic state scenarios where the effect of the dynamic nature of recharge and abstraction, as well as that of aquifer properties and well location, will be simulated. The model will subsequently be used to determine sustainable pumping rates as a function of the indicated factors.

3.2. Study area: *Querença-Silves* (M5) aquifer system

The QS aquifer system (Figure 3.1 and Figure 3.2) is a karstified carbonate rock aquifer formed by Jurassic (Lias-Dogger) carbonate sedimentary rocks, that extends over an irregular area of 324 km^2 from the Arade River (in the west) to the village of Querença (in the East) (Almeida et al 2000; Monteiro et al 2006; Monteiro et al 2007b). As the largest aquifer in the

Algarve (south Portugal) and the amount of recharge it is the most significant groundwater reservoir in the region.

The system is limited to the south by the Algibre thrust, the main onshore thrust in the Algarve Basin, separating the Lower/Early and the Upper/Late Jurassic, and to the north by Carboniferous shale and greywacke. Flow is mainly from East to West, with the main natural discharge area at the Estombar springs along the estuary of the Arade River. These springs support important and sensitive surface/groundwater ecotones, many of which are classified as protected areas (Silva et al 2012). Several streams cross the system from North to South and switch between being gaining and loosing along their path. Salvador et al. (2012) provided an initial attempt to quantify and simulate these exchanges, however further work is necessary to comprehend the complex nature of these surface/groundwater interactions.

The aquifer is divided into two compartments, evidenced by both the distinct change in topography (Figure 3.1) and temporal variation of hydraulic head measured in piezometers (Figure 3.3). Flow patterns in the East are complex, whilst in the West they indicate a well-connected karst with a clear east to west flow path. Recently Neves et al (2016) explored the temporal structure of a groundwater-level time series in the QS, confirming the distinct nature of the two sectors. They found that the western sector displays characteristics consistent with relatively large and uniform values of water storage capacity and transmissivity properties, while the eastern sector shows larger spatial and temporal heterogeneity.

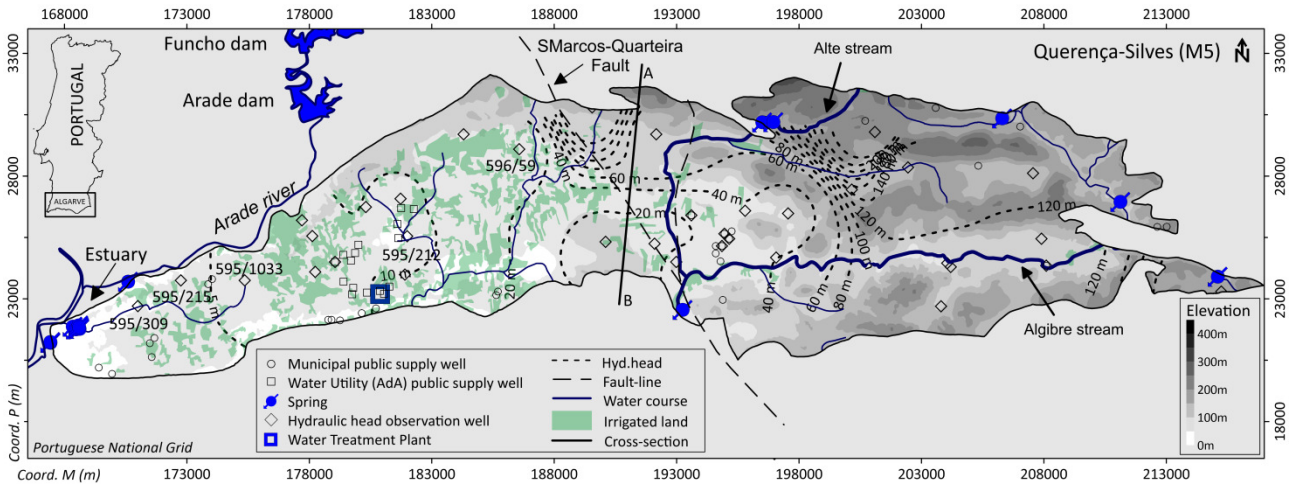

Figure 3.1 Location and main features of the Querença-Silves aquifer system.

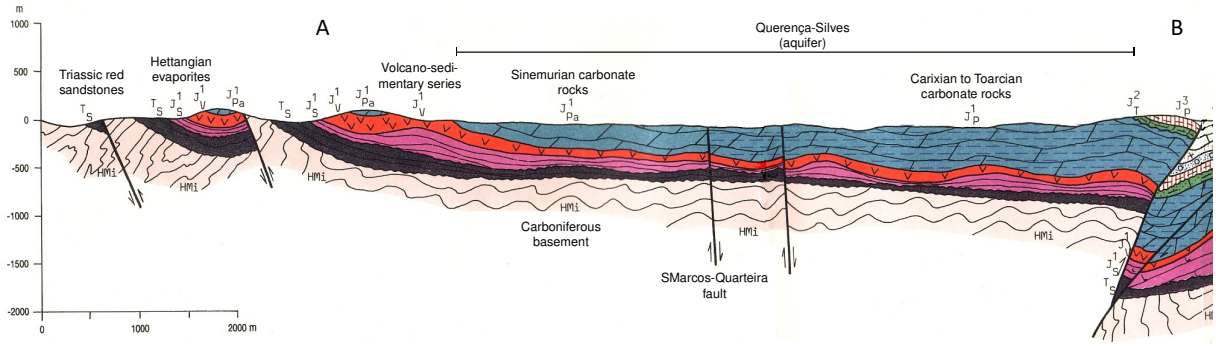

Figure 3.2 Geological cross section of the QS aquifer: Sinemurian (J1Pa) and Carixian to Toarcian carbonate rocks (J1P); and surrounding formations: Carboniferous basement (HMi), Triassic red sandstones (Ts), Hettangian evaporites (J1s) and volcano-sedimentary series (J1v). Location of cross-section is shown in Figure 3.1. (Adapted from Manuppella (1982)).

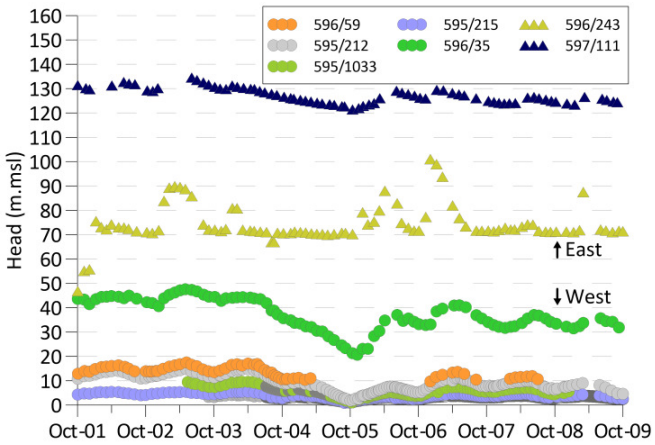

Figure 3.3 Selected groundwater level time series registered by the regional water management monitoring network.

Groundwater quality in the region is monitored by the Portuguese Environmental Agency with an extensive network of wells, boreholes and springs. Average chloride concentrations observed near the discharge area of the QS are presented in Figure 3.4 (left). Concentrations are low for most of the system, increasing in the proximity of the Arade estuary. Highest values are measured at the Estombar springs and well 595/262 which is in the vicinity of the springs. Figure 3.4 (right) presents time series of chloride measurements for selected wells. Unfortunately observations are sparse, however they do suggest that chloride concentrations in spring discharge increased during the 2004/05 drought and continued high during the subsequent years. Of note is the spike in concentration associated to the

large increase in groundwater levels in the winter of 2009, and subsequent improvement in water quality. In fact this occurs in every annual cycle, with concentrations increasing with the rise in water levels at the beginning of the wet season. It is likely that the increase in freshwater flow serves to flush saltwater that intruded during the prior dry period, lagging behind the recharge event.

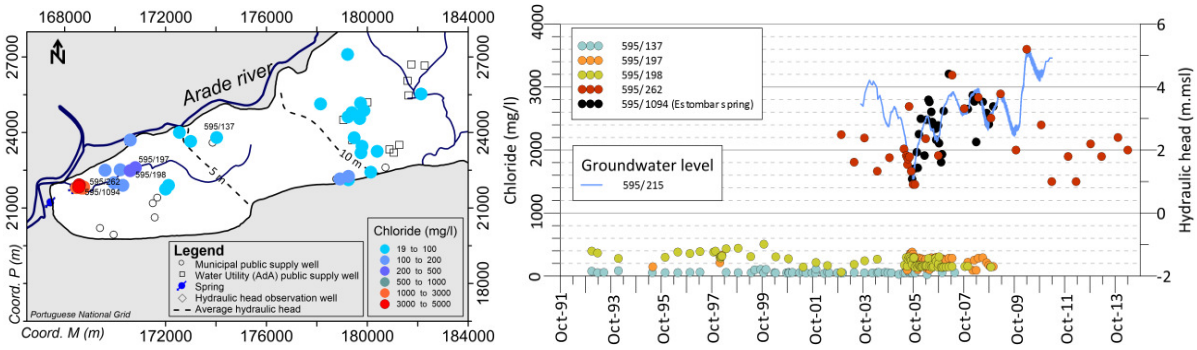

Figure 3.4 Groundwater quality monitoring network and average observed cloride concentration (left); time series of cloride concentration measured at selected stations (right).

3.2.1. Climate

The region has a warm Mediterranean climate, and the coastal zone is considered semi-arid due to the precipitation to potential evapotranspiration ratio (Estrela et al 1996). Rainfall is irregular, characterized by long dry summer seasons and heavy rainfall periods during the winter months, as well as large seasonal and annual variability (Stigter et al 2009). Average annual rainfall and temperature are 650mm and 17ºC respectively.

Current predictions are for an increase in frequency and intensity of droughts in the future (Giorgi 2006; Santos and Miranda 2006). Mean annual rainfall in the Algarve is expected to decrease slightly up to 2050, however significant reductions in rainfall are expected towards the end of the century (Stigter et al 2014). The most significant expected change in the short-term are shifts in seasonal distribution and inter-annual variability, with a greater concentration of rainfall in the winter season and large reductions in spring and autumn (Stigter et al 2014).

3.2.2. Recharge

Monteiro et al. (2006) originally estimated mean annual recharge for the QS at $93x10^6$ $m^3 \cdot yr^{-1}$. Oliveira et al. (2008) applied the FAO dual crop coefficient method using a sequential daily water balance model (BALSEQ_MOD), and obtained average annual recharge rates of $104x10^6$ $m^3 \cdot yr^{-1}$ along with a detailed spatial distribution of recharge.

Recent research by Stigter et al. (2009, 2014) on climate scenarios and their impacts on groundwater resources and dependent ecosystems in the Central Algarve, show that mean annual rainfall is expected to decrease slightly within the next 50 years (Table 3.1). The most significant change will be an increase in seasonal and inter-annual variability, with rainfall concentrated in the winter season, and large reductions in spring and autumn. Hugman et al. (2012) and Hugman et al. (2013) have shown that this increased seasonality will contribute to reducing the systems resilience to droughts and other extreme events. Within the next 100 years, a significant decrease in both rainfall and recharge is predicted.

Table 3.1 Estimated mean annual values for rainfall, recharge and crop water demand; average results for an ensemble of climate scenarios (adapted from Stigter et al. (2014)).

Parameter ($mm.yr^{-1}$)	Current	2020-2050		2069-2099	
		Absolute value	Change	Absolute value	Change
Rainfall	739	685	-7%	526	-29%
Total recharge	340	323	-5%	206	-39%
Net recharge	246	216	-12%	82	-67%
Crop water demand	94	107	+14%	124	+32%

3.2.3. Groundwater use

Up to the end of the 20th century public water supply in the Algarve was managed at a Municipal scale and was almost entirely dependent on groundwater. Lack of regional planning and unregulated groundwater use gave origin to a range of quantitative and qualitative problems (Monteiro and Costa 2004). Along with increasing water demand, these problems lead to the implementation of a water policy based on developing large surface water reservoirs, which now supply most public water demand in the Algarve. However, the severe drought of 2004-05 highlighted the fragility of this single source supply scheme and

has been caused a push towards an integrated water resource management (Stigter et al 2009).

The main pressure on groundwater resources in the QS comes from agriculture. Nunes et al. (2006) estimated an annual withdrawal of $31x10^6$ $m^3 \cdot yr^{-1}$ for irrigation, mostly located in the western part of the aquifer system (see Figure 3.1). Current groundwater abstraction for public supply is managed entirely by the regional water utility and is in the order of 4 to $10x10^6$ $m^3 \cdot yr^{-1}$. Prior to 1999, well-fields operated by municipal councils withdrew around $12x10^6$ $m^3 \cdot yr^{-1}$ (Monteiro et al 2006). The period with highest abstraction occurred during the 2004-04 drought, when municipal councils were forced to reactivate heir wells. An estimated $26.5x10^6$ $m^3 \cdot yr^{-1}$ of groundwater was used for public supply during this period (Monteiro et al 2006).

3.3. Methods

3.3.1. Numerical model

The model used in this paper is the result of ongoing research in relation with monitoring and modelling of aquifers at the University of Algarve. The first variants of this model implemented for the QS aquifer system were presented in Monteiro et al (2003) and Vieira and Monteiro (2003) and were related with understanding the control of the boundary conditions on the regional flow pattern and with the evaluation of recharge and evaluation of the order of magnitude of discharge in the different outflow areas of the aquifer. Monteiro et al (2006) performed an initial inverse calibration of transmissivity (*T*) for the model allowing a considerable improvement in the reliability of the simulation of the observed regional flow pattern. Subsequently, Monteiro et al (2007a) used the model to investigate stream-aquifer interactions, as these are relevant to the ecological conditions of these riparian groundwater dependent ecosystem. Stigter et al (2009) undertook simulations of hypothetical extraction scenarios as part of an effort to determine sustainable sources of groundwater for integration into a regional water supply system, in which the spatial distribution of abstraction for irrigation was refined and applied to the location of known irrigation wells.

Recent developments of the hydrogeological knowledge of the area, namely new estimates of the spatial distribution of recharge, have allowed for further refinements to the numerical groundwater flow model. Areal recharge rates were most recently quantified by Oliveira et al (2008). They estimated the average recharge as 45% of the rainfall and also obtained a new, more detailed spatial distribution of recharge, which was applied to both steady-state and transient versions of the model. Due to these new values of recharge, previously calibrated values of *T* are no longer result in the best representation of the hydraulic behaviour of the QS; therefore a new calibration was undertaken.

Abstraction for irrigation was applied to 150 nodes of the model, which represent 150 private wells known to be located within the irrigated area; the estimated annual volume of abstraction for irrigation was distributed equally among the nodes and, under transient condition, uniformly over the period of the last week of May to the end of September. Withdrawals for public water supply were applied to nodes representing wells that belong to the Water Utility *Águas do Algarve* (*AdA*) shown in Figure 3.1, who provided monthly values of abstraction volumes.

Presently, the boundary conditions are defined as constant head along the Arade estuary in the west (Figure 1) and no-flow for the remaining part. Since there is strong tidal influence in the estuary, a specified (non-constant) head boundary condition was tested; however it was found that the effect was not significant on a regional scale and therefore removed. Additional boundary conditions could have been defined for several small springs in the central and eastern sector, but model variants based on these conditions revealed a minor impact on the regional flow pattern and water balance.

The defined conceptual flow model was translated to a finite element mesh with 11 663 nodes and 22 409 triangular finite elements. The representation of the flow domain of karst systems as single continuum equivalent porous media, using concepts of hydraulic conductivity (*K*) and its bi-dimensional derivative *T*, is valid when modelling hydraulic heads and flow volumetrics on a regional scale, as is discussed by Scanlon et al. (2003). The direct solution was implemented using a standard finite-element model based on the Galerkin method of weighted residuals (Huyakorn and Pinder 1983)

T was estimated by inverse modelling under steady-state conditions. Calibration was performed using the Gauss-Marquardt-Levenberg method, implemented in the nonlinear parameter estimation software PEST (Doherty 2002). Optimization of the results proved a time-consuming procedure, where variants were tested to search for the best reproduction of the equipotential surface, meeting the water balance criteria. The entire aquifer system is supported by carbonate rocks, therefore, the hydraulic property zones cannot be defined based on geological evidence. Despite the lithologic uniformity the regional flow pattern of the aquifer reveals a complex internal heterogeneous structure, the zonation of which was established based on the available data (piezometric and discharge in natural outflow areas). In total 23 *T* zones were defined, where the behaviour of piezometers allowed a reasonable fitting of field data using a single value of *T*, as can be seen in Figure 3.5.

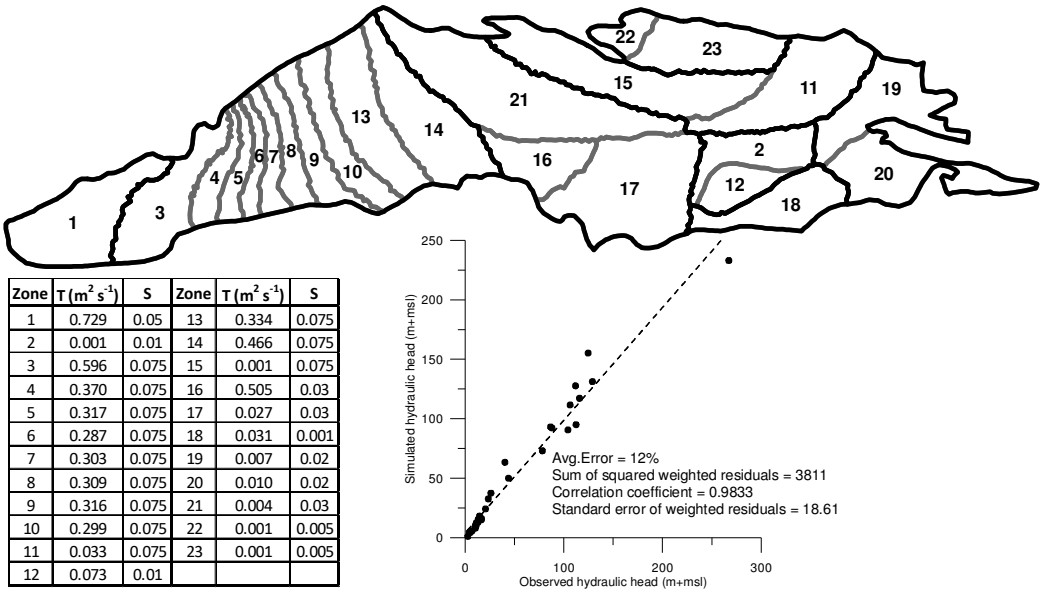

Zone	T ($m^2 s^{-1}$)	S	Zone	T ($m^2 s^{-1}$)	S
1	0.729	0.05	13	0.334	0.075
2	0.001	0.01	14	0.466	0.075
3	0.596	0.075	15	0.001	0.075
4	0.370	0.075	16	0.505	0.03
5	0.317	0.075	17	0.027	0.03
6	0.287	0.075	18	0.031	0.001
7	0.303	0.075	19	0.007	0.02
8	0.309	0.075	20	0.010	0.02
9	0.316	0.075	21	0.004	0.03
10	0.299	0.075	22	0.001	0.005
11	0.033	0.075	23	0.001	0.005
12	0.073	0.01			

Figure 3.5 Map with established zonation for estimation of transmissivity (grey lines) and storage coefficient (black lines) (top), optimized values obtained calibration (bottom left) and resulting plot of modeled versus observed hydraulic heads (bottom right).

For the transient model, the spatial distribution of the storage coefficient (*S*) was calibrated by trial-and-error for a model run from 2002 and 2006, using available piezometric data of eight wells, of the official monitoring network of the Regional Water Basin Administration (RWBA), and then validated for 2006-2009. All available data from piezometers in the

aquifer system was analysed and grouped according to the behaviour of hydraulic head to recharge and discharge events. This resulted in eight separate zones, the location of which was intersected with areas of equal *T*. The calibration of *S* was a difficult process and it was necessary to perform a recalibration of *T*, based on more accurate determinations of the relationship between hydraulic head distribution and water budget. In the end the results from the distribution of *S* showed a satisfactory fit with observed head time series for most of the observation wells, some examples of which are provided in Figure 3.6 (for location of the well see Figure 3.1). Estimated discharge rates were compared to measurements performed by the RWBA at springs of the Arade estuary that forms the imposed boundary condition in the model, shown in Figure 3.7 although direct calibration was not possible, as these springs only constitutes 25-35% of the total discharge from the aquifer (Stigter et al 2011a).

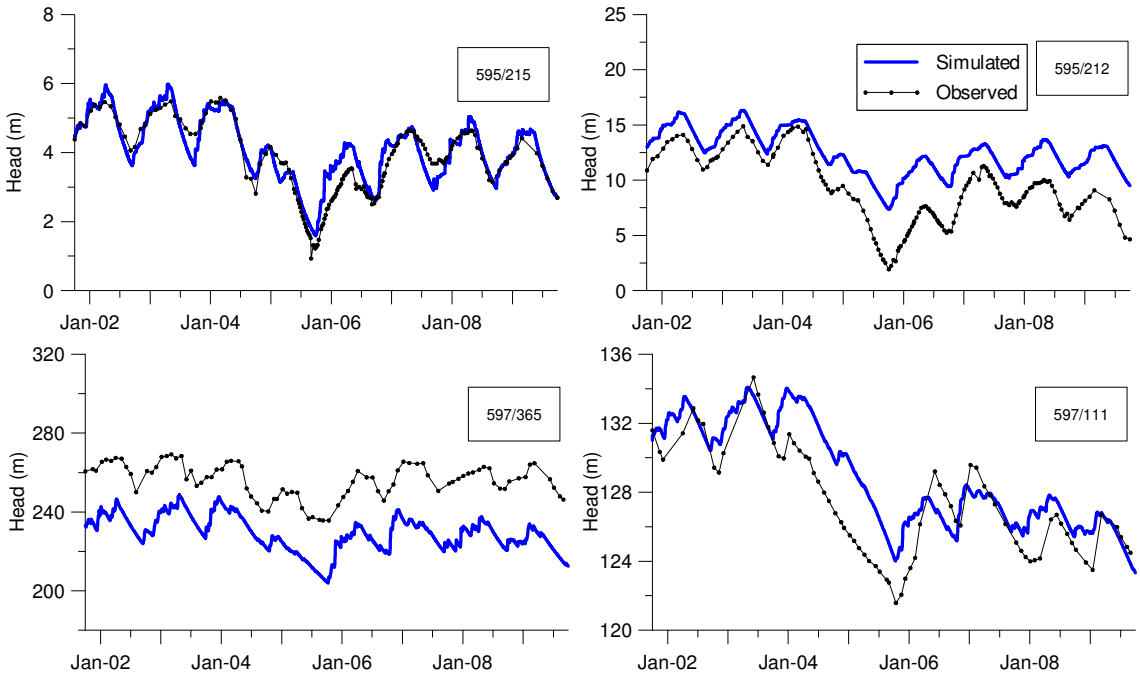

Figure 3.6 Observed and simulated hydraulic head at several observation wells used to calibrate and validate the Querença–Silves numerical flow model.

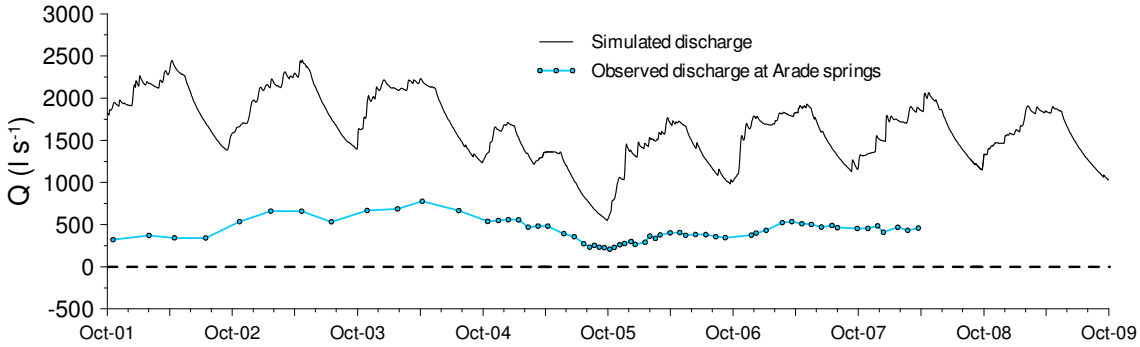

Figure 3.7 Observed and simulated discharge for the period between October 2001 and October 2009.

3.3.2. Scenario development

Several scenarios were developed in order to determine the effect of: i) aquifer properties ii) temporal distribution of recharge iii) temporal distribution of groundwater pumping and iv) spatial distribution of pumping wells on the hydraulic heads, storage and discharge rates of the QS aquifer system, as compared to a steady-state system. As was previously described, current climate predictions indicate a concentration of recharge in the winter period. On the other hand, currently the peak of groundwater abstraction occurs in the summer, for irrigation and public supply for tourism, an important economic activity. In the winter hardly any groundwater is withdrawn, as public supply is largely based on surface water.

Regarding recharge, two scenarios were developed in which the average annual value of recharge was distributed uniformly (1) over six months, from October to March and (2) over two months, November and December. The first scenario is a highly simplified variant of the present-day condition (as currently rainfall occurs mainly during six months, but follows a normal-type distribution), whereas the second is an extreme variant of the possible effect of climate change. With respect to abstraction, also two scenarios where considered: (A) 70% of the annual pumped volume was applied uniformly between April and September and the remaining 30% between October and March (low season), which roughly matches the currently observed temporal variation of abstraction rates for public supply; (B) constant rates of abstraction, a variant that allows evaluating the potential of attenuating the seasonality effect to a certain point. Both scenarios consider abstraction for irrigation distributed uniformly over the period of the final week of May to the end of September.

Despite the fact that a longer dry season is likely to raise the needs for irrigation over a longer period, abstraction for irrigation was not distributed uniformly over the remaining months as it this was not considered to be a reasonable scenario, and there is currently insufficient information to estimate how irrigation will evolve both quantitatively and over time.

Further scenarios where developed taking into account aquifer properties and well location. Regarding aquifer properties, the optimized storage coefficient *S*, scenario (i), was compared to a twofold (scenario ii) and fivefold (scenario iii) reduction of *S* over the entire area. Finally, scenarios on well location either considered abstraction wells for public supply located at the currently used well-fields (scenario a) or evenly distributed over the 150 private wells (scenario b), allowing the analysis of concentrated vs. distributed abstractions. The aim was to study the impact of the well field operated by the Regional Water Utility.

The scenarios are summarized in Table 3.2. All the described scenarios were run under a transient cyclic state until they reached equilibrium, i.e. with constant seasonal oscillations and no annual or longer-term changes in storage. Based on the foregoing, sustainable yields were determined for some of the developed scenarios, based on specific criteria rather than a fraction of mean annual recharge. One such criterion is the minimum hydraulic head that prevents gradient inversion and complete salinization of the estuarine springs at the end of the dry season, so as to preserve the current ecosystem status described by Silva et al (2012). Abstraction for irrigation was kept at 31 $hm^3.yr^{-1}$, only increasing the abstraction for public water supply to account for the remaining percentage of mean annual recharge. INAG (2005) which provides a characterization of the hydrographical regions of Portugal as part of the process of implementing the Water Framework Directive (WFD), defined 90% of mean annual recharge as the threshold over which groundwater abstraction applies a “potentially significant pressure” on a groundwater body. This threshold is one of several indicators applied by INAG (2005) to define the “quality status” of water bodies. Results were compared to this abstraction of 90% of mean annual recharge criterion.

Table 3.2 Overview of used scenarios and optimized sustainable yield.

Scenario	Distribution of *R*	Distribution of *A*	Storage coefficient	Location of PS wells	Sustainable yield	
					% recharge	hm^3
1Aia	Distributed	Seasonal	Optimized	Concentrated	73%	75.9
1Aib	Distributed	Seasonal	Optimized	Distributed	-	-
1Aiia	Distributed	Seasonal	Reduced 2x	Concentrated	70%	72.8
1Aiiia	Distributed	Seasonal	Reduced 5x	Concentrated	40%	41.6
1Bia	Distributed	Constant	Optimized	Concentrated	79%	82.4
1Bib	Distributed	Constant	Optimized	Distributed	79%	82.4
2Aia	Concentrated	Seasonal	Optimized	Concentrated	70%	72.8
2Aib	Concentrated	Seasonal	Optimized	Distributed	-	-
2Aiia	Concentrated	Seasonal	Reduced 2x	Concentrated	67%	69.7
2Aiiia	Concentrated	Seasonal	Reduced 5x	Concentrated	35%	36.4
2Bia	Concentrated	Constant	Optimized	Concentrated	76%	79
2Bib	Concentrated	Constant	Optimized	Distributed	74%	77

3.4. Results

The results of the different scenarios are illustrated by time series of hydraulic head (*h*) and discharge rate (*Q*) at the western boundary. Well 595/215 (see location in Figure 3.1) has been previously applied as an indicator of storage in the QS aquifer system (Stigter et al 2010) and Figure 3.8 shows that there is a good correlation between observed water level and storage calculated by the numerical model for the period 2001-2006.

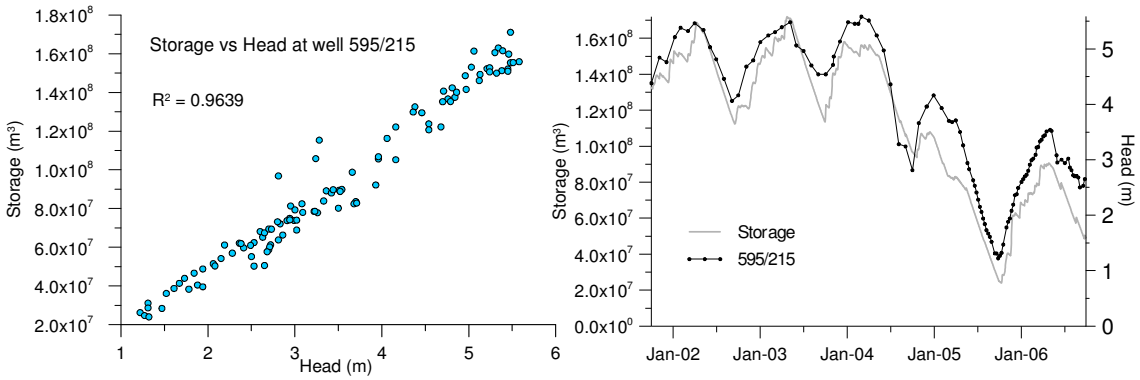

Figure 3.8 Comparison between hydraulic head at well 595/215 and calculated storage of the QS from 2001 to 2006.

The first scenarios compare distributed versus concentrated recharge and abstraction, presented in Figure 3.9. The time series are shown for one hydrological year plus the first

three months of the following year, to better illustrate the minimum values that occur at the end of the dry season and the recovery in the subsequent rainy period.

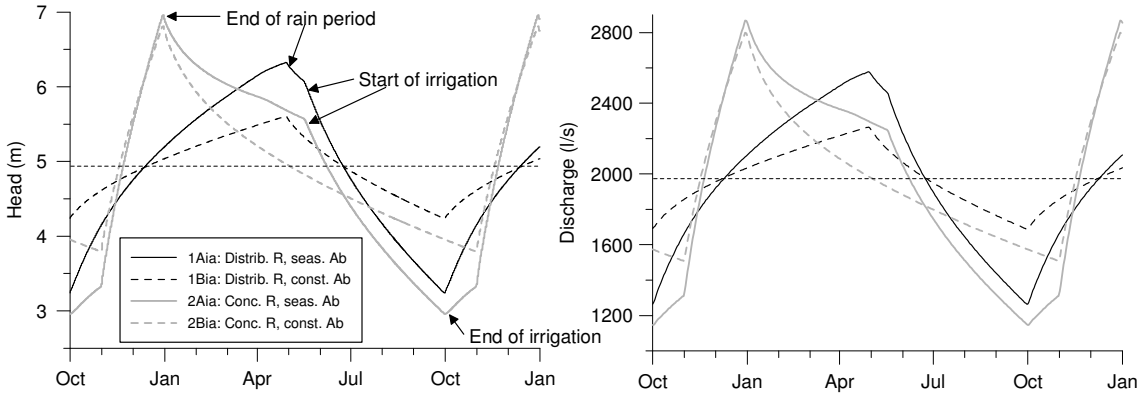

Figure 3.9 Variation of hydraulic head at well 595/215 (left) and aquifer discharge rate (right) for scenarios of different temporal distribution of recharge and abstraction.

In the present-day scenario, i.e. distributed recharge and seasonal variation in abstraction (1Aia), *h* starts to rise at the start of the rain season and reaches a maximum at the end of April, when rainfall stops. There is no observable time lag between the start/end of recharge and the rise/drop in *h*, which depicts the extremely rapid response of the aquifer. The behaviour of *Q* closely follows that of *h*, as it does for all scenarios. Groundwater pumping for irrigation causes a steep decline in *h* (ca. 3m) and *Q* (ca. 1500 l/s).

The concentration of rainfall and recharge in November and December (scenario 2Aia) results in significantly higher maximum values of *h* and *Q*. However, these values drop to values below those of the previous scenario already in March, before the start of the irrigation season and this situation is maintained until halfway into November, the first month of subsequent recharge. 42% of the total annual discharge occurs in the four months of highest discharge, i.e. November to March, vs. 36% in scenario 1Aia, a difference of 3.8 hm^3. It is interesting to note the recovery that occurs in October and that is not linked to recharge, which only occurs in November; this rise is solely due to the cessation of pumping for irrigation.

When the effect of seasonality of pumping is removed from the model by applying a constant abstraction rate throughout the year (scenarios 1Bia and 2Bia), there is a clear difference between maximum and minimum of *h* and *Q*. With a seasonal distribution of

recharge (1Bia) this is evident for both lower maximum *h* and *Q* at the end of the rain season and significantly higher minimum values at the end of the dry season. When recharge is concentrated, maximum *h* and *Q* are hardly affected by the more even distribution of abstraction, but the decline during the dry season is again much less pronounced. For scenarios 1Aia and 2Aia, respectively 59% and 61% of the annual discharged volume occurs during the six months of higher *h* and *Q* (December to June, see Figure 3.9), vs. 54% and 56% for the constant abstraction scenarios.

Figure 3.10 presents the effect of a two-fold and five-fold reduction of the storage coefficient on the time series of *h* and *Q*, considering a seasonal behaviour of abstraction and both the distributed and concentrated recharge scenarios. It is immediately clear that the lower the value of *S*, the higher the seasonal amplitudes. In fact, a five-fold lower *S* would result in minimum values of *h* and *Q* below 0, resulting in gradient inversion and subsequent seawater intrusion (negative discharge in Figure 3.10). In the scenario considering a seasonal distribution of recharge (1Aiiia), 57% of the annual volume is discharged in the four months of peak discharge, vs. 46% in scenario 1Aiia (two-fold lower *S*) and 36% in scenario 1Aia (optimized *S*). For concentrated recharge, the values are 88% (2Aiiia), 72% (2Aiia) and 42% (2Aia). Thus, the lower values of *S* increase the effect of the concentration of recharge, as also seen in *h*: a fivefold smaller *S* would result in Δh_{min}= 0.51m at the end of the dry season between distributed and concentrated recharge scenarios, vs. Δh_{min} = 0.28m for the optimized *S* scenario.

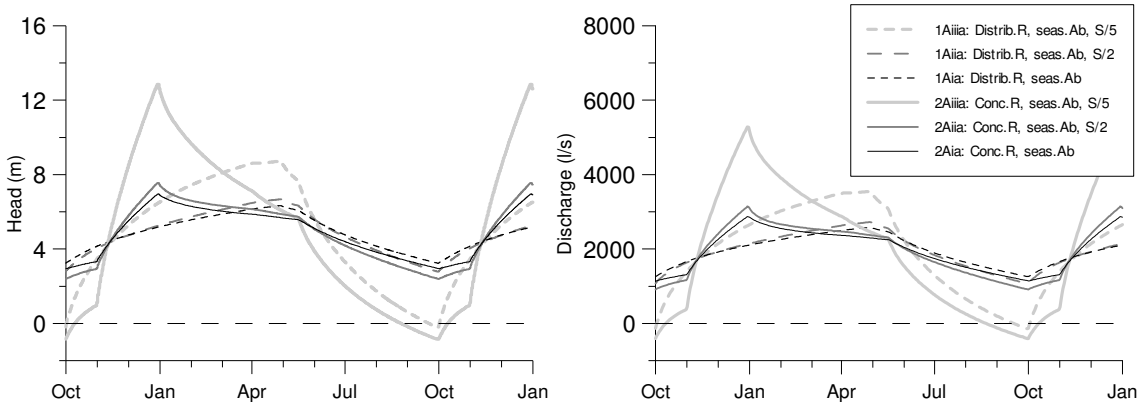

Figure 3.10 Variation of hydraulic head at well 595/215 (left) and discharge rate (right) for scenarios of different temporal distribution of recharge and a twofold and fivefold reduction of storage coefficient.

The impact of the spatial distribution of the public supply wells on the distribution of hydraulic heads in the aquifer is shown in the map of Figure 3.11, once again maintaining a seasonal behaviour of abstraction and considering scenarios of both distributed and concentrated recharge (1Aia vs. 1Aib and 2Aia vs. 2Aib). The map shows the spatial distribution of Δ*h* at the end of the dry season, where negative values indicate lower values of *h* related to the scenarios of spatially concentrated abstractions for public supply. These negative values occur in the western sector of the aquifer, and are concentrated around the well field operated by the Regional Water Utility. There is no observable difference between the concentrated and seasonal recharge scenarios.

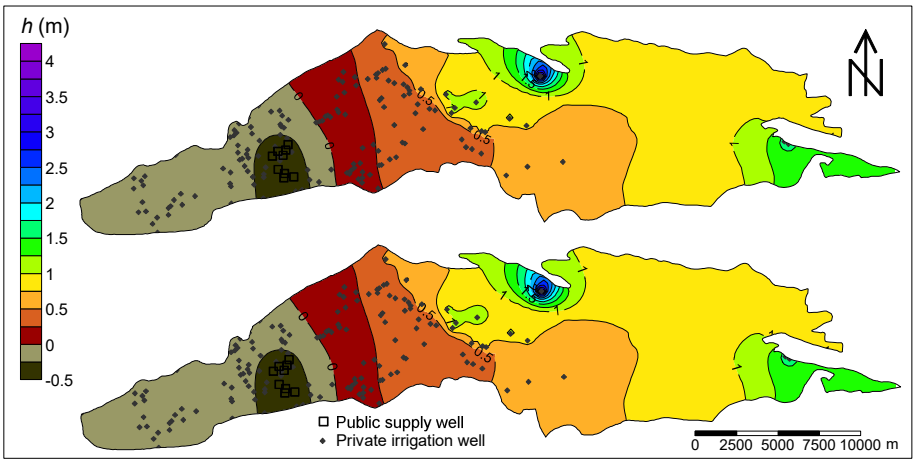

Figure 3.11 Difference in hydraulic head at the end of the dry season between scenarios with spatially concentrated and distributed public supply wells, with seasonal abstraction and distributed recharge (top, 1Aia and 1Aib) and concentrated recharge (bottom, 2Aia and 2Aib).

The effect of extracting 90% of mean annual recharge, the threshold for the definition of good quantitative status according to INAG (2005), on *h* and *Q* is shown in Figure 3.12. It shows that this fraction would clearly be unsustainable, resulting in negative values during almost four to five months, depending on whether recharge were to be distributed or concentrated. At the end of the dry season, negative heads would have occurred up to 15 km inwards. Figure 3.13 summarises the sustainable yields determined for relevant scenarios. Results show that, for the chosen criteria, the most significant effect is seen with the reduction of *S* with a difference of approximately 3 $hm^3.yr^{-1}$ (2x reduction) and 35 $hm^3.yr^{-1}$ (5x reduction) when compared to scenario 1Aia and 2Aia. Scenario 2Aia shows that

predicted changes in seasonal variability of rainfall will in fact have an effect on the sustainable yield, reducing it by 3 $hm^3.yr^{-1}$. The distribution of abstraction throughout the year, as was shown previously, has the opposite effect allowing for an extra 2 $hm^3.yr^{-1}$ to be sustainably abstracted. Although distributing abstraction over a wider area did reduce the effect on *h* at a local scale as can be seen in Figure 3.12, the effect on natural discharge was opposite to expected. The maximum sustainable yield for both 1Bib and 2Bib was lower than their spatially concentrated abstraction equivalents (although the difference between 1Bib and 1Bia was negligible), due to the reduction of *Q*, not *h*.

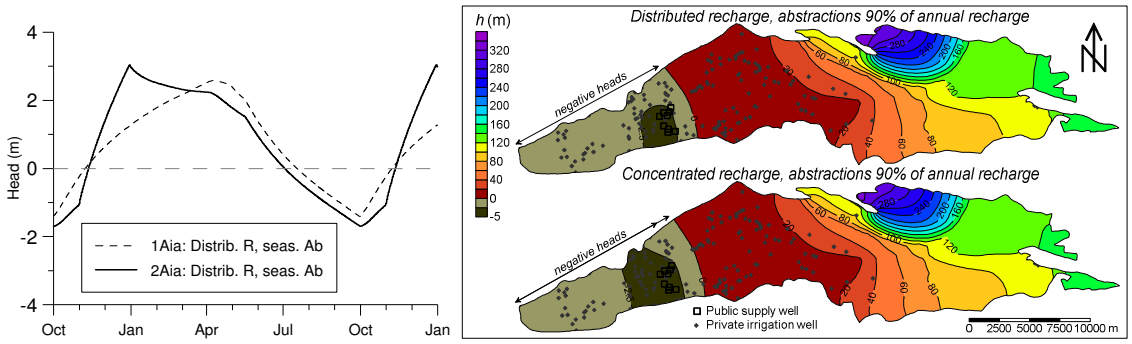

Figure 3.12 Variation of hydraulic head at well 595/215 (left) and spatial distribution of hydraulic head at the end of the dry season (right) for the scenario of abstraction of 90% of mean annual recharge, according to threshold of good quantitative status of the Water Framework Directive; arrows indicate extent of negative h, which is larger when recharge is concentrated (indicated by second arrow)

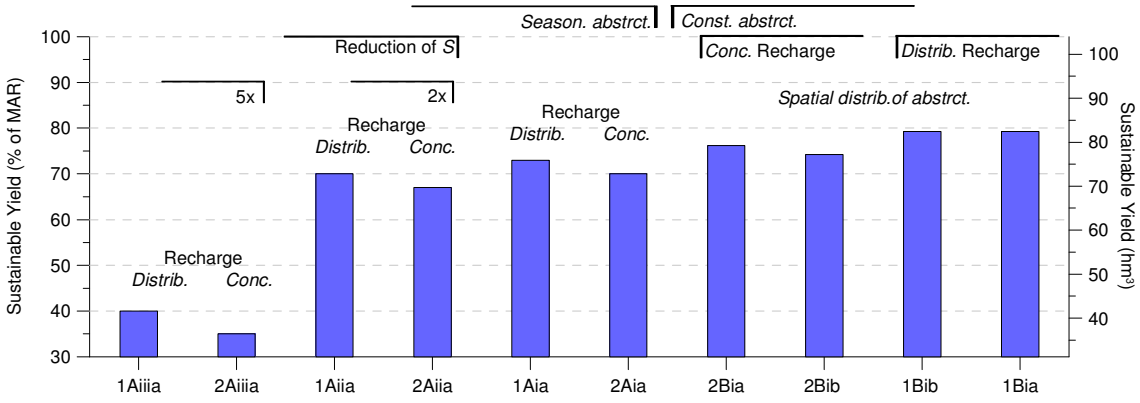

Figure 3.13 Comparison of the effect of values of S, temporal and spatial distribution of recharge and abstraction on sustainable yield.

3.5. Discussion

The simulations of abstraction of 90% of mean annual recharge show that significant seawater intrusion and cessation of freshwater discharge along the Arade estuary would occur, and although water levels recover during the wet season, water quality would be severely deteriorated over a significant part of the aquifer. This shows that it is not sufficient to consider a simple percentage of the mean annual recharge when defining a sustainable yield as it does not take into account the temporal and spatial variability inherent in these systems.

Regarding the temporal distribution of recharge, the results in Figure 3.9 demonstrate that under conditions of concentrated recharge aquifers will likely be more susceptible to negative impacts during droughts than under distributed recharge conditions. This is due to the fact that the concentration of rainfall in a short period of time leads to increased discharge, a loss of water that is not recoverable. One could argue that a higher rainfall intensity could decrease the fraction lost to evapotranspiration and therefore increase recharge. This however depends on the hydraulic conductivity of the soil and unsaturated zone, and its correlation to the degree of saturation, which together with topography, control the amount of surface runoff. In karst systems such as the aquifer of the study area, infiltration can be rapid and recharge can indeed increase with rainfall intensity. This was not considered under the current analysis and these scenarios could thus be somewhat pessimistic. On the other hand, the scenarios also do not consider the predicted future increase in temperature that will contribute to an increase in evapotranspiration rates (Stigter et al 2011a).

One way to mitigate the effect of the concentration of recharge is by increasing abstraction during the wet season, as proven by the scenarios of constant abstraction rates, i.e. where seasonality was removed from pumping. One could argue that in practice, this would be unrealistic, as irrigation and tourism are seasonal activities with higher water demands in the summer. Notwithstanding the truth of this fact, in many cases groundwater is not the only available source and integrated water resource management could use more groundwater in the winter to diminish the pressure on alternative sources such as surface water, an example

that clearly applies to Portugal. The occurrence of higher discharge rates of groundwater during recharge episodes is the main argument for considering groundwater as a valid additional water supply source the whole year round, rather than just in emergency situations such as droughts, when despite higher storage capacities, large volumes of groundwater have already been lost to discharge into rivers or coastal waters.

The model simulations with different values of *S* reveal the large storage capacity of the QS aquifer and the importance of this aspect for the resilience of the aquifer. Higher values of *S* clearly contribute to diminishing the impact of extreme events, and longer periods of drought can be sustained by retaining a larger fraction of recharge in storage. Clearly, aquifers with larger storage capacities will suffer less from the predicted concentration in rainfall in semi-arid regions (Figure 3.10), or from the seasonal impact of pumping.

The location of the pumping wells also determines the impact of groundwater abstractions on hydraulic heads and discharge rates. As was shown in Figure 3.14, the localised effects of abstraction on *h* are reduced by dispersing the location of public supply wells, although the effect on discharge rates (and therefore, in this case, sustainable yield) is inverted. This is likely due to that under the spatially distributed simulations abstraction is occurring closer to the discharge area and therefore having a more significant effect on discharge rates. The impact would naturally be greater if groundwater were to be pumped solely from the public supply well field and it would also increase in aquifers with lower storage capacities. This matches results obtained by Zhou (2009) which showed that the pattern of distribution of pumping had marginal effect on the dynamic development of capture and no effect on the water balance once a new equilibrium was obtained. However, in order to reduce localised effects, a more even distribution of pumping wells for public supply could be considered following a cost/benefit analysis, although probably not to the extent applied in the theoretical scenario presented here. Of note is the effect of seasonality of recharge on augmenting the reduction of discharge caused by the spatial distribution of abstraction. This can be seen in the difference between sustainable yields obtained for 2Bia and 2Bib and between 1Bia and 1Bib in Figure 3.13.

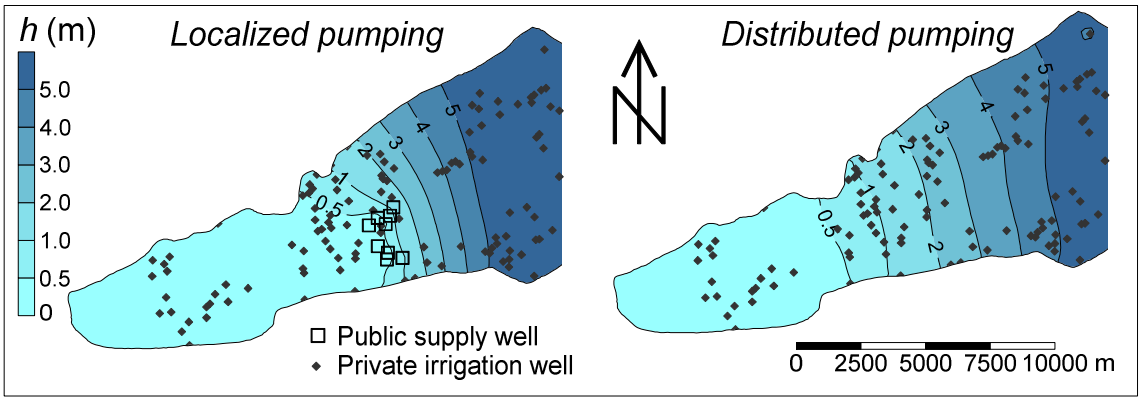

Figure 3.14 Comparison of the effect of the spatial distribution of abstraction for public supply on the distribution of *h* in the discharge sector of the Querença–Silves aquifer.

Although concentrating the location of pumping wells resulted in higher sustainable yield, the increased drawdown seen in these scenarios could have a significant effect on the location of the fresh-saltwater interface in a coastal aquifer such as the QS. This could lead to the salinization of deep wells and boreholes, making them unfit for abstraction for irrigation and public supply. In fact the location of this interface could also be applied as criteria in determining sustainable yield, will have an impact on the quality of groundwater and therefore influence the depth and location of practical abstraction. A density-driven flow model is currently in development and will contribute to analyzing these issues.

3.6. Conclusions

Sustainable yield is defined as the development and use of groundwater resource in a manner that can be maintained for an indefinite time without causing unacceptable environmental, economic, or social consequences. Much of the difficulty in determining this yield is related to identifying these impacts and defining acceptable limits. Once these limits have been defined the challenge is to link the predicted changes of groundwater levels and flows to the impacts on ecosystems and social benefits. Notwithstanding, the natural recharge alone cannot determine the sustainable yield; the impacts of the dynamic development of the capture must be assessed.

The influence of four factors on the determination of sustainable yields were analysed: i) aquifer properties ii) temporal distribution of recharge iii) temporal distribution of

groundwater pumping and iv) spatial distribution of pumping wells. By developing hypothetical scenarios with a numerical flow model it was demonstrated that the sustainable yield is dependent on the spatial and temporal distribution of abstraction and recharge. As well as that the storage coefficient of the aquifer has an important role in determining the resilience of the aquifer and therefore how intensely it is influenced by extreme events. Furthermore, the analysis of the effect of spatial distribution of abstraction showed that the magnitude of the effect of a factor on sustainable yield is dependent on the limit and/or indicator selected as a threshold for unacceptable impact.

For the purpose of this paper sustainable yields for the QS aquifer were considered to be those which did not cause an inversion of gradient and/or salinization of the estuarine springs. Sustainable yield under current climate and abstraction conditions was estimated at approximately 73% of mean annual recharge; significantly lower than the 90% of mean annual recharge criteria suggested by INAG (2005). Scenarios which take into account predicted changes in climate for the region indicate that, if no changes are made to abstraction regimes and rates, sustainable yield would drop to circa 70% of mean annual recharge. However, results indicate that a water management scheme which implements a temporal optimization of groundwater abstraction, perhaps to complement the use of surface water, could significantly raise the sustainable yield.

It must be highlighted that the obtained results are specific to the criteria and conditions considered in this paper. Moreover, sustainable yield is not merely a hydraulic result but the result of a series of agreed upon bounds on the level of changes that are acceptable in a given physical, environmental and social context that is susceptible to change. Once the changes in groundwater levels and flow can be linked and quantified to their social and environmental impacts, numerical models become invaluable tools in determining the sustainable yields, and in the process of optimizing proposed development scenarios.

4. Optimizing temporal scale for sustainable aquifer exploitation – the case of the *Querença-Silves* aquifer[3]

The numerical model described in the previous chapter is applied here to assess the impact of the time-scale at which sustainable yield is defined, in order to maximise groundwater use with minimum impacts. The analysis focuses on maximizing groundwater abstraction whilst minimizing the effect on natural groundwater discharge from the Querença-Silves coastal aquifer. The description of model development and the hydrogeology of the case study area can be found in Chapter 3.

4.1. Introduction: Dynamic Sustainable Yield

Maimone (2004) points out that the idea that there exists a single, correct sustainable extraction rate for a given system is inaccurate and thus sustainable yield must be defined for a specific period of time. It must be recognised that yield varies over time along with the conditions which influence it (Sophocleous 1997). Most recent attempts to determine maximum sustainable yields have made use of optimization-simulation techniques in order to establish the optimal abstraction rates for specific criteria of sustainability (Das and Datta 2001; Shiau and Wu 2007; Yin et al 2010; Roumasset and Wada 2010; Kang et al 2011), generally based on long-term averages or annual values. In a few cases a smaller time scale has been considered (Yin et al 2010; Peralta et al 2010; Kang et al 2011). Rejani et al (2008) retroactively determine the optimal distribution and monthly pumping rates for a specific time period. Shiau and Wu 2007, Yin et al (2010) and Sedki and Ouazar (2011) take into account the (four-) seasonal variation of maximum sustainable yield for representative average, wet and dry years. The defined sustainable yield in all of these cases ends up being based on historical averages and generally aimed at reducing and/or avoiding overexploitation by defining a single maximum value which is guaranteed not to cause

[3] The following chapter is adapted from **Hugman** R, Stigter TY, Monteiro JP (2013) The importance of temporal scale when optimising abstraction volumes for sustainable aquifer exploitation: A case study in semi-arid South Portugal. J Hydrol 490:1–10. doi: 10.1016/j.jhydrol.2013.02.053.

negative effects. However in regions where there is significant inter- and intra-annual variability, such as the Mediterranean, a single value of sustainable yield may not accurately represent the amount of groundwater available to be sustainably abstracted. Applying sustainable yields based on historic averages and not taking into account the variability inherent in these systems may in fact lead to an underestimation of sustainable yield and consequent freshwater loss through discharge.

Maximising the amount of an available freshwater resource is fundamental in regions where this resource is scarce, including Mediterranean regions such as Southern Portugal. Current climate change studies are predicting short-term shifts in seasonal distribution and an increase in inter-annual variability of rainfall in Mediterranean regions (Giorgi 2006; Santos and Miranda 2006; Stigter et al 2014). More specifically, rainfall is predicted to be concentrated in the winter, with significant reductions in spring and autumn. On an inter-annual basis, extreme events (high rainfall and droughts) will be more frequent. Hugman et al (2012) have shown that this increase in seasonal variability can lead to larger freshwater loss during the wet season, in particular if groundwater abstraction is largely concentrated during the dry months, which is often the case.

For the current study, a numerical finite element groundwater flow model for a case study in the south of Portugal is used to run a number of so-called transient cyclic state scenarios where the abstraction rates for public water supply are determined for various time-scales (ranging from daily to annual) as a fixed percentage of the recharge during the previous time-period. The purpose is to understand the effects and feasibility of defining groundwater abstraction rates at various time scales in integrated water supply systems to maximize sustainable yield and minimize freshwater losses.

4.2. Methods

The description of model development and the hydrogeology of the case study area can be found in the Chapter 3. The following sections describe the theoretical scenarios applied in the current analysis.

4.2.1. Transient cyclic state scenarios

Transient cyclic state scenarios were used to compare the effect of considering different time scales when determining sustainable yields. To simplify this theoretical exercise, it was only performed using the public supply wells, i.e. irrigation activities and their inherent seasonality were not considered in this case. Each scenario considered different time scales when calculating abstraction rates and timings, as shown in Table 4.1. Time scales were 1 day, 1 month, 3 months, 6 months and 1 year. Abstraction rates at public water supply boreholes for each time period (i.e.: day, month, 3 months, etc.) were calculated as 70% of total recharge during the previous time period. This value was derived from Hugman et al (2012) who showed that, under current climate conditions and pumping regimes, an abstraction rate of approximately 70% of mean annual recharge would be sustainable for the specific criteria of not causing gradient inversion at the border with the estuary. This "no-inversion" criterion is closely linked to that of continuous freshwater discharge into the estuary, thereby avoiding salinization of the estuarine springs at the end of the dry season, to preserve the current ecosystem status described by Silva et al (2012). 70% of mean annual recharge corresponds to a sustainable volume of approximately 70 $hm^3.yr^{-1}$, which coincidentally is roughly the average annual volume of water supplied by the Water Utility for public consumption in the Algarve region between 2008 and 2010 (Figure 4.1).

Two variants of temporal distribution of recharge were developed (Table 4.1): (a) recharge for the hydrological year (October to October) of 2007/08; and (b) recharge for the entire hydrological year of 2007/08 concentrated in the recharge events that occurred during the months of November, December and January. Variant (a) is representative of an average hydrological year, with recharge spread over eight months, whilst variant (b) represents predicted changes in seasonal distribution with the same amount of recharge concentrated in less time.

Table 4.1 Description of scenarios used to compare the effect of considering different time scales to determine pum ping rates on sustainable yield.

Scenario		Recharge	Time scale	Abstraction rates for public water supply	Irrigation
Transient cyclic-state	**a**	Cyclical recharge for the hydrological year (Oct to Sept) of 2007/08.	1 day	70% of recharge during the previous **day**	n/a
			1 month	70% of recharge during the previous **month**	
			3 months	70% of recharge during the previous **3 months**	
			6 months	70% of recharge during the previous **6 months**	
			1 year	70% of recharge during the previous **year**	
	b	Cyclical recharge for the entire hydro-year of 2007/08 concentrated during Nov-Jan.	1 day	70% of recharge during the previous **day**	n/a
			1 month	70% of recharge during the previous **month**	
			3 months	70% of recharge during the previous **3 months**	
			6 months	70% of recharge during the previous **6 months**	
			1 year	70% of recharge during the previous **year**	
Hypothetical abstraction (2001-2009)		Estimated recharge from October 2001 to September 2009.	1 day	40% of recharge during the previous **day**	31 hm^3.yr-1 from mid-May to the end of September
			1 month	40% of recharge during the previous **month**	
			3 months	40% of recharge during the previous **3 months**	
			6 months	40% of recharge during the previous **6 months**	
			1 year	40% of recharge during the previous **year**	
			5 years	40% of recharge during the previous **5 years**	

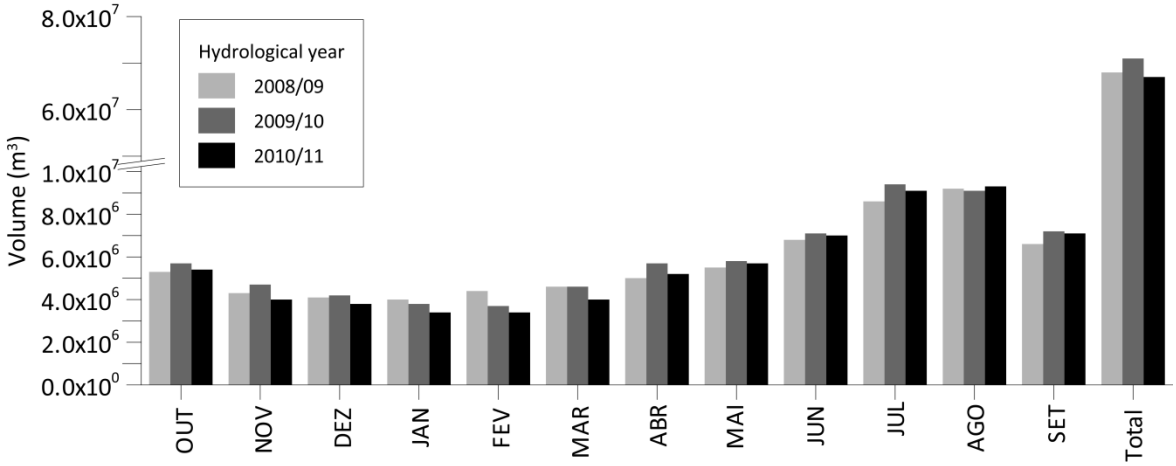

Figure 4.1 Monthly volumes of public water supp lied by the Water Utility to the region of the Algarve (AdA, 2012).

4.2.2. Hypothetical abstraction scenarios

In a subsequent phase, pumping rates for the same time scales were determined for the period between October 2001 and September 2009 based on observed rainfall data, and applied to the existent numerical model of this period. An additional time scale of five years was included, in which the withdrawal rate is based on the average of the five previous

years, in order to analyse the effect of not accounting for inter-annual variations in recharge (i.e. this scenario corresponds to a non-interactive water supply management). To make the current analysis more realistic (less theoretical), real estimated abstraction rates for irrigation (31 $hm^3.yr^{-1}$, c.a. 30% of mean annual recharge), distributed over a period from mid-May to the end of September, were maintained. In order to accommodate for this withdrawal volume for irrigation, public supply pumping rates were calculated as 40% of the recharge (instead of 70%) during the previous time period (Table 4.1). For the shorter time-scale, i.e. day and month scenarios, this means that abstraction for public supply mainly occurs outside the irrigation season (in autumn and winter), which is not the case for the longer time-scale scenarios.

Results were compared to calibrated simulations that consider actual withdrawal rates for irrigation and public supply. The goal of this exercise is twofold: i) see how much more groundwater could have been abstracted from the QS aquifer in the period 2001-2009 whilst confirming to the proposed sustainability criteria, thereby reducing the pressure on the surface water reservoirs and avoiding the disruption of the water supply system during the drought of 2005; ii) study the effect of different time scales on volume and timing of abstractions and the consequences for the status of the aquifer and dependent ecosystems, in response to the requirements of European Union (EU) Directive 2000/60/EC, known as the Water Framework Directive.

4.3. Results and Discussion

4.3.1. Transient cyclic state scenarios

Results for all scenarios are compared based on variations of hydraulic head at piezometers 595/215 and 597/211. Hydraulic head at monitoring point 595/215 demonstrates a good correlation with the variation of storage in the aquifer system (Figure 4.2Figure 4.3) and is therefore considered to be a good indicator for the state of the aquifer system. Hydraulic head at monitoring point 597/111 was included in order to observe the effect of the abstraction scenarios on the eastern sector of the aquifer system. Figure 4.3 shows the variation of hydraulic head simulated for the various time scales under scenario (a) and

scenario (b). The temporal distribution seen in the six-monthly time scale scenario is similar to that seen currently, with most of extraction occurring during the dry months and lowest values occurring at the end of September. This matches the current situation of higher extraction for irrigation and public water supply during the spring and summer months.

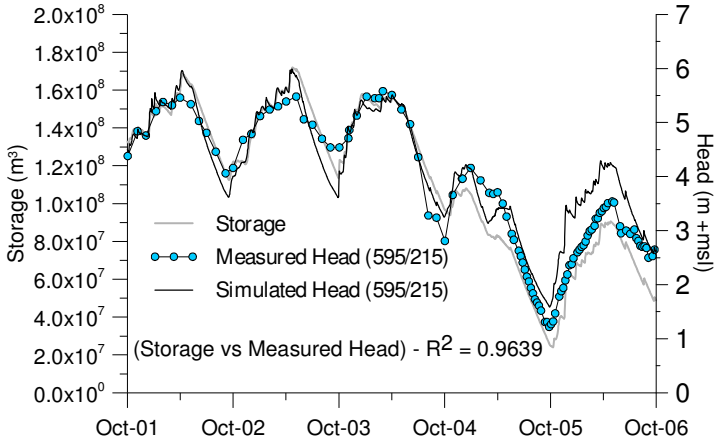

Figure 4.2 Observed and simulated hydraulic head at piezometer 595/215 and simulated storage of the QS.

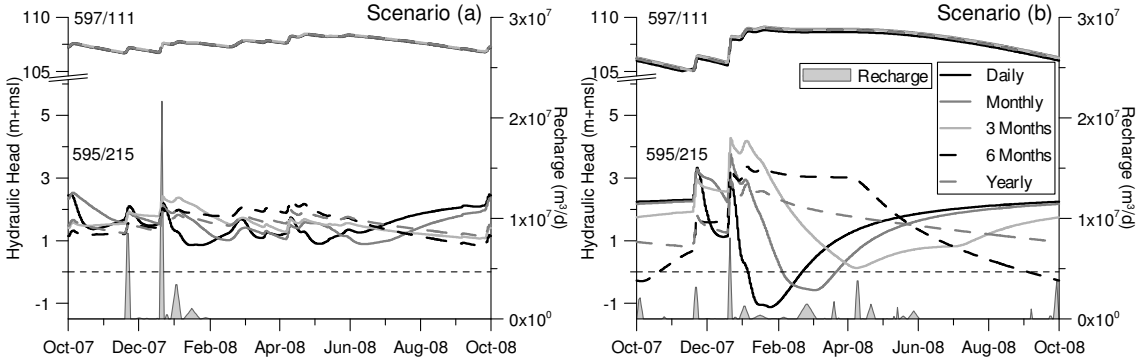

Figure 4.3 Variation of hydraulic head at piezometers 595/215 and 597/111 for the hypothetical abstraction rates considering current temporal distribution of recharge (scenario a, left) and considering predicted temporal distribution of recharge (scenario b, right)

Daily and monthly time scale scenarios both show sharp declines in hydraulic head during the wet months and a rise during the dry summer months at observation point 595/215. Scenarios which consider time scales larger than three months do not show this behaviour at this observation point, with hydraulic head declining during the dry months and less significant drops during the wet months. However variation of hydraulic head at observation

point 597/111 is the same across all time-scale scenarios. This effect is due to the location of the public supply wells in the south-western corner of the aquifer, near the main natural discharge area. In effect the shorter time-scales (daily and monthly) lead to high pumping rates during short pulses (i.e.: shortly after it rains) which captures the direct recharge in the south-western area, but mainly removes water from storage in this area and therefore has a significant effect on hydraulic head at 595/215. Subsequently, recharge that occurred in the eastern sector of the aquifer causes storage and hydraulic heads to recover in the west. On the other hand, longer time scales (particularly three and six months) lead to the recharge that occurs in the south-western area being lost as discharge, and the subsequent slow recharge being captured during the following months.

Lowest minimum hydraulic heads at observation point 595/215 are seen for daily, monthly and six-month time scales. For the two shorter time scales this is due to the characteristics of the public supply well (concentrated in space, relatively to the entire aquifer where recharge takes place) and those of the abstraction regime (concentrated in time). In the case of the six month time scale this is due to the temporal discrepancy between the occurrence of recharge and abstraction, with most of the abstraction occurring in the dry season, when a significant volume of recharge has been lost to natural discharge. Yearly time scale leads to hydraulic heads which are continuously closest to the average, although they also lead to declines during the dry months. Although this time scale seems to have the least impact, it represents an inefficient use of the freshwater resource, with high groundwater losses during the wet months.

Although the net yearly balance of all time scales in these theoretical scenarios are equal, shorter (daily and monthly) time scales lead to higher groundwater levels during the dry summer months. Consequently they also lead to enlarged freshwater losses during the summer. It can be argued that concentrating abstraction during the wet period, rather than during the dry period, would be more efficient and allow for recovery and a potential buffer if for any reason more groundwater would be needed due to drought or high demand. Moreover, lowering the hydraulic potential of an aquifer in the recharge season involves lower risks of possible negative consequences such as seawater intrusion or drying up of

springs and streams, due to a higher potential for recovery. The latter is also visible in scenario (b). The sharp declines in hydraulic heads at 595/215seen for the daily and monthly time scales are significantly more intense than in scenario (a), resulting in gradient inversions, although they recover rapidly. This demonstrates that the use of a fixed percentage of recharge to define maximum abstraction rate for a given time period is an inadequate method with which to determine maximum sustainable yield, and that it should be target based, such as a minimum discharge rate, water level and/or water quality standards. Based on such a target condition abstraction rates could be adapted at adequate intervals, to permit maximum withdrawal rates without causing undesired impacts. The recovery during the dry months indicates that overexploitation during the wet months, though it should be avoided, will likely lead to less severe negative effects than overexploitation during the summer, due to the protective buffer of storage which is significantly depleted after the winter. The six-monthly and yearly time scale scenarios have a similar though more pronounced behaviour to their equivalents in scenario (a): hydraulic heads reach lower values (and cause gradient inversion in the case of the six-monthly time scale scenario) due to a larger amount of recharge being lost to discharge caused by the concentration of recharge in a shorter time period. Unlike in scenario (a), the three-monthly time scale in scenario (b) shows a rise in hydraulic heads during the dry months. This is due to the longer dry season resulting in the cessation of abstraction in scenario (b), thus allowing heads to recover. The latter does not occur in scenario (a) as the dry season is too short.

The plot of cumulative abstracted volumes for each time scale for any given year in scenarios (a) and (b), shown in Figure 4.4, gives a clear image of the temporal distribution of abstraction for each time-scale. Figure 4.4 highlights that daily and monthly time scales for scenario (a) and additionally the three-monthly time scale for scenario (b) result in periods of no abstraction during the dry season. Taking this into account alongside the results shown for hydraulic head for the same scenarios (sharp declines during wet season with recovery during dry season) it shows that applying a single maximum value of percentage of recharge as an abstraction rate at a single time scale does not lead to the best solution for the QS aquifer. In addition, it should be noted that abstraction rates for the daily time scale scenario

are entirely unfeasible based on the pumping capacity at the municipal well field, so that this scenario is theoretical. Moreover, given the seasonality of water demand for irrigation and public supply (further enhanced by tourism), if no alternative water source would be available, such short time-scale abstraction regimes would be completely unfeasible. However, as will be discussed in the following section, in this area surface water reservoirs do provide a solid alternative (they currently in fact supply most of the drinking water). In addition, for systems with lower storage capacity, such as several smaller karst aquifers found in the Algarve region (Stigter et al 2009), short time scale abstraction regimes would likely be necessary, as recharge is rapidly lost through discharge.

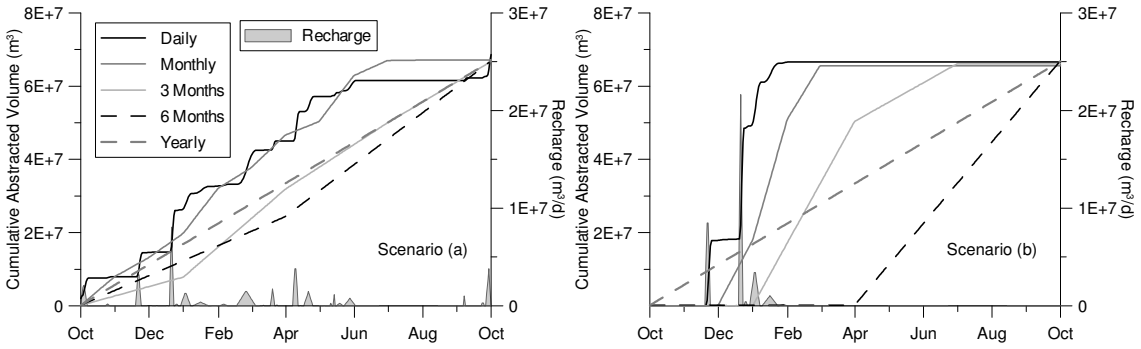

Figure 4.4 Cumulative abstracted volumes per cyclical year of the considered time scales for scenario a (left) and scenario b (right).

Abstraction rates need to take into account how the system reacts to recharge (for example when recharge reaches the well fields); therefore pumping schedules should be defined on the same time scale as the aquifer system's variation in order to maximise the sustainable yield. However, as was shown in Figure 4.3 the aquifer system does not work on a single time scale, with recharge from different areas of the aquifer reaching well-fields at different times, which makes defining the optimal time scale as well as the maximum sustainable yield a complex task. The optimal solution would be to have a monitoring network coupled to a numerical simulation-optimization model able to determine real-time estimates of maximum sustainable yield. In practice this is not yet feasible. A reasonable compromise would be to define an acceptable time scale for which to determine sustainable yields. Gleeson et al (2012) refer that for groundwater systems with a short residence time, the mean residence time is a good starting point for discussing planning horizons. There are

currently ongoing efforts to determine residence times for the QS aquifer using tracer tests. These studies should complement the analysis presented here and help to determine an optimal time scale for management of this system.

The QS aquifer offers an interesting case due to the location of most of the abstraction relative to the main recharge areas, which leads to the time-lag of several months for most of the recharge to reach the well fields. As is seen in particular in scenario b for the daily, monthly and three-monthly time scales, hydraulic head is still rising slightly five to six months after the last recharge event, which shows the significant storage capacity of the QS aquifer. This could allow for pre-emptive planning of pumping schedules and rates taking into account actual recharge events, leading to both an increase in efficiency of use of the renewable resource which is fresh groundwater, whilst also minimizing the risk of overexploitation during droughts.

As discussed by Gleeson et al (2012) and Holman and Trawick (2011), making the best use of available resources is, obviously, beneficial for the sustainable development of groundwater resources. Amongst other measures, Holman and Trawick (2011) suggest offsetting the timing of peak demand and timing of least resources. This principle could be applied to the QS by offsetting demand on surface water sources by using alternative groundwater sources for supply. Gleeson et al (2012) go on to underscore the need for an adaptive management, able to adjust to changing conditions in order to reach long term sustainability goals. Such a management scheme would be more robust and able to cope with an uncertain environment, and it would need to be adjusted at the optimal time scale for a given aquifer system in order to maximize its efficiency.

4.3.2. Hypothetical abstraction scenarios

Figure 4.5 presents total annual abstraction volumes resulting from the pumping schemes determined for each of the considered time scales from October 2001 to September 2009, as compared to measured withdrawals by *AdA* (the Water Utility) during the same period. Values of estimated yearly recharge are also shown. As is to be expected, intra-annual (daily, monthly, three-monthly and six-monthly) time scale abstractions result in similar annual

volumes, which follow inter-annual variations in recharge. Annual time scale pumping follows the same distribution, but with a one-year time lag, whilst the five year time scales result in abstraction volumes without correlation with inter-annual variations. All hypothetical scenarios result in significantly higher annual abstraction volumes than measured for all years except during the drought year 2004/05. One-yearly and five-yearly time scales lead to a higher total abstracted volume during the entire eight year period than the remaining time scales. This is due to the fact that (due to their larger temporal extent) abstraction rates are determined based on recharge values from previous years (2000/01 in the case of 1 year time scale and 1996/97 to 2000/01 for 5 year time scale). As the recharge during these previous periods was larger than that during the periods covered by the remaining time scales, total abstraction rates become higher.

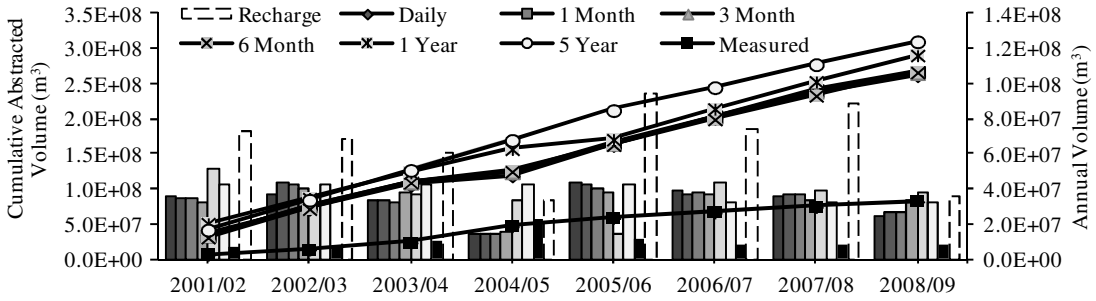

Figure 4.5 Cumulative and annual abstracted volumes determined at the various considered time-scales (time scale of the columns increases from left to right) and actual volumes abstracted by the AdA Water Utility and from municipal wells during 2001–2009; also shown are values of estimated yearly recharge.

Effects of the hypothetical pumping rates calculated for the period of 2001 to 2009 for the different time scales, are compared with calibrated simulations of actual pumping rates for the same period in Figure 4.6. Up to a six-monthly time scale, variations in hydraulic head show that their seasonal amplitude increases with the length of the time scale used to determine pumping rates. This is explained by the fact that for the shortest (daily and monthly) time-scales abstraction for public supply occurs in the wet seasons (autumn and winter), capturing groundwater and keeping heads relatively low (or attenuating their rise), whereas in the spring and summer seasons, groundwater is only withdrawn for irrigation, not for public supply, avoiding larger drawdown. Irrigation was considered in these runs to

make the application more realistic, as it will be difficult for farmers to obtain water from an alternative source, despite the ongoing debate on the reuse of treated wastewater (Costa 2006). Increasing time-scales cause greater shifts between the timing of abstraction for public supply and that of recharge. The most extreme scenario, provided by the six-monthly time-scale, results in all abstractions, for public supply and irrigation, concentrated in the spring and summer months. This scenario, currently in practice, basically corresponds to the philosophy of groundwater as a strategic resource to be used exclusively in the dry season. The simulations show that this scenario results in the largest amplitudes of variations of hydraulic head, indicating a larger amount of freshwater loss (mainly in autumn and winter), as well as the lowest minimum values, with lower storage at the end of the simulation period. The high oscillations in discharge in this scenario, with high peaks in the winter and near-zero discharge in the summer, contrast with those of the one-monthly time scale scenario, where discharge is much more constant. This clearly reveals that for the QS aquifer shorter time scales lead to a more sustainable exploitation, also in terms of environmental flows, with potential for higher sustainable yields.

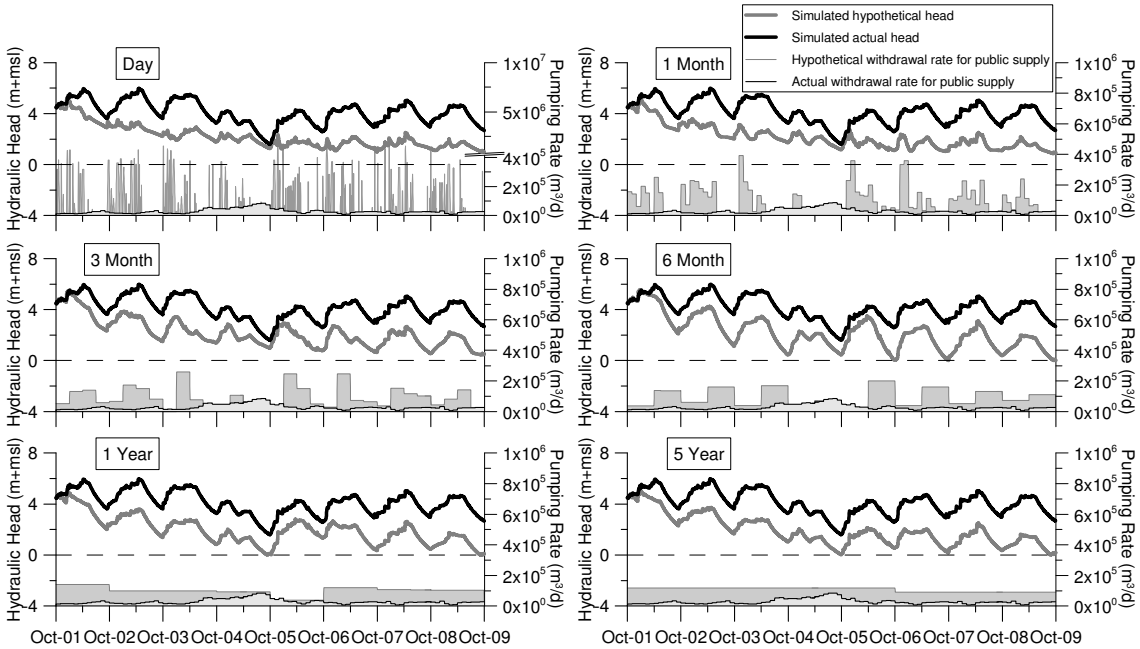

Figure 4.6 Variation of hydraulic head at piezometer 595/215 for the considered hypothetical maximum abstraction scenarios; extractions for irrigation during spring and summer months are considered in the model, but not represented here.

Increasing the time scale to a year and longer mostly reduces the amplitude of variations again, as some of the seasonality of abstraction is removed and a single pumping rate for public supply is maintained all year round. Notwithstanding, these time scales do not take into account the intra-annual variability and therefore may lead to larger losses of freshwater during the recharge season than shorter time scales. Coupled with the results of Hugman et al (2012), which showed that discharge is accelerated during recharge periods, these results show that the current concept of using aquifers in the Algarve exclusively for storage during the winter is not the most adequate in terms of maximising the use of available freshwater, as a significant fraction can be lost before it is needed. Vieira et al (2011) show, by creating a water allocation optimization model, that an integrated water resource management in the region, with interannual planning time horizons, can help to cope with future shortages, by positively enhancing the conjunctive use of the different system water sources.

Although hydraulic head and discharge rates in all hypothetical scenarios are continuously lower than actual values due to hypothetical abstraction rates being largely superior to actual abstraction rates, they show a stabilizing trend following the drought of 2004/05. Up to three-monthly time scales, discharge and head values for that year are approximately equal to those observed. This is achieved with significantly lower abstraction rates (circa 35% or 8 hm^3, see Figure 4.5) during 2004/05 for the hypothetical scenarios, which highlights that the method applied to determine sustainable yield leads to lower maximum sustainable yields for public supply during time periods when water is needed the most. It should be noted however that these short-scale scenarios show that much larger volumes of water (400% or 75 hm^3) could have been abstracted during the previous three years when merely considering gradient inversion as a sustainability criteria.

It must be kept in mind that the values shown here are considered to be sustainable yields considering the specific criteria of non-occurrence of inversion along the Arade estuary boundary and do not take into account any other potential effects of the pumping regimes. When defining the sustainable yield it is important to take into account all the effects of pumping. For example in the current case, if the limit for acceptable impact was solely

defined based on the natural discharge rate then, although the simulated scenarios would be considered to be sustainable, they would not take into account the drawdowns that occur in the northern areas of the aquifer system. Figure 4.7 exemplifies this with the difference between simulated hydraulic head at the end of September 2009 with abstraction rates based on a monthly time scale and actual abstraction rates. These drawdowns would likely have an effect on the aquifer-stream interactions, and subsequently on the ecosystems which depend on them, though it is currently not clear to which extent. On the other hand, they could also enhance recharge from the streams carrying water from runoff from the little permeable Paleozoic schists and greywackes upstream, through infiltration in the streambeds. This is presently already an important phenomenon that is being studied in more detail (Salvador et al 2012).

The location and depth of fresh-saltwater interface in a coastal aquifer such as the QS could also be applied as criteria in determining sustainable yield, as it will have an impact on the quality of groundwater and therefore influence the depth and location of practical abstraction. Of course, this kind of water supply management would only be feasible where an alternative water source exists, as is the case in the Algarve, where large surface water reservoirs currently supply most of the drinking water to the region. Although both these sources are subject to the highest pressures at the same time (i.e.: summer and/or drought), these scenario calculations show that a more efficient water resource management would be possible by coordinating the use from both sources. More groundwater could be abstracted for public supply during the winter months (mixing it with a smaller amount of surface water, reducing treatment problems derived from higher turbidity in surface waters and benefiting from the groundwater's natural hardness), avoiding large depletions of the surface water reservoirs. This would create a source of public supply during the dry season, when groundwater would largely be used for irrigation.

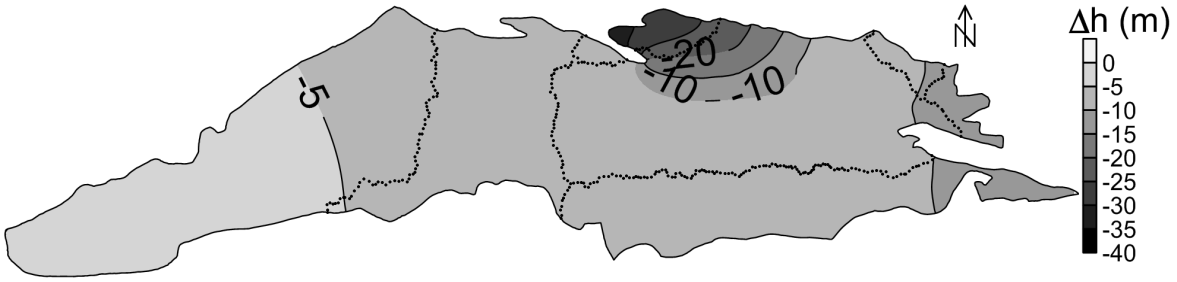

Figure 4.7 Difference between simulated hydraulic heads at the end of September 2009 with maximum abstraction rates based on a monthly time scale and simulated heads in the same period with measured abstraction rates.

Apart from the issues of availability, there are also technical issues of the feasibility of pumping at such high pumping rates. For the daily scenarios pumping rates would not be viable at the present public supply well field. Moreover, representing the karstic nature of the QS aquifer with a single continuum equivalent porous media model, whilst adequate when representing flow at regional scales, may result in significant uncertainty when simulating smaller scale effects such as locations of well fields. Apart from spatial scales, equivalent porous media models do not represent the dual nature of flow in a karst aquifer. To properly quantify time scales for an aquifer such as the QS aquifer, although an equivalent porous media model is adequate, a discrete continuum model would allow for a more detailed comprehension of the various time scales at which the aquifer works.

4.4. Conclusions

Sustainable yield must be defined based on a "target condition", not just a regional water budget, and is dependent on the spatial and temporal dynamics of the systems response to influencing factors such as recharge and pumping. In practice, most efforts to determine sustainable yields define a single value based on long-term averages or annual values of recharge. However, in particular in areas with high seasonal and inter-annual variability such as Portugal, these time scales are too coarse for the systems to which they are being applied and can lead to over- as well as under-exploitation.

The effect of adapting pumping rates based on recharge occurring during the previous time period at several temporal scales was analysed. By developing hypothetical scenarios with a

numerical model it was demonstrated that defining a single value based on long term averages does not give an accurate value of sustainable yield. Results show that, for the carbonate rock aquifer of QS, reducing the time scale at which abstraction rates are adapted allows for an increase in withdrawal volumes without surpassing the here considered sustainability criterion of non-occurrence of gradient inversion along the Arade estuary. In fact, not reducing the temporal scale leads to an irretrievable loss of freshwater during recharge periods. Furthermore, scenarios show that predicted seasonal changes in rainfall for the south of Portugal will make taking the temporal scale of the system into account more important, as the concentration of recharge into a shorter period will lead to faster depletion and therefore larger freshwater loss.

Currently groundwater in the Algarve is mainly used for irrigation. Results show that a significant part of annual recharge of the QS aquifer is lost through discharge during the winter which could be used for public water supply allowing water in dams to be conserved for use during the summer. Taken together with the predicted increase in water demand and decrease in availability due to climate change, this is a strong argument in favour of an integrated and adaptive water management scheme for the region, leading to a more robust water supply system within a climate of increasing uncertainty in regards to the availability of freshwater.

5. Numerical modelling assessment of climate change impacts and mitigation measures on the Querença-Silves coastal aquifer (Algarve, Portugal)

Continuing the numerical assessment of the Querença-Silves, the following chapter discusses the development and application of a density-coupled flow and transport model to assess the impact of climate change on seawater intrusion in this coastal aquifer. Several adaptation measures are assessed and once again the issue of defining sustainable yield is addressed, this time taking into account seawater intrusion. Some comparisons between the previously discussed flow model and the density-coupled model are made, to highlight their respective applicability and advantages.

5.1. Introduction: Climate Change and Seawater Intrusion

SWI in coastal aquifers is a common problem in areas where water supply is dependent on groundwater (Custodio 2002) and is often particularly severe in semi-arid and arid areas where recharge is low (Abarca et al 2007). The balance between freshwater and saltwater can be disrupted by natural (e.g. droughts/floods) or anthropogenic causes (e.g. abstraction, soil impermeabilization), which can cause seawater to move toward or away from land. Concern over climate change has stimulated research on the expected impacts on groundwater systems during the last few years, reviews of which can be found in Green et al (2011) and Taylor et al (2012). The impact of climate change on seawater intrusion has mostly been focused on theoretical studies of boundary condition (BC) controls on SWI processes using simplified numerical and analytical models (e.g. Werner and Simmons 2009; Watson et al 2010; Chang et al 2011; Ferguson and Gleeson 2012; Chang and Clement 2012) and site specific assessments (e.g. Carneiro et al 2010; Payne 2010; Oude Essink et al 2010; Rozell and Wong 2010; Loáiciga et al 2012; Sulzbacher et al 2012; Rasmussen et al 2012; Green and MacQuarrie 2014). These studies mostly carry out simulations for a range of combinations of predicted sea-level rise (Loáiciga et al 2012), change in recharge (Carneiro et al 2010; Payne 2010; Rozell and Wong 2010; Green and MacQuarrie 2014) and surface water elevation(Oude Essink et al 2010; Rasmussen et al 2012) applying average long-term values without considering inter-annual or seasonal variability. However, Michael et al (2005) have shown that seasonal recharge causes the fresh-saltwater interface to oscillate seasonally, may account for a large component of SGD in areas of the world with significant

seasonal cycles in net recharge. Yet, few or no studies have taken into account the impact of expected changes in recharge regimes on SWI and SGD.

Studies of the impact of climate change incorporate several sources of uncertainty: carbon dioxide emission and socioeconomic scenarios (IPCC 2014), selected circulation models and applied downscaling methods (Holman 2006; Jackson et al 2011). Error inherent to methods used to translate climate data into runoff or recharge (e.g soil water balance models, 1-D variably saturated flow models and empirical relationships) can introduce further uncertainty, as they can respond differently to temporal variations in rainfall whilst providing similar long-term averages (Holman et al 2012). In their guide to best practices for groundwater climate change studies, Holman et al (2012) suggest that analyses should include a range of scenarios that take all these sources of uncertainty into account. This of course requires a large number of model runs, which can be problematic when dealing with computationally expensive models required to simulate coastal aquifer dynamics.

Groundwater in the Algarve region (south of Portugal), as in most of the Mediterranean basin, is under growing pressure from the combined effect of rising sea level, reduced rainfall and increasing crop water demand caused by global warming (Giorgi 2006; Santos and Miranda 2006). Water management policy needs to adapt to this changing environment in order to guarantee water supply as well as maintain the sustainability of the resource and other dependent systems. The QS is a coastal aquifer and one of the main sources of freshwater supply for irrigation in the region, as well as serving as a backup to the public water supply system during prolonged droughts (Stigter et al 2009). Stigter et al (2013) and Stigter et al (2014) have shown that climate change will have significant impacts on groundwater levels and spring discharge rates of the this aquifer. Apart from the reduced availability of groundwater for anthropogenic use, changes in discharge to springs and streams will have impacts on sensitive groundwater dependent ecosystems (Silva et al 2012). Previous studies have shown that the intensification of seasonality has a significant effect on the sustainable level of exploitation when considering freshwater discharge to the coast (Hugman et al 2012; Hugman et al 2013b), however so far the impact on SWI has not been extensively explored.

The aim of this study is to determine the potential for SWI in the QS aquifer system for a range of climate change and groundwater use and adaptation scenarios, as well as assess the impact of seasonal variability on the extent of SWI. An ensemble of climate scenarios previously developed by Stigter et al (2014) are applied to a local-scale cross-sectional coupled-density flow and transport model. Results incorporate uncertainty from climate modelling by including input from three climate models, two downscaling methods and two soil water budget methods to determine monthly recharge rates and crop water demand. Innovative aspects include the simulation of seasonal and inter-annual variation and assessment of the impact of changes in recharge regimes on SWI. Identified adaptation measures are subsequently simulated for the worst case climate scenario to determine their relative effectiveness in reducing SWI.

5.2. Materials and methods

5.2.1. Horizontal plane model: regional scale flow

The development and application of the horizontal plane model of the QS is described in Chapters 3 and 4. This model has previously been applied by Stigter et al. (2014) to run an ensemble of climate change scenarios to assess the impact of anthropogenic use on resource availability and groundwater dependent ecosystems. The previously developed climate scenario simulations using the horizontal plane flow model are used here to provide input to a smaller scale density-coupled flow and transport model, as described below.

5.2.2. Cross-section model: density-coupled flow and mass transport

The computational burden of solving this system, and the need for high spatial and temporal resolutions of the finite-element mesh and time-stepping schemes to guarantee numerical stability, often makes the development of large scale three-dimensional models impractical (Oude Essink 2001a). As the western section of the QS is relatively uniform, with little lateral variation, a simplified 2D cross-section representation was considered sufficient to provide a representation of the interaction between fresh and saltwater within the aquifer.

The representation of the flow domain of karst systems as a single continuum equivalent porous media (EPM) is valid when modelling processes at a regional scale (Scanlon et al 2003). At a local scale the presence of fractures and karstic features can have a significant effect on the distribution of flow and transport and require fracture network or dual porosity modelling approaches to be adequately simulated. However, these approaches require a large amount of information on the geometry and hydraulic parameters that can only be obtained in certain cases and is subject to a large amount of uncertainty (Papadopoulou et al 2010). The lack of detailed data, scale of the system and focus on overall assessment of groundwater resources (as opposed to a need for detailed assessment of localized effects of SWI) makes the EPM approach particularly applicable to the current study.

The representative cross-section model extends 23.5 km from the Arade estuary to the S.Marcos-Quarteira fault line, and a further 500 m into the estuary. To simplify construction, the modelled domain was considered to have an average width of 5 km. A three-dimensional geological model of the system, developed by Monteiro et al (2007b) was used to define the lower boundary of the model. The upper boundary was determined from maximum observed head values. A finite-element mesh was generated with 37,412 triangular finite elements and 19,888 nodes. The characteristic length of elements is equal to or less than 20 m to guarantee numerical stability. All simulations were run using a Forward Euler/Backward Euler (FE/BE) time integration scheme for automatic time-step control, as recommended for variable density problems by Diersch (2014), with a maximum time-step of one day.

Imposed flow BC (2^{nd} type, Neuman) are used to represent direct recharge from rainfall within the modelled domain and lateral flow from the north-eastern section of the QS system (along the eastern vertical border). Imposed flow rates are obtained from the plane model described in Chapter 3 for both steady-state and transient model runs. Abstraction for irrigation within the modelled domain is distributed across 12 well BCs, roughly scattered according to the spatial distribution of irrigated land; withdrawals for public water supply are grouped into five representative well-fields and imposed on well BCs at the approximate distance of these fields from the estuary.

The estuary is represented with constant freshwater head conditions along the top and lateral limit of the model in the West. Equivalent freshwater head values are determined according to equation (5.1):

$$h_f = h_s + \frac{(\rho_s - \rho_f)}{\rho_f} \cdot (h_s - z) \qquad 5.1$$

in which, h_f is equivalent freshwater head [*L*], h_s is saltwater head [*L*], ρ_s [ML^{-3}] and ρ_f [ML^{-3}] are salt-water density (1025 kg.m^{-3}) and freshwater density (1000 kg.m^{-3}) respectively and z is elevation of the node [*L*] (Diersch 2014).

For mass transport, boundary nodes corresponding to the estuary were assigned a relative chloride concentration value (C_{max} = 1), representing 100% fraction of seawater. A boundary constraint condition, in which the presence of a constant concentration is defined according to the flux direction, was included to allow for the formation of an outflow face. Thus, when mass-flux is positive (entering the system) the constant mass BC is maintained, whilst when it is negative (leaving the system) the concentration is computed and automatically assigned as a flux-BC (Diersch and Kolditz 1998; Diersch 2014). This technique has previously been applied for use in large-scale models (i.e. Kopsiaftis et al. 2009; Nocchi and Salleolini 2013).

Several zones of uniform hydraulic conductivity (*K*) were defined and the ratio between vertical (K_v) and horizontal (K_h) conductivity assumed to be 0.1. An initial approximation of *K* was obtained using a flow model under steady-state conditions and PEST (Doherty 2002) to adequately represent values of average hydraulic head at selected monitoring wells. Subsequently, transport and density effects were included and *K* was refined through trial-and-error. Values of *K* for the various zones are relatively uniform (+\- 100 m.d^{-1}), except for at the discharge area where it was consistently higher (259 m.d^{-1}). Higher conductivity at the discharge area is reasonable in carbonate rocks, which are soluble in water. Groundwater flow may dissolve the limestone, thus increasing the hydraulic conductivity of the aquifer. The amount of dissolution depends mainly on the magnitude of the groundwater flow (Kiraly 1975). As all flow within the QS is channelled through the discharge zone, it is reasonable to assume that this area is subject to the most karsification.

A uniform value (0.00025) for specific storage (S_y) was calibrated by trial-and-error for the period from October 2001 to October 2009. Initial conditions for head and mass were obtained by allowing the model at equilibrium to drain (by deactivating the recharge BCs), until it reached groundwater levels representative of the end of summer in 2001.

There is a lack of data on dispersion parameters for the QS. Values for molecular diffusion (10^{-9} $m^2.s^{-1}$) and longitudinal and transverse dispersivity (20 m and 2 m, respectively) were selected as a compromise between values suggested in the literature for aquifer type and scale (Gelhar et al 1992; Neuman 2005) and finite-element size. Lower dispersivity values lead to increased numerical instability and oscillations in the results, whilst refining the mesh further would lead to a significant increase in computation time. A uniform value of 0.3 was assumed for porosity.

5.2.3. Climate change scenarios

Climate scenarios have previously been developed for the study area by Stigter et al. (2014) as part of larger analysis of the effect of climate change on coastal aquifers in the Mediterranean. These authors obtained temperature and rainfall data from scenarios from the ENSEMBLES project (van der Linden and Mitchell 2009), that result from the combination of a Regional Climate Model (RCM) and a Global Circulation Model (GCM), with a 25x25 km resolution and a balanced CO_2 emission scenario A1b. Three climate models cover the study area and period up to 2100: CNRM-RM5, C4IRCA3 and ICTP-REGCM3. Obtained data was bias corrected using a control period from 1980 to 2010. Two approaches were applied, in order to compare their applicability and include method uncertainty in the results: (1) calculation of anomalies and (2) monthly linear regression between observed and simulated values. Bias-corrected values were then applied to develop total and net (taking into account crop water demand) groundwater recharge scenarios, using the soil water budget. The sensitivity of the results to the choice of soil water budget method was assessed by comparing the results using the Thornwaite-Mather (TM) and Penman-Grindley (PG) methods. The differences between the two methods were not significant when compared to the variability between climate scenarios. Consequently, only the TM soil water budget was used in the subsequent analyses.

An in-depth description of the development and results from these climate and recharge scenarios can be found in Stigter et al. (2014). The multiple combinations of RCMs, bias correction and recharge estimation methods resulted in nine recharge scenarios. Of these, six were selected to be applied in the present study. Calculated total recharge was imposed on the groundwater models as direct recharge. Estimated values of monthly crop water demand (assuming current agricultural area is maintained) was imposed on wells within irrigated areas. Monthly pumping rates measured at public water supply wells during the hydrological year 2006/07 were applied cyclically, so as to replicate the conditions used by Stigter et al. (2014) with the regional scale model. A linear sea level rise of 1 m by 2100 was considered at the seaward boundary. Spatial distribution of head (flow model) and seawater ratio (flow and transport model) obtained from the final time-step of the 2001-2009 model run were used as initial conditions for all climate scenario simulations.

5.2.4. Adaptation scenarios

The following section describes five adaptation measures to increase the QS resilience to climate change. To assess the effect of these measures, simulations are run for a single climate change scenario: ICTP-REGCM3 bias corrected with monthly linear regression (henceforth referred to as ICTP-lin.reg). As will be shown further on, this represents the worst case scenario in terms of freshwater discharge and extent of SWI.

The greatest pressure on groundwater is clearly caused by agriculture, due to both large withdrawal volumes as well as the extensive spatial distribution. The first adaptation scenario considers a decrease in groundwater use for irrigation, which could be the result of a combination of adaptation measures such as decreasing irrigated land, increasing agricultural efficiency or promoting the use of alternative water sources. Two scenarios are considered in which groundwater use for irrigation is decreased by 25% and 50%. A scenario with no groundwater withdrawals for irrigation is simulated to determine the impact of public supply abstraction. Additionally a single model run with no abstraction was also simulated. These last two scenarios are not considered to be realistic adaptation measures, serving merely to determine the impact of reduced recharge and highlight the influence of groundwater users.

The second measure focuses on increasing groundwater supply through managed aquifer recharge (MAR).The on-going FP7 Project, Demonstrating Managed Aquifer Recharge as a Solution to Water Scarcity and Drought (MARSOL) aims to demonstrate MAR as a sound, safe and sustainable strategy that can be applied to optimize water resources management through storage of excess water to be recovered in times of shortage or by influencing gradients. For the QS aquifer, existing large diameter wells would be used to infiltrate surplus water from the large surface water reservoirs currently used for public water supply. Injection and tracer tests have demonstrated the technical feasibility of applying MAR at the location of one such well (Leitão et al 2014; Costa et al 2015b; Costa et al 2015c). An infiltration test demonstrated the capacity to infiltrate 40 m^3 in 20 minutes (equivalent to $1.05x10^6$ m^3yr^{-1}). This does not represent the long-term infiltration capacity, but is so far the only measurement for this site. The MAR site is located close to the Alcantarilha water treatment plant (location in Fig. 1), which is supplied by three large surface water dams. At peak capacity the pipeline can carry $6.74x10^5$ m^3d^{-1}, however at most the treatment plant can process $2.59x10^5$ m^3d^{-1}. The unused capacity of the pipeline could be used to transport surplus surface water to be injected into the QS, thus increasing water storage and reducing the SWI. The amount of water available for MAR will thus be constrained by (1) pipeline capacity and (2) surface water availability. Three adaptation scenarios are simulated with continuous injection rates of 1.05, 5.25 and 10.5 $x10^6$ m^3yr^{-1}.The first is the estimated maximum recharge at the single well site already being studied. The latter two values represent a five- and ten-fold increase of the observed infiltration capacity (and coincidentally correspond to approximately 50% and 100% of withdrawals for public water supply), to assess the potential effect of expanding the site.

The third adaptation measure considered is another potential MAR solution to enhance infiltration from streams that cross the QS. There are two main stream networks that cross the QS: the Meirinho stream (West) and the Alte and Algibre streams (East) (location in Fig. 1). These intermittent streams bring run-off from the low-permeability Paleozoic rocks north of the system, a portion of which contributes to allogenic recharge, with the remainder (along with some additional base flow from the aquifer system) flowing south towards the sea. Infiltration of this excess stream flow could be passively enhanced through the use of

small dams or weirs and increasing the infiltration capacity of the stream bed. Salvador et al. (2012) determined several exponential relationships between average rainfall and the surface water outflow from the area overlying the aquifer taking into account uncertainties in measured stream flow values. These authors estimate that the surface outflow for the Meirinho stream is negligible but average annual outflow from the Alte and Algibre stream network ranges between $16.5x10^6$ $m^3 \cdot yr^{-1}$ and $22.6x10^6$. The most conservative rainfall/surface outflow relationship was applied to the ICTP-lin.reg rainfall series to determine how much excess streamflow could potentially be available for MAR from the Alte and Algibre streams. This relationship may no longer be representative under future climate conditions, however it serves as an initial estimate. A simulation was run considering all the excess as added recharge along the streams, which on average accounts for and additional recharge of $10.9x10^6$ $m^3 \cdot yr^{-1}$.

To study the impact of spatial spreading of groundwater abstractions, the baseline model run using the ensemble of climate scenario simulations was compared to one where the abstraction for public water supply in the QS was concentrated in the AdA (Water Utility) well-field. The baseline model run considers abstraction for public supply from both AdA and Municipal well-fields. This approach does not represent current management practices, but was chosen in order to replicate the simulations by Stigter et al. (2014). Effectively, the distribution of abstraction over several well-fields represents a potential adaptation measure in which the negative effects of exploitation are dispersed (Hugman et al 2012). To study the effect of this measure, a single model run with a public supply abstraction of $9.85x10^6$ $m^3 \cdot yr^{-1}$ (total public water supply withdrawals in the western sector of the QS) applied entirely to the AdA well-field is simulated.

Finally, the fifth adaptation measure is a seasonal distribution of abstraction, by concentrating public supply abstraction during the winter period. As with the spatial distribution, this does not represent current pumping schemes but is representative of a scenario in which the integrated management of surface and groundwater sources of supply allows for a more efficient water resource use. In practice, withdrawals are concentrated during the months in which groundwater levels are already lowest, increasing the risk of

short-term negative effects (e.g. insufficient freshwater discharge to GDEs). Distributing withdrawals over the year, or even concentrating them during the periods of high water levels, not only reduces this risk but reduces the amount of freshwater which would otherwise be "lost" to the sea. This of course raises other issues, such as what to do with unused surface water during the wet season, however the point here is to assess whether reducing the seasonality of abstraction contributes to reducing SWI.

Table 5.1 Summary of simulated adaptation scenarios.

Adaptation measure	Scenario			Δ Abstraction*	Δ Recharge*
Decrease groundwater use	No pumping			-45.5	-
	Irrigation	100% decrease		-35.6	-
		50% decrease		-17.8	-
		25% decrease		-8.9	-
Increase recharge	MAR	Injection in well	C1	-	+10.5
			C2	-	+5.3
			C3	-	+1.05
		Stream infiltration		-	+10.9
Spatiotemporal distribution of public supply abstraction	Spatial	Concentrated (Water Utility well field)			
		Distributed (Water Utility and municipal well fields)			
	Seasonal	Concentrated in dry season			
		Concentrated in wet season			

*average annual change ($x10^6$ $m^3.yr^{-1}$)

5.3. Results and Discussion

5.3.1. 2D cross section model: 2001-2010

The density-coupled model provides a good fit to observed variations in hydraulic head between 2001 and 2009 (Figure 5.1). Results provide an improvement on previous models of the QS (i.e. Hugman et al. 2012; Salvador et al. 2012), as they more accurately represent the drawdowns observed during the 2004-05 drought. This was achieved by increasing withdrawals for irrigation two-fold during the drought years, which highlights the need for a better understanding of the temporal variability of water demand and recharge rates. To achieve a similar result with the regional scale flow model, a five-fold increase was necessary. This can be due to several reasons: 1) increasing abstraction in the cross section model does not induce more recharge from the north, which occurs in the regional model; 2)

different spatial distribution of *T* in the two models; and/or 3) effect of the fresh-saltwater interface, which reduces the rate of flow from the estuary BC.

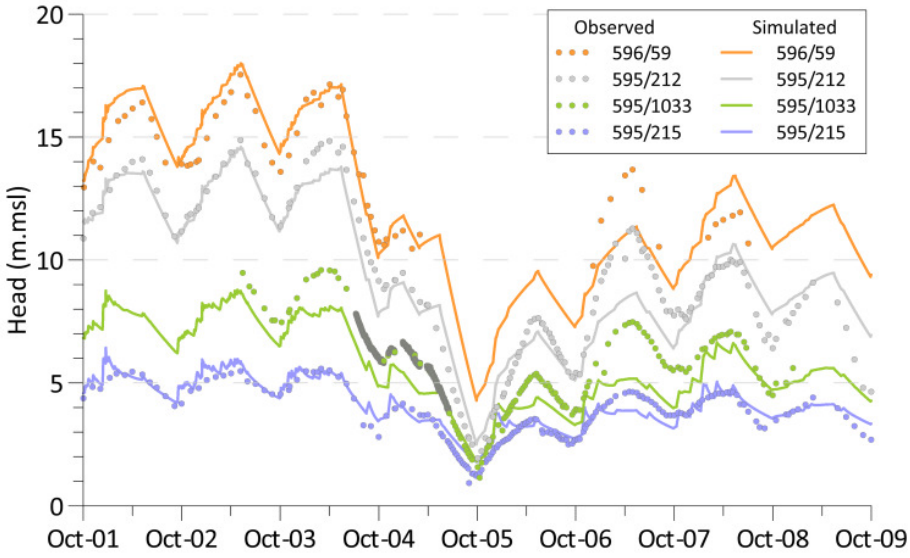

Figure 5.1 Observed and simulated hydraulic head time-series at selected monitoring wells (location in Figure 3.1).

Simulated discharge rate at the coastal boundary also follow measured variation in flow rates at springs along the Arade estuary (Figure 5.2). Model results are significantly higher, as measured values only represent the sum of flow at several springs and do not take into account diffuse seepage or un-monitored springs. The comparison between total discharge and flow into the model domain along the coastal boundary shown in Figure 5.2 shows that during a brief period at the end of the 2004-05 drought, there was more saltwater entering the system, than there was discharge. This does not mean that no freshwater discharge occurred along the boundary, but merely that the overall balance was towards seawater intrusion.

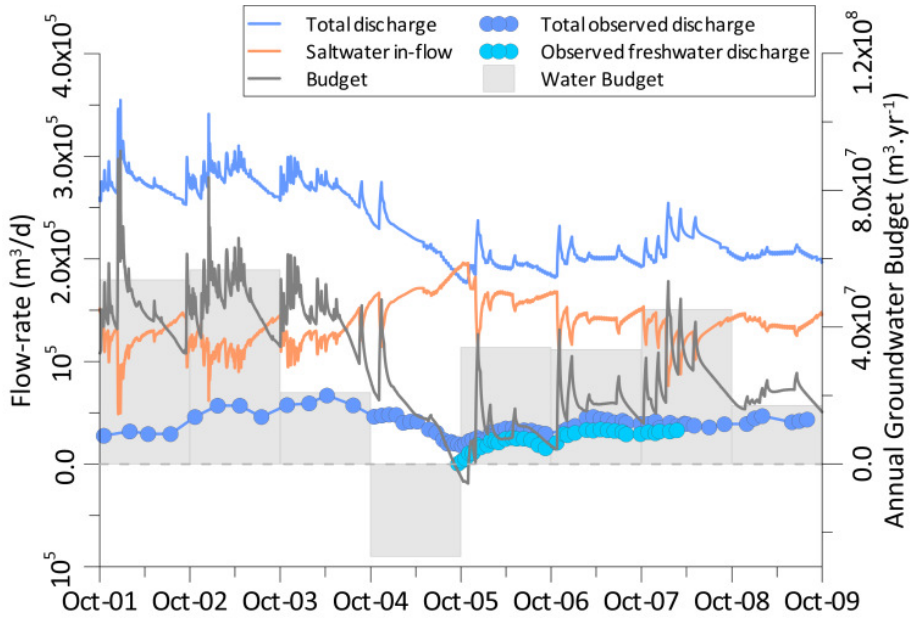

Figure 5.2 Comparison between measured discharge at springs and simulated flows through the Arade estuary boundary condition.

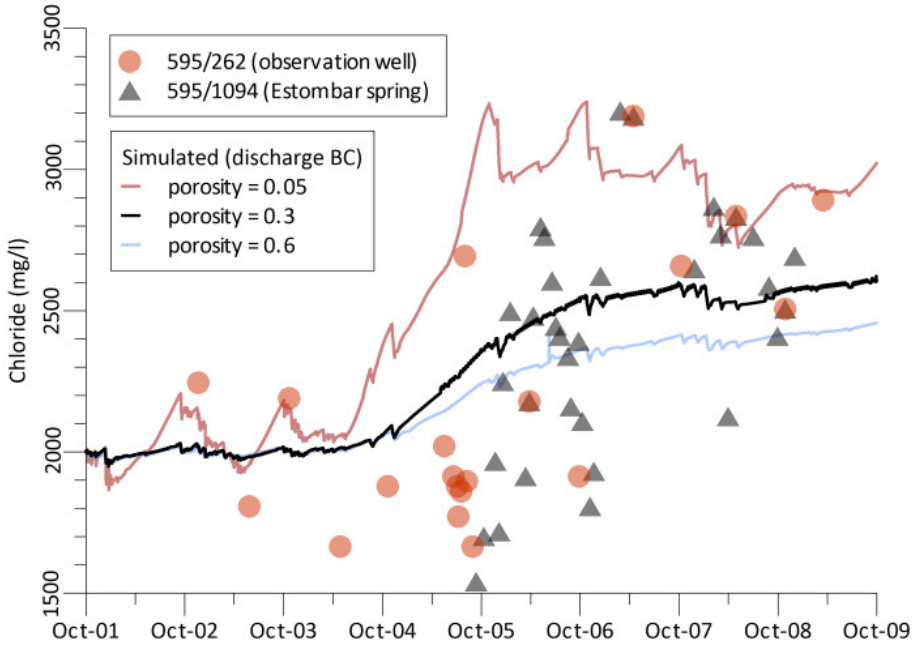

Figure 5.3 Comparison between time series of chloride concentration observed at well 595/262 and simulated discharge to the estuary.

Simulated chloride concentration in groundwater discharged at the Estombar springs is representative of observed inter-annual variation at the springs and observation wells in the vicinity, but fails to represent seasonal fluctuations (Figure 5.3). Both observed and

simulated concentrations increase most at the end of 2005 and remain elevated in the subsequent years. Two simulations were run with porosity at the extreme range of physically acceptable values (0.05 and 0.6) to highlight the parameters effect. Lower values of porosity do in fact lead to slightly faster changes in spring salinity, but in this case overestimate the observed inter-annual increase. In practice, it is likely that spring flow is associated with highly conductive karst channels with rapid changes in water quality, and the EPM model does not provide an adequate tool to simulate the local-scale processes.

Due to a lack of data on the three-dimensional distribution of the fresh-saltwater interface, the simulated spatial distribution of saltwater cannot be validated. Available data mostly include measurements from springs, shallow wells and some boreholes, which do not provide a comprehensive image of the variation of salinity with depth. Figure 5.4 shows that inter-annual variability can have a significant effect on SWI for systems with low porosity by affecting the time-scale at which intrusion occurs. Although the difference between 0.3 and 0.6 is not very significant, results for the simulation with 0.05 show SWI extending over a kilometre further inland, with a significantly thicker transition zone. Low porosity systems are thus more vulnerable to impacts of extreme events such as droughts or to more intense seasonal fluctuation. The effect of hydraulic conductivity and storage parameters on the time-scale of SWI processes is well documented (e.g. Souza and Voss 1987; Watson et al 2010) however no assessments of the impact of porosity on the transient nature of the fresh-saltwater interface were found in the literature.

Assuming that a porosity of 0.3 is representative based on simulated concentration in spring discharge and extent of SWI (Figure 5.4), by the end of the simulated period the saltwater interface has yet to reach any significant well-fields (Figure 5.4 (middle)). Despite the reduction in abstraction and increase in recharge after 2005 (and subsequent recovery in groundwater levels and discharge), the toe continues to move in-land up until the end of the simulated period, although at a slower pace. These results agree with those of Michael et al (2005), who observed large-scale saline discharge as a result of seasonal movement of the freshwater-saltwater interface driven by, but lagging behind, seasonal recharge. In the case of the QS during the simulated period, the high inter-annual variability in recharge and

abstraction appears to have a greater impact on the interfaces movement than the seasonal fluctuations. This explains the continued high salinity in spring discharge in the three years after the drought in 2004/05, as groundwater salinity continues to increase near the coast. As was shown in Figure 3.4, chloride concentrations in spring discharge only decrease after the year 2009/10, after a period of very intense recharge. Unfortunately this is not included in the model as input data was not available at the time of model development.

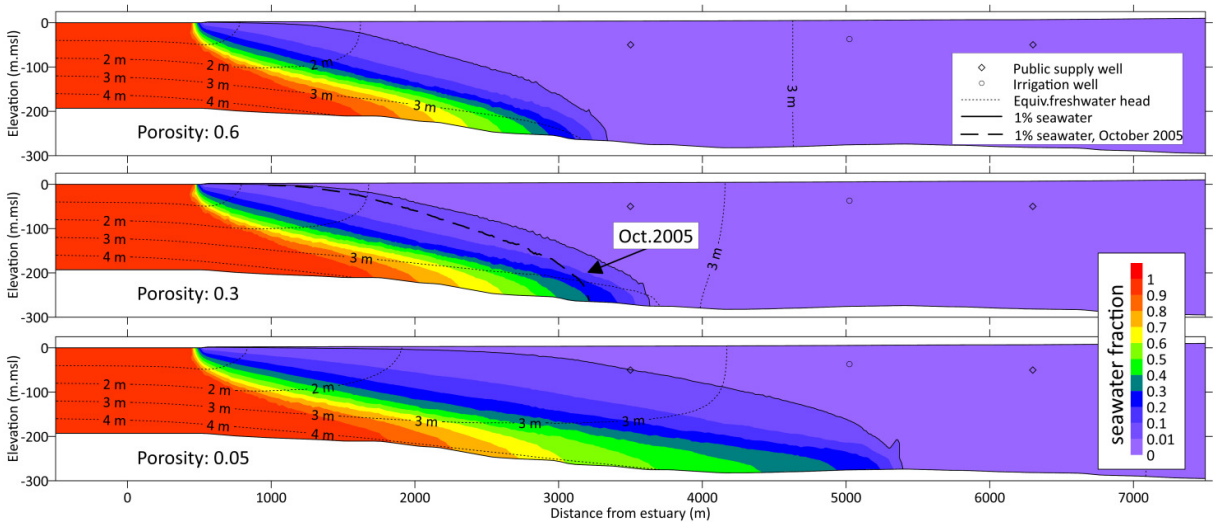

Figure 5.4 Comparison of the effect of porosity on the simulated extent of seawater intrusion and freshwater head for October 2009.

5.3.2. Climate change scenarios: 2010-2099

The range of simulated total discharge and (seawater) in-flow rates at the coastal boundary from all climate change scenarios are shown in Figure 5.5. Results for the ICTP-REGCM3 (linear regression corrected) climate scenario are highlighted for comparison.

As is to be expected, simulated discharge (Figure 5.5) show the same inter-annual and seasonal variations as obtained by Stigter et al. (2014). Discharge rates from the cross-section model are consistently higher than from the regional model, as they include a portion of recirculated seawater. Results show the largest variation between climate scenarios occurring in the near future (between 2020 and 2050) with a decreasing range of simulated results towards the end of the century. In part this is due to the greater number of simulations, as anomaly corrected scenarios only span the years 2020-2050 and 2069-2099, and thus the range of simulated values tends to be larger during these periods. Furthermore,

as initial conditions for the 2069-2099 anomaly corrected scenarios are based on values from the end of the 2050, the effect of variations in the interim are removed, which increases the uncertainty of the results. Even so, the convergence of all scenarios is unlikely to be a consequence of artefacts of the groundwater model and is most likely attributable to climate predictions. As previously discussed by Stigter et al. (2014), the long-term climate signal becomes stronger than the seasonal and short-term variability. Similar results were obtained by Goderniaux et al (2011), who showed that despite consistently large confidence intervals around projected groundwater levels, the climate change signal becomes stronger than that of natural climate variability by 2085.

There is a slight increase in in-flow for all (linear regression) scenarios up to 2020. However, between 2020 and 2050, discharge and in-flow rates do not show an overall trend. During the first half of the century only the ICTP-REGCM3 linear regression corrected (henceforth referred to as ICTP-lin.reg) scenario shows occurrences of less discharge than in-flow, as simulated during the 2004-05 drought. These match hydraulic head gradient inversions identified by Stigter et al. (2014). Regular occurrences ensue for several scenarios from the 2060's forward, even over several consecutive years. This coincides with a general decrease in discharge rates across all scenarios. The ICTP-lin.reg climate scenario usually presents the lowest discharge and highest in-flow rates and was therefore selected to simulate adaptation measure scenarios.

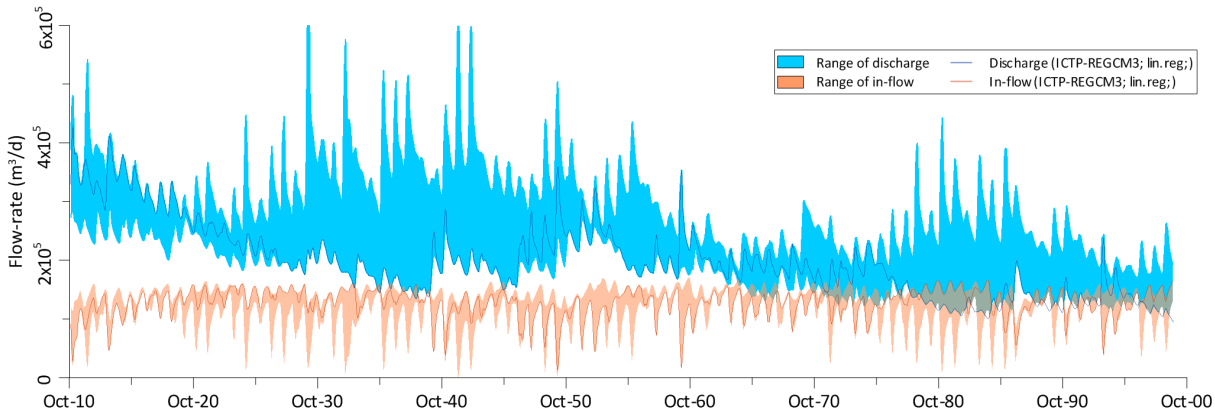

Figure 5.5 Ensemble of simulated discharge and seawater in-flow rates at the coastal boundary.

The extent of seawater encroachment simulated for the ensemble of climate scenarios (Figure 5.6) reflects the range of uncertainty inherent to the climate models. Depending on the climate scenario, by 2050 the position of the fresh-saltwater ranges between receding 500 m to encroaching 2 km in-land. The majority of the scenarios show the interface at approximately the same location as at the end of 2009, indicating that as long as current groundwater use is maintained there is not a significant risk of SWI in the near future, despite the increased seasonal and inter-annual variability. For the worst case scenario, only one municipal well-field would be potentially at risk along with a small patch of agricultural land.

The main impact during this period will be the concentration of freshwater discharge into shorter periods, reflecting the concentrated recharge periods as discussed by Hugman et al. (2013), which may have impacts on associated groundwater dependent ecosystems. However, increased seasonality in and of itself does not have an immediate effect on SWI in the QS due to the relatively slow movement of the fresh-saltwater interface. In practice it may lead to changes in groundwater use (as was seen for example during 2004/05), which can induce changes in the systems equilibrium and cause lasting effects. However, the lack of impact of seasonality on SWI in the QS may not be the case under other hydrogeological conditions. For example, Michael et al (2005) showed that the interface oscillates seasonally, the extent of which is controlled by a complex function of recharge forcing, aquifer parameters, and location within the aquifer. Thus, depending on local conditions, the area affected by SWI may be substantially underestimated if seasonal effects are ignored.

Predicted reduction in recharge during the second half of the century has a clear impact with significant SWI for all scenarios. The simulations indicate that the fresh-saltwater interface will move between 2 km to 3.5 km further inland. In all cases the municipal well-field nearest to the coast would be contaminated. In the worst case scenario, saltwater would reach as far in-land as the second municipal well-field, putting it at risk. Simulated salinity in boreholes up to 6 km from the estuary exceeds usable values for irrigation purposes.

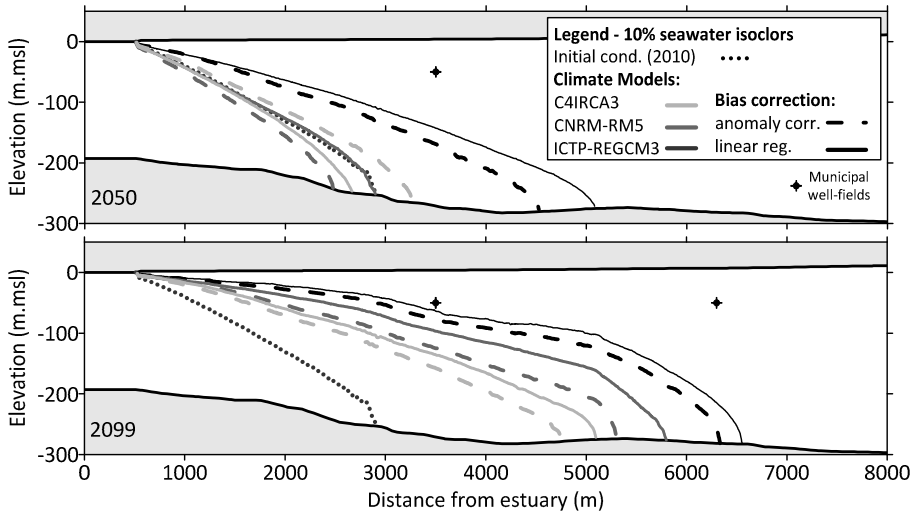

Figure 5.6 Comparison of simulated location of the 10% seawater isocline for the ensemble of climate scenarios at the end of the dry season in 2050 and 2099.

5.3.3. Climate change adaptation measures

Comparison between simulated extents of SWI when adaptation measures are considered are shown in Figure 5.7. The impact of anthropogenic groundwater use is highlighted by the "no pumping" scenario, in which the fresh-saltwater interface actually recedes up to 2050 and even in 2099 only slightly exceeds the current in-land extent. The effect of public supply abstraction is relatively small, as demonstrated by the "no irrigation" scenario with almost no change by 2050 and only a slight increase by 2099. In fact, the entire withdrawals for public water supply represent approximately a quarter of the effect of pumping for irrigation. As the seasonal effect of abstraction for irrigation greatly outweighs that of public supply, the effect of seasonal optimization of abstraction for public supply on both extent of SWI and discharge rates is practically indistinguishable. Likewise, spatial distribution of public supply withdrawals only has a very slight effect on the extent of the saltwater toe by 2099. Previously Hugman et al (2012) and Hugman et al (2013) showed that seasonal and spatial optimization of groundwater use had a significant impact on discharge rates. However, their analysis assumed that all abstraction (pubic supply and irrigation) would be optimized. The results obtained here suggest that this is only the case when a significant portion of abstraction is optimized.

Most significant results are obtained by substantially reducing withdrawals for irrigation, as these represent the greatest pressure on the system. Stigter et al. (2013) suggest that the most likely socio-economic development scenario for the area would lead to a decrease in irrigation water demand of approximately $8x10^6$ $m^3 \cdot yr^{-1}$. This roughly coincides with the scenario in which withdrawal for irrigation is reduced by 25% (average reduction of $8.9x10^6$ $m^3 \cdot yr^{-1}$). However, even so this level of abstraction would not be sustainable for the worst case climate scenario simulated here, as the fresh-saltwater interface moves in-land almost 1.5 km affecting a municipal well-field and irrigation wells.

Comparing the relative volumes used for irrigation, public water supply and increased infiltration in Figure 5.8 and the respective simulations in Figure 5.7, shows that the extent of SWI is directly related to the overall water budget of the system. Reducing irrigation withdrawals by 25% and 50% reduce the extent of SWI by approximately 500 m and 1000 m, respectively. Excess stream flow, as well as the $10.5x10^6$ m^3yr^{-1} injection scheme, represent on average 30% of annual irrigation demand (Figure 5.8), and have similar effects on the extent of SWI as reducing irrigation withdrawals by 25%. In a similar fashion, the model run including solely public supply withdrawals (which correspond to 25-30% of irrigation demand) cause approximately the same change in extent of SWI. An increase of $10x10^6$ m^3yr^{-1} in the groundwater budget roughly coincides with a decrease of 500 m in the extent of SWI.

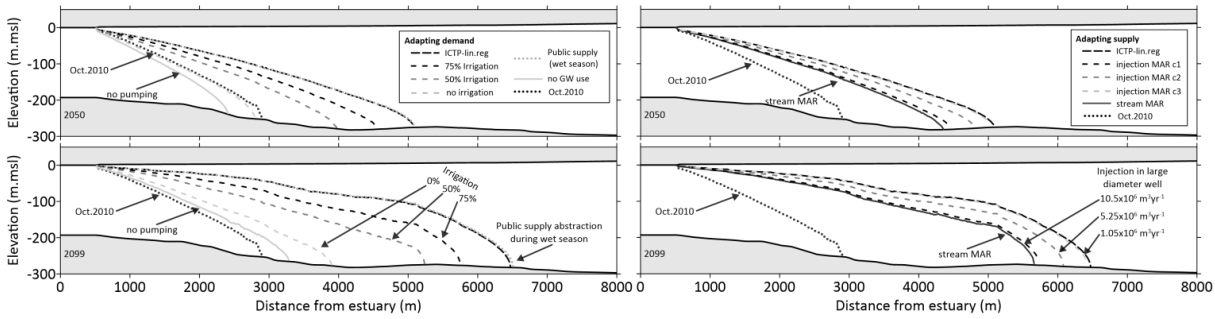

Figure 5.7Comparison of the effect of simulated adaptation measures on the 10% seawater isocline location by 2050 (top) and 2099 (bottom).

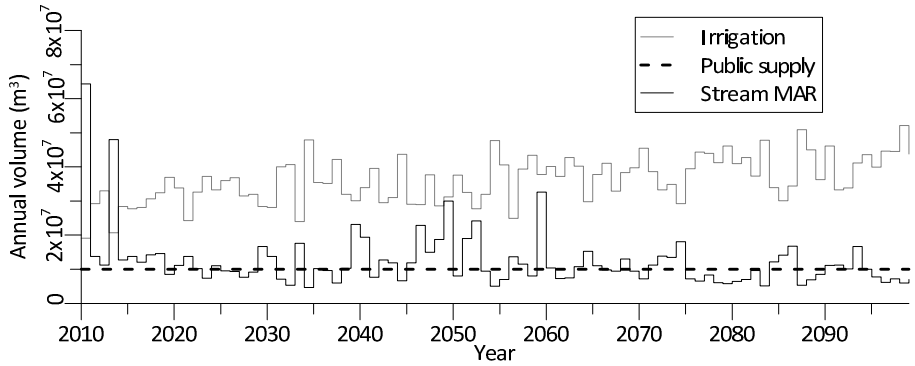

Figure 5.8 Simulated annual withdrawals for irrigation and public supply and enhanced stream infiltration for climate scenario ICTP-lin.reg.

In the specific case of the QS, if the sole criteria for sustainability is the extent of SWI, then the long-term groundwater budget provides a useful estimate of the sustainable yield of the system. The results for the no-pumping scenario show that if the current (c.a. 2010) position of the fresh-saltwater interface is to be maintained, then an average annual discharge of $50x10^6$ m^3yr^{-1} (average annual recharge from 2080-2099) must be maintained. This is significantly lower than the $30x10^6$ m^3yr^{-1} (70% current mean annual recharge) estimated by previous authors (Hugman et al 2012; Stigter et al 2014) and the $10x10^6$ m^3yr^{-1} (90% current mean annual recharge) defined by INAG (2005). Current results are insufficient to define the scale at which this average needs to be defined. Future work should address this issue, to aid in defining what could be referred to as sustainable levels of groundwater mining (e.g. over-exploiting during short periods) such as occurred during the 2004/05 drought.

The impact on SWI of current groundwater abstraction for public water supply could be mitigated by either of the simulated MAR solutions. However there are large differences between the two solutions in terms of their impacts on groundwater levels in the north-eastern sector of the QS (Figure 5.9). Additional stream infiltration raises water levels in the north-eastern sector of the QS significantly. Although average annual recharge for the simulated period is similar to those of the C1 injection scheme, recharge during high rainfall years is stored in the eastern sector. This increased storage provides a buffer of discharge to the western sector as well as a larger reserve of freshwater, increasing the aquifers resilience to short-term extreme events and providing source of water supply.

The alternative of using large diameter wells to infiltrate surplus water from the reservoirs is a feasible solution to reduce the risk of SWI, as long as a significant amount of excess surface water can be maintained. As this scheme would require significant investment in terms of infrastructure, a comprehensive assessment of available surplus and the capacity to maintain MAR under future climate conditions is required. Although a comprehensive cost/benefit analysis has yet to be carried out, it is likely that implementing the stream infiltration scheme would be significantly easier from a technical and financial perspective. On the other hand, the estimated excess stream flow is subject to a large amount of uncertainty and values applied here do not take into account the need to maintain ecological flows in the streams nor the practical issues of implementing such a scheme.

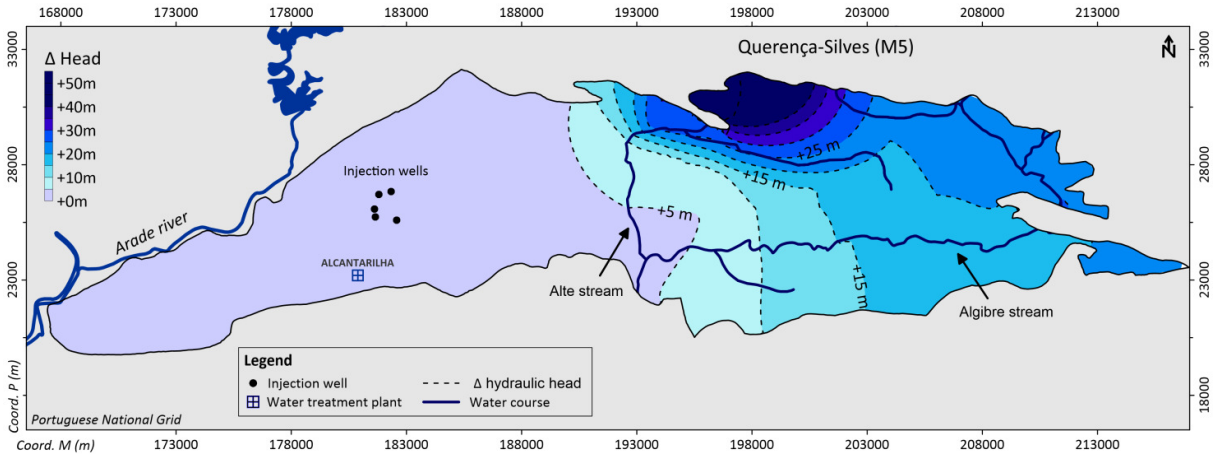

Figure 5.9 Difference between simulated hydraulic head at the end of 2099 for the stream infiltration and C1 injection MAR schemes.

5.4. Comparison between model results

The following section compares the results from the flow and density-coupled flow and transport models. The aim is to verify the impacts of ignoring density effects on simulated groundwater levels and discharge rates.

Figure 5.10 compares discharge simulated by the regional flow model with discharge from the density-coupled flow and transport model. As to be expected, total discharge from the density-coupled model is consistently higher as it includes a portion of re-circulated saltwater. The amount of freshwater discharge is obtained by subtracting the amount of seawater entering the model from the total discharge (inflow - outflow in Figure 5.10). As

can be seen, freshwater discharge from the density-coupled model and the flow model show a good fit over the entire hundred year period.

Thus, density effects do not have a significant effect on regional scale discharge rates and can be ignored if the aim is merely to determine the freshwater component of coastal groundwater discharge. Estimates of sustainable yield, focusing on maintaining an ecological baseflow to coastal springs can therefore be obtained using more simple and "cheaper" flow models. However, these will not consider increasing salinity in groundwater discharge associated to decreasing freshwater, which may have a significant impact on GDEs.

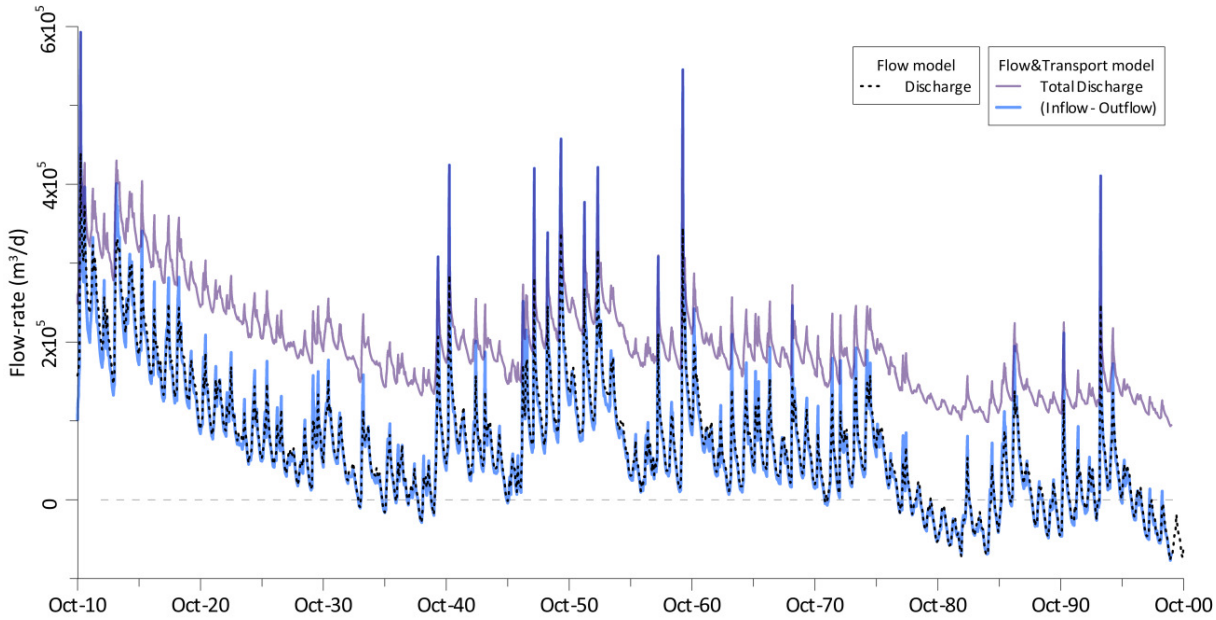

Figure 5.10 Comparison between discharge rates simulated by the flow and density-coupled models for the ICTP-lin.reg scenario.

However, when comparing simulated groundwater levels in Figure 5.11, the impact of ignoring density effects is evident. Although during the first couple of decades simulated heads are similar, hydraulic head in the flow model gradually decreases over time in comparison to the density-coupled model. The effect decreases with distance from the coast, being more apparent at observation point 595/215 (c.a. 5 km inland) than at 595/212 (c.a. 10 km inland). In the density-coupled model, the landward movement of the fresh-saltwater interface effectively reduces the thickness of the medium through which freshwater can flow. This is comparable to reducing the transmissivity of the system, leading

to higher hydraulic heads for the same amount of flow. Thus, as the system moves further away from current day conditions (e.g. position of the interface), the flow model becomes less accurate in simulating groundwater levels near the coast.

As the calibrated parameters of the flow model take into account the effect of the current day position of the interface, and as any changes in position are relatively slow, the flow model provides accurate representation of groundwater levels in the short term. However, long-term or steady-state simulations will lead to inaccurate estimates of groundwater levels. As the effect decreases with distance from the coast, predicted effects on heads in-land will likely still be reasonable. However, near the coast they will consistently be underestimated. Therefore, any assumptions on the depth of the fresh-saltwater interface based on simulated hydraulic pressure and the Ghyben-Herzberg relation will be overestimated. This can be beneficial, as any assessments based on their results will provide conservative estimates of the risk of SWI.

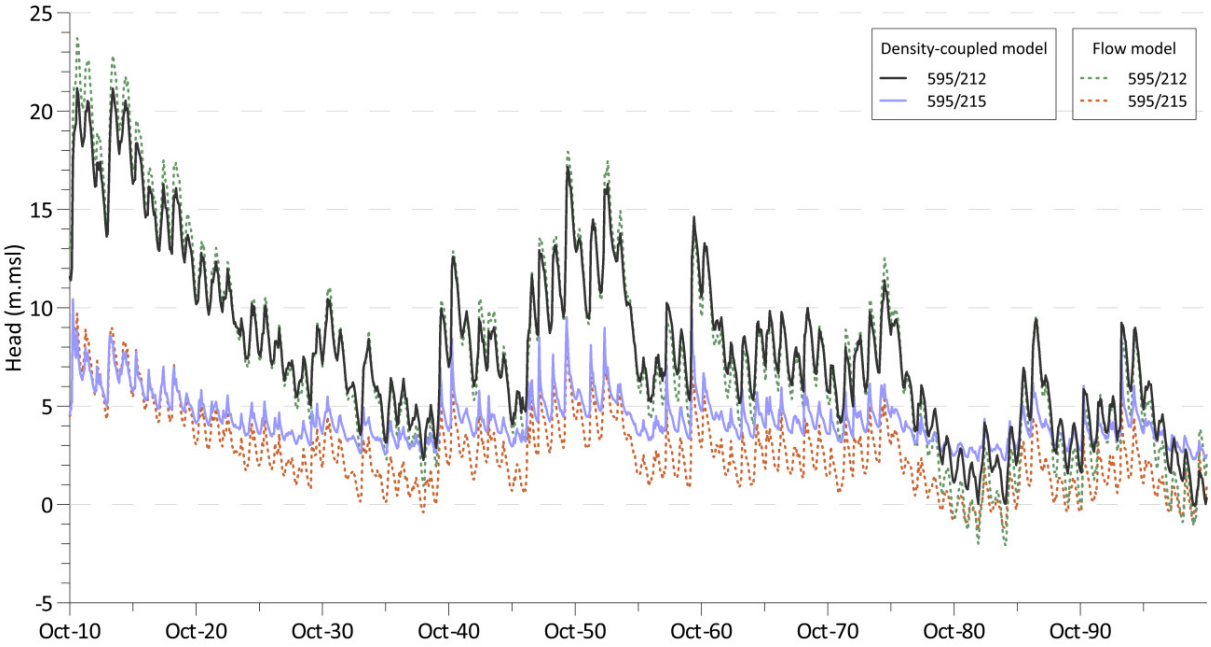

Figure 5.11 Comparison between hydraulic heads simulated by the flow and density-coupled models for the ICTP-lin.reg scenario.

5.5. Final remarks

Simulations using a density-coupled groundwater flow and transport model demonstrated the effect of predicted changes in recharge, crop water demand and adaptation scenarios on SWI in the QS aquifer system. By considering several climate models, bias correction and recharge calculation methods a degree of uncertainty was included in the results. Uncertainty related to climate change models is evident in the short-term results (2050), with simulated scenarios ranging from a decrease in SWI to significant increase in SWI. Changes in rainfall regimes will have an immediate effect on the seasonal variation of discharge, however the effect on SWI is attenuated by the fresh-saltwater interfaces' comparatively slow rate of movement. More accurate predictions of SWI will only be possible if more detailed information is collected on the fresh-saltwater interface and its reactions to changes in the hydrogeological system.

In the long-term (2100), the scenarios converge. All simulations show significant increase (between 2 to 3.5 km) in SWI by the end of the century. Despite predicted encroachment of the fresh-saltwater interface, simulations indicate that public water supply wells managed by the regional water utility are not under risk of salinization if current water management practices are maintained. However users within a few kilometres from the coast will be adversely affected. These include several agricultural areas and two municipal well-fields currently maintained as reserves to supplement public water supply, as well as the estuarine GDE. Adaptation measures will be necessary to maintain current groundwater quality in the long-term.

Comparing the effects of proposed adaptation measures confirms that the extent of SWI in the QS is controlled by the long-term water budget. The effectiveness of both demand (e.g. reduced withdrawals, alternative sources, optimized spatiotemporal abstraction) and supply (managed aquifer recharge) oriented measures on the extent of SWI is directly related to the change in water budget. However this is specific to SWI and ignores other sustainability criteria, such as maintaining ecological flows to GDE. Taking these issues into account, the single most effective measure would be a MAR scheme to increase infiltration of run-off from the Palaeozoic rocks north of the system, which would counteract the effect of

decreasing recharge from climate change. Research is required to better understand the surface/groundwater interactions in this system, as well as estimate the effects of climate change on surface water availability, in order to assess the practical feasibility of either MAR scheme.

Previous authors estimated sustainable yield for the QS as 70% of the mean annual recharge, in order to maintain freshwater discharge at the Estombar springs. However, the impact on SWI and the salinization of spring discharge was not taken into account. Current results show that these latter two criteria are mostly controlled by the long-term water budget of the system, and that to maintain both current ecological status of the GDEs and groundwater quality, mean annual discharge should be in the order of $50x10^6$ m^3yr^{-1} (c.a. 50% of current mean annual recharge).

6. Modelling the spatial and seasonal distribution of groundwater discharge for different water use scenarios under epistemic uncertainty[4]

In the current chapter a new study area of the Albufeira-Ribeira de Quarteira and Quarteira aquifer systems is presented. A numerical flow model is developed to assess the spatial and seasonal distribution of groundwater discharge to the coast, taking into account uncertainty in regards to hydraulic parameters and surface/groundwater interaction in the system. Concepts of sustainable yield discussed in chapters 3 and 4 are subsequently applied to provide an initial assessment of sustainable levels of groundwater use.

6.1. Introduction

Integrated approaches considering groundwater and surface water bodies as a single resource must be adopted for sustainable management (Winter et al 1998; Sophocleous 2002). Water use for anthropogenic needs must take into account effects on other environmental users in order to fit the concept of sustainability (Alley et al 1999; Sophocleous 2002; Custodio 2002). This has led to a large body of work on the interaction between groundwater and fresh water bodies such as rivers, lakes and wetlands (e.g. Sophocleous 2002; Eamus and Froend 2006). However, until recently research on the interactions between groundwater and the sea has been mainly focused on seawater intrusion (Ghassemi et al 1996; Zhang et al 2004; Kerrou et al 2010; Watson et al 2010; Lu et al 2011; Koussis et al 2012; Gaaloul 2012) despite recognition that submarine groundwater discharge (SGD) can have a significant impact on marine ecology (Taniguchi et al 2002; Burnett et al 2006).

[4] The following chapter is adapted from and expands upon:

Hugman, R., Stigter, T.Y., Monteiro, J.P., Costa, L., Nunes, L.M., 2014. Modeling the spatial and temporal distribution of coastal groundwater discharge for different water use scenarios under epistemic uncertainty: case study in South Portugal. Environ. Earth Sci. 73, 2657–2669.

The term Submarine Groundwater Discharge (SGD) has been given several definitions, depending on whether it merely takes into account freshwater discharge or also includes re-circulated water seepage (Taniguchi et al 2002). The most consensual definition is described in Burnett et al. (2006) as “any flow of water out across the sea floor”. Whether or not SGD includes a large component of freshwater, also referred to as coastal groundwater discharge (CGD), depends on the local hydrogeological conditions, i.e. aquifer lithology, aquifer type and hydraulic gradients, as well as the groundwater balance and how it is affected by human activities (abstractions).

SGD or CGD may be determined using different methodologies, depending on the scale of interest. For small-scale local estimates of groundwater discharge field measurements are most adequate, for instance using seepage meters or tracer methods (Burnett et al. 2006). These may be accurate locally but difficult to upscale to regional values. In the latter case, regional water balances may be set up to get initial estimates of shallow and deep freshwater outflow at the coastline (e.g. Stigter et al. 2013b). For more representative estimates of such freshwater discharge fluxes along the coastline groundwater flow models tend to produce the most reliable estimates (e.g. Andersen et al. 2007). Such models may consider or neglect the fresh-saltwater interface and density driven flow, depending on the purpose of the study (Ghassemi et al 1996; Zhang et al 2001; Koussis et al 2012; Bakker and Schaars 2013; Llopis-Albert and Pulido-Velazquez 2013). The advantage of groundwater flow models is that they can be used to test hypotheses of outflow, boundary conditions and groundwater extraction scenarios, and subsequently be used to show the past or future evolution of fresh groundwater outflow under changing pumping practices, and consequences for groundwater dependent ecosystems (GDEs). Notwithstanding, a crucial task when using such models is to characterize and assess the different levels of uncertainty that are inherent to the process. Uncertainty may be divided into epistemic uncertainty and variability. The first is related to the modeler’s uncertainty of how to represent the phenomenon, or the lack of information to fully describe the phenomenon. Some of this uncertainty is reducible by collecting more data. The latter is due to the complex behavior of natural processes and can only be partially diminished by collecting more data. Hence, uncertainty analysis must take these two sources into account.

CGD and SGD are known to occur and have been observed at several locations in the Algarve region in the south of Portugal, in the Ria Formosa lagoon near the capital of Faro (e.g. Leote et al. 2008, Stigter et al. 2013b), and 25 km west of this city, where submarine springs have been observed and their impact on local ecosystems have been studied (Encarnação et al., 2013). The aquifers in these areas are mostly in contact with the sea, discharge occurring at sea level and as SGD. The increase of tourism along the coast during the 1970s led to a rise in water demand, in particular for public supply and green area irrigation. Irrigated agriculture also required large amounts of water. Initially demand was met with groundwater (Monteiro and Costa 2004), and the increase in groundwater abstraction led to a decrease in water quality in some areas, partly due to local overexploitation and consequent seawater intrusion. At the beginning of the 21st century, surface water replaced groundwater for public supply and currently all publicly owned boreholes are either inoperative or held in reserve in case of lack of water emergencies. However, the drought during 2004 and 2005 highlighted the limitations of this single source strategy as well as the crucial role of groundwater as part of the more complex concept of integrated water resource management (Stigter et al 2009).

Reintroducing groundwater abstraction as part of an integrated management scheme requires quantifying and understanding available resources to avoid overexploitation. Several efforts during the past few years have begun to analyze the factors that influence sustainable groundwater use in the region (Hugman et al 2012; Salvador et al 2012; Stigter et al 2013a; Hugman et al 2013b; Stigter et al 2014). Apart from issues of adequate groundwater quantity and quality for human needs, there is a need to determine criteria for sustainability which take into account other users such as GDE. Various GDEs have been identified in the Algarve, mostly related to springs and streams connected to groundwater bodies (Reis 2007; Salvador et al 2012; Fernandes 2013), but little attention has been given to the dependence of marine ecosystems on fresh groundwater discharge.

The main goal of this chapter is to assess and characterize the epistemic uncertainty with regard to the parameterization and the definition of boundary conditions while building a groundwater flow model to provide estimates of the spatial and temporal distribution of

freshwater discharge along the coastline at a regional scale. This is done for two coastal aquifer systems in the Algarve region for which preferential CGD and near-shore SGD has been observed at specific locations, the cause of which is studied with the help of the groundwater flow model. Off-shore SGD is being investigated in the scope of a multidisciplinary research project that seeks to identify and characterize groundwater flow from the coastal strip towards the continental platform, taking into account structural geology, marine geology and the effects of the hydrological/ hydrogeological conditions on associated ecosystems. The model is further used to simulate different past and present scenarios of groundwater pumping, to provide an estimate of sustainable yields based on a predefined criteria, and to analyze the importance of well location on these yields.

6.2. Study area: the Albufeira-Ribeira de Quarteira (M6) and Quarteira (M7) aquifer systems

The Albufeira-Ribeira de Quarteira (ARQ) and Quarteira (QRT) are two coastal aquifer systems that occur in the area between the cities of Albufeira and Quarteira in the southernmost region of Portugal (Figure 6.1). In their compilation of the hydrogeological knowledge of the region, Almeida et al. (2000) classified these systems as two units, with the aim of defining inventory and management units for the national and local water authorities. This classification has since been applied by most regional studies of groundwater resources and is used in the regional river basin management plans. The following analysis will aim to maintain the currently used nomenclature but considers the two units as a connected system.

A thorough hydrogeological description of the region was made by (Almeida et al 2000). Subsequent research in the area has contributed to the further understanding of the ARQ and QRT aquifer systems (e.g. Monteiro et al. 2002; Monteiro et al. 2005; Costa 2006; Monteiro et al. 2007; Bronzini 2011; Costa et al. 2013; Francés et al. 2014; Hugman et al. 2014). The following section comprises a synthesis of the available information.

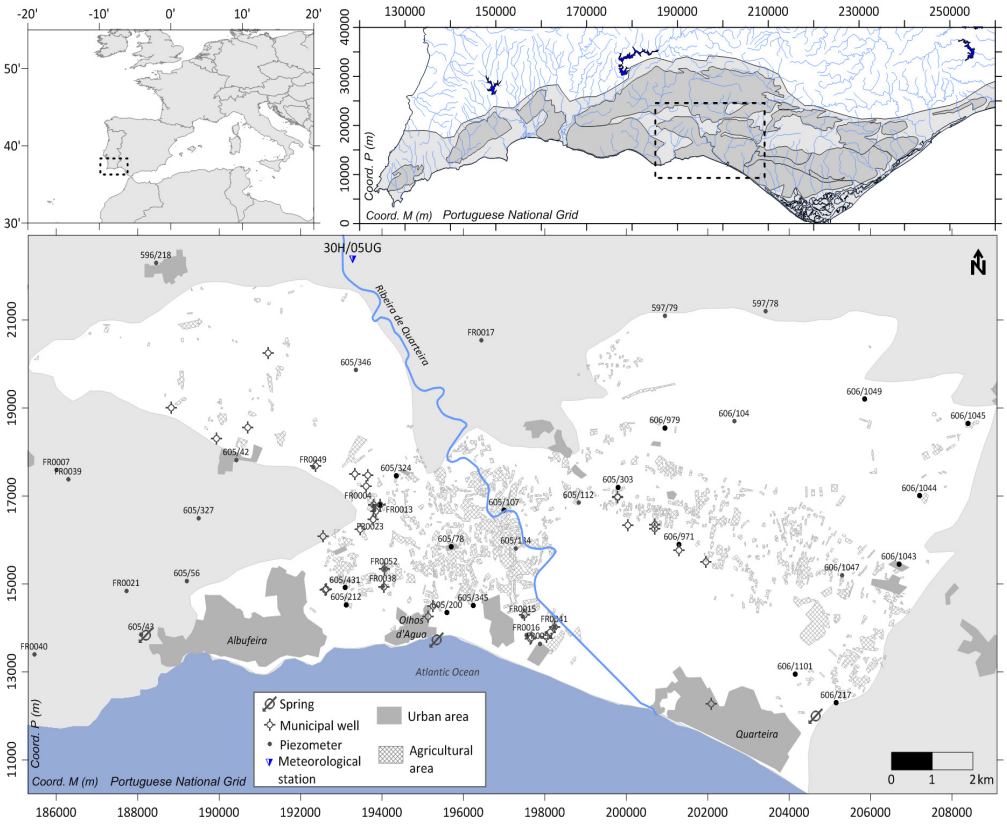

Figure 6.1 Location of the main aquifer systems of the Algarve (top right, adapted from Stigter et al. (2009)) and extent of the Albufeira-Rib.Quarteira and Quarteira aquifer systems (bottom) according to Almeida et al. (2000).

6.2.1. Climate

The Algarve region, the southernmost province of Portugal, is characterized by a warm Mediterranean climate, and the coastal zone can be defined as semi-arid based on the precipitation to potential evapotranspiration ratio (Estrela et al 1996). For the Algarve mean annual temperature and precipitation are around 17^{o}C and 650 mm, respectively. The precipitation regime is irregular, having intermittent periods with heavy rains in the winter and a long dry period in the summer.

The region is subject to large seasonal and annual variations in rainfall (Stigter et al 2009) and research points towards an increase in frequency and intensity of droughts in the future (Giorgi 2006; Santos and Miranda 2006). For the Central Algarve, although mean annual rainfall is expected to decrease only slightly in the short-term, i.e. up to 2050, and despite a

certain degree of uncertainty inherent in climate change scenarios, significant shifts in seasonal distribution and inter-annual variability are predicted. Rainfall will be more concentrated in the winter season, with large reductions in spring and autumn. In the long-term, 2070–2100, a significant reduction in both rainfall and recharge is predicted (Stigter et al 2014).

6.2.2. Geology

The aquifer ARQ and QRT aquifer systems develop mostly within productive Miocene and Jurassic lithologies, occasionally separated by low permeability Cretaceous formations, and overlain with a low permeability layer from the Plio-Quaternary (Figure 6.2).

Jurassic lithologies are composed of two main formations, (1) the Dolomites and Dolomitic Limestones of Santa Barabara de Nexe and (2) the Escarpão Limestone (Almeida et al 2000). The first are composed of thick bands of dolomites and dolomitic limestones with a pink colour from the Kimeridgian age and reaching up to 165 m thickness (Terrinha et al 2010). These outcrop in the north-eastern area of the system, coinciding with the Jurassic outcrops of the QRT aquifer system, and are partially divided by an E to W band of marly limestone (Peral Marls in Figure 6.2 and Figure 6.3) which creates a low permeability barrier to groundwater flow. The Escarpão Limestone is essentially composed of limestones and dolomites, with a clay component which increases towards the top. It can reach up to 500m thickness and outcrops in the north-western area of the system forming what is locally known as the Escarpão Plateau (Almeida et al 2000; Terrinha et al 2010). Both these formations outcrop in the north, and are overlain by the Miocene and Cretaceous layers to the south.

The base of the Cretaceous layer consists of marly-limestones of purbeck facies (65m thick), overlain with alternating layers of sandstone and limestone with quartz, conglomerates and clays (135m thick) (Terrinha et al 2010). This formation outcrops to the East of the ARQ limits as defined in Almeida et al. (2000a), where it overlies the Escarpão Limestone formation (Manuppella 1992). It extends to the south-west, where it is covered by the Miocene formations, outcropping once again to the East of the QRT system.

The Miocene formations are formed by occasionally karstified fossiliferous limestone, which dip 6° in an S-SW direction. Thickness increases towards the S and E, reaching at most 80m thickness in the ARQ and up to 180m in the QRT aquifer system. Outcrops occur in the south-western area of the system, extending from the Cretaceous outcrop and into the sea. The outcrop continues offshore for approximately 6km (Sousa et al 2014). They are almost entirely covered by low permeability argillaceous sandstone deposits of the Mio-Plio-Quaternary, which can reach 40m thickness.

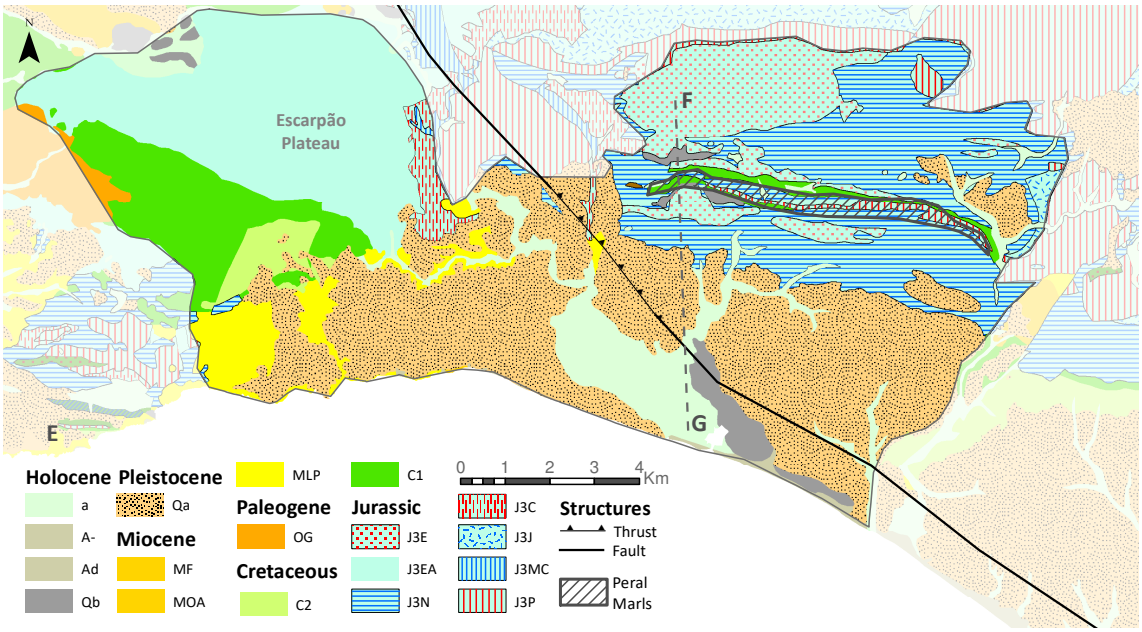

Figure 6.2 Geological map of the study area, adapted from Manuppella (1992) and (Francés et al 2015).

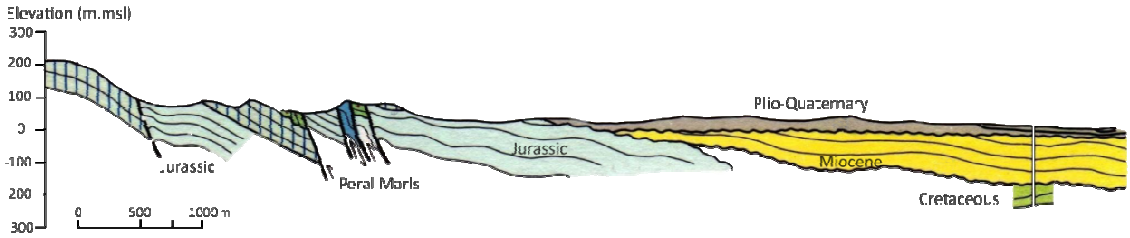

Figure 6.3 Geological cross-section (F-G), adapted from Manuppella (1992); location in Figure 6.2

6.2.3. Hydrogeology

The water-bearing formations are composed by detrital-carbonate rocks dating from Miocene and Upper Jurassic (Figure 6.2). Both aquifers can be in direct contact or separated by the Cretaceous aquitard as shown in Figure 6.3. In some sectors, depositional and structural conditions allow the contact between the two water-bearing formations, making hydraulic connection possible. The Miocene aquifer is mostly covered by the Plio-quaternary formations. In some locations this low permeability layer causes the underlying aquifer to become confined, which is evidenced by the existence of artesian wells in some areas close to the city of Quarteira (Almeida et al 2000).

The aquifer system boundaries are defined by three tectonic major accidents. Along the northern border they are limited system by the Algibre flexure. The ARQ is currently considered to be limited to the west by outcrops of impermeable Cretaceous lithologies and the Albufeira diapir (Almeida et al 2000). The NE-SW S. Brás de Alportel – Loulé – Quarteira fault line limits the system to the East. The NW-SE S.Marcos da Serra-Quarteira fault, which coincides with the Ribeira de Quarteira stream, creates a low permeability barrier between the ARQ and QRT however groundwater levels indicate that some transfer occurs (Almeida et al 2000).

The Miocene aquifer discharges into the sea as well as into the Quarteira stream (Almeida et al 2000; Reis 2007). The Quarteira stream is ephemeral, with flow occurring mostly during the wet winter season. Along its upper reaches it has an influent behaviour (contributing to groundwater recharge), with the occurrence of sinkholes in several locations. However the lower reaches are effluent and support groundwater dependent ecosystems (Fernandes 2013). Of further interest are several inter- and sub-tidal freshwater springs along the ARQ coast line, in particular at the Olhos d'Agua beach. One of the earliest references, Lopes (1841), described this discharge as follows "Between Albufeira and the Valongo fort, several freshwater springs break out along the beach, hence they call this place Olhos d'Agua and within the sea in the same direction and not far out another very large one breaks out". Recently Encarnação et al. (2013) compared meiofauna assemblages at Olhos d'Agua and a control site, and found that the discharge of groundwater stimulated an increase in

biodiversity, which leads to a more robust ecosystem with the ability to support a more diverse range of organisms at higher trophic levels. On the eastern border the system also discharges to a spring, locally known as the Fonte Santa. This spring flows year round and feeds into the Almargem coastal lagoon to the East.

A portion of flow in the Jurassic aquifer flows to the north and northeast, as shown by tracer tests carried out by Almeida and Crispim (1987). Until recently most of the groundwater in the Jurassic aquifer was presumed to flow south towards the sea, passing through the Miocene aquifer. However recently acquired data indicates potential freshwater SGD occurring up to five kilometres from the coastline (Sousa et al 2014). This suggests that the Jurassic aquifer extends under the sea and that the confining Cretaceous layer permits the offshore continuation of a fresh groundwater wedge.

6.2.4. Hydraulic parameters

Transmissivity was estimated in 30 boreholes exploiting the Miocene formation of the ARQ, ranging between 84 e 3080 $m^2.d^{-1}$, with average of 540 $m^2.d^{-1}$ and median of 235 $m^2.d^{-1}$ (Almeida and Silva 1990). Almeida (1985) estimated transmissivities in the QRT aquifer between 24 and 7740 $m^2.day^{-1}$, with an average of 1145 $m^2.d^{-1}$ and median of 750 $m^2.d^{-1}$. Lourenço (1992) estimated transmissivity in 32 boreholes in the Miocene and Jurassic aquifers of QRT and obtained an average of 2700 $m^2.day^{-1}$ and median 868 $m^2.d^{-1}$. Lourenço (1992) refer that there are two main areas separated by the E to W band of marly limestone: (1) high transmissivity to the south in both the Miocene and Jurassic aquifers, and (2) low transmissivity to the north.

Almeida and Silva (1990) obtained storage coefficient values of 0.02-0.03 for several pumping tests in the ARQ Miocene aquifer, and refer a value of $2x10^{-5}$ to $2x10^{-4}$ for fracture flow. Almeida et al. (2000) refers that the Santa Barabara de Nexe Limestone formations (Jurassic) have similar properties to those observed in the neighbouring Almasil-Medronhal aquifer (transmissivity of 4000 $m^2.d^{-1}$ and storage coefficient of 0.04). The hydraulic conductivity of the Plio-Quaternary deposits, obtained from insitu and permeater tests is

respectively of the order of 10^{-5} and 10^{-4} m.d^{-1}. Specific yields vary from 0.02 to 0.04 (Almeida and Silva 1990; Lourenço 1992).

6.2.5. Groundwater use

Public water supply in the Algarve was largely dependent on groundwater prior to the switch to a regional system dependent on surface water dams in 1999. Since the switch to surface water, public supply wells have been deactivated and are currently held as an emergency reserve. The effect of this switch is visible in the groundwater level time series, in particular at the piezometer 605/324 perhaps due to its proximity to one of the largest municipal well-fields. As can be seen in Figure 6.5, up until the year 2000 groundwater levels have a strong seasonal fluctuation and a pronounced response to periods of low rainfall (i.e the droughts in 1994-95 and 1998-99). After the surface water supply system was put into place, the intra-annual variation in groundwater level is reduced from an average of approximately 10 m to 5 m. Even during the 2004-05 drought, groundwater levels were higher than the average of values measured between 1994 and 2000. As is to be expected, this effect is not so evident in piezometers located in the QRT aquifer system.

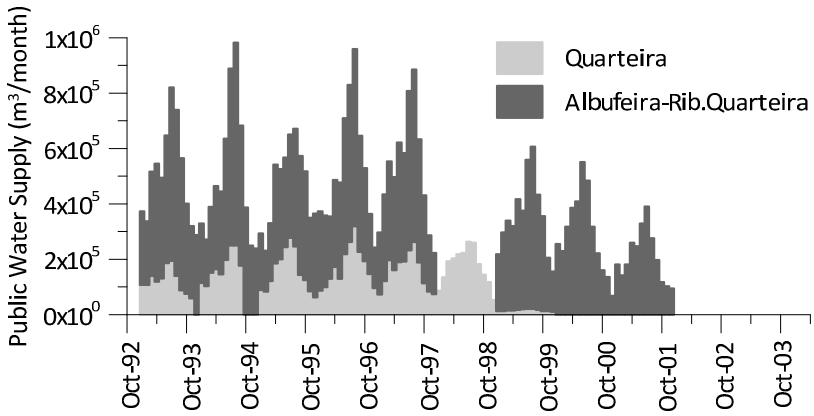

Figure 6.4 Monthly volumes of groundwater abstraction for public water supply for the Quarteira and Albufeira-Rib.Quarteira aquifer systems.

Almeida et al. (2000) estimated groundwater abstraction for irrigation as 3.5×10^6 m^3.yr^{-1} and 9×10^6 m^3.yr^{-1}, for the ARQ and QRT aquifer systems respectively. Using land use maps from 2007, supplied by the local water authority (APA, ex-ARH Algarve), irrigated land in the study area was calculated. A total area of 9.0×10^6 m^2 is used for agricultural purposes. Of this area,

92% is taken up by citrus crops. Assuming crop water need values for the area, as presented in the River Basin Management Plan for the Algarve (RBMP 2012), groundwater abstraction for agricultural purposes is estimated at 3.56×10^6 $m^3.yr^{-1}$. Information from the local water authority indicates that an additional 5.93×10^6 $m^3.yr^{-1}$ is used to irrigate golf courses, and 0.12×10^6 $m^3.yr^{-1}$ is pumped at a cement factory. Data supplied by the factory shows an average annual abstraction of 0.13×10^6 $m^3.yr^{-1}$ up to 1999.

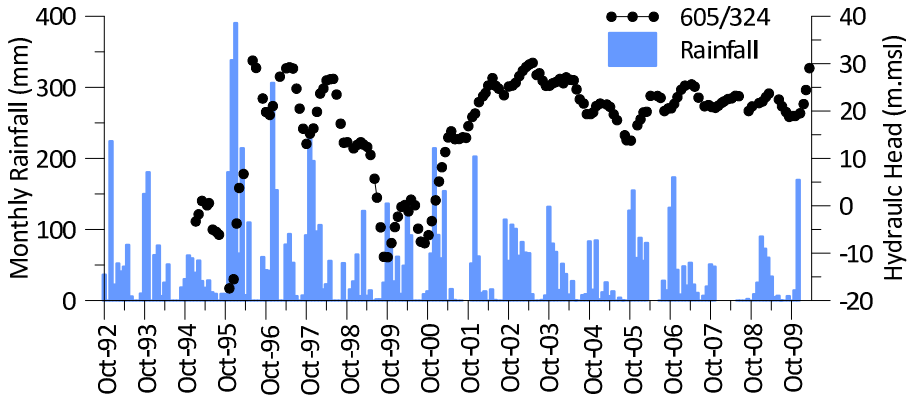

Figure 6.5 Comparison between groundwater levels measured at 605/324 and monthly values of rainfall measured at the Paderne meteorological station (30H/05UG), location in Figure 6.1.

6.2.6. Water budget

Due to the presence of the low permeability layer, recharge rainfall to the Miocene aquifer is reduced. Most direct recharge occurs on the Jurassic outcrops in the north, which then enters the Miocene where the two formations are in contact. Almeida and Silva (1990) originally roughly estimated $8.7\text{x}10^6$ $m^3.yr^{-1}$ for the ARQ, based on an average rainfall of 500 mm and considering recharge rates of 50% for the outcropping limestone and 20% to the confined Miocene lithologies. Almeida et al. (2000) suggest similar recharge rates for QRT, resulting in an estimated recharge of $15\text{x}10^6$ $m^3.yr^{-1}$ with an average 600 mm of rainfall. Based on these values the average annual recharge for the two systems is $23.7\text{x}10^6$ $m^3.yr^{-1}$.

Applying representative recharge rates per lthology as suggested by (Almeida et al 2000; Monteiro et al 2003; Vieira and Monteiro 2003) to the spatial distribution of rainfall determined by Nicolau (2002) and the outcropping areas as presented in Francés et al (2014) leads to an average annual recharge of 25.4 $\text{x}10^6$ $m^3.yr^{-1}$. Table 6.1 presents the water

budget components according to aquifer lithology and groundwater management unit. The only sub-unit with a negative water budget is the miocene aquifer within the QRT unit. The fact that groundwater levels in this area are relatively high and constant shows that the jurassic and miocene aquifers are well connected here.

Sousa et al (2014) detected offshore SGD up to 5 km in the area between the city of Albufeira and Olhos d'Agua (see location in Figure 6.1), which can be explained by an offshore continuation of the Jurassic aquifer, confined by the Cretaceous aquitard. According to Francés et al (2014), the jurassic aquifer in the eastern part of the system is composed by the c.a. 650m thick Escarpão limestone which outcrops in the northeast. A portion of the recharge that occurs on this outcrop is believed to recharge the miocene aquifer. As recharge occurring directly on the miocene aquifer is sufficient to account for current levels of abstraction, it must be presumed that, at most, 8.91×10^6 $m^3.yr^{-1}$ may occur as offshore SGD. However it is likely less.

Table 6.1 Average annual groundwater budget post-2000.

Management Unit	Component	Miocene	Jurassic ($x10^6 m^3.yr^{-1}$)	Total
ARQ (M6)	Recharge	1.75	9.29	11.0
	Abstraction	1.34	0.38	1.72
	Budget	**0.40**	**8.91**	**9.32**
QRT (M7)	Recharge	1.08	13.3	14.3
	Abstraction	7.14	0.85	7.98
	Budget	**-6.05**	**12.4**	**6.35**

6.2.7. Groundwater levels

The local water authority (APA) maintains a regional piezometric monitoring network with measurements usually taken once a month, in some cases since 1978. The Albufeira municipal council also collects groundwater level measurements from their deactivated boreholes, albeit sporadically. The location of APA piezometers and measurements provided by the municipal council are shown in Figure 6.1. During the FREEZE project attempts were made to measure groundwater levels from private boreholes. Unfortunately it was found that most privately owned boreholes were inaccessible or completely sealed, making

measurements hard to obtain. Several previous studies have collected data in the area, however they do not provide a system wide coverage during a single time period. Figure 6.6 presents an interpolated map of groundwater level based on the median of data (1) presented in Almeida and Silva (1990), Lourenço (1992) and Costa (2006), (2) data obtained from APA and the Municipal Council and (3) data collected during the FREEZE project (Francés et al 2014; Francés et al 2015). This map is not representative of the system at any given time or aquifer layer, however it does supply a general overview of the systems behaviour. The right hand map in Figure 6.6 is the result of the interpolation of median values of data collected from the APA groundwater monitoring network, for points in which there are continuous time series for the period between 2001 and 2014. Values of 0 m above mean sea level (msl) were considered along the coast where Miocene outcrops, and equal to equivalent freshwater head at the top of the Miocene layer along the rest of the coastline. Equivalent freshwater heads were calculated presuming that the entire overlying Plio-quaternary layer is saturated with seawater. This is the minimum value of head that would lead to equilibrium between fresh and seawater in the semi-confined Miocene aquifer along the coastline, and is therefore likely underestimated.

Flow is predominantly from north to south. In the northwest there is some flow northwards. This is in agreement with tracer tests carried out by Almeida and Crispim (1987). There is a sink in the south, west of the Quarteira stream, due to either the concentration of abstraction (see agricultural areas in Figure 6.1) or preferential flow lines coinciding with the discharge area at the Olhos d'Agua springs. The groundwater table in the south-east area has very low gradient, from the Marga do Peral division, until the S.Marcos-Quarteira fault line.

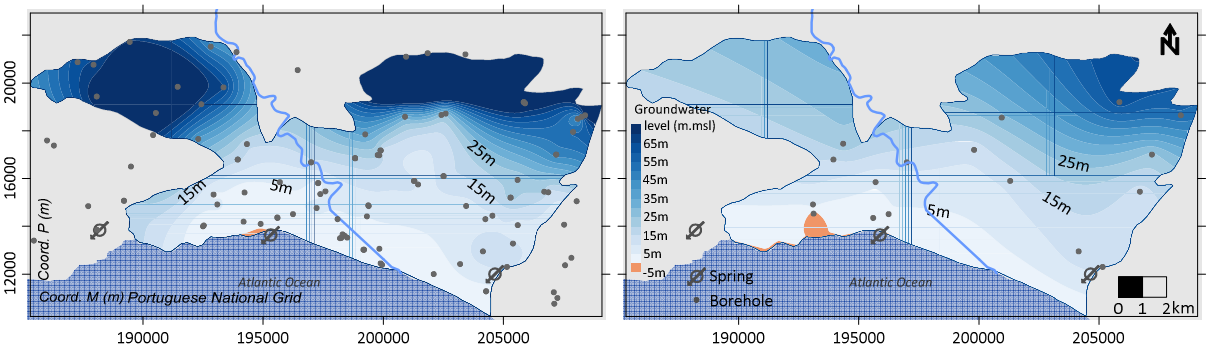

Figure 6.6 Interpolated map of groundwater level of median values from all available data (left) and from median values from 2001-2014 from selected time series (right).

Figure 6.7 presents time series from selected piezometers with the most complete datasets between October 1995 and December 2014 collected from the APA monitoring network. Several zones are identifiable, in agreement with Figure 6.6 (right):

i) Large inter-annual variations (10-20m) with sharp responses to years with extreme rainfall in the north-eastern Santa Barbara de Nexe limestone outcrops (i.e. 606/1049);

ii) Less accentuated inter-annual variation (<10m) and response to rainfall events, that stretches along the eastern limit of the system all the way from north of the Marga do Peral division to the coastline (i.e. 605/1045 and 605/217). In the southern area, it extends through the Miocene aquifer to the western limit, although with lower values (i.e. 605/78 and 605/200);

iii) The only observation point with regular measurements in the Escarpão limestone outcrops (605/326, not shown in graph) does not appear to be representative of the system. This observation point is not located in a well or borehole, but is the water table in an abandoned open air mine. Despite being in agreement with groundwater levels measured in the area (see Figure 6.6, left), the time-series shows little variation (<1m) and is likely measuring a local perched aquifer.

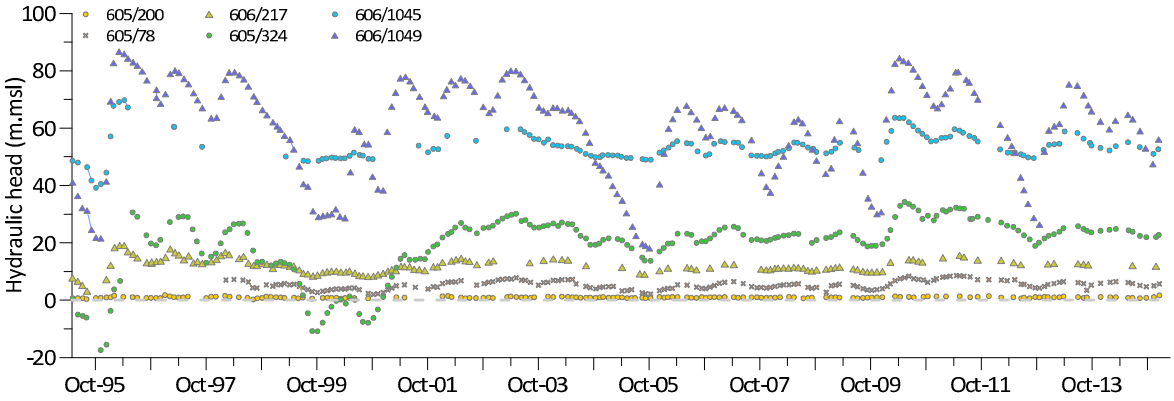

Figure 6.7 Selected groundwater level time series from the APA monitoring network; locations in Figure 6.1.

6.3. Methods

Several efforts to simulate the ARQ and QRT aquifer systems using numerical models have been undertaken for various purposes (Monteiro et al 2002; Monteiro et al 2003; Costa 2006; Monteiro et al 2007b; Costa et al 2013). The focus of the development of these models has been towards the accurate representation of regional hydraulic head and potential for seawater intrusion, with little attention being given to the spatial distribution of discharge along the coastline and stream. As of yet none of these numerical models have presented a definitive representation of the surface/groundwater interface, mostly due to a lack of field data to properly define them. All previous variants of the numerical model considered aquifer limits as defined by Almeida et al. (2000), a constant head boundary condition (BC) equal to mean sea level along the coastline, and no-flow BC at the remaining limits. Previous authors proposed various conceptualizations for stream BC. Constant head BC equal to terrain elevation were imposed on nodes coinciding with the entire reach of the Quarteira stream by Costa (2006). This resulted in groundwater discharge into the stream simulated along stream reaches that are known to be influent, mostly upstream. To resolve this Monteiro et al. (2007) applied constant head BCs (equal to terrain elevation) only along the lower reaches of the stream where a connection between groundwater and stream is known to exist. Subsequently Costa et al. (2013) applied flow constraints in an attempt to eliminate infiltration that was still being simulated along lower reaches of the stream.

Boundary condition types and conceptualization for groundwater flow models, as defined in this paper, are well explained in Reilly (2001). All these conceptualizations suffer limitations in representing the behaviour of the system. Boundary conditions as defined in Costa (2006) and Monteiro et al. (2007) lead to groundwater discharge along stream reaches which are known to be influent, whilst the constraints applied by Costa et al. (2013) ignore infiltration observed along the upper reaches of the stream. Although influent and effluent reaches of the Quarteira stream have been identified, currently there is insufficient data on stream flow for additional calibration of the model.

6.3.1. Numerical Model

The numerical model follows the aquifer limits as defined by Almeida et al. (2000), a constant head boundary condition (BC) equal to mean sea level along the coastline, and no-flow BC at the remaining limits.

The recharge rate determined by Oliveira (2006) (approximately 40%) was applied to the spatial distribution of rainfall proposed by Nicolau (2002), resulting in 33.1 $x10^6$ $m^3.yr^{-1}$ of average annual recharge.

Transmissivity (*T*) values were estimated by Costa (2006) through inverse modelling under steady-state conditions taking into account pumping for public water supply. He first proposed the spatial zoning and distribution of *T* and then performed calibration using the Gauss–Marquardt–Levenberg method, implemented in the nonlinear parameter estimation software PEST (Doherty 2002). Costa et al. (2013) applied the same values of *T* obtained by Costa (2006) as the correlation between observed and simulated hydraulic head was adequate and did not justify the effort of re-calibration. As shown in Figure 6.8, changes in BC do not significantly affect the correlation between observed and calculated hydraulic heads.

The defined conceptual flow model was translated into a 2-D finite element mesh with 5453 elements and 2914 nodes, and solved using the groundwater flow modelling code FEFLOW (Diersch, 2014).

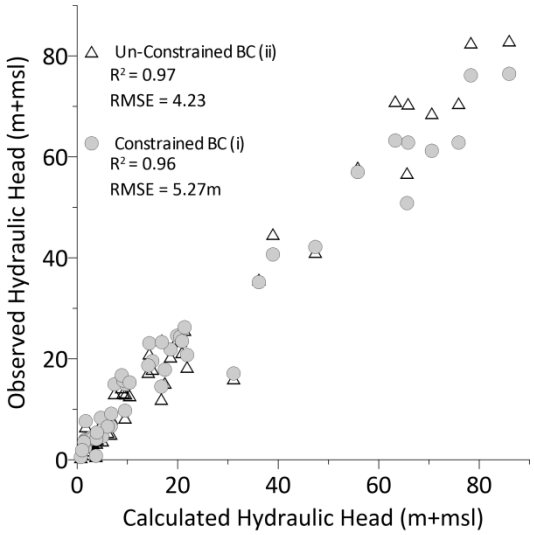

Figure 6.8 Plot of observed *versus* calculated hydraulic head obtained from model with un-constrained (ii) and constrained (i) stream BCs variants, as well as their respective correlation coefficients (R^2) and root mean square error (RMSE)

6.3.2. Steady State Simulations - Epistemic Uncertainty and Groundwater Use Variability

The model variants and scenarios described in this section are all simulated under steady state conditions. To represent the epistemic uncertainty, two model variants are applied representing the two extremes of BC conceptualization: (i) constant head equal to elevation along the lower effluent reach, with constraints to guarantee no recharge from the stream to the aquifer, according to Costa et al (2013); and (ii) constant head equal to elevation along the entire stream without constraints, according to Costa (2006).

Boundary conditions in FEFLOW can be constrained by physical limits, allowing the representation of a broad variety of specific boundary properties (examples include seepage faces, pumps with a minimum water level, and temporal rivers) (Diersch, 2014). Constant head BCs can be constrained by a minimum and maximum flow rate. Stream BCs in scenario (i) are constrained by a maximum flux = 0 $m^3.d^{-1}$, which means that the head BC is only active in case of water flowing out.

Variability in groundwater abstraction is simulated using several abstraction scenarios. Previously described generations of the numerical model simulated both the natural state of the system, with no pumping (scenario a), as well as taking into account pumping for public

water supply (scenario b). Withdrawal rates for public water supply, determined from Municipal Council data, were imposed on nodes corresponding to the location of public supply wells. Withdrawals for private use had so far been ignored due to a lack of definitive data. In order to obtain a better understanding of the range of possible discharge rates, additional abstraction rates for private use for each aquifer system, estimated by Almeida et al. (2000), were distributed uniformly over nodes corresponding to the location of private boreholes currently in use. Abstraction for private supply is taken into account in two scenarios: abstraction for public and private supply (scenario c); and only abstraction for private supply (scenario d). Scenario (c) represents groundwater use at the end of the 1990s, whilst scenario (d) should be indicative of current groundwater use, after public supply wells were abandoned. Table 6.2 presents a summary of all model variants and groundwater use scenarios.

Table 6.2 Summary of water use scenarios and BC model variants applied in the analysis

BC Variant		Water Use Scenario		Code	Transient
i	Constant head equal to elevation along lower effluent reaches; constraints imposed to only allow discharge.	a	Natural state/no abstraction	ia	x
		b	Abstraction for public supply	ib	
		c	Abstraction for public and private supply	ic	
		d	Abstraction for private supply	id	x
ii	Constant head equal to elevation along the entire stream.	a	Natural state/no abstraction	iia	x
		b	Abstraction for public supply	iib	
		c	Abstraction for public and private supply	iic	
		d	Abstraction for private supply	iid	x

6.3.3. Sustainable Extraction Scenarios

Several simulations were developed to analyze the effect of groundwater abstraction for public supply on the sustainability of the aquifer system. Pumping rates to public supply wells were determined as a percentage of average annual recharge, and varied by 5% across a range of transient simulations. Total amount of annual abstraction equal to a percentage of average annual recharge, was distributed over the year according to average monthly values registered for public supply wells between 1991 and 2001. Abstraction from private supply wells was not varied (hence maintained at the levels of scenarios (c) and (d)), as this represents a more likely scenario for water management. The obtained pumping rates were

applied to the model variant with lowest storage coefficient (S = 0.01) representing the worst-case scenario: (see section 0). In order to test whether locating abstraction further away from sensitive areas (coast and stream) would increase the sustainable abstraction rate, all public supply wells within 1.5 km were removed and all pumping concentrated in the remaining wells.

6.4. Results and Discussion

6.4.1. Steady State BCs and Groundwater Use Scenarios

Figure 6.9 shows simulated discharge rates for the various BC variants and groundwater use scenarios of the steady state simulations. Here the discharge rates for the various discharge areas (stream, ARQ Coast, and QRT Coast) are compared.

Stream BC type does not appear to have a significant impact on coastal discharge under natural conditions. On the other hand, groundwater discharge to the stream increases in scenario (ii) to compensate for the recharge from the stream (infiltration) in other reaches. Stream infiltration increases once groundwater withdrawals are included. It is interesting to note that this induced recharge reduces the effect of abstraction on coastal discharge rates for the (ii) BC scenarios. Subsequently, the difference between coastal discharge estimates for different BC variants increases with increase in groundwater abstraction. An average annual flow of 43.2×10^6 m^3, from 2001 to 2012, was measured by a stream gauge installed at the northern limit of the aquifer systems (location in Figure 6.1). Therefore, recharge from the stream can be considered as being within an acceptable range. However, as there are no stream flow measurements for the lower reaches of the stream, it is impossible to determine how accurately the model simulates this process.

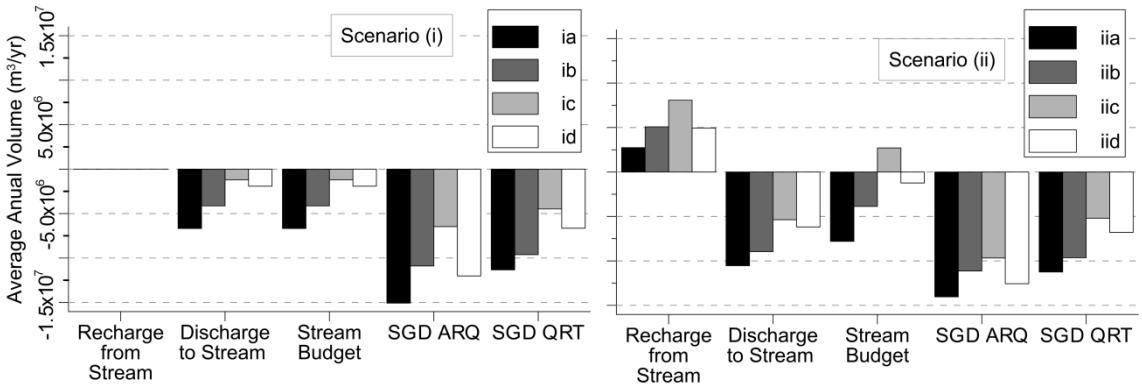

Figure 6.9 Comparison of water budget components for the two boundary condition model variants (i and ii) and groundwater use scenarios (a-d)

The only scenario to result in an influent stream budget is scenario (iic). This is due to the drawdown caused by the pumping close to the stream, which leads to both a decrease in discharge to the stream and increase in induced recharge from the stream. Considering the large seasonal variability in the region of both rainfall (and therefore stream flow) and water use, it is likely that this induced recharge may be overestimated as drawdown will be greatest during periods in which the stream is most frequently dry. This is discussed further in the following section when discussing the cyclic transient state scenarios.

As described previously, the interaction between the stream and aquifer system is not yet clear. Water can be seen in the stream all year round from the mouth to approximately 7 km upstream. Stream elevation at this point is approximately 15 m above mean sea level, meaning that the water is fresh and not intruding from the sea. There is no data on whether the stream gains or losses water above this point during the wet season. However, it is certain that it does not gain water during the dry season. The cumulative plot of simulated discharge values along the stream length gives a representation of flow down the length of the stream (Figure 6.10). For the constrained BC variant (i) no interaction occurs above the 7 km point. Downstream from the 7 km point, the stream is effluent for water use scenarios (a) and (b). Once abstraction for private use is taken into account, aquifer contribution to stream flow reduces significantly and only occurs within the last kilometre. Thus, scenarios (ia) and (ib) match observed behaviour, whilst (ic) and (id) do not. This suggests that private use may be overestimated or the spatial distribution of the abstraction rates is inaccurate

and too concentrated near the stream. The surface/groundwater interaction for BC variant (ii) is almost completely opposite. All water use scenarios have an overall effluent stream behaviour between km 2 and km 9 from the aquifer's northern border. There are small occurrences of groundwater recharge from the stream, but they are not significant. The stream becomes influent at km 9 in all scenarios. In the natural state scenario (iia), it quickly recovers, becoming effluent for the remainder of its course. The remaining water use scenarios only revert to effluent streams much closer to the sea. Scenario (iic) is the only water use scenario in which the stream is simulated as dry along the lower (known to be) effluent reach. This is likely due to the same reasons discussed for scenarios (ic) and (id). There is sufficient discharge along the upstream reaches in scenarios (iia), (iib) and (iid) to offset any losses along the lower reach and thus maintain water in the stream. However, there is no data or reports of discharge along the upper reaches of the stream to validate this conceptualization.

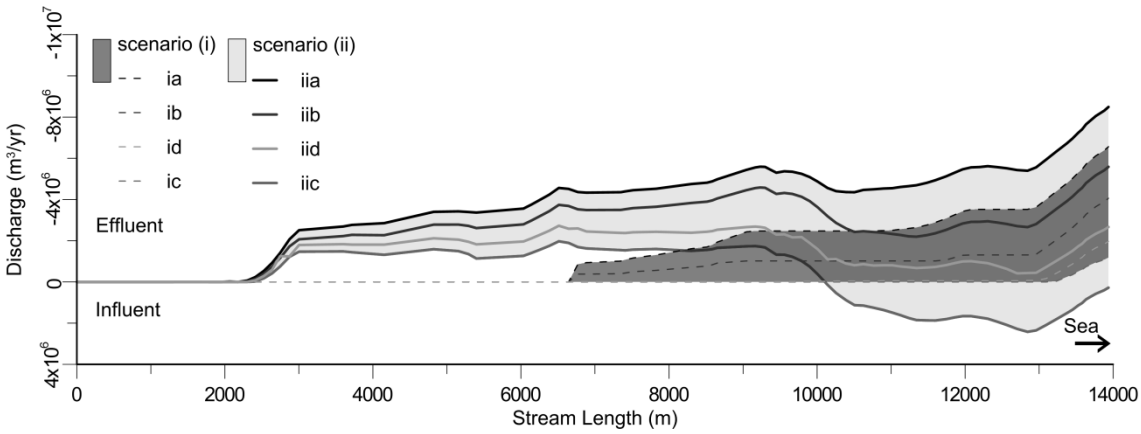

Figure 6.10 Cumulative simulated discharges along the Quarteira stream; water use scenarios are, from top to bottom, a, b, d and c

Scenario results show that abstraction from private boreholes has a greater impact on stream discharge and QRT coastal discharge than abstraction for public supply, whilst the opposite occurs for ARQ coastal discharge to a lesser extent. This is due to the spatial distribution of pumping over the two systems. As shown in Figure 6.1 there is a large concentration of private boreholes located near the stream, and private supply abstraction is estimated at 2.5 times higher from QRT than from ARQ. On the other hand, public supply

abstraction is greater from the ARQ, hence the greater impact on coastal discharge from this system for scenarios (b) and (c).

Taking a closer look at the spatial distribution of discharge along the coastline reveals that although discharge along the QRT is relatively uniform, ARQ shows a more heterogeneous distribution. Figure 6.11 illustrates the variation in discharge rate for scenario (ia), in which no abstraction is in effect, to remove any potential interference from pumping. Higher discharge rates along the ARQ coast coincide with inlets at the coastline. Effectively this is due to the BC being further inland, and therefore creating a higher hydraulic gradient at these points. The area with the highest discharge rate coincides with the Olhos d'Agua beach where many significant intertidal springs exist. In fact, between 30-35% of ARQ coastal discharge occurs along the inlet corresponding to Olhos d'Agua. Apart from coinciding with the most inland point of the coastline, it is also the most direct path between the high recharge Jurassic lithologies to the north and the discharge area. Although there is no definitive data on sub- and intertidal spring flow rates or distribution to confirm these simulations, the results do offer an explanation for the high concentration of springs at Olhos d'Agua. The model is an equivalent porous model and does not in fact represent conduit flow, characteristic of limestone areas. However, the dissolution process associated to karst conduit development accelerates along preferential flow paths (more water leads to more dissolution) (Groves and Howard 1994; Domenico and Schwartz 1997). Therefore, it is conceivable that the preferential flow suggested by the model could have favored karst development along the path to Olhos d'Agua.

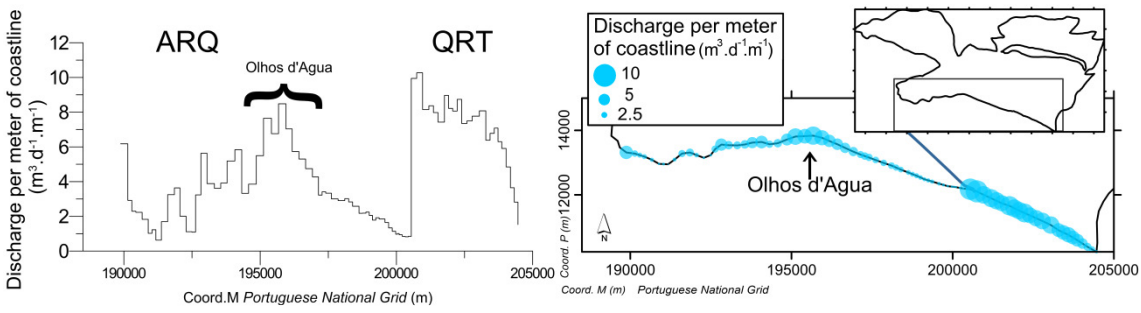

Figure 6.11 Calculated coastal freshwater discharge per meter of coastline for scenario (ia)

On the other hand, this behaviour may also just be an artefact of the conceptual model. Some authors suggest that the Jurassic lithologies may extend under the low permeability Cretaceous formation in the west portion of the ARQ (see Figure 6.2 and Figure 6.3), and connect with the Miocene in the south (Bronzini 2011). However, due to the complex geological structure of the area it is unclear whether a hydraulic connection exists. Ongoing fieldwork is currently attempting to answer this question, applying geophysical methods to determine the thickness and angle of the overlying cretaceous layer. Should these results show that there is a connection, overall groundwater budget values will not change, however the spatial distribution of discharge from the ARQ system will probably be different.

Spatial variation in discharge rates reinforces the need to take into account the location of abstraction when defining sustainable yields (Hugman et al 2012). On one hand there is a greater likelihood of seawater intrusion if abstraction is located closer to low discharge rate areas, and on the other there will be a greater effect on intertidal springs and SGD (and subsequently any GDEs) if pumping is closer to these areas. This is a highly complex matter and the available groundwater resources and the needs of the various water users have yet to be properly identified and quantified. Impact of SGD on the marine ecosystems has been demonstrated (Encarnação et al 2013) but a quantifiable relationship has yet to be defined. Currently there are ongoing efforts to identify and measure SGD along the ARQ and QRT coast which should lead to a better comprehension of ecosystem variations between sites seen by Encarnação et al. (2013).

Transient Cyclic Scenarios of Seasonal VariationFigure 6.12 and Figure 6.13 present the range of aquifer discharge rates obtained from the transient cyclic scenarios with a range of values of *S* for both BC variants. The effect of pumping and its seasonality, as well as the seasonal distribution of recharge on discharge rates is evident. Furthermore, the seasonal variation in discharge rates at the coast is generally greater than the difference in discharge rate between the two BC variant estimates. This underlines the importance of taking into account seasonality when assessing epistemic uncertainty in groundwater modelling.

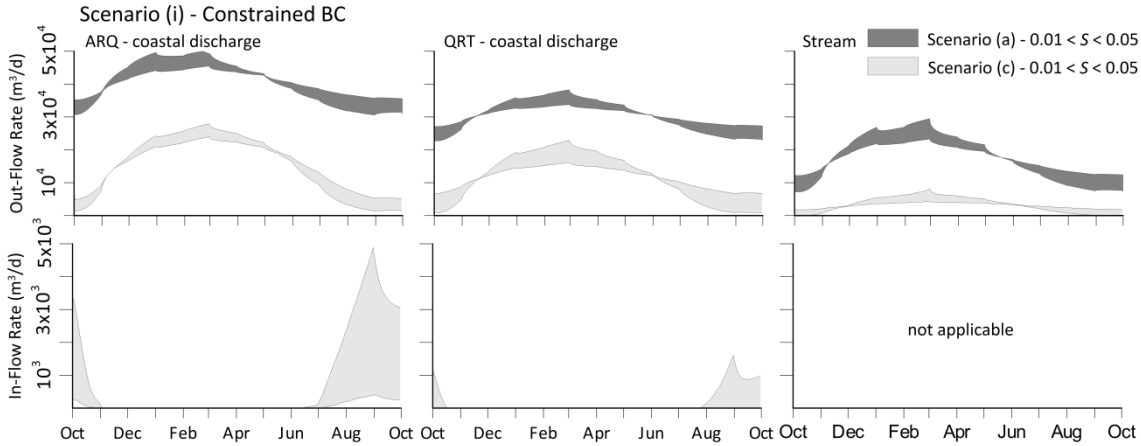

Figure 6.12 Range of calculated flow out (top) and in (bottom) to the aquifer system along the ARQ coastline, QRT coastline and stream (left to right) for an average recharge year, considering constrained BCs at the stream (Scenario i)

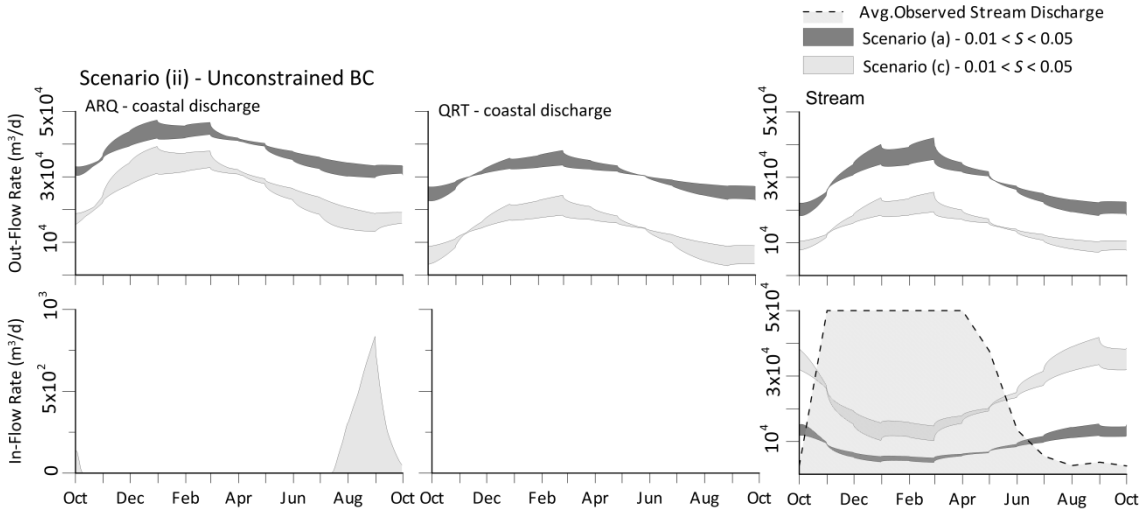

Figure 6.13 Range of calculated flow out (top) and in (bottom) to the aquifer system along the ARQ coastline, QRT coastline and stream (left to right) for an average recharge year, considering un-constrained BCs at the stream (Scenario ii)

Encarnação et al. (2013) found that there was an increase in species diversity during the spring season at the location under SGD influence, but not at the control location. This matches the highpoint of simulated discharge rate (see Figure 6.12 and Figure 6.13). Simulation results confirm that this localized seasonal variation in biodiversity is linked to discharge from the aquifer system. Natural state scenarios (ia) and (iia) do not present significant differences in terms of coastal discharge for the two BC variants. Groundwater abstraction (scenario c) leads to both a decrease in overall discharge rates as well as an increased amplitude of seasonal variation of discharge. The latter is due to the periods of

greater abstraction coinciding with low recharge. This increased amplitude is more evident for BC scenario (ic) than (iic) due to the attenuating effect of induced recharge from the stream in scenario (ii). This effect is partially artificial due to constant BCs, as will be discussed below.

Unlike the steady state scenario, transient scenarios (ic) and (iic) show occurrences of localized gradient inversion during short periods along the ARQ and the QRT, though much less significant for the unconstrained BC model variant (ii). Despite the systems recovering rapidly at the beginning of the subsequent rain season, water quality in the area could be at stake due to an increased risk of seawater upconing and localized seawater intrusion, particularly in karstified limestone aquifers. Once more, these results demonstrate that ignoring seasonal variation can lead to misleading results. Likewise, the inter-annual variation in recharge will likely have a significant effect on discharge rates. By applying average monthly and yearly rainfall values to determine recharge, this effect has not been considered. Considering that current climate change predictions for the region indicate greater inter-annual variation and greater seasonal concentration of rainfall (Stigter et al., 2014), a more comprehensive analysis of the effect of changes in recharge is necessary.

Induced recharge in BC scenarios (ii) has an inverse behavior to stream discharge. As mentioned previously, the only stream gauge is located at the uppermost limit of the aquifer system (see Figure 6.1 for location). Therefore, there is no data on how much water is gained/lost between the aquifer and stream. However, this gauge does provide a value of total available water in the stream before crossing the aquifer. Therefore, it can be stated that this is close to the maximum amount of water that may become recharge, ignoring surface runoff in the small downstream catchment area. Monthly averages of existing data (from 2001 to 2012) are compared to simulated recharge from the stream in the lower right plot of Figure 6.13 (maximum values are cut off at $5x10^4$ $m^{3.}d^{-1}$ in order to fit the plot). During the rainy season (November to May) stream flow is sufficient to satisfy simulated values of groundwater recharge. However during the remaining months it is significantly lower and thus the model is largely overestimating recharge from the stream during this period, explaining the largely reduced inflow rate at the coastline, as compared to the

constrained BC model variant (i). These results show that a more complex model, with time-varying BCs to match the seasonal variation of stream flow, is needed to simulate this effect and further constrain the range of results.

6.4.2. Determining Sustainable Groundwater Abstractions

Defining *sustainable use* is a complex matter. Different criteria can be taken into account, depending on what is considered necessary in order for groundwater use to be sustainable. From a resource management point of view, maintaining groundwater quantity and quality is foremost. From an environmental point of view, maintaining ecological flow to GDEs should be added to the previous criteria. The Water Framework Directive (WFD) requires that EU member states implement action plans (which are a mandatory part of the River Basin Management Plans) to meet the general goals of attaining good quantitative and qualitative status of groundwater bodies, as well as good chemical and ecological status of (inland, transitional and coastal) surface water bodies, which in many areas constitute GDEs at least to a certain degree. As such, the main concern for the ARQ and QRT in regards to water quantity and quality relates to avoiding seawater intrusion and protecting the GDE associated to the effluent reaches of the Quarteira stream and submarine springs. Although a relationship between biodiversity and SGD has been identified in the area (Encarnação et al., 2013), minimum flow rates required by the ecosystems have thus far not been determined. In an estuary located nearby the macroinvertebrate community structure was also seen to respond to the seasonal differences in salinity between summer and winter, with a higher impact from groundwater discharge into the channel during winter (Silva et al 2012). It was therefore concluded that changes in macroinvertebrate communities can constitute early warnings of reductions of aquifer discharge, which is particularly useful where monitoring submarine groundwater discharge is difficult. Despite not yet being able to set a minimum target flow for GDEs as one of the criteria for sustainable use, it is possible to say what the effect of a given pumping scheme will have on the flow distribution and rate. On the other hand, the seawater intrusion criterion is clearly an important one, as it impairs the use of groundwater for drinking water or irrigation, and has been found to occur to a moderate extent in municipal public supply wells in the studied aquifers.

Table 6.3 summarizes the effects of varying public supply pumping rates and well location. Results from the current numerical model do not take into account the effects of varying density nor transport phenomena between fresh and seawater. Thus, the effect of pumping on the location of the salt-freshwater interface is not analyzed. The inversion of the hydraulic head gradient is used as the criteria for sustainable yield, keeping in mind that, due to the above mentioned phenomena, it is possible that water quality problems may occur prior to reaching these abstraction levels.

Table 6.3 Minimum simulated discharge rates along the coast and occurrence of seawater intrusion for a range of public supply ($P_{pub.s}$) pumping rates; P - pumping rate; R – recharge; $P_{private\ supply}$ - 1.25E+07 $m^3.yr^{-1}$

Scenario	$P_{pub.s}$ ($m^3.yr^{-1}$)	$P_{pub.s}/R$	P_{total} ($m^3.yr^{-1}$)	P_{total}/R	Gradient Inversion	Min.Discharge Rate ($m^3.d^{-1}$)
(ia)	0.00E+00	0%	0.00E+00	0%		6.10E+04
(ic)	0.00E+00	0%	1.25E+07	38%		2.57E+04
	1.66E+06	5%	1.42E+07	43%		2.04E+04
	3.31E+06	10%	1.58E+07	48%		1.53E+04
	4.97E+06	15%	1.75E+07	53%	x	1.02E+04
	6.62E+06	20%	1.91E+07	58%	x	5.97E+03
	8.28E+06	25%	2.08E+07	63%	x	3.36E+03
(ic) conc. abstraction	0.00E+00	0%	1.25E+07	38%		2.58E+04
	1.66E+06	5%	1.42E+07	43%		2.04E+04
	3.31E+06	10%	1.58E+07	48%		1.57E+04
	4.97E+06	15%	1.75E+07	53%		1.08E+04
	6.62E+06	20%	1.91E+07	58%	x	6.66E+03
	8.28E+06	25%	2.08E+07	63%	x	4.18E+03

Inversion of the hydraulic head gradient, allowing coastal waters to flow inland, occurs with public supply rates equal or higher than 15% of the annual recharge with all public wells in use (total pumping rate exceeding 53%). This amounts to $3.31x10^6$ $m^3.yr^{-1}$, significantly lower than the $8.43x10^6$ $m^3.yr^{-1}$ registered during 1999. When abstraction is concentrated to wells at least 1.5 km away from BCs, gradient inversion only occurs once annual abstraction values are 20% of annual recharge ($4.97x10^6$ $m^3.yr^{-1}$). In agreement with Hugman et al. (2012), these results demonstrate that the spatial distribution of abstraction has as significant impact on sustainable yields in coastal aquifers. Furthermore, the difference in minimum

discharge rate between distributed and concentrated abstraction increases with the increase in pumping rate. Therefore, although a sustainable level of abstraction to guarantee ecological flow cannot be specified, it can be stated that well location will influence the maximum rate of abstraction that can be maintained without affecting other groundwater users.

6.5. Conclusions

A numerical groundwater flow model supplied initial estimates of coastal freshwater discharge for the ARQ and QRT systems as well as sustainable levels of groundwater use. Uncertainty regarding the surface-groundwater interactions along the Quarteira stream was included in the results by simulating two conceptualizations of the BC. Steady state simulations indicate that the system contributes a range of average annual freshwater to coastal discharge between 6.5 $x10^6$ $m^3.yr^{-1}$ and $15x10^6$ $m^3.yr^{-1}$ from the ARQ, and 4.5 $x10^6$ $m^3.yr^{-1}$ and 11.3 $x10^6$ $m^3.yr^{-1}$ from the QRT. Furthermore, there is significant spatial variation, in particular for the ARQ, with almost 30% of the discharge from this system occurring at the Olhos d'Agua area.

Seasonal variation in discharge rates is greater than the difference between the two BC variants estimates of average annual discharge rates under steady state. Despite steady state simulations resulting in consistently positive water budgets, seasonal variability inherent to these systems can lead to inversions of the hydraulic head gradient during short periods. It is likely that the effect of seasonality will increase with the higher concentration of rainfall during shorter periods predicted to occur during the next 50 years in this region. Furthermore, transient simulations of scenario (ii) demonstrated that this conceptualization of the BC leads to overestimates of stream recharge. Future efforts to simulate the ARQ and QRT systems should take into account the seasonal variation of stream flow to characterize the ground/surface water interaction and thus further constrain the range of results.

A preliminary analysis of sustainable levels of groundwater abstraction for public supply was developed, considering the worst-case model variant. Results indicate that historical levels of abstraction are not sustainable, but up to $3.31x10^6$ $m^3.yr^{-1}$ could be abstracted from

existing well fields without causing an inversion of the hydraulic head gradient. However, by placing abstraction further from the coast, sustainable yield can be increased significantly. As these values are based on simulations that ignore the existence of a saltwater wedge (caused by differences in density between fresh and saltwater), it is likely that water quality problems would occur at lower abstraction rates.

These results reflect the significant uncertainty that still exists in regards to the hydrogeological knowledge of these systems. In order to constrain coastal discharge estimates further, more detailed data on recharge, stream flow and abstraction rates is required. Although the discussed 2D flow model supplies an estimate of discharge values and distribution, considering the coastal nature of the aquifer system, developing a model that takes into account the fresh-saltwater interface effect could significantly improve results. Such a model, taking into account the 3D structure of the system, would further constrain discharge rates as well as be a powerful tool to determine areas where freshwater SGD is more likely to occur.

7. Offshore Freshwater in the Albufeira-Ribeira de Quarteira aquifer system – Algarve, Portugal

Recent data acquired by the multidisciplinary research project FREEZE (PTDC/MAR/102030/2008) identified signs of SGD several kilometres from the shoreline of the Albufeira-Ribeira de Quarteira (described in the previous chapter), which has led to a new conceptual model of the aquifer system to be proposed. In the following chapter, numerical models are applied to test the feasibility of the conceptual model. Due to the high computational demand of variable density modelling, in an initial phase simplified two-dimensional cross-section models are used to test the conceptual model and reduce uncertainty in regards to model parameters for future work.

7.1. Introduction

The *Albufeira-Ribeira de Quarteira* (ARQ) aquifer system on the south coast of Portugal is an important source of groundwater for agriculture and tourism, as well as contributing to significant freshwater discharge along the coast in the form of inter- and sub-tidal springs, and maintaining groundwater dependent ecosystems along the *Quarteira* stream (Hugman et al 2014).

The ARQ aquifer system is described in Almeida et al. (2000) and has been described in detail in the previous Chapter 6. The aquifer systems develop mostly within lithologies dating from the Miocene and Jurassic, believed to be separated by low permeability Cretaceous formations. The two water bearing layers are thought to be connected in the central/eastern section, where the Miocene directly overlies the Jurassic (see Figure 7.1).

Geophysical methods have recently been applied to update the existing hydrogeological conceptual model, along with an analysis of available borehole logs and water level and quality (Francés et al 2015). Results verified the existence of the confining Cretaceous formation in the south; however, were unable to confirm explicitly the connection between Jurassic and Miocene formations. Furthermore, during several offshore field campaigns

submarine springs and indications of freshwater discharge were found several kilometres from the shoreline (Sousa et al 2014).

Submarine groundwater discharge (SGD) in the area was investigated within the scope of a multidisciplinary research project FREEZE (PTDC/MAR/102030/2008), which aimed to identify and characterize groundwater flow from the coastal strip towards the continental platform, taking into account structural geology, marine geology and the effects of the hydrological/hydrogeological conditions on associated ecosystems. As well as near shore submarine springs, signs of SGD were found several kilometres from the shoreline during offshore CTD and geophysical surveys (Francés et al 2014; Sousa et al 2014; Fernandes et al 2015). On-land geophysical and offshore seismic surveys supplied data to update the conceptual model of the aquifer system (Francés et al 2015). These authors propose the existence of an offshore continuation of freshwater, created by the existence of a confining layer overlying the water bearing Jurassic aquifer.

Numerical models were applied to test the possibility of an offshore continuation of fresh groundwater over several kilometres under local conditions. Due to the high computational demand of variable density modelling, in an initial phase simplified 2D cross section models were used to test the conceptual model and reduce uncertainty in regards to model parameters for future work. This represents the initial step in developing and calibrating a three-dimensional regional scale model of the system, which aims to supply an estimate of the spatial distribution of SGD as well as serve as a decision support tool for the local water resources management agency.

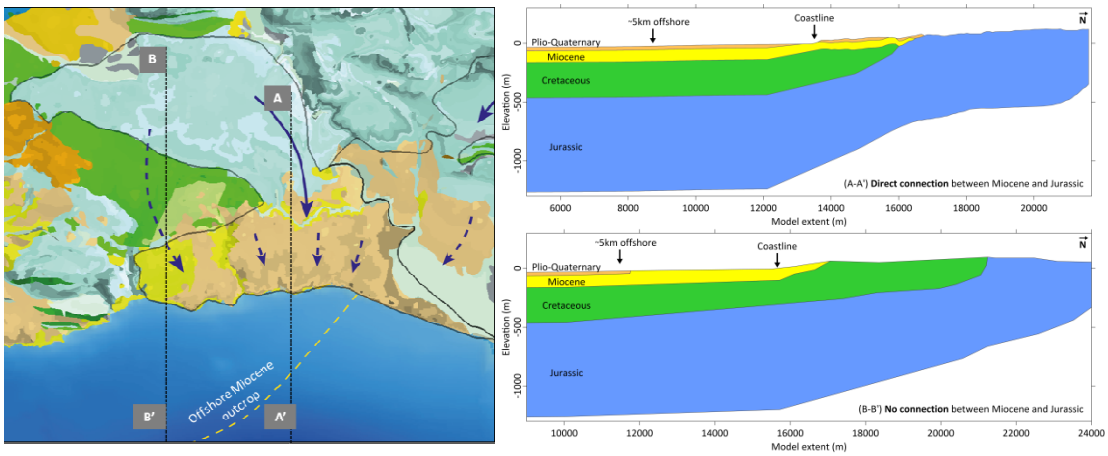

Figure 7.1 Hydrogeological conceptual model (left) and cross-sections of the geological model developed by Francés et al (2015) (right).

7.2. Numerical flow and transport model

Two cross-section density-coupled flow and transport model of the ARQ were developed, and solved using the finite element method as applied in the commercial code FEFLOW (Diersch 2014). Finite element meshes were generated based on the two representative cross-sections of the hydrogeological model previously developed by Francés et al (2015) with an additional 15 km offshore extent.

Constant equivalent freshwater head (flow) and saltwater fraction (mass) BC were assigned along the border of the models corresponding to the sea. Recharge was imposed using flux BC, along the borders corresponding to the outcrops of Miocene and Jurassic units. Recharge over the Cretaceous was ignored as most rainfall over these outcrops is considered to be lost to runoff. When simulating post-development periods, abstraction was subtracted directly from imposed recharge to avoid localized effects of pumping.

Uniform values of hydraulic conductivity (*K*) were assigned to the three geological units, assuming a 0.1 anisotropy ratio between horizontal and vertical conductivity. Data from pumping tests and estimated from transmissivity and borehole depths in the literature was used to obtain a range for *K* values for Miocene and Jurassic units (

Figure 7.2). Parameter values where then calibrated by trial-and-error for all units, aiming to improve the fit between simulated and average observed values of on-shore hydraulic head and obtain a 5 km offshore extent of freshwater.

Longitudinal and transversal dispersivity were assumed as 30 m and 3 m respectively. A uniform value of 0.3 for effective porosity was assigned to the entire domain, according to values referenced in Silva (1988).

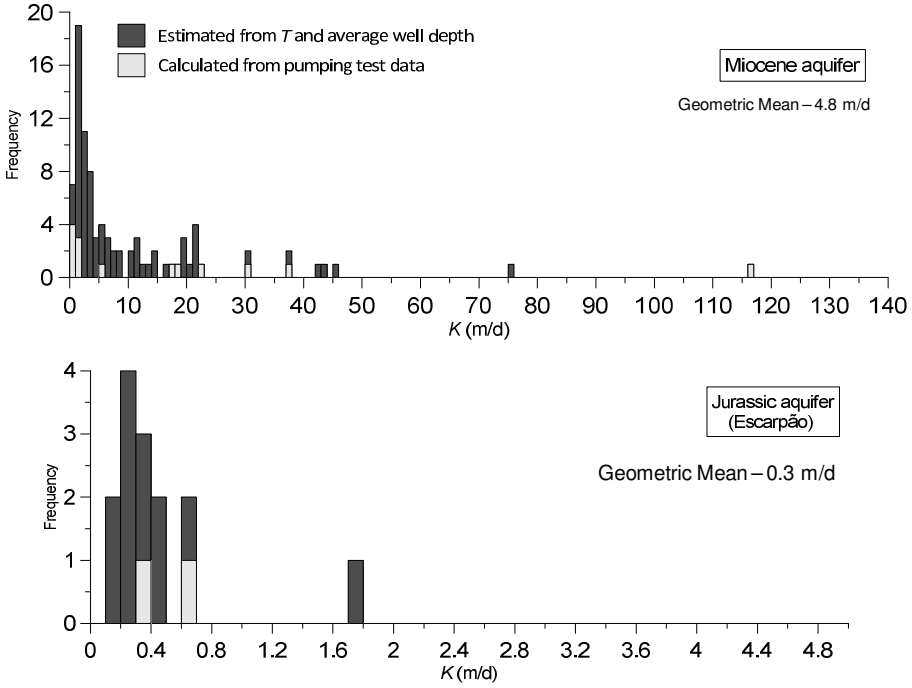

Figure 7.2 Histogram of hydraulic conductivity collated from pumping tests and estimated from transmissivity and borehole depth data in the literature.

7.3. Results and Discussion

Figure 7.3 presents the simulated distribution of seawater within the ARQ for both model variants. In both cases fresh or brackish water extends up to approximately five kilometres offshore. The thickness of the mixing zone is significantly different between the two variants. When the Miocene and Jurassic layers are directly connected the mixing zone is approximately twice the width of the un-connected variant.

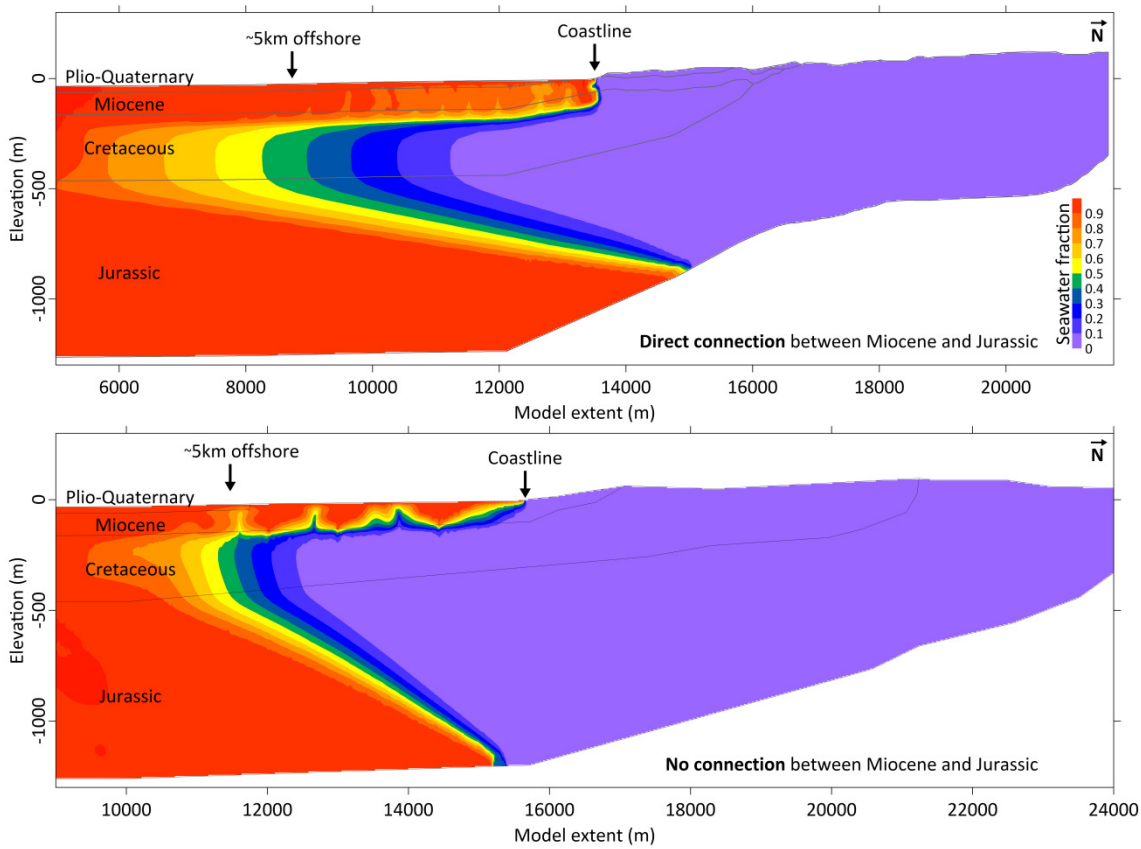

Figure 7.3 Simulated position of the fresh-saltwater interface after 50 years of groundwater withdrawals for both conceptual models of the ARQ.

The relative proportions of offshore diffuse SGD and discharge at the coastline are also distinct. In the connected variant, essentially all (99%) of freshwater discharge occurs at the coastline. When the Miocene and Jurassic are entirely separated by the Cretaceous, discharge at the coastline merely accounts for 80% of total SGD with the remaining 20% occurring as diffuse seepage offshore. In practice offshore SGD probably occurs via fractures and dissolution channels. In fact the surveys by Sousa et al (2014) show greatest indications of SGD at depths of 13-20m, which coincide with paleo-coastlines during the last the thousand years as defined by (Dias et al 2000). According to Fleury et al (2007), discharge from karst aquifers creates dissolution networks and springs at the at the lowest outcrop point of the carbonate rocks, which in coastal aquifers is sea-level. Marine transgression floods these springs, but the submerged networks can continue to discharge the groundwater, creating submarine springs (Fleury et al 2007).

These results show that, in the directly connected case, the offshore freshwater is effectively stagnant. Any additional recharge to the system will tend to flow out through the Miocene aquifer. In this case the position of the fresh-saltwater interface is controlled by the equilibrium between seawater and freshwater pressure within Jurassic aquifer, where it becomes confined. On the other hand, the position of the interface and ratio of coastal to offshore SGD in the un-connected variant is controlled by the vertical resistance to flow and the on-shore length of the aquifer layers. Further work in understanding the relative impacts of these factors and how they influence temporal dynamics of flow and discharge is necessary to understand how these systems are affected by seasonal variability and changes in groundwater use.

Both model variants are able to adequately represent average on-shore groundwater levels and maintain a 5 km offshore freshwater extent. However, the variant which assumes a direct connection between the Jurassic and Miocene layers requires higher *K* for the Miocene aquifer (20 $m.d^{-1}$ *vs* 5 $m.d^{-1}$). Despite being higher, these values are within the acceptable range and cannot be ruled out. The area in which the Miocene is thought to directly overly the Jurassic is a relatively small portion of the system. Higher *K* can be accounted for if the direct connection between the two layers is considered as a localized effect, enhanced by the presence of karsification. This would agree with the proposed hypothesis that preferential flow paths have contributed to accelerated karst conduit development (Kiraly 1975; Groves and Howard 1994; Domenico and Schwartz 1997) towards the Olhos d'Agua springs discussed in the previous Chapter 6.

It is likely that in practice connectivity between the layers varies within the system. Not connected in the western section where the Cretaceous layer outcrops and connected in the east where it does not. Model results do not provide a definitive answer on the connectivity of the two aquifer layers. However they do show that in either case offshore freshwater is feasible, re-enforcing the hypothesis for the existence of an offshore freshwater wedge.

Simulated results are far from being a definitive representation of the ARQ, as this aquifer system has large lateral heterogeneity (there are significant changes from east to west in thickness, lithology, abstraction, etc.). A fully three-dimensional model is necessary to

properly assess the hydrogeological behaviour of this system. However, these simple cross-section models do provide a computationally (relatively) cheap manner in which to test basic assumptions regarding the conceptual model of the aquifer.

7.4. Conclusions

Numerical model results support field studies that identified freshwater SGD several kilometres off the coast of the ARQ aquifer system. This represents the initial step in developing and calibrating a 3D regional scale model of the system, which aims to supply an estimate of the spatial distribution of SGD as well as serve as a decision support tool for the local water resources management agency.

Although far from definitive, simulations suggest that the regional behaviour of the ARQ is better represented by the conceptual model that considers no direct connection between the Jurassic and Miocene aquifer layers. In this case offshore SGD accounts for 20% freshwater discharge to the ocean. Allowing for a direct connection between the aquifers leads to all discharge occurring at the coastline, which does not agree with observed offshore SGD.

Confirming the existence of this potential offshore freshwater would be of interest from a management perspective, as it could represent a significant volume available at less risk from saltwater intrusion.

7.5. General remarks on offshore fresh groundwater management and potential in the Algarve

Studies using numerical and analytical models have shown that freshwater can extend far beyond the coastline in aquifers that are overlain by low permeability layer (Kooi and Groen 2001; Bakker 2006). SGD from these offshore extents occurs slowly by upward flow through the confining layer across extensive areas (Moore 2010; Post et al 2013). For carbonate aquifers with dissolution-formed flow conduits, discharge is often in the form of submarine freshwater springs (Taniguchi et al 2002; Fleury et al 2007; Moore 2010). However, when

compared with the near-shore zone, relatively little is known about the dynamics of submarine groundwater systems at this scale (Bratton 2010).

The existence of extensive, low permeability formations can results in large quantities of trapped freshwater stored offshore. These were usually formed during previous periods in which sea-level was lower and the current seabed was exposed to freshwater recharge (Ouazar and Cheng 2003). Sea level rise to present day conditions will naturally cause a decrease in the offshore freshwater volume, although the fresh-saltwater interface may remain offshore depending on aquifer properties. In either case, this process of natural SWI can be in the scale of thousands of years.

As a side note, this fact makes obtaining a numerical representation of the system at dynamic equilibrium very time consuming. Models that are already computationally expensive, need to be simulated for extremely long run times before equilibrium (i.e. steady-state) is achieved.

Groundwater abstraction from confined and semi-confined coastal aquifers can significantly accelerate the SWI process (Ouazar and Cheng 2003). Any increase in abstraction will cause a decrease in on-shore freshwater pressure and thus landward movement of the fresh-saltwater interface. This is effectively the same as a decrease in recharge. However, in practice groundwater withdrawals can be mining the offshore freshwater instead of capturing renewable recharge. This is particularly the case in highly permeable systems with low storage and subject to high seasonal variability in recharge and abstraction (Hugman et al 2013a). However, abstraction can still occur for decades with no observed decrease in on-shore groundwater quality.

The dynamics and time-scales of these systems provide both challenges and opportunities for groundwater resource management. On one hand, if the hydrogeological systems and processes are not well understood by users and managers and a significant portion of withdrawals are mining offshore freshwater, then coastal groundwater resources may be over-allocated and over-exploited as there are no visible negative impacts in the short- to mid-term. However, once SWI reaches the onshore portion of the aquifer, decreasing water quality will force users to find alternative sources of supply. An example of this is the

Campina de Faro (CF) aquifer (Algarve), where there have been large drawdowns near the coast for over 30 years but water quality has only started to decrease during the last few years. Considering current climate change predictions for increased water scarcity, this may have significant economic and social impacts on regions dependent on these coastal aquifers. Depleting offshore freshwater and thus reducing or eliminating offshore freshwater SGD will also cause negative impacts on unique coastal groundwater dependent ecosystems. It is important to pre-emptively identify aquifer systems with adequate characteristics for offshore freshwater and put comprehensive management plans into place in order to protect both the resource and the various competing users.

On the other hand, confined or semi-confined coastal aquifers may provide useful conditions as water reservoirs. As the fresh-saltwater interface moves at a slow rate and is located offshore (can reach tens or hundreds of kilometres, depending on the characteristics of the system), groundwater mining can be used in the short-term without significant impacts. This makes these systems particularly useful as backups or sources for emergency water supplies during periods of drought, as they can be overexploited without immediate risk of SWI. They also present practical characteristics for managed aquifer recharge. By increasing recharge to the system, onshore hydraulic pressure will induce saltwater movement away from land and increase the volume of offshore freshwater. As in any coastal aquifer, increased recharge will eventually be lost as discharge to the sea, however the longer residence times in a semi-/confined system will make injected water available for re-capture for longer, making them more useful for inject and store MAR schemes.

There are several aquifer systems in the Algarve with characteristics that may allow for the formation of offshore freshwater. As shown in the current chapter, there is strong evidence that the ARQ system has extensive offshore SGD and freshwater reserves. The neighbouring *Quarteira* (M7) system, described in Chapter 6, presents similar conditions with an additional confining layer overlying the Miocene aquifer.

Further east, the main aquifer systems within the Ria Formosa catchment (M8-M15 in Figure 7.4) are characterized by limestone and highly karstified dolomites from the Jurassic and marl limestone from the Cretaceous, overlain to the south by sandy-limestone and detritic

(sands and silt) formations from the Miocene and Plio-Quaternary. Freshwater within the *Campina de Faro* (M12) is known to extend beneath and discharge into the Ria Formosa lagoon. However there is no data on the position of the fresh-saltwater interface. SWI processes in this system are further discussed in Chapter 9. Although the Cretaceous formations in this sector of the Algarve are productive, they are composed of intercalated layers of limestone and marl. These layers create confining conditions for both the Cretaceous and Jurassic formations. The highly karstified limestone of the Jurassic formations are characterized by high permeability and recharge rates, but low storage capacity. Despite the significant amount of recharge and low abstraction rates, there are no large springs or other evident surface discharge zones to account for excess water budget. Recharge over these formations has been assumed to provide lateral recharge to the downstream aquifers, however a portion may flow beneath the confining layers (Stigter et al 2007) and occur as offshore SGD either at the embayment or shelf scale (Bratton 2010).

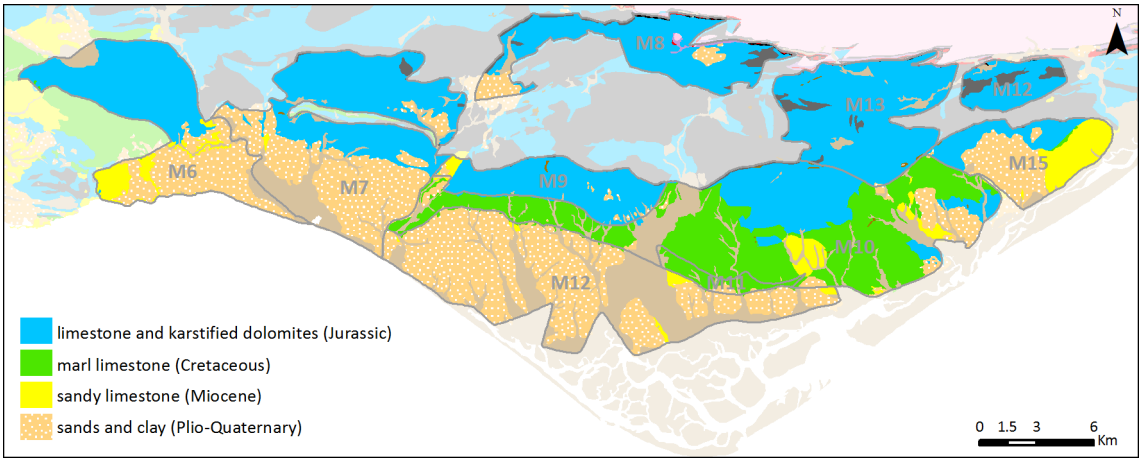

Figure 7.4 Simplified geological map of selected aquifer systems in the Algarve (adapted from Manuppella (1992)).

The paragraphs above present a general discussion of aquifers in the Algarve that may provide conditions for the existence of offshore freshwater, but are far from providing a definitive analysis on the subject. Although in some cases it seems highly probable (M6, M7 and M12), the remainder are merely supposition. Most of these systems are still not very well characterized and would greatly benefit from more comprehensive study. Given the

growing pressures on water resources and the predicted increase in water scarcity for the region, having a sound understanding of physical characteristics of these coastal groundwater bodies is fundamental for an efficient and sustainable management of available water resources.

8. Modelling nitrate-contaminated groundwater discharge and seawater intrusion: aquifer systems of the Ria Formosa coastal lagoon (Algarve, Portugal) [5]

Chapter 8 describes the development and application of a two-dimensional flow and mass transport model, for a selected group of aquifer systems that discharge directly to the Ria Formosa. Density effects are ignored, as the large extent of the model domain would lead to prohibitive run-times. These would affect local flow patterns near the coastline, however the simulation of regional scale flow patterns is not likely to be significantly affected. The aim is to assess the spatial and temporal distribution of groundwater discharge to the coastal lagoon and associated nitrate contamination. During model development processes that contribute to elevated nitrate concentrations are assessed and the potential for irrigation return flow on nitrate concentration levels is analyzed. Subsequently the relative effect of potential mitigation measures are compared. The same model is applied to assess the long-term impacts of changes in groundwater use and climate on the potential extent of SWI, highlighting areas of particular concern and which require more detailed assessment.

8.1. Introduction

In the past, the joint pressures of overexploitation and inadequate agricultural practices in southern Portugal caused nitrate contamination and seawater intrusion problems in several groundwater systems in the Algarve region of southern Portugal.

---

[5] The following chapter is adapted from:

Hugman R, Stigter TY, Monteiro JP, Costa L, 2016. Modelling nitrate-contaminated groundwater discharge to the Ria Formosa coastal lagoon (Algarve, Portugal). *In:* 15th Water Rock Interaction International Symposium. Procedia Earth and Planetary Science, Elsevier. Évora, Portugal, p. 4.

and,

Hugman, R., Viegas, J., Góis, A., Costa, L., Monteiro, J.P., Stigter, T.Y., 2015. Re-Assessing Coastal Groundwater Management Policy in the Algarve : Estimating the Potential for Seawater Intrusion. *In*: Aqua 2015 - 42nd IAH Congress. Rome, Italy, p. 1.

The overexploitation in some coastal aquifers in the Algarve during the final decades of the 20th century led to a gradual decrease in their water quality. The local water authority responded by prohibiting the drilling of new boreholes along the coast. However, since the switch to a surface-water-based public supply in the region, groundwater levels have stabilized and water quality has improved in the majority of these aquifer systems.

The current regulatory agency (the Portuguese Environment Agency - APA) is under growing pressure from end users to emit groundwater use permits within the restricted area. To deal with this issue, the Algarve regional branch of APA is developing a Specific Water Management Plan (SWMP) for the coast in accordance with the European Water Framework Directive. However, the currently available data on seawater intrusion and the effects of predicted changes in groundwater use, climate and sea level in the region is still scarce.

Changes in water use and improved agricultural practices have led to improvements in most of the region. However the group of aquifers that drain in to the Ria Formosa coastal lagoon still suffer from high nitrate concentrations. In fact, the only two nitrate vulnerable zones (NVZ) designated according to the EU's Nitrate Directive in the Algarve are within this area (Figure 8.1). Continuous monitoring provides clear evidence of the continued elevated levels of nitrate and movement of the contamination plume towards the lagoon (Stigter et al 2007).

The Ria Formosa is recognized as an important wetland at both European and International level and is designated as a Natura 2000 and a Ramsar site. Coastal lagoons are particularly vulnerable to eutrophication as they are regions of restricted exchange with the adjacent ocean and may accumulate nutrients supplied by the surrounding watershed (Newton et al 2003). The role of groundwater discharge as a vector for nutrient transport to the lagoon has been well established (Leote et al 2008; Ibánhez et al 2011; Stigter et al 2013b; Rocha et al 2015; Malta et al 2016). Initial estimates of the contribution of groundwater borne nitrogen (N), based on a regional water balance and N loads suggests that total transport towards the lagoon is in the order of 300 ton.yr^{-1}, significantly larger than the annual contributions from surface run-off (6 ton) (Malta et al 2016), though lower than the point source contribution from waste water treatment plants (477 ton). However, a recent study in the area has

shown that the N loading alone does not explain the high values of nitrate observed in the field (Stigter et al 2015), and that salinization processes caused by irrigation return flow may be an additional driver.

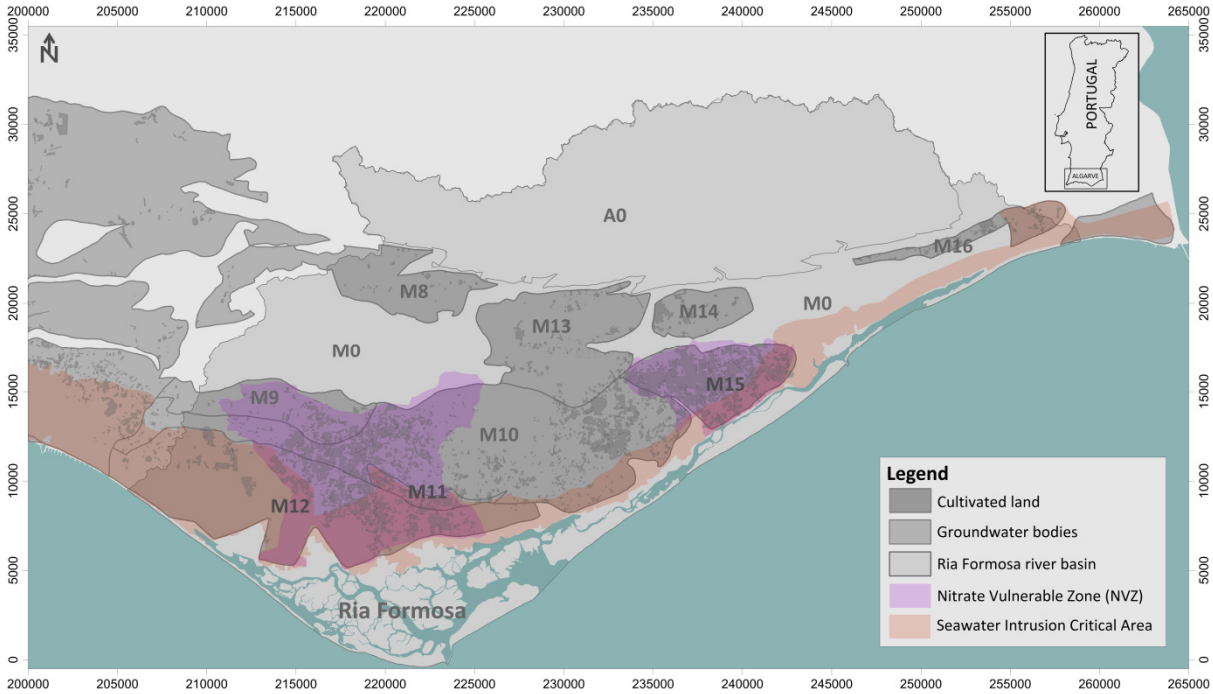

Figure 8.1 Location of the study area, main groundwater bodies and vulnerable zones.

This chapter describes the development and application of a numerical flow and mass transport model for a selected group of aquifer systems that discharge directly to the Ria Formosa, to evaluate the potential effect of return flow on nitrate concentration levels and assess the relative effect of potential mitigation measures. The same model is applied to assess the long-term impacts of changes in groundwater use and climate on the availability of freshwater resources and highlight the areas most likely to suffer from SWI.

8.2. Study area

The onshore Meso-Cenozoic Algarve basin is an east-west trending sedimentary basin, with a south-dipping monocline structure, lying on Carboniferous schists and greywackes (Manuppella 1992). The main aquifer systems within the Ria Formosa catchment (M8-M15 in Figure 8.1) are characterized by limestone and highly karstified dolomites from the Jurassic and Cretaceous, overlain to the south by sandy-limestone and detritic (sands and

silt) formations from the Miocene and Plio-Quaternary. The catchment includes two areas of low-permeability: the Palaeozoic schists and greywackes to the north (A0 in Figure 8.1) and outcrops of marls from the upper Jurassic (M0 in Figure 8.1). The detailed characterization of each system is provided by Almeida et al (2000).

For the purposes of this modelling exercise, only the aquifer systems that are directly interconnected (M9-M13 and M15) were considered. M8, M14 and M16 are geographically separated from this group by outcrops of M0 and are thus not considered to function as a unit. It is unclear whether M8 and M14 provide discharge to the lagoon or deep flow towards the Atlantic Ocean (Stigter 2005; Stigter et al 2007; Malta et al 2016).

8.3. Methods

8.3.1. Water budget and N load

The spatial distribution of rainfall (Nicolau 2002) and recharge ratios according to outcropping lithology (Almeida et al 2000) were cross-referenced to estimate total available groundwater recharge. Current groundwater use in the area is mostly for agricultural purposes. Irrigation water demand was estimated based on land use mapping for 2007 provided by the regional environmental agency (APA-ARH Algarve) and average crop water demands presented in RBMP (2012) by crop type and occupied area. Net loss to irrigation is calculated taking into account the irrigation efficiency in the same report (76.5%) and irrigation return flow (estimated to be 15% for drip irrigation systems used in the area (Beltrão 1985; Keller and Bliesner 1990)).

Annual N requirements for the crops grown in the area are in the order of 200-300 $kg.ha^{-1}$. An average N loss of 20% to the groundwater, suggested by previous authors (Stigter et al 2007), is applied to land use data to estimate the total N load to groundwater. Leaching of domestic effluents from septic tanks is an important point source of nitrogen in areas not connected to the sewerage network (c.a. 20% of the population), which is clearly revealed by the microbiological contamination observed in many groundwater wells (Stigter et al 2007). The total N load from septic tanks was estimated assuming the same values as previous

authors (Stigter et al 2007) (average population density in the Ria Formosa basin of 165 hab.km^{-2}, water use per capita of 150 l.day^{-1}, 70 mg.l^{-1} N concentrations in wastewater and N removal efficiency of the treatment system of 25%). The contribution from atmospheric deposition was calculated based on the spatial distribution of rainfall (Nicolau 2002) and average concentration of N in rainwater (20 μmol.l^{-1}) measured in the area (Stigter et al 2007; Malta et al 2016).

8.1 Calculated groundwater budget for the selected groundwater bodies.

Groundwater body		**Rainfall** x10^6 m^{3}yr^{-1}	**Recharge ratio**	**Recharge** x10^6 m^{3}yr^{-1}	**Irrigation (net loss)** x10^6 m^{3}yr^{-1}	**Budget**
M9	Almansil - Medronhal	14.4	0.50	7.2	-1.8	5.4
M10	S.João da Venda-Quelfes	71.5	0.20	14.3	-14.5	-0.2
M11	Chão Cevada-Qta João Ourem	3.3	0.50	1.7	-1.5	0.3
M12	Campina de Faro	49.1	0.20	9.8	-10.2	-0.4
M13	Peral - Moncarapacho	31.2	0.40	12.5	-0.9	11.6
M15	Luz-Tavira	16.8	0.25	4.2	1.6	5.8
	Total	192.2		49.7	-27.3	22.4

8.3.2. Numerical flow and transport model: setup and calibration

A two-dimensional flow and transport model of the aquifer systems that discharge directly into the Ria Formosa was developed using finite element code FEFLOW (Diersch 2014). The geometry of the groundwater management units, geological outcrops and main hydrogeological features were used to generate a triangular finite element mesh with 193,709 elements and 98,208 nodes (Figure 8.2).

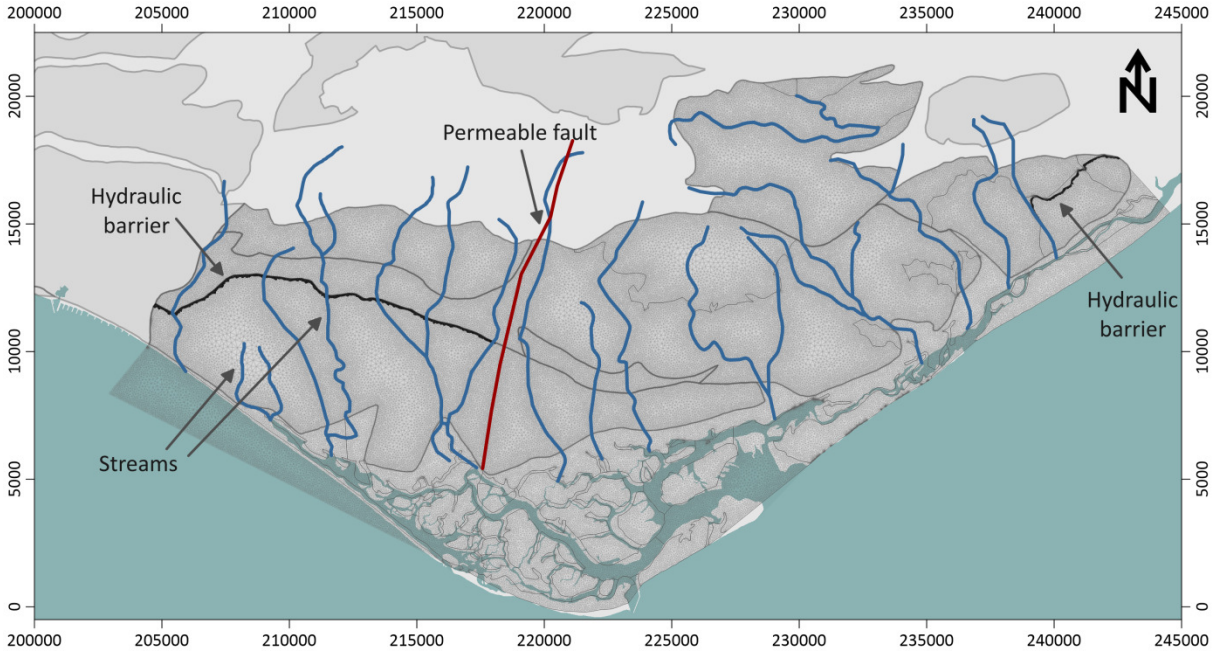

Figure 8.2 Finite element mesh and main hydrological features included during mesh generation.

Constant head BC equal to 0 m above mean sea level were imposed along the coastline and channels of the coastal lagoon. Constant head BC equal to surface elevation were imposed on nodes coinciding with the main streams. Constraints were imposed to only allow water to exit the model, with no recharge from the streams considered.

Well boundary conditions were assigned to nodes within irrigated areas. Abstraction rates were spatially distributed according to calculated water demand for each specific plot of land. Recharge and atmospheric deposition of N was assigned according to the spatial distribution of rainfall (Nicolau 2002) and recharge ratios according to outcropping lithology (Almeida et al 2000). Additionally, irrigation return flow was added to recharge over agricultural areas.

A source of mass was assigned to elements corresponding to irrigated areas to represent excess N from fertilization. Leaching from domestic effluent was distributed uniformly over all non-agricultural areas.

Spatial distribution of transmissivity (*T*) was estimated by inverse modelling under steady-state conditions, using the Gauss-Marquardt-Levenberg method as implemented in the

nonlinear parameter estimation software PEST (Doherty 2002). Uniform hydraulic property zones were considered for all aquifers except the *Campina de Faro (*M12) and *São João da Venda-Quelfes* (M10), as the spatial distribution of hydraulic head in these two aquifers is relatively heterogeneous. As there is little geological evidence on which to base sub-division of property zones, the pilot-point method (Doherty 2003) was used to describe the spatial distribution of *T* in these two aquifers. The pilot-point method of spatial parameter definition is that hydraulic parameter values are assigned to a set of points within the model domain, instead of directly to the mesh elements. Parameter values are then assigned to the elements of the model through spatial interpolation, resulting in a smooth variation over the selected domain (Doherty 2003). This method removes the need to define parameter zones, allowing the calibration process itself to determine where heterogeneity must exist within the model, with the trade-off being the increased number of model runs required during calibration. Therefore, uniform parameter zones wherever possible, and the pilot-point method was applied to aquifers with large variability in hydraulic head, not clearly associated to a known hydrogeological feature.

Transport parameters (effective porosity (n_e) and aquifer thickness (b)) were manually calibrated by trial and error for a 17-year simulation between 1995/96 and 2012/13, to obtain the best fit with average observed nitrate concentrations in 2012/13. Initial conditions were interpolated from average observed values during 1995/96. Simulated results were not very sensitive to b, with an overall value of 100 m obtained for all systems. Values for n_e range from 0.01 to 0.4, with an average per aquifer system of 0.1. Obtained values are realistic for all systems, with the exception of M15 and M11 which obtained the best fit with 0.01. Although this value is physically acceptable, it is at the lower end of the acceptable range for the aquifer type. Given that the model presents simplified representations of the system, ignoring vertical heterogeneity and temporal dynamics, optimal fit parameters will not necessarily be realistic, as they may be compensating for unaccounted for factors (e.g. greater vertical mixing or the impact of flushing from high recharge years).

Longitudinal and transverse dispersivity were assumed as 20 m and 2 m respectively as a compromise between numerical stability and realistic parameter values according to the literature (Gelhar et al 1992; Roseiro 2009), as discussed in Chapter 2.

Initially, transport simulations were carried out under steady-state conditions to assess the long-term spatial distribution of N for a range of parameter values and whether the estimated N load could account for nitrate concentrations observed in the field. Subsequently, a 30-year simulation in which N recycling through irrigation return flow is re-applied to the model in five-year periods was simulated and compared to observed concentrations in the 1990s'.

8.3.3. Numerical flow and transport model : nitrate mitigation scenarios

Five technical and management solutions to improve groundwater quality by the EU imposed limit of 2027 were simulated in order to compare the relative effects of each on nitrate concentration in groundwater and discharge to the coastal lagoon.

First, a baseline, *business as usual* (BAU) scenario was simulated to demonstrate the effect of continuing current groundwater management and use. Abstraction for irrigation and N recycling is continued as before.

Second, the effect of removing a source of contamination by improving agricultural practices (higher efficiency in the application of fertilizers and taking into account the existing concentration in abstracted groundwater) was simulated, maintaining abstraction and return flow for irrigation but removing excess N input from agricultural areas.

Third, a change in water source for irrigation purposes was also considered in which groundwater is replaced by surface water supply (as is already the case for the *Luz-Tavira* (M15) aquifer), thus removing the effect of recycled nitrate and the impact of abstraction.

Finally, two managed aquifer recharge (MAR) schemes were considered: (1) increased infiltration along the Rio Seco stream (Roseiro 2009), and (2) injection of rainwater harvested from greenhouse run-off, into large diameter wells in the *Campina de Faro* (M12) (Costa et al 2015a). Locations of the selected MAR sites are shown in Figure 8.3. Roseiro

(2009) previously estimated available average stream flow for infiltration at $2x10^6$ m^3yr^{-1} and simulated the effect using a local scale model, but did not take into account the effect of return flow or nitrate recycling. Costa et al (2015) calculated available average annual rainfall occurring over selected greenhouses on the *Campina de Faro* (M12) at $1.63\ x10^6$ m^3yr^{-1}, although in practice this value may be slightly lower due to technical issues related to rainwater collection and transfer to the injection wells.

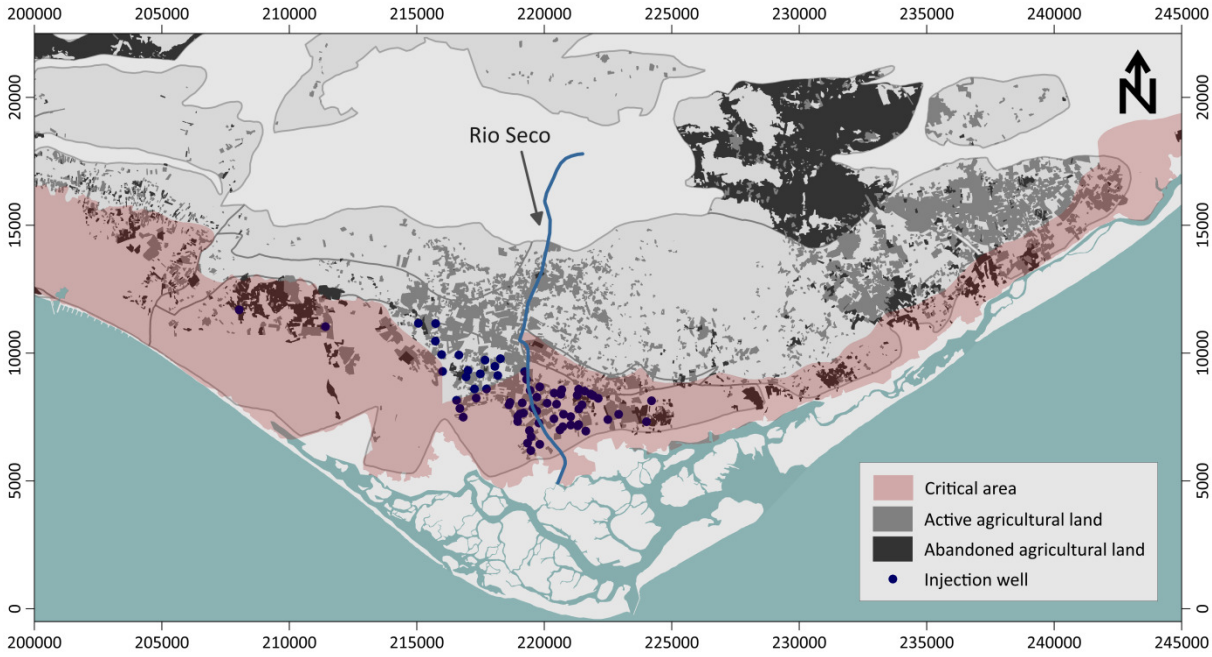

Figure 8.3 Location of MAR sites and changes in irrigated area considered in the hypothetical scenarios

8.3.4. Numerical flow and transport model: climate change scenarios

Stigter et al (2014) present values for an ensemble of climate scenarios for the central Algarve. Average values from the ensemble are used here to estimate the impact of reduced average annual recharge on hydraulic head.

The impact of the "critical area" restriction is assessed by simulating two scenarios for an increase in water demand for irrigation, assuming that currently abandoned areas of the National Agricultural Reserve are re-developed for agriculture. In the first scenario, all abandoned land is re-developed. In the second scenario only territory that is not within the

restricted area is considered. In both cases abstraction rates for the new agricultural areas are calculated assuming current water demand for citrus crops.

Applying the Ghyben-Herzberg relation and the depth of the groundwater bearing layer to the obtained distribution of head provides a rough estimate of the extent of potential seawater intrusion. As was shown in Chapter 5, this method will likely overestimate the extent of SWI. However, it does provide insight into where SWI is more likely to occur as well as the relative impacts of changes in the environment and water use.

8.4. Results and Discussion

8.4.1. Water budget and nitrate load

Table 1 presents calculated values of abstraction, return flow and agricultural contribution to nitrate load for the selected aquifer systems. Input from domestic effluents was estimated at 31.1 ton.yr^{-1} for the model area and atmospheric deposition at 63.8 ton.yr^{-1}. A total N load of 255 ton.yr^{-1}r is estimated for the whole area, of which agriculture accounts for 73% of total load, and domestic effluent and atmospheric deposition for the remaining 9% and 18% respectively.

Table 8.2 Calculated current abstraction, return flow and N load from agriculture for the aquifer systems in the study area.

Aquifer System	Unit	Irrigated area (km^2)	Return-flow (x10^6 m^{3}yr^{-1})	Abstraction (x10^{6}m^{3}yr^{-1})	N (ton.yr^{-1})
S. João da Venda - Quelfes	M10	19.7	2.5	17	98.3
Chão de Cevada - Quinta João de Ourem	M11	1.9	0.25	1.7	9.4
Campina de Faro	M12	11.9	1.8	12	59.5
Malhão	M13	1.4	0.17	1.1	7.2
Luz - Tavira	M15	14.0	1.6	-	70.1
Almancil - Medronhal	M9	2.2	0.32	2.1	10.8
Total		**53.5**	**6.6**	**33.4**	**255.3**

8.4.2. Numerical model: nitrate transport

A steady-state simulation of average conditions shows that the model does not explain high values of nitrate observed in the field with calculated values of N loading. Sensitivity analysis shows that even at the extreme ranges of physically acceptable parameter values

(dispersivity and transmissivity) simulated concentrations are generally an order of magnitude below observed values (Figure 8.4). Previous studies have suggested that irrigation with contaminated groundwater is a likely cause of the elevated concentrations (Stigter 2005). In fact, model results show abstracted mass accounting for 70% of average annual nitrate load to the system, with only the remaining 30% occurring as discharge to the lagoon. Although this could be a consequence of the 2D nature of the model, which does not account for vertical flow across multiple layers.

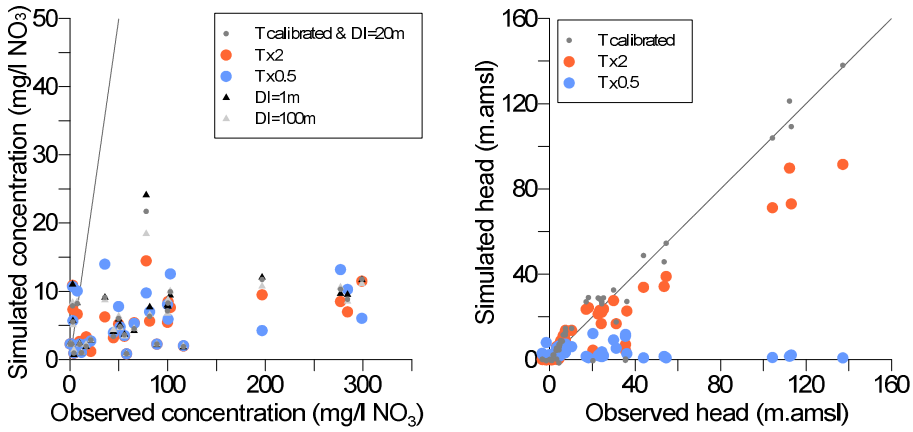

Figure 8.4 Comparison between average values of nitrate(left) and hydraulic head (right) observed in 1995/96 and values simulated for a range of parameters.

To test this hypothesis, a 30-year simulation was carried out in which mass removed via abstraction is re-applied with return-flow in five-year periods. Model results corroborate the idea that return flow accounts for recycling of nitrate and the increasing concentrations and observed spatial distribution. However, 80-100 years (depending on parameters) of recycling are necessary for concentrations to reach observed levels in the late 1990s', and even so concentrations in individual wells are not well represented in the model. This is assuming an average loss of 20% of crop N requirements.

In practice, higher loads are likely to have occurred in the past (Stigter et al 2007), which would account for the accelerated rate of increase in concentrations observed in the field. Spatial heterogeneity of hydraulic and transport parameters, abstraction and fertilization rates as well as the two-dimensional simplification of the three-dimensionally heterogeneous real world system are the likely culprits for the models' inability to simulate

accurate concentrations in individual wells. However, the regional spatial distribution is reasonably represented (Figure 8.5), suggesting that the simulated processes provide an acceptable explanation for observed nitrate concentrations.

Agricultural areas in the *Campina de Faro* (M12) suffer the greatest increase in loading, as wells in this system are re-circulating contamination that flows from aquifers upstream. Nitrate concentrations in the central northern part of the model (M9 and M10) are underestimated. This is likely to be due to inaccurate spatial distribution of nitrate sources (e.g. higher concentration of domestic effluent due to lack of sewage network) or unaccounted for sources of contamination from groundwater bodies and/or run-off further north.

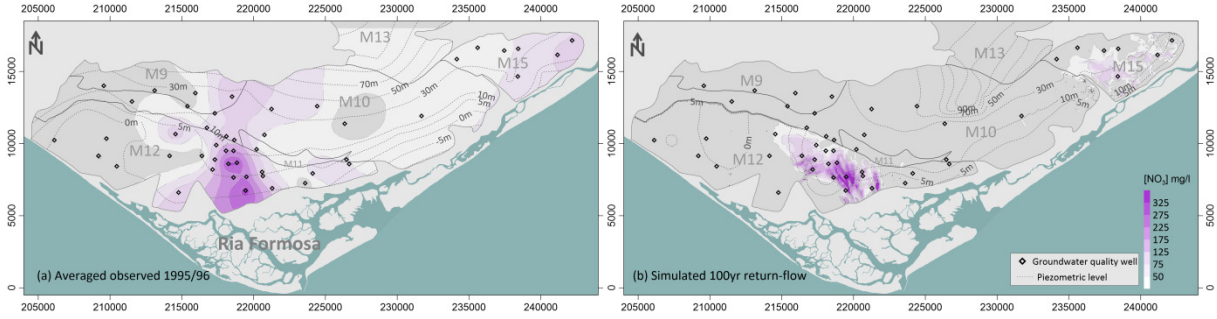

Figure 8.5 Concentration of nitrate, interpolated average observed values in 1995/96 (left) and simulated for a 100 years of return flow (right).

To test the effect of mitigation measures, a simulation is run starting from observed distribution of nitrate in 1995/96 until 2013 and considering N recycling via return-flow. The model is able to represent the overall change in nitrate concentrations, and shows a good fit with average values measured in 2013 (Figure 8.6 and Figure 8.7). This is mostly due to the effect of the interpolated initial conditions, which provide higher concentration levels and a wider spread over the model domain than long-term simulations, which then drain out of the system under current estimated N load. These results support the idea that historically N loss to groundwater could have been significantly higher.

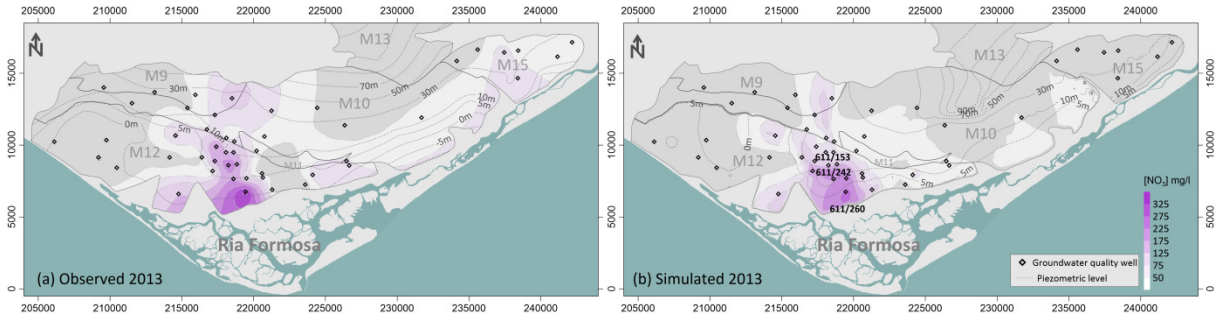

Figure 8.6 Interpolated average observed (left) and simulated (right) hydraulic head and concentration of nitrate in 2013.

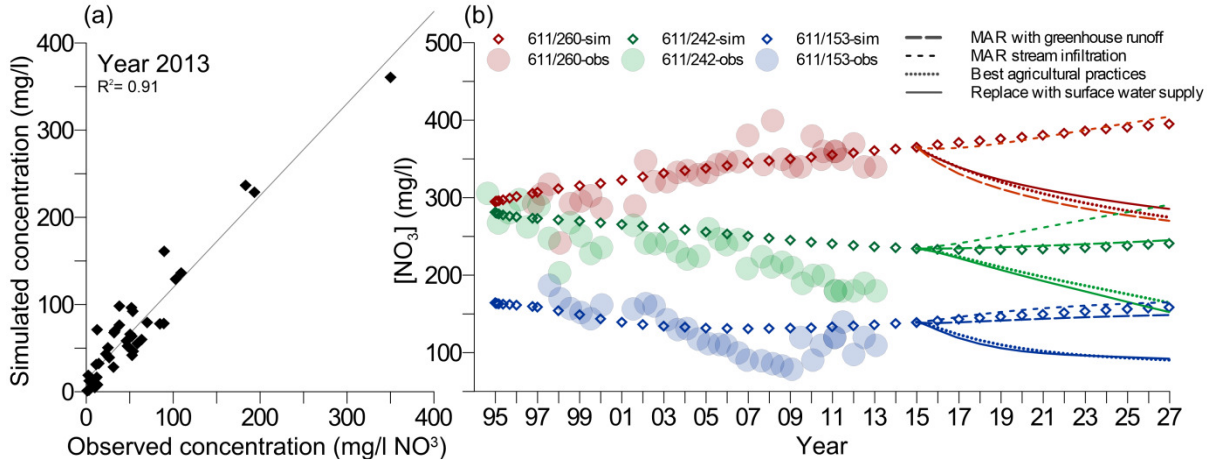

Figure 8.7 (a) observed versus simulated nitrate concentrations in 2013; (b) observed and simulated time series of nitrate concentration at selected monitoring points.

The effect of several mitigation measures are compared in Figure 8.7(b), Figure 8.6 and Figure 8.10. If *business as usual* (BAU) is maintained, nitrate levels in most of the systems would stabilize at current values or decrease slightly as the excess nitrate is slowly flushed to aquifers downstream. The exception is aquifer M12 near the coast, where concentrations would be expected to continue to increase in the mid to short term (Figure 8.7) as nitrate continues to be recycled (see Figure 8.8). Simulated values for observation wells 611/242 and 611/153 follow the observed decrease, with a slight increase predicted for the BAU scenario (Figure 8.7). This may be an artefact of the model, as re-circulated mass from the entire system is distributed uniformly over agricultural areas within the aquifer, thus abstracted mass is being artificially migrated back upstream.

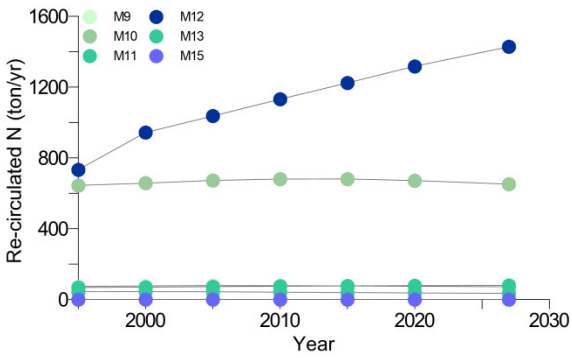

Figure 8.8 Annual rate of nitrate recycling per aquifer system.

Replacing irrigation supply with surface water and improving agricultural fertilization practices contribute the most to reducing nitrate concentrations. The effect is mostly due to the removal of the recycling effect, as can be seen by the similar spatial distributions in Figure 8.9.

Managed aquifer recharge schemes (increasing stream infiltration and injecting rainwater harvested from greenhouses) have a localized effect, as seen for well 611/260 in Figure 8.7(c) and the overall distribution in Figure 8.9. The increased stream infiltration MAR scheme causes higher concentrations observed at 611/242 and 611/153, despite reduced concentrations along the stream bed (Figure 8.9) as previously shown by Roseiro (2009). This is due to local changes in flow direction, with added infiltration "pushing" contamination away from the stream causing higher concentrations in these areas.

However, even in the best case scenario, the physical characteristics of the system will not allow the existing contamination plume to dissipate within a short time period and that to reach good quality status by 2027.

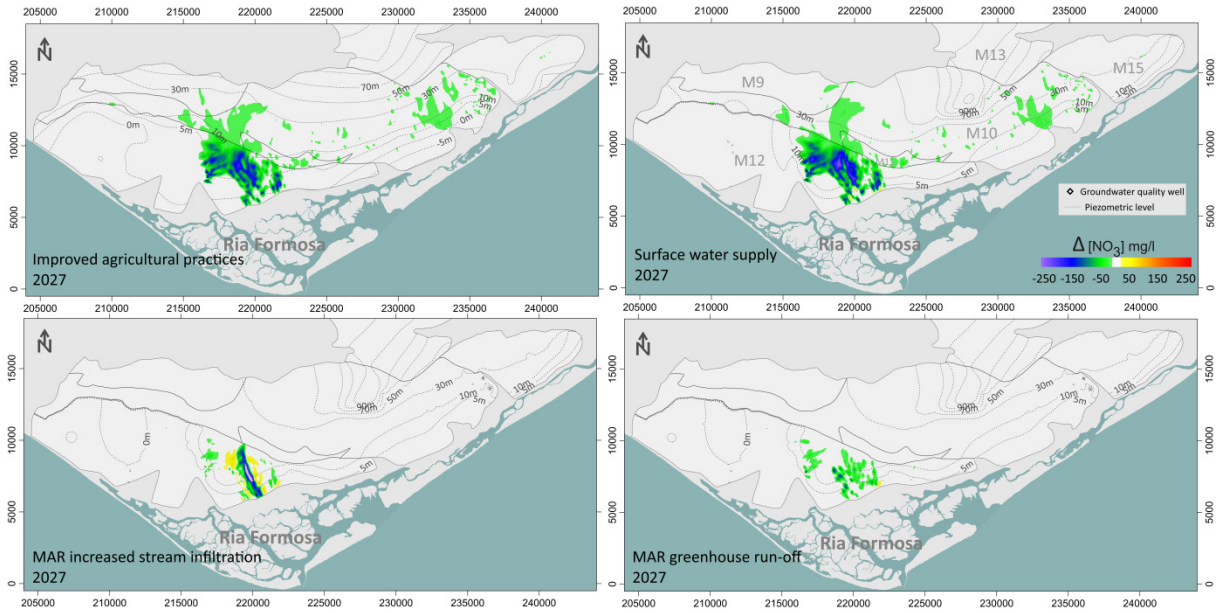

Figure 8.9 Simulated impact of mitigation measures on the spatial distribution of nitrate and hydraulic head by 2027.

Nitrate discharge rates to the lagoon are most significantly altered by switching the source of water for irrigation (Figure 8.10). As is to be expected, the increase in groundwater discharge increases the flushing of the system, and in the short term leads to greatly increased mass flow into the lagoon. These values do not represent values effectively reaching the lagoon, as biogeochemical processes in the lagoon sediment may act as a sink prior to reaching the surface water body. Additionally, simulated discharge rates are potentially overestimated due to the imposed initial conditions. Even so, this represents a large increase in nutrient loads to the lagoon which would likely have a significant impact on water quality. A similar effect is evident for the MAR schemes, albeit at a lesser scale.

Improving agricultural practices on the other hand leads to a decrease in nitrate discharge, as nitrate is exported from the system in agricultural products, effectively acting as a pump-and-treat solution, and thus reducing the impact on the lagoon. Even so simulated average annual discharge of nitrate is in the order of 1000 ton.yr^{-1}, significantly higher than calculated by previous mass balance estimates (350 ton.yr^{-1}). Accounting for nutrients already available in abstracted groundwater and avoiding excess fertilization would likely reduce agricultural costs. Whether they would offset the cost of implementing improved practices is unknown and should be assessed in future work. Simulated discharge rates may

be overestimated due to the imposed initial conditions, which assume homogeneous vertical mixing and should only be considered comparatively and not as absolute values. To improve on estimated values, a fully 3D model would be necessary, taking into account the vertical distribution of mass and accounting for historical levels of loading to obtain accurate values of total mass within the system.

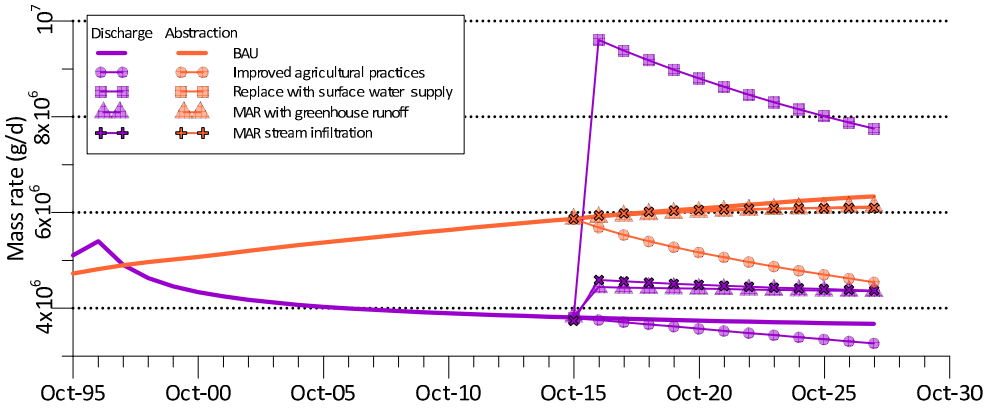

Figure 8.10 Simulated N discharge to the lagoon and abstraction rates.

8.4.3. Numerical model: seawater intrusion

Figure 8.11 presents simulated long term-average hydraulic heads as well as depth and extent of the fresh-saltwater interface based on the Ghyben-Herzberg relation and average thickness of the aquifer layers. As was shown in Chapter 5, the inland extent of the fresh-saltwater interface will be overestimated using this method, but it does provide a useful assessment of the relative impacts of the various factors influencing SWI. Estimates represent long-term effects, which would be expected to occur if the system were to reach equilibrium under the given conditions. Calculated results show significant SWI in the *Campina de Faro* (M12) and to a lesser extent along the coastline of the *S.João da Venda-Quelfes* (M10) aquifer due to reduced hydraulic heads. The time-scale at which this would occur is unknown, but would likely be in the order of decades due to the slow movement of the SWI interface.

Data available from the official groundwater quality network does not show indications of SWI in the study area, with the exception of the western sector of the *Campina de Faro* (M12) where chloride concentrations have begun to increase during the last few years (this

is discussed in further detail in the following Chapter 9). However, there are no monitoring points in the affected area within the M10 aquifer. Previous studies have shown occurrences of SWI here in the past (Silva 1988; Carreira et al 2014), however there are no recent surveys to assess the evolution of groundwater quality.

Despite several decades of overexploitation and water levels below sea-level, chloride concentrations in the western sector of the *Campina de Faro* (M12) aquifer have only recently started to increase. This supports the supposition that this system is not yet at equilibrium and that the fresh-saltwater interface is still moving land-ward. In practice groundwater abstraction would be discontinued once groundwater quality decreased too far for irrigation(see irrigated areas in Figure 8.3), thus SWI would never in fact reach this point, however the purpose of the simulation is merely to demonstrate that current abstraction rates are not sustainable in the long-term.

Comparing the maps for current groundwater use (Figure 8.11, top left) and irrigation demand (Figure 8.11, top right), shows that without the implementation of surface water for irrigation in the eastern sector, the Luz-Tavira (M15) aquifer would also still be at risk of SWI, although there were no indications of SWI occurring in the past. Once again, this can be attributed to the slow movement of the fresh-saltwater interface and hydraulic properties of the system.

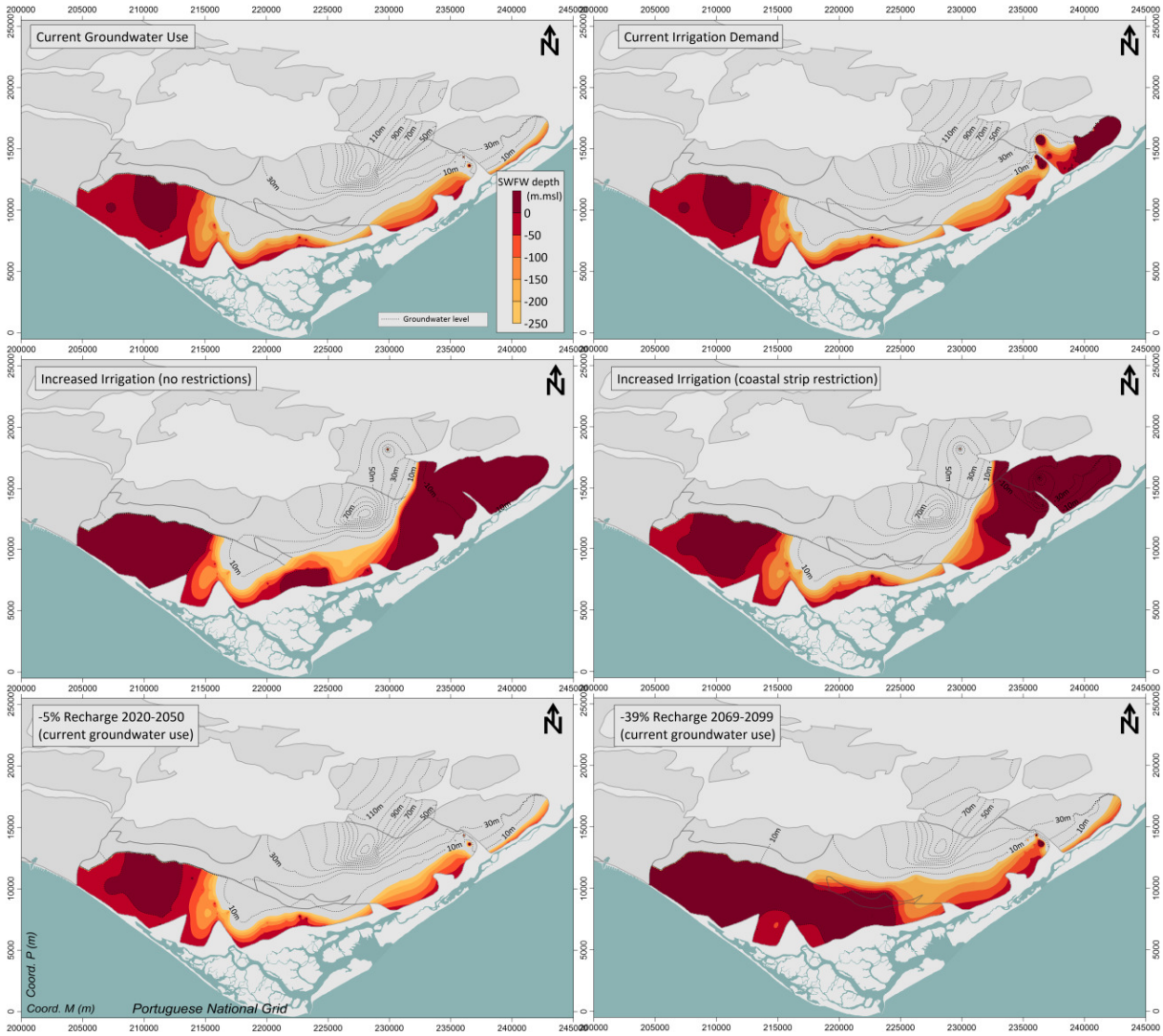

Figure 8.11 Simulated long-term average hydraulic head and depth of the fresh-saltwater interface for the proposed climate and water use scenarios.

The increased irrigation scenario shows drastic impacts in the eastern sector. Figure 8.3, shows the largest increase in agricultural land in the north-eastern M13 aquifer, which was previously mostly occupied by non-irrigated crops. Thus, the proposed increase in irrigated land is likely exaggerated. As shown in Figure 8.11 (middle) and Figure 8.12, in the long-term, the coastal strip restriction does not have a significant effect on the extent of SWI, with the exception of a small area in the centre of the study area. If withdrawals are to increase significantly inland, the long-term impact will be similar whether there is abstraction along the coast or not. However, the restriction may increase the systems resilience to short term fluctuations of the interface and avoid local occurrences of SWI, as well as delay seawater

encroachment. Further research on the effectiveness of this management scheme is still necessary, with a particular focus on local scale heterogeneity and the effect of preferential pathways such as karst conduits or faults.

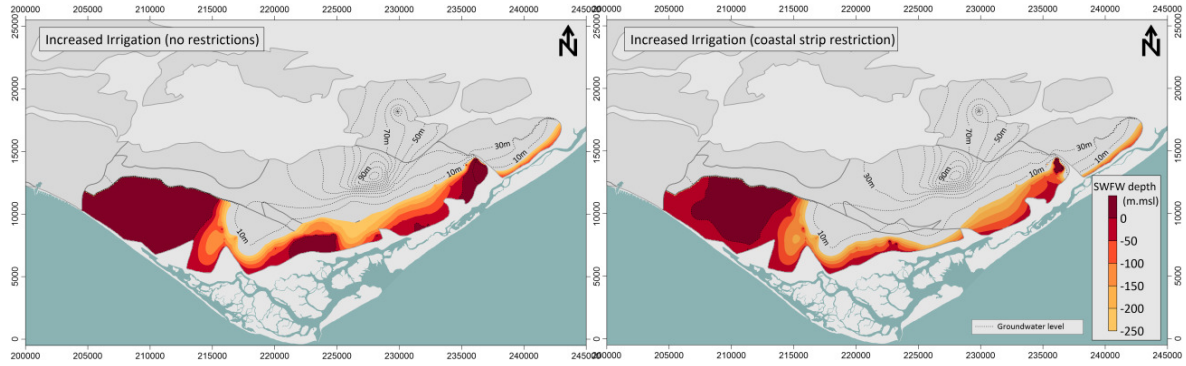

Figure 8.12 Simulated long-term average hydraulic head and depth of the fresh-saltwater interface for increased irrigated area scenarios, assuming surface water supply for irrigation in the eastern sector.

Simulations with reduced recharge show that even if groundwater use is not increased, there is a significant potential for seawater intrusion, in particular for *Campina de Faro* (M12) and *Chão de Cevada-Quinta João de Ourem* (M11). Even though the average annual budgets for each scenario (Figure 8.13) show that the total groundwater discharge is higher for the 2069-99 scenario than the increased irrigation (no restriction) scenario, the reduced recharge leads to a larger affected area.

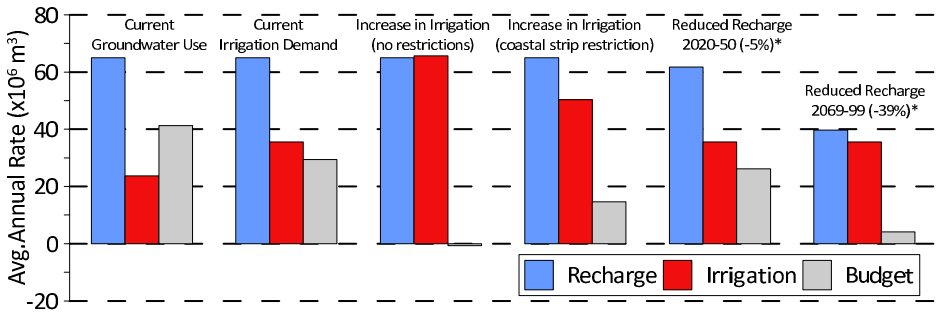

Figure 8.13 Water budget components for the proposed climate and water use scenarios.

The spatial distribution of SWI is markedly different for the climate and water use scenarios. The increased abstraction scenarios has the greatest change in the East. This is due to the fact that current irrigation needs are supplied by surface water, and the simulated scenario assumes that all water demand is met by groundwater.

Figure 8.12 shows results for the increased irrigation, assuming that areas currently supplied by surface remain so, and as can be seen, the extent of SWI is significantly less. In the reduced recharge (climate) scenarios SWI in this sector is minor, as the eastern areas are still subject to additional recharge from surface water irrigation, with the greatest impact in the central and western sectors associated to a concentration of agricultural areas.

Thus, as previously shown by Hugman et al (2012), the spatial distribution of abstraction can have a significant impact on the sustainable use of groundwater, as spatially concentrated pumping is more likely to cause localized drawdown's and increase SWI. Furthermore, contrary to the results discussed in Chapter 5 the fact that these aquifer systems have a relatively large discharge area in comparison to the in-land extent (unlike for example the *Querença-Silves* (M5), with a ca. 5 km discharge area and ca. 50 km inland extent) the overall long-term budget by itself is not sufficient to define the sustainable level of abstraction.

The impact of proposed mitigation scenarios are presented in Figure 8.14, assuming current climate and groundwater use. Only replacing groundwater use with surface water has any noticeable impact on SWI, despite increasing hydraulic head in-land. In part the effect of added recharge is offset by increased discharge to streams crossing the system, as hydraulic heads reach surface level.

In all cases the western sector of *Campina de Faro* (M12) is still under risk due to the large abstraction for golf courses and the hydraulic barrier along the northern limit, which reduces recharge here. Due to its physical isolation, specific measures would need to be implemented within the affected area in order to increase recharge or decrease abstraction and thus avoid SWI. This will be addressed in further detail in the following Chapter 9.

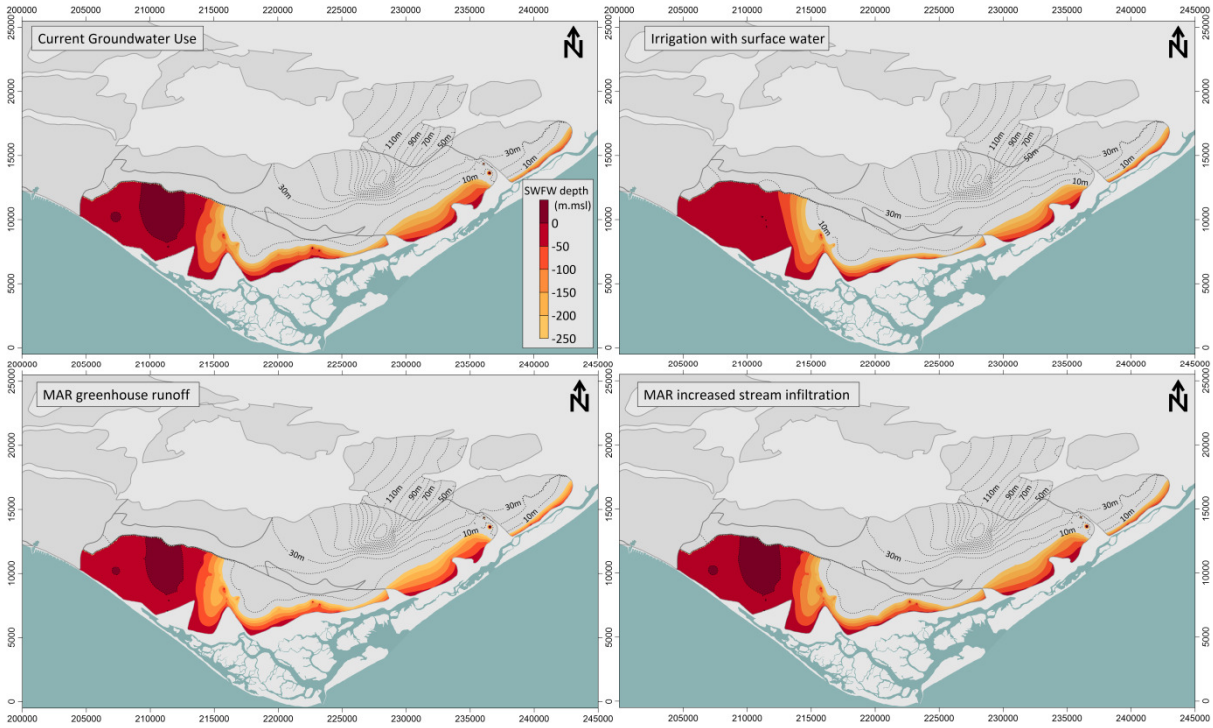

Figure 8.14 Simulated long-term average hydraulic head and depth of the fresh-saltwater interface for increased mitigation scenarios.

8.5. Final remarks

Despite the simplifications inherent to the approach, this large scale model supplies an important first assessment of the potential for SWI and nutrient discharge to the coastal lagoon, and provides a basis on which to decided where further research should be focused.

Aquifers in the Algarve are classified as “Groundwater Management Units”, following the systematic classification by Almeida et al (2000), which has led to most resource assessments and management policies being applied at the scale of individual units. The connections between them and the existence of underlying water bearing layers is often ignored or not well understood. These could represent important sources of freshwater supply and require further study. The simplified large scale model of the aquifer systems that discharge into the Ria Formosa highlights that these systems should not be considered as individual groundwater bodies, as water and land use practices associated to one system can cause impacts on others.

Simulations show that current groundwater use will not be sustainable in the long term for predicted changes in climate in some areas. The coastal strip restriction on new water use permits will not significantly change current groundwater use patterns and other measures will need to be taken in these areas. The western sector of the *Campina de Faro* (M12) aquifer is already at risk as well as the most affected by decreasing recharge. Proactive measures should be put in place to avoid salinization of this aquifer. There is on-going work to assess the feasibility of managed aquifer recharge schemes, aiming at solving nitrate pollution, which could be adapted to deal with SWI. The *Luz-Tavira* (M15) aquifer is currently under-exploited, however if the entire irrigation demand in this area should become dependent on groundwater once more, the aquifer would not be able to sustain current or future water-demand. On the other hand, fresh groundwater resources are being underused. An integrated use of surface and groundwater for the entire area should be considered in order to increase the efficient resource management, and could provide a solution to reduce the potential for SWI.

Nutrient recirculation via return flow provides an explanation for the elevated levels in the *Campina de Faro* (M12), where contamination from upstream is being captured by abstraction and re-applied in this area. Although the large scale model provides a useful first assessment, simulations ignore important local scale effects (in particular vertical heterogeneity). As greatest impacts are by far in the *Campina de Faro* (M12) a local scale model of this system should be developed to assess mitigation measures with a greater degree of certainty. Several mitigation measures to reduce elevated levels of nitrate were assessed, however even the most optimistic scenario does not lead to acceptable contamination levels in the near future. Meaning that it is unlikely that good quality status will be attained within the deadlines imposed by the EU. From both an environmental and economic perspective, the most beneficial measure would be the implementation of improved agricultural practices, taking into account existing nitrate levels in irrigation water and avoiding excess fertilization. Future efforts should be made to assess the socio-economic feasibility of implementing such measures if groundwater quality and the ecological status of the Ria Formosa is to be improved and protected.

9. Numerical modelling contributions to understanding seawater intrusion processes in the *Campina de Faro* aquifer system (Algarve, Portugal)

Results from chapter 8 highlighted the potential for SWI problems in the Campina de Faro aquifer. In the following chapter a three-dimensional density-coupled model for the system is developed to assess the existing conceptual model and provide insight into local SWI processes. The model provides a preliminary representation of the system and highlights several data requirements. Although still preliminary, the model is used to simulate several potential SWI mitigation scenarios in order to provide an initial estimate of their relative effectiveness.

9.1. Introduction

In the past, the joint pressures of overexploitation and inadequate agricultural practices in southern Portugal caused nitrate contamination and seawater intrusion problems in several groundwater systems in the region. When groundwater was replaced by surface water as the main source for public supply in 1999, and agricultural practices improved to certain extent (partly using surface water), groundwater levels and quality recovered large parts of the region. A notable exception is the *Campina de Faro* (CF) coastal groundwater system, where groundwater levels remain below sea level in certain sectors, and measured nitrate concentrations are high in others (reaching 350 mg/l).

In Chapter 8, a large scale two-dimensional flow model was developed for the aquifer systems that discharge into the Ria Formosa coastal lagoon, which included a simplified representation of the CF. Model results suggested that the western sector of the CF was at significant risk of SWI, given current groundwater use. However, despite low groundwater levels during the last several decades, only recently has there been any indication of seawater encroachment.

A three-dimensional density-coupled flow and transport model is developed to improve the conceptual understanding of this multi-layer aquifer system and assess the impact of current and future groundwater use and climate conditions on SWI.

9.2. Study area: *Campina de Faro* (M12) aquifer system

9.2.1. Hydrogeology

A succinct description of the hydrogeology of the CF (main features in Figure 9.1 and Figure 9.2) can be found in Almeida et al. (2000), who summarize previous studies in the area (e.g. Almeida 1985; Silva 1988; van Oijen et al. 1996; Stigter et al. 1998), and is further developed in Stigter (2005) and Roseiro (2009).

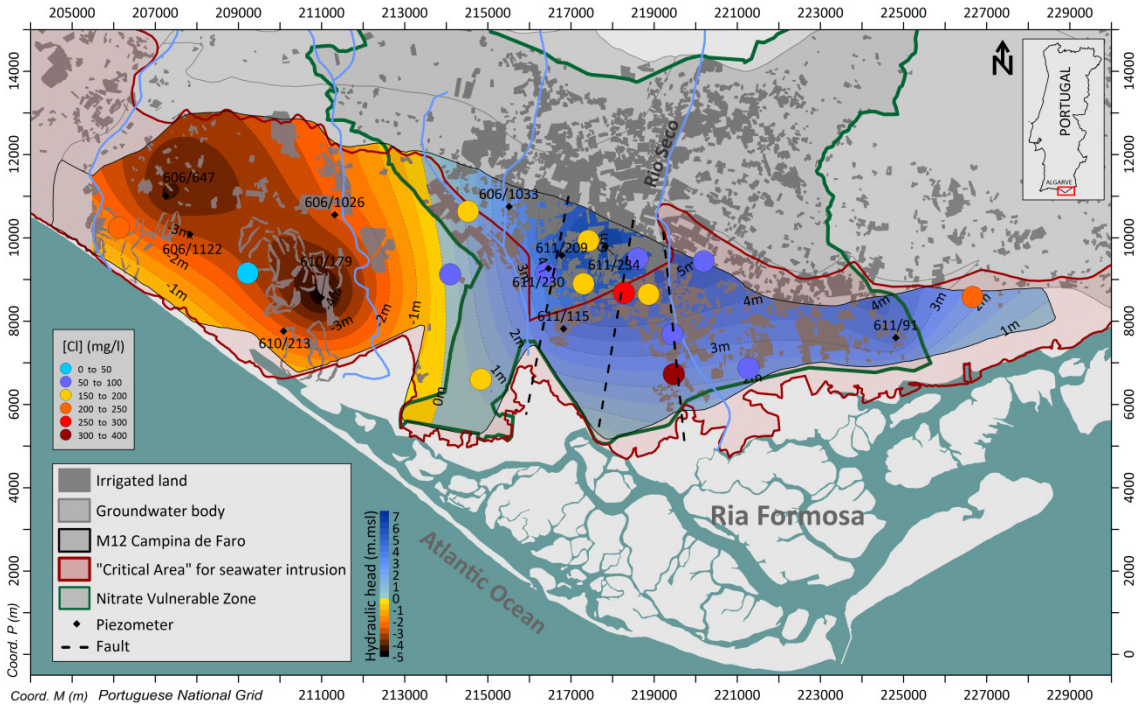

Figure 9.1 Location, main hydrological features, nitrate vulnerable zone delimitation, average hydraulic head in the sandy-limestone layer and chloride concentration during 2001-2008 of the *Campina de Faro* aquifer system.

Fossil-rich sandy limestone of the Miocene period, deposited in a graben-like structure bordered by large N-S trending faults, make up the lower semi-confined aquifer layer. Thickness increases towards the coast and can exceed 200 m near the city of Faro (Silva 1988). This formation does not outcrop, being covered by fine sand of Miocene age, and deposited in the same graben-like structure. Along with the overlying Plio-Quaternary sands and gravels, these sediments support the uppermost phreatic aquifer, which has a maximum thickness of about 50 m in the centre of the study area, but can be somewhat thicker below

the hill of Faro (Stigter 2005). Fluvial and marine erosion took place during Holocene times, followed by the deposition of a layer of clay and silt in a large part of the area, however it is often too thin and the silt content too high to confer a confined character to the upper aquifer (Stigter 2005).

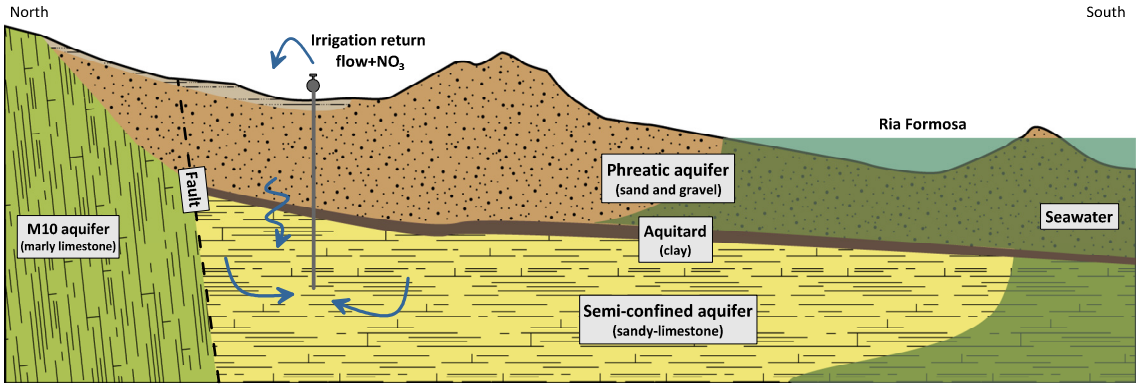

Figure 9.2 Conceptual model of the *Campina de Faro* multi-layer aquifer system (adapted from Stigter (2005)).

Some authors refer the existence of an aquitard, separating the upper phreatic aquifer from the underlying semi-confined sandy limestone aquifer. This is supported by a clay layer identified in borehole logs, pumping tests that demonstrate the hydraulic independence between the two layers and historical references of artesian boreholes (Silva 1988; Almeida et al 2000; Roseiro 2009). However, the existence of local connections between the two layers cannot be ruled out. This connection may be due to natural discontinuities in the regional distribution of the clay layer, or artificially created by the practice of drilling boreholes at the bottom of traditional large wells (van Ooijen et al 1996; Almeida et al 2000). In fact, van Oijen et al (1996) did not find evidence of a separating layer between the two aquifers during geo-electrical soundings. However, the distinct seasonal variation in groundwater level within the two aquifers supports the idea that the clay layer affects the connectivity at a regional scale.

Groundwater flow is generally N-S, which is increased by the preferential flow paths formed by N-S trending faults (Stigter 2005). Discharge occurs along the coastline, into the Ria Formosa coastal lagoon and the Atlantic ocean. The northern and eastern limit of the system coincides with a W-E trending fault and the outcrop of Cretaceous marl-limestone, which

have been considered by most previous authors as being hydraulically disconnected from the water bearing layers of the CF (Silva 1988; Almeida et al 2000; Roseiro 2009). To the West the system is limited by a N-S trending fault line and up-doming of the Cretaceous marl-limestone, however there are indications that some connection with the neighbouring *Quarteira* (M7) aquifer system may exist (Almeida et al 2000).

9.2.2. Recharge

Recharge to the upper phreatic aquifer occurs directly from rainfall and is estimated by Almeida et al. (2000) as $10x10^6$ $m^3.yr^{-1}$, assuming an average rainfall of 550 mm and infiltration rate between 15% and 20%. Lobo-Ferreira et al (2006) estimated recharge as $12x10^6$ $m^3.yr^{-1}$, with a daily sequential water balance developed, using the BALSEQ_MOD numerical model (Oliveira 2004).

The system is crossed by several ephemeral streams. Of these, the Rio Seco is the most significant and contributes to the recharge of the upper detritic aquifer (Silva 1988; Roseiro 2009). Roseiro (2009) estimated that average annual recharge from the Rio Seco as $0.24x10^6$ m^3, however this would be concentrated in short periods during the wet season.

Recharge to the semi-confined sandy limestone aquifer is assumed to occur indirectly through lateral inflow from the Jurassic and Cretaceous limestones which crop out to the North (Almeida et al., 2000). This assumption is based on several factors: (1) groundwater abstraction from the CF is equal to or greater than average annual recharge, yet piezometric levels do not show a decreasing trend (Almeida 1985; Silva 1988; Stigter 2005); (2) faults identified during field campaigns, using geophysical methods and remote sensing (Silva 1988; Manuppella 1992; Stigter et al 1998); and (3) distinct water types identified during hydrogeochemistry surveys and higher temperatures associated with large N-S trending faults (Geinaert et al 1982; Silva 1988; Stigter et al 1998). However, this lateral recharge has yet to be quantified.

9.2.3. Groundwater use

Groundwater in the area is currently the main source of supply for irrigation for agriculture and several golf courses. Data supplied by the regional regulatory agency (APA-ARH Algarve) suggest approximately $2.7x10^6$ $m^3.yr^{-1}$ is pumped for golf course irrigation, whilst the most recent river basin management plan (RBMP 2012) estimates $3.6 x10^6$ m^3. RH8 (2012) estimates net groundwater loss to irrigation at $14.4x10^6$ $m^3.yr^{-1}$, of which $10.8x10^6$ $m^3.yr^{-1}$ is for agriculture. The same report estimates that irrigation efficiency is 76.5%, thus total abstraction for agriculture should be around $13.3 x10^6$ $m^3.yr^{-1}$, similar to the $12x10^6$ $m^3.yr^{-1}$ suggested by Almeida et al. (2000). The previous generation of river basin management plans (RBMP 1999), also estimated similar values for water crop demand ($9.7x10^6$ $m^3.yr^{-1}$) and abstraction ($11.9x10^6$ $m^3.yr^{-1}$).

Detailed estimates of agricultural water demand were determined by analysing land use maps, supplied by APA-ARH Algarve, obtained from the analysis of aerial photography of the region in 2007. Within the limits of the CF, $1.2x10^7$ m^2 of land is used for agricultural purposes. Citrus plantations occupy 68% of this area, the remainder being mostly occupied by greenhouse crops and horticulture. Applying average crop water demands presented in RBMP (2012) by crop type and occupied area, results in an average annual demand of $8.8x10^6$ $m^3.yr^{-1}$. Assuming the efficiency presented by the same authors, results in an estimated abstraction volume of $10.9x10^6$ $m^3.yr^{-1}$. Irrigation return flow is estimated to be 15% for drip irrigation systems used in the area, accounting for an additional $1.6\text{-}2x10^6$ $m^3.yr^{-1}$ of recharge to the upper phreatic aquifer from return flow (Beltrão 1985; Keller and Bliesner 1990).

In the past, two well-fields abstracting from the sandy limestone Miocene aquifer were used for public supply, one near the city of Faro in east and the other in the western Vale do Lobo sector. However, these were abandoned in 1999 when public supply was switched to a regional system supported by large surface water dams. According to Stigter (2005), registered abstraction for the city of Faro within the sandy limestone Miocene aquifer was relatively minor, reaching approximately $0.5x10^6$ $m^3.yr^{-1}$ at its peak in 1994/95. Almeida et al.

(2000) refers a peak abstraction of $2.3x10^6$ m^3 for the entire system in 1994, suggesting that total pumping for public supply was un-evenly distributed between the two sectors.

9.2.4. Groundwater level and quality

As previously discussed by Stigter (2005), piezometric time series in the sandy phreatic aquifer and the sandy limestone aquifer present distinct behaviours. Groundwater levels in shallow boreholes and traditional wells (e.g 611/233) show lower intra-annual variation, whilst deeper boreholes (e.g. 611/234 in the proximity of 611/233) present accentuated seasonal amplitudes. Inter-annual variation in both is clearly linked to rainfall.

The long-term behaviour of groundwater levels in the sandy limestone aquifer varies from East to West. On average, groundwater levels in both layers were at or below sea level during the 1980's. Since then, levels in the Western sector have not recovered as well as the rest of the system and have remained below mean sea level during most of this period. Abstraction in this sector is mostly for irrigating golf courses (which began during the early 1980's), some agriculture and historically for public supply. However, the greatest pressure on the system is located in the central and eastern sector of the CF where extensive agricultural plots rely on groundwater for irrigation. As this central area coincides with the N-S trending faults, higher groundwater levels despite the concentration of abstraction supports the idea that these faults form preferential flow paths for lateral flow to the sandy limestone aquifer.

There is no clear connection between seasonal and inter-annual variation in hydraulic head and chloride concentration (Figure 9.3). Higher values are mostly observed in the phreatic aquifer (see 611/242 in Figure 9.3), with a decreasing trend up to around the year 2004, after which they stabilize. This has previously been discussed in Stigter et al (2011b), where increasing concentrations at some locations are attributed to irrigation return flow (an important mechanism of salinization) and decreasing concentrations due to flushing after the late 1990's due to increased discharge. There are localized occurrences of increases in concentrations measured at deep boreholes (as shown for 611/246 in Figure 9.3), but in general values measured in the central sector have been relatively constant during the last

decade, matching the stable trend in groundwater level. In fact, the concentration spikes occur in high rainfall periods, suggesting that they are not associated to SWI but more likley caused by other processes. On the other hand, during several field campaigns in 1982/83 Silva et al (1986) identified an elongated area with higher chloride concentrations, and proposed the existence of a paleo-channel along which SWI was occurring. This area coincides with the boreholes referred to above.

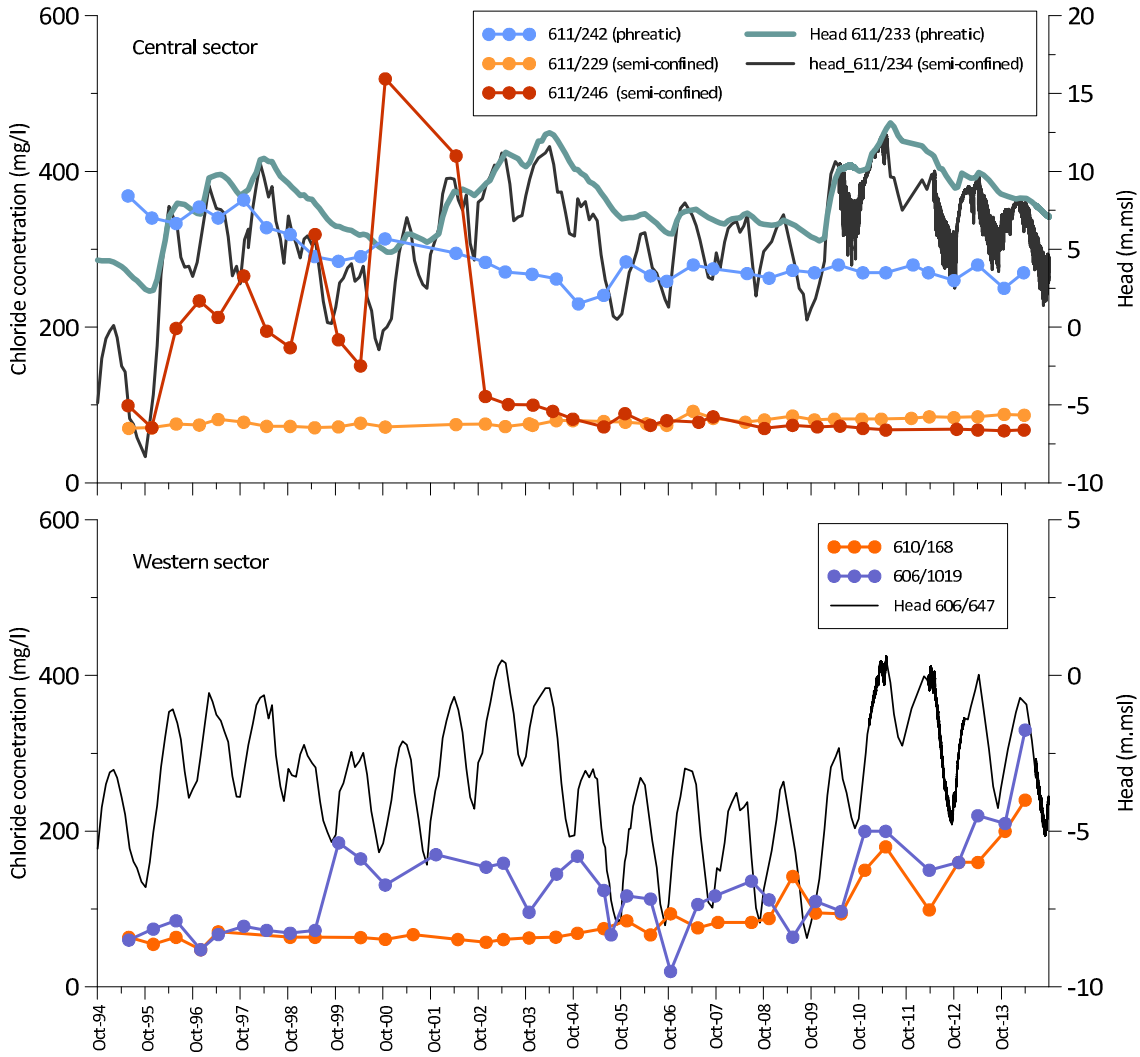

Figure 9.3 Comparison between chloride concentration and groundwater level time series in the central and western sectors of the CF.

Despite groundwater levels below mean sea level over several decades in the western sector, chloride concentrations have remained relatively low and stable until the most recent drought in 2004/05. Since then, observed values show a steady increase at

piezometer 610/168 and a significant rise at both observation points as of 2009/10. This last event could be associated with the implementation of a new golf course in the area, leading to higher abstraction. However, the fact that chloride concentrations remain low over several decades despite negative groundwater levels suggests that the intrinsic characteristics of the system are the cause for the slow occurrence of SWI. The confined nature of the sandy-limestone aquifer may have allowed the for the formation of an offshore extent of freshwater, which has been depleted over the last few decades and only now is the fresh-saltwater interface reaching the onshore area. On the other hand, simply the slow rate of movement of the fresh-saltwater interface and the hydraulic properties of the system may be sufficient to account for the delayed impact of SWI.

9.3. Materials and methods

9.3.1. Three-dimensional density-coupled flow and transport model setup

Solving density-coupled flow and transport problems requires the solution of a complex system of coupled non-linear partial differential equations. This system is solved using the finite element method, as applied within the commercial modelling software FEFLOW (Diersch 2014). Detailed descriptions of the governing equations and theoretical development and benchmarking of the FEFLOW code can be found in Kolditz et al. (1998), Diersch and Kolditz (1998) and Diersch (2014).

A three-dimensional (3D) geological representation of the three layers (sandy phreatic aquifer, clay aquitard and sandy limestone aquifer) of the CF was created, based on a digital elevation model (DEM), data collected from borehole logs (supplied by APA) and results from previous geophysical studies (Geinaert et al 1982; van Ooijen et al 1996; Roseiro 2009). On-shore, the outer limits were set according to the M12 groundwater body as defined by Almeida et al (2000) and extended to include the coastal lagoon and a 500 m offshore extent where the CF connects directly with the Atlantic ocean. Elevation of the sea-floor was based on detailed bathymetry data, obtained from the Centro de Investigação Marinha e Ambiental da Universidade do Algarve (CIMA) project LiDAR, as previously attempted by Viegas (2015).

A finite-element mesh was generated with 505,720 triangular prism finite elements and 272,244 nodes, divided into 20 layers and 21 slices. Mesh generation takes into account the location of the geological units, fault-lines, main streams and channels of the lagoon. All simulations were run using a Forward Euler/Backward Euler (FE/BE) time integration scheme for automatically time-step control with a maximum time-step of one day (Diersch 2014).

All density-coupled flow and transport simulations are by necessity transient. To simplify model development and reduce run-time, some simulations here are run under constant conditions (i.e. no temporal variation recharge or abstraction). These are used to obtain pre-development conditions and to accelerate the calibration process, as described below. Henceforth, mention of transient simulations refers to those that consider temporal variability in recharge and abstraction.

Recharge from rainfall was assigned to the top layer, with a uniform value of 17.5% of average annual rainfall (Almeida et al 2000). Monthly rainfall data is used to determine recharge for transient simulations. Flux-BC (2nd type, Neuman) were assigned to nodes along the northern limit of the confined sandy limestone layer that coincide with the main fault-lines identified in previous studies, to simulate inflow from the North. In the transient simulations a constant value is applied per year, based on the annual budget of the area contributing lateral inflow. Fractures are represented using two-dimensional plane discrete features, solely within the confined aquifer. Flow is simulated using the Hagen-Poiseuille law, assuming an arbitrary cross-section thickness of 0.01 m. Calculated stream infiltration from the Rio Seco was imposed at nodes along the streams upper reaches, with monthly data being used for transient simulations.

Coastal BC are represented with constant freshwater head. Mass transport BC are assigned to nodes corresponding to the estuary with a relative concentration value (C_{max} = 1), representing 100% seawater fraction. A boundary constraint condition, in which the presence of a constant concentration is defined according to the flux direction, was included to allow for the formation of an outflow face. Thus, when mass-flux is positive (entering the system) the constant mass BC is maintained, whilst when it is negative (leaving the system) the concentration is computed and automatically assigned as a flux-BC (Diersch and Kolditz

1998; Diersch 2014). This technique has previously been applied for use in large-scale models (i.e. Kopsiaftis et al. 2009; Nocchi and Salleolini 2013). The remaining out-limits of the model domain are considered as no-flow boundaries.

Crop water demand and irrigation efficiency were used to determine annual abstraction for irrigation within the CFs limits, and assigned to nodes coinciding with boreholes inventoried in agricultural areas. Fifteen percent of abstraction for irrigation was re-applied to the top slice, using flux-BC assigned to agricultural areas. Estimated abstraction rates for the several golf courses active within the aquifer limits were assigned to boreholes inventoried within their respective areas of operation. Abstraction for agriculture was arbitrarily distributed with 25% in the phreatic and the remaining 75% in the semi-confined aquifer. Transient simulations consider constant abstraction for irrigation concentrated from mid-May to mid-September.

9.3.2. Initial conditions and parameter calibration

The computational burden of solving variable density flow problems, and the need for high spatial and temporal resolutions of the finite-element mesh and time-stepping schemes to guarantee numerical stability, often makes the development of large scale 3D models impractical (Oude Essink 2001a). During model development, the impact of refining the mesh and decreasing the dispersivity parameter on hydraulic head at on-shore observation points was found to be insignificant, as it mostly affects the thickness of the transition zone which is located off-shore. Therefore a relatively coarse mesh, with a lower computational burden, was considered acceptable for current modelling purposes. Values for longitudinal and transverse dispersivity (100 m and 10 m, respectively) were selected as a compromise between values suggested in the literature for aquifer type and scale (Gelhar et al 1992; Neuman 2005) and finite-element size as discussed in chapter 2.

Roseiro (2009) presents a recent compilation of available data on hydraulic parameters of the CF. Uniform values of hydraulic conductivity (K) and storage parameters (S_y and S_s) were defined for the three geological layers and the ratio between vertical (K_v) and horizontal (K_h) conductivity assumed to be 0.1. Average values of K from the range presented in Roseiro

(2009) were assigned initially, and the model was run under pre-development conditions until reaching dynamic equilibrium, followed by a 20 year run under pre-2000 conditions, to obtain initial conditions of hydraulic head and mass distribution.

K and *b* were calibrated by trial-and-error for the period between 2000-2007. This period was chosen for the large amount of continuous time-series and seasonal variability was ignored to reduce computation time and accelerate the calibration process. Constant average recharge and groundwater use for this period was imposed on the model, and storage parameters were placed very low. In practice this means that hydraulic head will quickly reach pseudo steady-state conditions for a given position of the fresh-saltwater interface, assuming that the interface does not change significantly during this relatively short period. This provides a faster means for which to calibrate these parameters, reducing the number of variables during the calibration as well as the computation time.

Subsequently storage parameters (S_y and S_s) were calibrated by trial-and-error using transient data for the period between 1990 to 1999. Simulated variation in hydraulic head was compared to measured values from the official monitoring network. Results were validated by extending the simulation to 2007 (limit of available rainfall time series).

Porosity affects the rate of contaminant movement, with lower values allowing for faster transport. A lack of data on the position and movement of the fresh-saltwater interface makes it difficult to calibrate transport parameters. Therefore minimum values from the literature were assumed, as they represent the worst case scenario (SWI occurs faster).

Table 9.1. Hydrogeological parameter ranges in the literature.

Layer	Porosity	Specific Yield (S_y)	Hydraulic Conductivity (K) ($m.d^{-1}$)
Phreatic (sand)	0.22-0.38 *	0.20-0.35 *	0.0167-46.32 *
Aquitard (clay)	0.35-0.60 **	0.00-0.05 *	0.005 *
Semi-Confined (sandy-limestone)	0.05-0.40 **	0.001 ***	0.19-3.97 ***

*(Roseiro, 2009); **(Fitts, 2002); ***(Silva (1988)

9.3.3. Estimation of lateral inflow

To determine the potential amount of lateral recharge to the CF, the average annual groundwater budget of the area to the north was estimated. The spatial distribution of rainfall determined by Nicolau (2002) and recharge ratios according to outcropping lithology as proposed by Almeida et al. (2000) were cross-referenced. Total available recharge over this area amounts to 14.5×10^6 $m^3.yr^{-1}$. This value could be significantly higher if M0 and M8 groundwater bodies were also taken into account, however these were not included so as to obtain a conservative estimate. Current groundwater use in the area is mostly for agricultural purposes. According to the land use map provided by APA-ARH Algarve and crop water demands suggested by RBMP (2012), net groundwater use for irrigation is 9.4×10^6 $m^3.yr^{-1}$, which results in a excess of 5.2×10^6 $m^3.yr^{-1}$ that may contribute to the CF. According to Almeida et al. (2000), prior to 1999 several significant well-fields in this area were used for public water supply and accounted for an average 6.5×10^6 $m^3.yr^{-1}$. These were abandoned when the regional multi-municipal water supply system was implemented and large dams replaced groundwater as the main source for public supply.

A transient analysis of the water budget from 1983 to 2008, using monthly rainfall data and assuming constant abstraction rates for irrigation during between May-September, shows that both inter-annual and seasonal variability is large (Figure 9.4). However, the average (14.8×10^6 $m^3.yr^{-1}$) is similar to that obtained using average annual rainfall values from Nicolau (2002) and recharge ratios of outcropping lithologies in the area. The average water budget from 1983 to 1999, assuming constant irrigation and public water supply demands, results in a excess water budget of 1.0×10^6 $m^3.yr^{-1}$. Rainfall data from the official monitoring network is currently only available up to 2008. With the decrease in abstraction for public water supply from 1999 to 2008, average groundwater available for lateral recharge is estimated at 4.2×10^6 $m^3.yr^{-1}$. This value is subject to a large amount of uncertainty and calls for further work in constraining the estimate of lateral inflow, as this is an important part of the CF water budget. A rough assessment of the impact of this uncertainty on model results is carried out, however future research should aim to quantify and understand the temporal dynamics of the processes controlling lateral inflow to the CF.

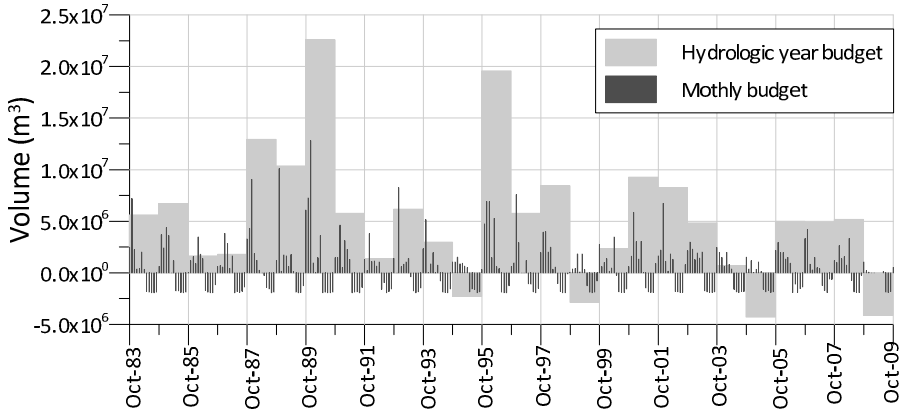

Figure 9.4 Transient water budget of the area to the north of the *Campina de Faro* aquifer system

9.3.4. Mitigation scenarios

Four mitigation scenarios are simulated, focusing on both decreasing demand and increasing supply. Simulations were arbitrarily run for twenty years, starting at the end of the calibration simulation (i.e. October 2007). As the model is inadequate to provide predictions on the time-scales at which SWI will occur, the aim of these simulations is merely to compare the relative effects on the movement of the seawater. Thus twenty year model-run was selected as it is sufficient time for the model to show changes in the position of the interface, without requiring extremely long run-times.

First, two previously proposed managed aquifer recharge (MAR) schemes are simulated: (1) increased infiltration along the Rio Seco stream (Roseiro 2009), and (2) injection of rainwater harvested from greenhouse run-off, into large diameter wells in the *Campina de Faro* (M12) (Costa et al 2015a).

Roseiro (2009) previously estimated available average stream flow for infiltration at $2x10^6$ m^3yr^{-1} and simulated the effect using a local scale model, but did not take into account the effect on the western sector of the system.

Costa et al (2015) calculated available average annual rainfall occurring over selected greenhouses on the CF at $1.6x10^6$ m^3yr^{-1}, although in practice this value may be slightly lower due to technical issues related to rainwater collection and transfer to the injection wells. Both of these schemes enhance recharge to the phreatic aquifer, as they were

designed to help mitigated nitrate contamination. The simulations presented here aim to assess whether the added recharge would also contribute to counteracting SWI.

Lastly, two additional scenarios are considered, in which groundwater abstraction for (3) agriculture and (4) golf courses is abandoned. These represent scenarios in which either demand is reduced or alternative sources of water are obtained. Results will highlight the impact of each user group and provide insights on where efforts to reduce abstraction would provide the most benefits.

9.4. Results and Discussion

9.4.1. Numerical model: calibration and sensitivity analysis

Simulated hydraulic head shows a close fit to average values observed from 2000-2008, with an even distribution of error across the model domain (Figure 9.5). Optimal fit was obtained with *K* values of 5.62 $m.d^{-1}$ (phreatic), 0.0045 $m.d^{-1}$ (aquitard) and 0.95 $m.d^{-1}$ (semi-confined), and *b* of 0.006 m. Values of *K* are within an acceptable range. Although physically acceptable, the value of *b* is not directly comparable to realistic values, as the geometry of the fractures was arbitrarily assumed and not based on observation.

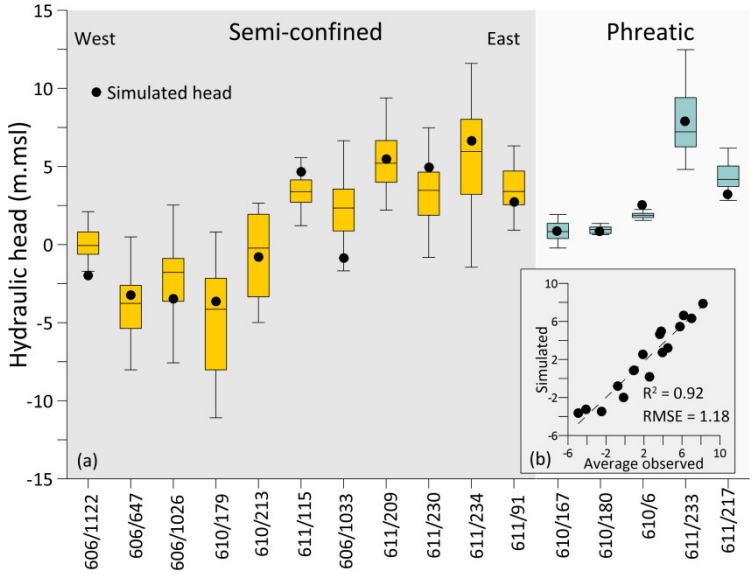

Figure 9.5 (a) Variability of observed hydraulic head for 2000-2008 and (b) correlation between average observed and simulated hydraulic head.

The sensitivity of the model changes in parameter and recharge values was investigated varying selected factors one-at-a-time, under constant conditions based on average values for 2001-2008 (i.e. pseudo steady-state). However, due to long model run-times an extensive analysis was not conducted. The impact on simulated hydraulic head of values of *K*, lateral inflow, direct recharge and fracture hydraulic aperture (*b*) varied by +/-50% is presented in Figure 9.6.

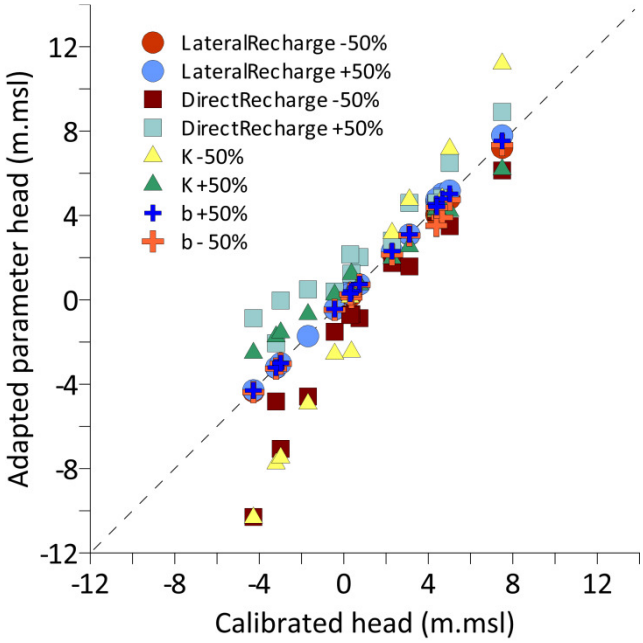

Figure 9.6 Comparison of the effect of relative parameter changes on simulated hydraulic head.

Simulated heads at the observation points are not sensitive to changes in hydraulic aperture, suggesting that the calibration value is still subject to a degree of uncertainty. The western sector (negative values) is evidently the most sensitive to changes to *K* and direct recharge, with no significant effect from changes to lateral inflow (via faults) as the northern boundary in this sector is a no-flow boundary. Hydraulic head in this sector is thus controlled by the ratio of direct recharge and *K* and is relatively sensitive to these two factors. Although not assessed here, it is evident from the spatial distribution of simulated head (Figure 9.10) that the abstraction rate and spatial distribution also has a significant effect on results, the effect of which is increased with lower values of *K*. These results show that decreasing recharge

rates due to reduced rainfall (i.e. predicted climate change for the region) will have the most significant impacts on the western sector.

The central sector is most affected by decreasing *K*, without significant impacts from the remaining factors. This is due to the increased retention of lateral recharge, causing higher hydraulic gradients. The impact of changes in lateral and direct recharge is similar, as their relative contribution to the water budget in this area are equivalent. The fact that the remaining factors do not significantly affect results in the central sector suggests that the models ability to represent hydraulic behaviour here under different conditions is still subject to some uncertainty. Future work should aim to improve knowledge on the geometry and hydraulic properties of the hydrogeological features in this sector, as well as determine the rate and processes that control lateral inflow to constrain the range of acceptable values for model parameters and BC.

Simulated temporal variation in hydraulic head for the 1990-2007 period is compared with observed values for selected piezometers in Figure 9.7, Figure 9.8 and Figure 9.9. Best fit was obtained with an S_y of 0.05, 0.01 and 0.2 for the phreatic, aquitard and semi-confined layers respectively. Both phreatic and aquitard layers were not sensitive to S_s, and the default 0.0001 m^{-1} was maintained, whilst the best fit for the semi-confined layer was obtained with a value of 0.0003 m^{-1}.

Simulated values for the central sector (Figure 9.7 and Figure 9.8) show a good match with observed inter- and intra-annual variability in both the phreatic and semi-confined layers. The exception being two occurrences in 1997 and 2003, where the model was unable to match the increase in measured values. This can be explained by inaccurate estimate of recharge or unaccounted for change in groundwater use or even due to lateral inflow being uniformly distributed over the year. In subsequent years, although offset, simulated values follow the observed pattern.

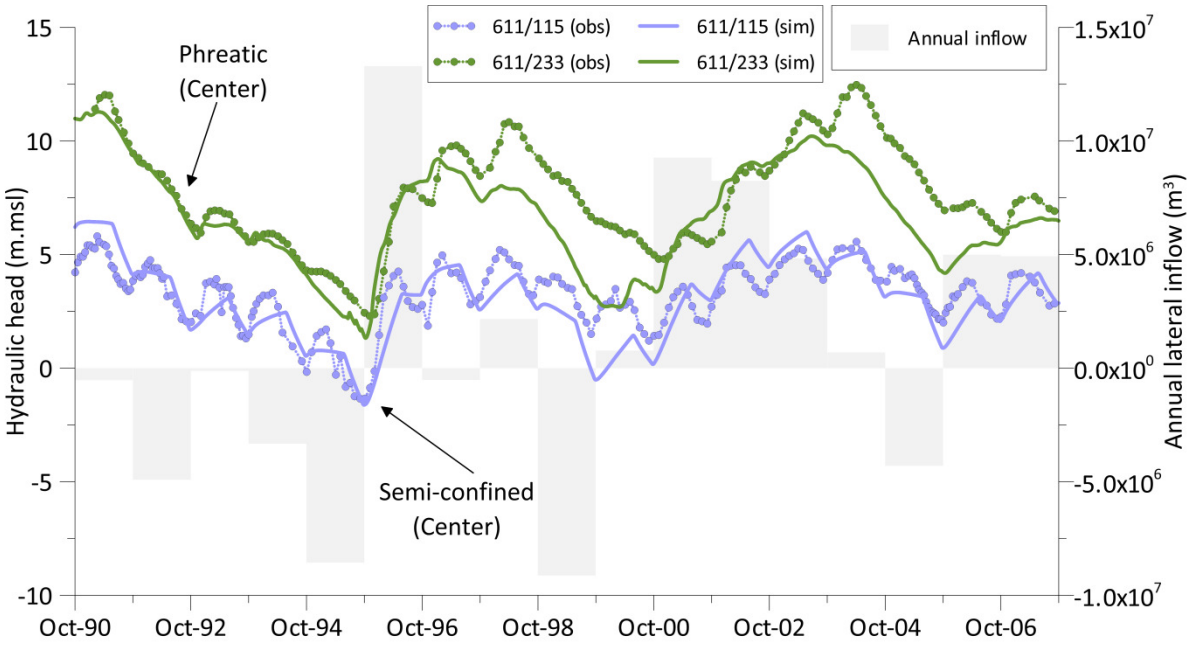

Figure 9.7 Time-series of simulated and observed hydraulic head between 1990 and 2007 in the central sector of the CF.

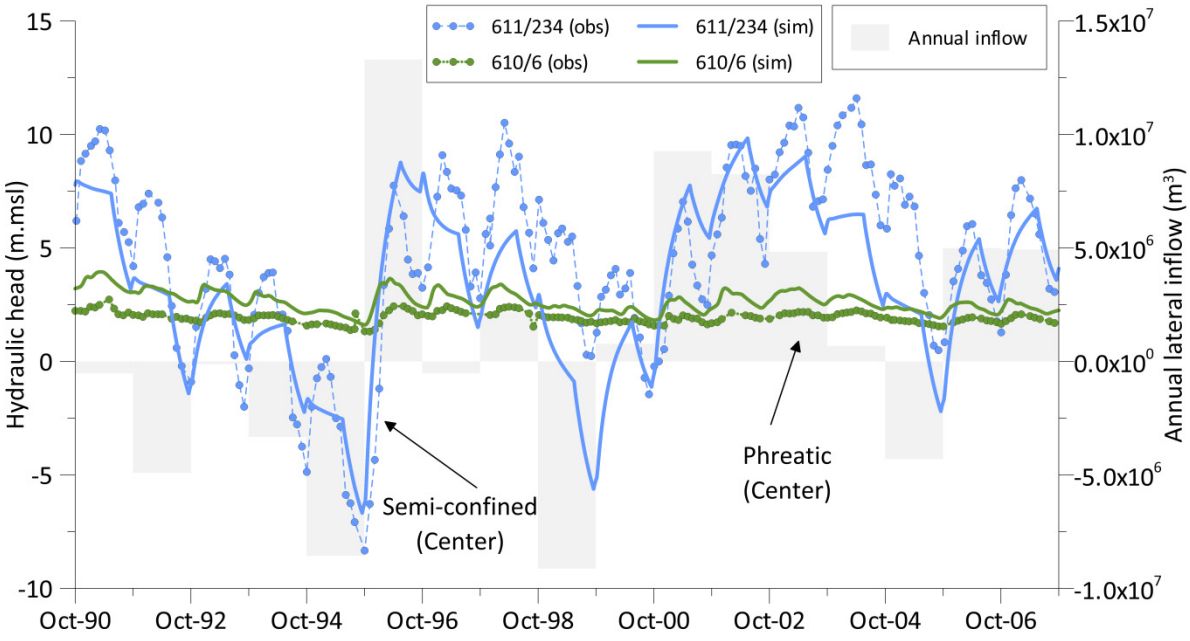

Figure 9.8 Time-series of simulated and observed hydraulic head between 1990 and 2007 in the central sector of the CF.

Simulated hydraulic head in the western and eastern sectors matches observed seasonal variation, but does not follow inter-annual fluctuations (Figure 9.9). The observed inter-

annual pattern in the semi-confined layer is similar across the entire system, however only simulated head in the central sector shows the same behaviour. This suggests that lateral inflow has as a strong control on the inter-annual variability in head in the system, and that it is not as concentrated through the central faults as is currently considered in the model. There is an evident need for future research to focus on improving understanding of the both the physical processes and dynamics of recharge to the CF. In particular understanding the spatial distribution of lateral inflow is important in order to better define the water budgets of each sector.

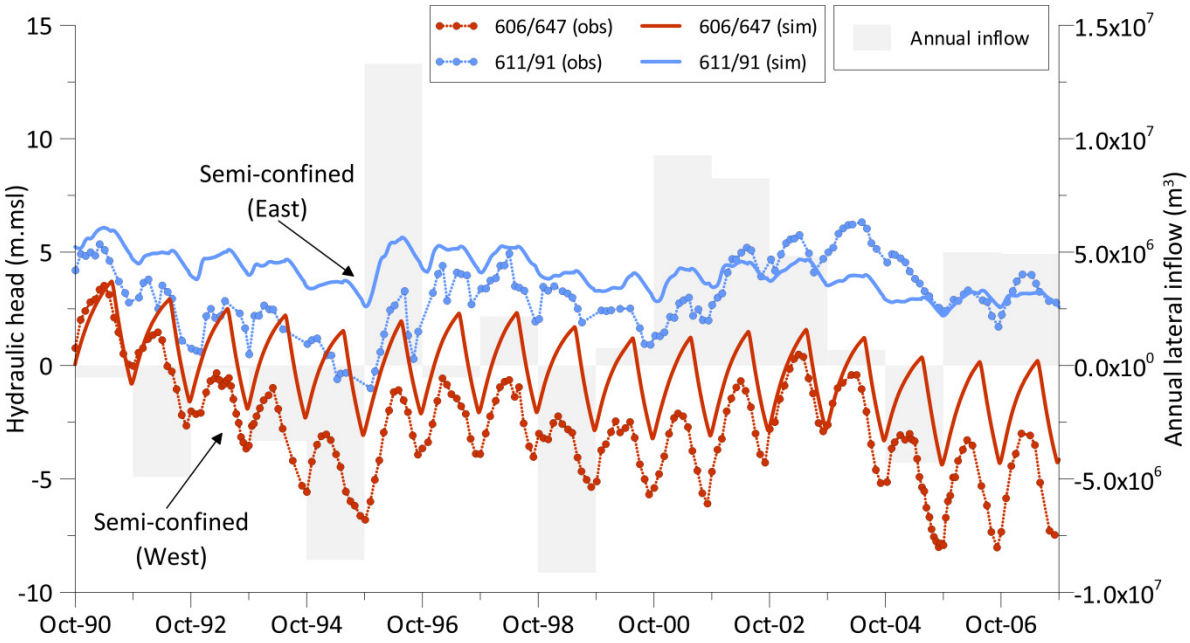

Figure 9.9 Time-series of simulated and observed hydraulic head between 1990 and 2007 in the east and west sectors of the CF.

9.4.2. Numerical model: SWI

Under pre-development conditions (i.e. no abstraction) the model shows freshwater extending below the Ria Formosa (Figure 9.10, top). To the west, the model domain may be too small as the offshore extent of freshwater along the western sector (directly connected to the Atlantic) is limited by the imposed BC. The effort of redesigning the mesh was not considered worthwhile as the aim of the model was to test conceptual ideas of the system and not provide precise predictions of changes to groundwater quality.

The impact of pumping on SWI is very localized, although not in the over-exploited western sector as might be expected. SWI occurs fastest in the highly permeable fractures within the semi-confined aquifer, even though hydraulic heads in this area are the highest in the system. The area affected by SWI along the faults is likely overestimated by the model as it reaches relatively far in-land, affecting several agricultural areas, of which there are no reports. The overestimate can be attributed to several factors: 1) inadequate transport and/or hydraulic parameters for the faults; 2) artificially large dispersivity, which in practice is likely to be smaller, concentrating SWI along a narrower path and creating a sharper transition zone; or 3) underestimated lateral inflow prior to 1990.

Large-scale heterogeneity created by structures such as faults and karst conduits, can form preferential flow paths along which rapid transport may occur (Calvache and Pulido-Bosch 1997; Werner et al 2013) and are often the primary mechanism dominating transport in coastal settings (Fleury et al 2007). Added to this, the depth of the aquifer bottom also influences the onshore extent of SWI (Abarca 2006; Werner et al 2013). The fault lines within the model coincide with the thickest (e.g. deepest) section of the aquifer, which allows the seawater toe to reach further in-land (albeit at greater depth).

Silva et al (1986) sampled groundwater quality during 1982/83 to assess and determine the source of salinization. They identified an elongated area with higher concentration of chloride, and suggested the existence of a paleo-channel along which SWI was occurring. This area coincides with one of the faults, which re-enforces the hypothesis that these provide preferential flow paths for SWI in the CF. As previously discussed, existing data on groundwater quality cannot be used directly to calibrate transport parameters due to both a lack of information to characterize the distribution of saltwater and the coarse nature of the model. However, comparing the (horizontal) spatial distribution of measured chloride concentration and the simulated distribution of seawater, shows that higher observed values coincide with permeable fault-zones along which the model simulates the most SWI.

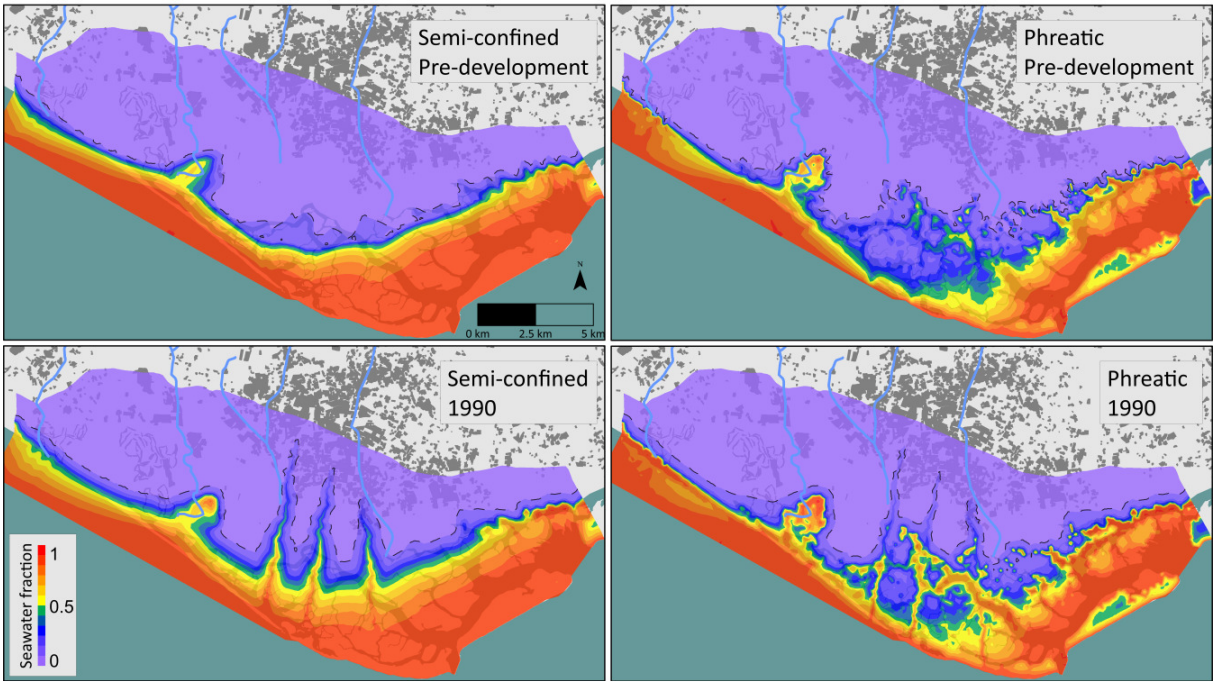

Figure 9.10 Average measured chloride concentrations during 2000-2008 and simulated distribution of seawater under pre-development conditions (top) and at 1990 (bottom).

Figure 9.11 presents the change in seawater distribution from 1990 to 2000 and from 2000 to 2008. These two periods represent the two distinct phases of groundwater use in the region, before and after the abandonment of groundwater as the source for public water supply. During the 1990's seawater continues to move landward across much of the system, with the most significant increases occurring along the fractures and in the western sector.

The impact of the switch in water source is evident, with a groundwater rapidly quality improving along the fractures, although SWI continues in the western sector. Given that the model overestimates groundwater levels in this sector, it likely underestimates the rate and extent of SWI here as well. On the other hand, the extent of SWI along the fractures is likely overestimated, due to the inadequate initial conditions as discussed above. Improving data collection and the characterization of the spatial and temporal variability of the fresh-saltwater interface is of particular importance to both validate the model and understand the importance of permeable faults as a pathway for SWI in the CF.

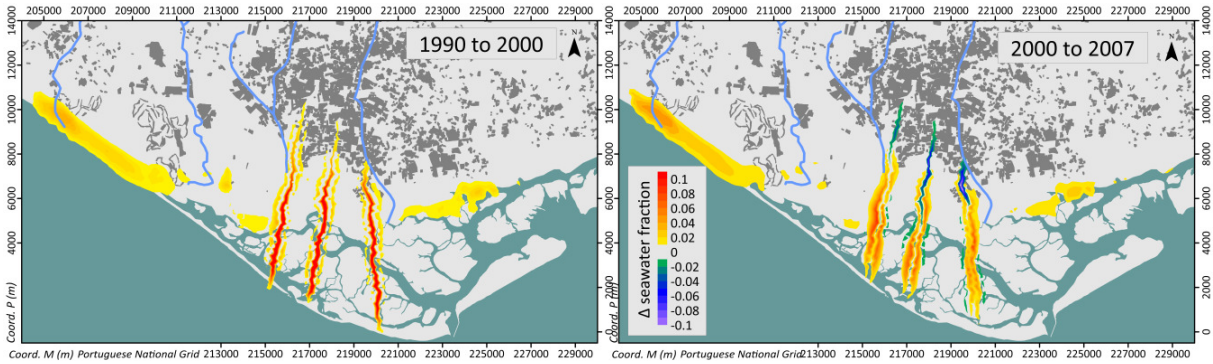

Figure 9.11 Change in seawater distribution in the semi-confined aquifer between 1990 and 2000 and between 2000 and 2007.

Model results suggest that current groundwater use from the CF is un-sustainable, in particular in the western sector. However, even ignoring expected impacts of climate change, the central sector is at risk of some SWI in the long term (Figure 9.12). Although changes along the highly permeable fractures are likely to occur over short periods, the movement of seawater within the porous media occurs over several years or decades. Thus it is possible, or even likely, that the fresh-saltwater interface in the CF is not yet at equilibrium. As shown in Figure 9.12, significant encroachment would be expected under current climate and groundwater water use conditions, making abstraction for golf course irrigation unfeasible and completely reducing the offshore freshwater wedge beneath the Ria Formosa lagoon. Fortunately the long time-scales at which SWI occurs allows for further study to refine the representation of the system and provide more accurate predictions, in time for adequate management measures to be put into place.

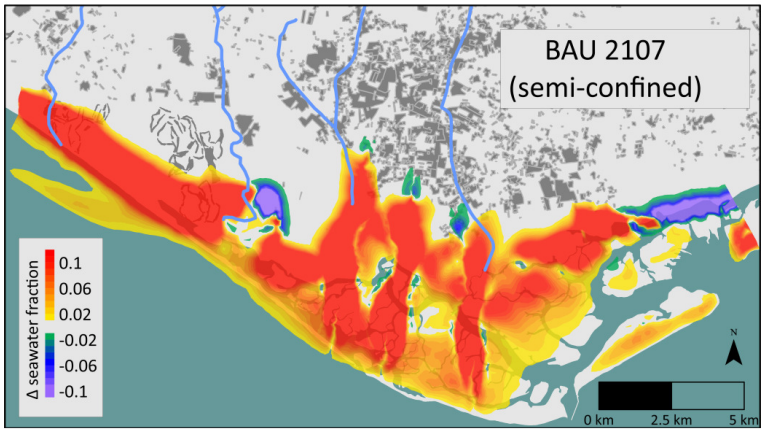

Figure 9.12Change in seawater distribution after 100 years of *business as usual*.

9.4.3. Mitigation scenarios: SWI

The impact of proposed mitigation scenarios on SWI within the semi-confined aquifer is shown in Figure 9.13. Results do not represent the final position of the interface, merely the impact after twenty years, with the aim to compare the relative change for each scenario.

Both MAR schemes have negligible effects on SWI, with stream infiltration having a slightly greater impact. This is likely due to MAR being concentrated within a smaller area, thus causing a greater localized increase in hydraulic gradient. An additional scenario was simulated in which greenhouse runoff was injected directly into the semi-confined layer, but results (not shown for brevity) were very similar.

As is to be expected changes to groundwater use have the greatest impact, as they represent the largest change to water budget. Replacing groundwater as the source of supply for agriculture causes most change, with improvements across the entire system. However, despite the large increase in groundwater levels, boreholes abstracting water for the golf courses are still at risk of salinization, as they still capture water from the seaward boundary due to their proximity to the coastline.

Removing abstraction for the golf courses reduces SWI in the western sector, but has little effect elsewhere. And in fact, improvements in the western sector are similar to those observed for the no abstraction for agriculture scenario. Either solution is only feasible in practice if alternative sources of water are found. The area supplied by the large surface water dams could be expanded to include agriculture within the CF. Other solutions to protect groundwater use for the golf courses could include the re-use of treated wastewater as (1) an alternative source for irrigation, (2) as a source for a *store and recover* MAR scheme and/or (3) as a hydraulic barrier to avoid further seawater encroachment. Cost/benefit analyses are necessary to assess the economic feasibility of any of these solutions, alongside more detailed assessments of the local hydrogeological characteristics of the system to assess the practical feasibility.

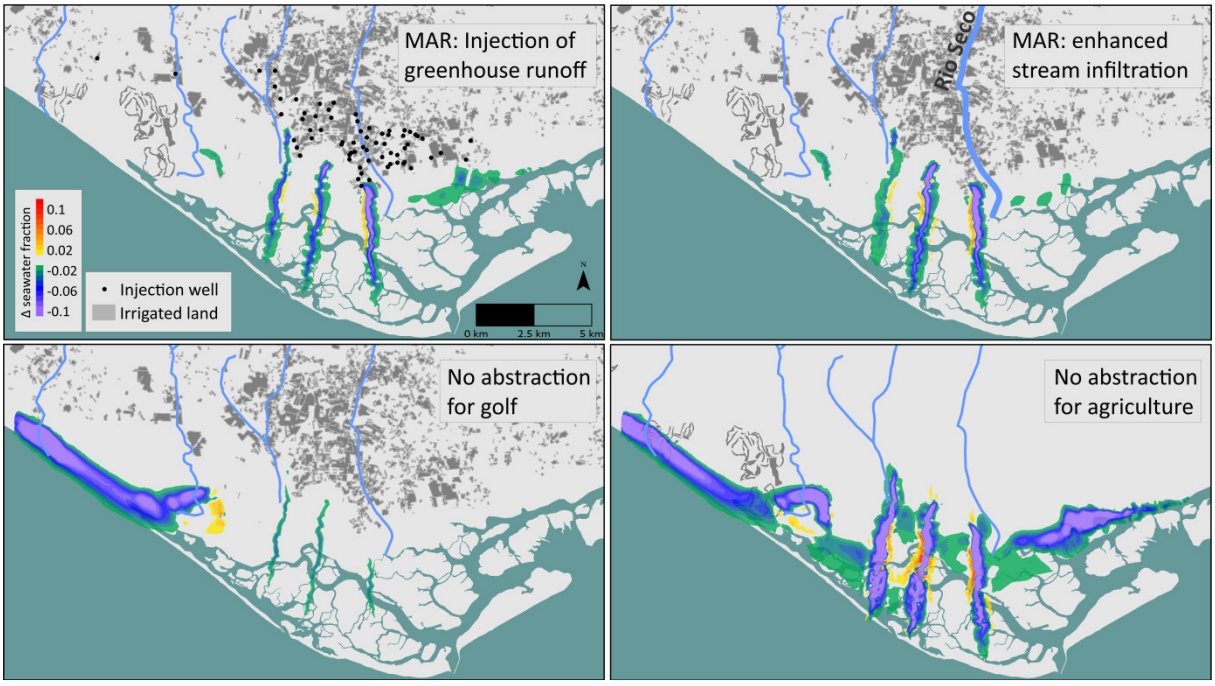

Figure 9.13 Effect of mitigation scenarios on spatial distribution of seawater in the semi-confined aquifer in comparison to the effect of *business as usual*.

9.5. Conclusions

A density-coupled flow and transport model was developed for the CF multi-layer aquifer system, validating the existing conceptual model. Due to a lack of adequate groundwater quality data, transport parameters are not calibrated. Thus the model provides insights into the general behaviour of the system, but cannot be used in a predictive capacity.

The first estimate of current lateral inflow to the CF was calculated at 5.2×10^6 $m^3.yr^{-1}$ (approximately 50% of direct recharge). Even so, groundwater removed from the CF for human use is almost equal to total estimated recharge, placing the system at risk of SWI. The good fit between observed and simulated hydraulic heads, for an acceptable range of hydraulic parameters, corroborates the conceptual model of lateral inflow through fractures contributing to groundwater budget of the system. However, discrepancies in simulated results for the western and eastern sectors suggest that lateral flow is spatially distributed across the system and not concentrated in the central sector as was considered in the model.

Simulated results provide an explanation for the lack of evidence of SWI despite significant drawdown in the western sector during the last several decades. The delayed effect of SWI can be explained by the effect of (1) hydraulic parameters of the semi-confined aquifer and/or (2) offshore freshwater created by the confining clay layer. The joint evidence of increasing chloride concentrations since 2009 and model results show that the western sector is currently overexploited. Adaptation measures are necessary if groundwater quality is to be protected. The proximity to the seaward boundary of abstraction wells that supply the golf courses in the western sector, places these at particular risk of salinization. Simulations comparing the effect of several mitigation measures show that intervention upstream does not guarantee the protection of these well-fields.

Unexpectedly, simulations suggest that the rest of the system is also at risk of SWI despite elevated groundwater levels and no observed decrease in quality. However, the interfaces slow rate of movement and offshore extent means that it will probably take several decades to reach existing monitoring wells, which provides an opportunity for pre-emptive measures to be put into practice. Further work should focus on identifying and characterizing the spatial and temporal variability of the interface, in order to assess the validity of these results. In particular the influence of the water bearing faults requires further study, as the model suggests that they provide an important pathway for SWI.

Simulated mitigation scenarios suggest that significant changes in water use practices are needed to counteract SWI. In particular the well fields that supply golf courses in the western sector are at risk, due to their proximity to the sea and the hydraulic properties of the system. Further work is still needed to improve the understanding of the system and provide reliable predictions of the impact of changes to water use and climate. However, the preliminary results provided here already show that groundwater management needs to be adapted to avoid problems in the future.

10.Conclusions and Final Remarks

Numerical models of varying scales and degrees of complexity were applied to study issues related to coastal aquifer management in the Algarve. Theoretical questions related to maximizing sustainable yield taking into account spatiotemporal variability were analyzed and insights into the hydrogeological behaviour of several aquifer systems were provided. These insights contribute to improving the management of these groundwater bodies by (1) supplying estimates of sustainable yield, (2) re-enforcing existing or new conceptual models of system behaviour and (3) providing insight into potential SWI mechanisms and guidance on further data needs.

Sustainable yield cannot be defined on a simple ratio of long-term average recharge if the sustainability criteria include maintaining a given rate of SGD. However, adapting the time-scale at which sustainable yield is defined allows for an effective increase in abstraction, whilst maintaining the same average discharge. In fact, not reducing the temporal scale leads to an irretrievable loss of freshwater during recharge periods. Furthermore, predicted seasonal changes in rainfall for the south of Portugal will make taking the temporal scale of the system into account more important, as the concentration of recharge into a shorter period will lead to faster depletion and therefore larger freshwater loss if abstraction is concentrated during the dry period.

However, sustainable yield may be defined based on long-term averages in coastal aquifers for which maintaining SGD is not of concern and that have a relatively small discharge area in comparison to their in-land extent (such as the QS). In these cases the time-scale for SWI will be strongly influenced by the permeability and porosity of the system, but will be larger than the time-scale for impacts on SGD. On the other hand, the spatial distribution of abstraction can have a significant impact on sustainable yield when the ratio between discharge area and in-land extent is large. Concentrating abstraction, in particular if near the coast, leads to drawdown that can cause localized SWI problems, as was shown for the remaining case studies.

Simulated effects of climate change on recharge rates and groundwater demand show that these will cause SWI in the long-term, if current water use and management practices are

maintained. As mentioned above, changes in seasonal rainfall patterns will affect SGD within the short-term however the impacts on SWI will require longer to take effect. Fortunately this provides the opportunity to put adaptation and mitigation measures into practice before the onset of negative impacts. Several management and technical solutions to mitigate the impact of climate changes are feasible and simulations show that they do contribute to reducing SWI. Even so, the joint application of measures that reduce demand and increase supply will be necessary to counteract growing water scarcity.

Density effects were shown to not have a significant effect on regional scale discharge rates and can be ignored if the aim is merely to determine the freshwater component of coastal groundwater discharge. However, ignoring changes in fluid density leads to inaccurate representations of groundwater levels in long-term simulations that depart from the conditions under which the model was calibrated (e.g. climate change scenarios). Therefore, cheaper flow models are an efficient choice to study discharge rates at a regional scale, but more complex variable density models are necessary of SWI is to be assessed.

New insights in to the hydrogeology of several aquifer systems, obtained from field observations and complemented with numerical modelling, suggest the existence of potential offshore freshwater reserves in the Algarve. These could provide interesting opportunities for groundwater management as water reservoirs. As the fresh-saltwater interface moves at a slow rate and is located offshore, groundwater mining can be used in the short-term without significant SWI. This makes these systems particularly useful as backups or sources for emergency water supplies during periods of drought, as they can be temporarily overexploited without immediate risk of SWI. They also present practical characteristics for managed aquifer recharge. By increasing recharge to the system, onshore hydraulic pressure will induce saltwater movement away from land and increase the volume of offshore freshwater. As in any coastal aquifer, increased recharge will eventually be lost as discharge to the sea, however the longer residence times in a semi-/confined system will make injected water available for re-capture for longer, making them more useful for store and recover schemes. There are several aquifer systems in the region with characteristics that may allow for the formation of offshore freshwater, however there is still a significant

lack of data to characterize them in sufficient detail. Given the growing pressures on water resources and the predicted increase in water scarcity for the region, confirming the existence of freshwater reserves and having a sound understanding of physical characteristics of these coastal groundwater bodies is fundamental for an efficient and sustainable management of available water resources.

Despite an extensive continuous monitoring network and a wealth of groundwater level and quality data in the region, there is still a lack of data to accurately characterize the hydrogeological conditions that describe three-dimensional flow and transport under variable-density conditions. As was shown, SWI can be significantly affected by the heterogeneity of the subsurface, be it in the form of vertical resistance from aquitard or preferential flow paths created by faults or karst conduits. Improving the characterization of geological and structural features of these systems is fundamental for any future development of numerical models to describe and predict SWI with a greater degree of certainty.

The same holds for the distribution of the fresh-saltwater interface. Current groundwater monitoring is almost entirely based on point measurements in boreholes or wells, few of which are adequately located to capture the interface. Although these can act as triggers for managers to enact emergency measures to avoid further SWI (Werner et al 2011), they are far from sufficient to provide a detailed image of the position or movement of saltwater, necessary for the numerical model development and calibration. As discussed by Post (2005), effective subsurface characterization for SWI modelling requires methods that provide information on lateral variations in lithology, hydraulic properties and salinity, such as two- and three-dimensional geo-electrical, airborne electromagnetic and seismic methods. Future studies in the region should aim to apply these, along with complementary methods (e.g. environmental tracers and isotopic techniques) to improve knowledge on recharge processes and connectivity between groundwater bodies.

Large-scale density-coupled flow and transport models are still computationally demanding, requiring very long run-times on most common processors. Understanding the physical processes and the particular issues in modelling them also has a steep learning curve,

requiring a large amount of time to master. All this makes developing and applying variable density models expensive and impractical when solving real-world problems. This is particularly the case when available data is scarce and the amount of uncertainty is large, as this can require both greater efforts during model development and calibration, as well as increasing the amount of model runs to include all the sources of uncertainty within obtained results. As such, as stated twenty years ago by Oude Essink and Boekelman (1996), and despite the improvements in computation power during the last two decades, in practice the application of three-dimensional large-scale models of SWI to real-world problems remains limited. This can be circumvented in certain cases by applying coarser meshes and artificially high dispersivity to maintain numerical stability, thus reducing run-times. However, any predictions on the evolution of SWI are likely to be inaccurate. Thus these coarse models can serve the "preliminary modelling" purpose as outlined in chapter 1, but further refinement (and increasing computational cost) is mostly likely required to provide predictive capacity with a greater degree of certainty.

11.References

Abarca E (2006) Seawater intrusion in complex geological environments. Technical University of Catalonia,

Abarca E, Carrera J, Sánchez-Vila X, Voss CI (2007) Quasi-horizontal circulation cells in 3D seawater intrusion. J Hydrol 339:118–129. doi: 10.1016/j.jhydrol.2007.02.017

Alley WM, Leake SA (2004) The Journey from Safe Yield to Sustainability. Ground Water 42:12–16.

Alley WM, Reilly TE, Franke OL (1999) Sustainability of Ground-water Resources - U.S. Geological Survey Circular 1186. U.S. Geological Survey, Denver, Colorado

Almeida C, Crispim JA (1987) Traçagens com uranina no Algarão do Escarpão. 9–16.

Almeida C, Mendonça JJL, Jesus MR, Gomes AJ (2000) Sistemas Aquíferos de Portugal Continental. INAG, Lisbon

Almeida C. e M., Silva L (1990) Hidrogeologia do Miocénico entre Albufeira e Ribeira de Quarteira. Geolis IV:199–216.

Almeida CA da C (1985) Hidrogeologia do Algarve Central. Universidade de Lisboa

Andersen MS, Baron L, Gudbjerg J, et al (2007) Discharge of nitrate-containing groundwater into a coastal marine environment. J Hydrol 336:98–114. doi: 10.1016/j.jhydrol.2006.12.023

Bakker M (2006) Analytic solutions for interface flow in combined confined and semi-confined, coastal aquifers. Adv Water Resour 29:417–425. doi: 10.1016/j.advwatres.2005.05.009

Bakker M, Schaars F (2013) Modeling steady sea water intrusion with single-density groundwater codes. Ground Water 51:135–44. doi: 10.1111/j.1745-6584.2012.00955.x

Barlow PM (2003) Ground Water in Freshwater-Saltwater Environments of the Atlantic Coast. U S Geol Surv - Circ 1262 Circular 1:121.

Bear J, Cheng AH-D, Sorek S, et al (1999) Seawater Intrusion in Coastal Aquifers — Concepts, Methods and Practices. doi: 10.1007/978-94-017-2969-7

Bear J, Verruijt A (1987) Modeling Groundwater Flow and Pollution. doi: 10.1007/978-94-009-3379-8

Bekesi G, McGuire M, Moiler D (2009) Groundwater Allocation Using a Groundwater Level Response Management Method—Gnangara Groundwater System, Western Australia. Water Resour Manag 23:1665–1683. doi: 10.1007/s11269-008-9346-5

Beltrão (1985) Rega localizada (Localized irrigation). Faro, Portugal

Bettencourt P, Alcobia S, Monteiro JP, et al (2013) Planeamento e gestão de massas de água subterrânea no Alentejo e Algarve – abordagens inovadoras e necessidades subsequentes de aprofundamento do conhecimento. 8º Congr Ibérico Gestão e Planeam da Água 775–784.

Bratton JF (2010) The Three Scales of Submarine Groundwater Flow and Discharge across Passive Continental Margins. J Geol 118:565–575. doi: 10.1086/655114

Bredehoeft JD (1997) Safe Yield and the Water Budget Myth. Ground Water 35:929–929.

doi: 10.1111/j.1745-6584.1997.tb00162.x

Bronzini S (2011) Etude Hydrogeologique de la zone de Albufeira (Algarve, Portugal) et Analyse des Mecanismes de Salinisation des Eaux Souteraines. Université de Neuchâtel

Burnett WC, Aggarwal PK, Aureli a, et al (2006) Quantifying submarine groundwater discharge in the coastal zone via multiple methods. Sci Total Environ 367:498–543. doi: 10.1016/j.scitotenv.2006.05.009

Calvache ML, Pulido-Bosch A (1997) Effects of geology and human activity on the dynamics of salt-water intrusion in three coastal aquifers in southern Spain. Environ Geol 30:215–223. doi: 10.1007/s002540050149

Carneiro JF, Boughriba M, Correia A, et al (2010) Evaluation of climate change effects in a coastal aquifer in Morocco using a density-dependent numerical model. Environ Earth Sci 61:241–252. doi: 10.1007/s12665-009-0339-3

Carreira PM, Marques JM, Nunes D (2014) Source of groundwater salinity in coastline aquifers based on environmental isotopes (Portugal): Natural vs. human interference. A review and reinterpretation. Appl Geochemistry 41:163–175. doi: 10.1016/j.apgeochem.2013.12.012

Chang SW, Clement TP (2012) Experimental and numerical investigation of saltwater intrusion dynamics in flux-controlled groundwater systems. Water Resour Res 48:n/a–n/a. doi: 10.1029/2012WR012134

Chang SW, Clement TP, Simpson MJ, Lee K-K (2011) Does sea-level rise have an impact on saltwater intrusion? Adv Water Resour 34:1283–1291. doi: 10.1016/j.advwatres.2011.06.006

Costa JPP (2006) Calibraçao Inversa de um Modelo de Escoamento Subterraneao com Aplicaçao daos Sistemas Aquiferos de Albufeira-Ribeira de Quarteira e Quarteira. Universidade Tecnica de Lisboa

Costa L, Hugman R, Monteiro JP (2013) Modelação da Descarga de Águas Subterrâneas dos Aquíferos de Abufeira-Ribeira De Quarteira e de Quarteira (Algarve,Portugal). 9o Semin. sobre Águas Subterraneas da APRH. Lisbon, pp 82–85

Costa L, Monteiro JP, Leitão T, et al (2015a) Estimating harvested rainwater at greenhouses in south Portugal aquifer Campina de Faro for potential infiltration in Managed Aquifer Recharge . EGU Gen. Assem. 2015. Copernicus GmbH, Vienna, Austria, p 10415

Costa L, Monteiro JP, Oliveira M, et al (2015b) Modelling Contributions of the Local and Regional Groundwater Flow of Managed Aquifer Recharge Activities at Querença-Silves Aquifer System . EGU Gen. Assem. 2015. p 11930

Costa LRD, Monteiro JP, Oliveira MM, et al (2015c) Interpretation of an injection test in a large diameter well in south Portugal and contribution to the understanding of the local hydrogeology. 10.º Semin. sobre Águas Subterrâneas. APRH, Evora, Portugal, pp 2013–2016

Custodio E (2002) Aquifer overexploitation: what does it mean? Hydrogeol J 10:254–277. doi: 10.1007/s10040-002-0188-6

Das A, Datta B (2001) Application of optimisation techniques in groundwater quantity and quality management. Sadhana 26:293–316. doi: 10.1007/BF02703402

Dausman AM, Langevin C, Bakker M, Schaars F (2010) A comparison between SWI and SEAWAT – the importance of dispersion , inversion and vertical anisotropy. 21st Salt Water Intrusion Meet. Azores, pp 271–274

Dias JMA, Boski T, Rodrigues A, Magalhães F (2000) Coast line evolution in Portugal since the Last Glacial Maximum until present — a synthesis. Mar Geol 170:177–186. doi: 10.1016/S0025-3227(00)00073-6

Diersch HJG (2014) FEFLOW: Finite Element Modeling of Flow, Mass and Heat Transport in Porous and Fractured Media. doi: 10.1007/978-3-642-38739-5

Diersch H-JG, Kolditz O (1998) Coupled groundwater flow and transport: 2. Thermohaline and 3D convection systems. Adv Water Resour 21:401–425. doi: 10.1016/S0309-1708(97)00003-1

Doherty J (2002) Model-Independent Parameter Estimation, 4th edn. Watermark Numerical Computing

Doherty J (2003) Ground water model calibration using pilot points and regularization. Groundwater 41:170–177.

Domenico PA, Schwartz FW (1997) Physical and Chemical Hydrogeology, 2nd edn. Wiley, New York

Eamus D, Froend R (2006) Groundwater-dependent ecosystems: the where, what and why of GDEs. Aust J Bot 54:91. doi: 10.1071/BT06029

Encarnação J, Leitão F, Range P, et al (2013) The influence of submarine groundwater discharges on subtidal meiofauna assemblages in south Portugal (Algarve). Estuar Coast Shelf Sci 130:202–208. doi: 10.1016/j.ecss.2013.04.013

Estrela T, Marcuello C, Iglesias A (1996) Water Resources Problems in Southern Europe. Copenhagen, Denmark

Ferguson G, Gleeson T (2012) Vulnerability of coastal aquifers to groundwater use and climate change. Nat Clim Chang 2:342–345. doi: 10.1038/nclimate1413

Fernandes J, Carrara G, Terrinha P, et al (2015) Descargas do sistema aquífero Albufeira-Ribeira e Quarteira em meio marinho - métodos e cartografia. 10.º Semin. sobre Águas Subterrâneas. APRH, Evora, Portugal, pp 4–7

Fernandes NP (2013) Ecossistemas Dependetes de Água Subterranea no Algarve - Contributo para a sua Identificaçao e Caracterizaçao. University of the Algarve

Fleury P, Bakalowicz M, de Marsily G (2007) Submarine springs and coastal karst aquifers: A review. J Hydrol 339:79–92. doi: 10.1016/j.jhydrol.2007.03.009

Francés AP, Ramalho EC, Fernandes J, et al (2015) Contributions of hydrogeophysics to the hydrogeological conceptual model of the Albufeira-Ribeira de Quarteira coastal aquifer in Algarve, Portugal | Contributions de l'hydrogéophysique au modèle conceptuel hydrogéologique de l'aquifère côtier Albufeira-R. Hydrogeol J 23:1553–1572. doi: 10.1007/s10040-015-1282-x

Francés AP, Ramalho EC, Fernandes J, et al (2014) Hydrogeophysics contribution to the development of hydrogeological conceptual model of coastal aquifers – Albufeira-Ribeira de Quarteira aquifer case study. 8a Assem. Luso Esp. Geod. e Geofis. Evora, pp 533–542

Gaaloul N (2012) Simulation of Seawater Intrusion in Coastal Aquifers: Forty Five-Years Exploitation in an Eastern Coast Aquifer in NE Tunisia. Open Hydrol J 6:31–44. doi: 10.2174/1874378101206010031

Geinaert W, van Beers PH, de Vries JJ, Hoogeveen H (1982) A Geo Electric survey of the Miocene Aquifer between Quarteira and Olhao. Vrije Universiteit, Amsterdam, Netherlands

Gelhar LW, Welty C, Rehfeldt KR (1992) A critical review of data on field-scale dispersion in aquifers. Water Resour Res 28:1955–1974. doi: 10.1029/92WR00607

Ghassemi F, Jakeman AJ, Jacobson G, Howard KWF (1996) Simulation Of Seawater Intrusion With 2D And 3D Models: Nauru Island Case Study. Hydrogeol J 4:4–22. doi: 10.1007/s100400050251

Giorgi F (2006) Climate change hot-spots. Geophys Res Lett 33:L08707. doi: 10.1029/2006GL025734

Gleeson T, Alley WM, Allen DM, et al (2012) Towards sustainable groundwater use: setting long-term goals, backcasting, and managing adaptively. Ground Water 50:19–26. doi: 10.1111/j.1745-6584.2011.00825.x

Goderniaux P, Brouyère S, Blenkinsop S, et al (2011) Modeling climate change impacts on groundwater resources using transient stochastic climatic scenarios. Water Resour Res 47:n/a–n/a. doi: 10.1029/2010WR010082

Green NR, MacQuarrie KTB (2014) An evaluation of the relative importance of the effects of climate change and groundwater extraction on seawater intrusion in coastal aquifers in Atlantic Canada. Hydrogeol J 22:609–623. doi: 10.1007/s10040-013-1092-y

Green TR, Taniguchi M, Kooi H, et al (2011) Beneath the surface of global change: Impacts of climate change on groundwater. J Hydrol 405:532–560. doi: 10.1016/j.jhydrol.2011.05.002

Groves CG, Howard AD (1994) Early development of karst systems: 1. Preferential flow path enlargement under laminar flow. Water Resour Res 30:2837–2846. doi: 10.1029/94WR01303

Holman IP (2006) Climate change impacts on groundwater recharge- uncertainty, shortcomings, and the way forward? Hydrogeol J 14:637–647. doi: 10.1007/s10040-005-0467-0

Holman IP, Allen DM, Cuthbert MO, Goderniaux P (2012) Towards best practice for assessing the impacts of climate change on groundwater. Hydrogeol J 20:1–4. doi: 10.1007/s10040-011-0805-3

Holman IP, Trawick P (2011) Developing adaptive capacity within groundwater abstraction management systems. J Environ Manage 92:1542–9. doi: 10.1016/j.jenvman.2011.01.008

Hugman R, Stigter TY, Monteiro JP, et al (2014) Modeling the spatial and temporal distribution of coastal groundwater discharge for different water use scenarios under epistemic uncertainty: case study in South Portugal. Environ Earth Sci 73:2657–2669. doi: 10.1007/s12665-014-3709-4

Hugman R, Stigter TY, Monteiro JP, et al (2015) Modeling the spatial and temporal

distribution of coastal groundwater discharge for different water use scenarios under epistemic uncertainty: case study in South Portugal. Environ Earth Sci 73:2657–2669. doi: 10.1007/s12665-014-3709-4

Hugman R, Stigter TY, Monteiro JP (2013a) The importance of temporal scale when optimising abstraction volumes for sustainable aquifer exploitation: A case study in semi-arid South Portugal. J Hydrol 490:1–10. doi: 10.1016/j.jhydrol.2013.02.053

Hugman R, Stigter TY, Monteiro JP (2013b) The importance of temporal scale when optimising abstraction volumes for sustainable aquifer exploitation: A case study in semi-arid South Portugal. J Hydrol 490:1–10. doi: 10.1016/j.jhydrol.2013.02.053

Hugman R, Stigter TY, Monteiro JP, Nunes L (2012) Influence of aquifer properties and the spatial and temporal distribution of recharge and abstraction on sustainable yields in semi-arid regions. Hydrol Process 26:2791–2801. doi: 10.1002/hyp.8353

Huyakorn P, Pinder G (1983) Computational Methods in Subsurface Flow. Academic Press, Inc, New York

Ibánhez JSP, Leote C, Rocha C (2011) Porewater nitrate profiles in sandy sediments hosting submarine groundwater discharge described by an advection–dispersion-reaction model. Biogeochemistry 103:159–180. doi: 10.1007/s10533-010-9454-1

INAG (2005) Relatório Síntese Sobre a Caracterização das Regiões Hidrográficas Prevista na Directiva-Quadro da Àgua (Report on the Caracterization of the Hydrographic Regions as per the Water Framework Directive). Lisbon, Portugal

IPCC (2014) Climate Change 2014: Impacts, Adaptation, and Vulnerability. Part A: Global and Sectoral Aspects. Contribution of Working Group II to the Fifth Assessment Report of the Intergovernmental Panel on Climate Change. Clim Chang 2014 Impacts, Adapt Vulnerability - Contrib Work Gr II to Fifth Assess Rep. doi: 10.1016/j.renene.2009.11.012

Jackson CR, Meister R, Prudhomme C (2011) Modelling the effects of climate change and its uncertainty on UK Chalk groundwater resources from an ensemble of global climate model projections. J Hydrol 399:12–28. doi: 10.1016/j.jhydrol.2010.12.028

Johannes R (1980) The Ecological Significance of the Submarine Discharge of Groundwater. Mar Ecol Prog Ser 3:365–373. doi: 10.3354/meps003365

Kalf FRP, Woolley DR (2005) Applicability and methodology of determining sustainable yield in groundwater systems. Hydrogeol J 13:295–312. doi: 10.1007/s10040-004-0401-x

Kang F, Jin M, Qin P (2011) Sustainable yield of a karst aquifer system: a case study of Jinan springs in northern China. Hydrogeol J 19:851–863. doi: 10.1007/s10040-011-0725-2

Keller J, Bliesner RD (1990) Sprinkle and Trickle Irrigation. The Blackburn Press

Kerrou J, Renard P, Tarhouni J (2010) Status of the Korba groundwater resources (Tunisia): observations and three-dimensional modelling of seawater intrusion. Hydrogeol J 18:1173–1190. doi: 10.1007/s10040-010-0573-5

Kiraly L (1975) Rapport sur l'état actuel des connaissances dans le domaine des caractères physiques des roches karstiques (Report on the Present Knowledge on the Physical Characters of Karstic Rocks). In: Burger A, Dubertret L (eds) Hydrogeol. karstic terrains. International Association of Hydrogeologists (IAH), Paris, France, pp 53–67

Kolditz O, Ratke R, Dierschb HG, Zielke W (1998) Coupled groundwater flow and transport : 1 . Verification of variable density flow and transport models. 21:

Konikow LF, Kendy E (2005) Groundwater depletion: A global problem. Hydrogeol J 13:317–320. doi: 10.1007/s10040-004-0411-8

Kontar AY, Newton A (2009) Study of the Impact of Submarine Groundwater Discharge on the Bio-Geochemical Parameters of Coastal Waters off Southern Portugal. AGU Fall Meet Abstr -1:0932.

Kooi H, Groen J (2001) Offshore continuation of coastal groundwater systems; predictions using sharp-interface approximations and variable-density flow modelling. J Hydrol 246:19–35. doi: 10.1016/S0022-1694(01)00354-7

Kopsiaftis G, Mantoglou a., Giannoulopoulos P (2009) Variable density coastal aquifer models with application to an aquifer on Thira Island. Desalination 237:65–80. doi: 10.1016/j.desal.2007.12.023

Koussis AD, Mazi K, Destouni G (2012) Analytical single-potential, sharp-interface solutions for regional seawater intrusion in sloping unconfined coastal aquifers, with pumping and recharge. J Hydrol 416-417:1–11. doi: 10.1016/j.jhydrol.2011.11.012

Lee CH (1915) The determination of safe yield of underground reservoirs of the closed basin type. Transactions of the American Society of Civil Engineers, New York

Leitão TE, Lobo-Ferreira JP, Carvalho T, et al (2014) MARSOL : Demonstrating Managed Aquifer Recharge as a Solution to Water Scarcity and Drought. 10.º Semin. sobre Águas Subterrâneas. APRH, Evora, Portugal, p 4

Leote C, Ibánhez JS, Rocha C (2008) Submarine Groundwater Discharge as a nitrogen source to the Ria Formosa studied with seepage meters. Biogeochemistry 88:185–194. doi: 10.1007/s10533-008-9204-9

Llopis-Albert C, Pulido-Velazquez D (2013) Discussion about the validity of sharp-interface models to deal with seawater intrusion in coastal aquifers. Hydrol Process n/a–n/a. doi: 10.1002/hyp.9908

Loáiciga H a., Pingel TJ, Garcia ES (2012) Sea water intrusion by sea-level rise: Scenarios for the 21st century. Ground Water 50:37–47. doi: 10.1111/j.1745-6584.2011.00800.x

Lobo-Ferreira JP, Diamantino C, Moinante M, et al (2006) GABARDINE project - Groundwater artificial recharge based on alternative sources of water : advanced integrated technologies and management. Deliverable D51 – Test sites and their characteristics. Lisbon, Portugal

Lohman S., Bennett RR, Brown RH, et al (1972) Definitions of selected ground-water terms, revisions and conceptual refinements.

Lopes JB da S (1841) Corografia: ou, Memoria economica, estadistica, e topografica do Reino do Algarve. Typ.da Academia [R.das Sciencias de Lisboa]

Lourenço M (1992) Almeida , C . e M . Lourenço da Silva (1992) Hidrogeologia do sistema aquífero de Quarteira Geolis , revista da Secção de Geologia Ec . e Aplicada , vol . HIDROGEOLOGIA DO SISTEMA AQUÍFERO DE QUARTEIRA. VI:61–79.

Lu W, Yang Q, Tang G (2011) A numerical modelling of seawater intrusion with a 3D density dependent model in Shenzhen. 2011 Int Conf Electr Control Eng 5181–5184. doi:

10.1109/ICECENG.2011.6058228

Maimone M (2004) Defining and Managing Sustainable Yield. Ground Water 42:809–814. doi: 10.1111/j.1745-6584.2004.tb02739.x

Maimone M, Harley B, Fitzgerald R, et al (2003) Coastal Aquifer Planning Elements. Coast Aquifer Manag Model Case Stud. doi: 10.1201/9780203493496.ch1

Malta E, Stigter TY, Pacheco A, et al (2016) Effects of External Nutrient Sources and Extreme Weather Events on the Nutrient Budget of a Southern European Coastal Lagoon. Estuaries and Coasts 1–18. doi: 10.1007/s12237-016-0150-9

Manuppella G (1992) Notícia Explicativa da Carta geológica da região do Algarve (escala 1/100000) [Explanatory note of the geological map of the Algarve region].

MED-EUWI (2007) Mediterranean Groundwater Report: Technical report on groundwater management in the Mediterranean and the Water Framework Directive.

Michael H a, Mulligan AE, Harvey CF (2005) Seasonal oscillations in water exchange between aquifers and the coastal ocean. Nature 436:1145–1148. doi: 10.1038/nature03935

Monteiro J, Ribeiro L, Reis E, et al (2007a) Modelling Stream-Groundwater Interactions in the Querença-Silves Aquifer System. XXXV AIH Congr. Groundw. Ecosyst. Lisbon, Portugal, pp 41–42

Monteiro JP, Costa MS (2004) Dams, Groundwater Modelling and Water Management at the Regional Scale in a Coastal Mediterranean Area (The Southern Portugal Region–Algarve). Larhyss J 3:157–169.

Monteiro JP, Martins P, Martins R (2005) Estudo Hidrogeologico para o Dimensionamento do Sistema de Abastecimento de Água do Campo de Golfe e Estruturas Turisticas Associadas de Vila Sol. Actas do 7º Simpósio Hidráulica e Recur. Hídricos dos Países Língua Of. Port. Evora, p 110

Monteiro JP, Nunes L, Vieira J, et al (2003) Síntese Bidimensional dos Modelos Conceptuais de Funcionamento Hidráulico de Seis Sistemas Aquíferos do Algarve, Baseada em Modelos Numéricos de Escoamento Regional (Bidimensional Sythesis of Conceptual Models of Six Aquifers oif the Algarve, Based on Reg. In: L R, Peixinho de Cristo F (eds) As Águas Subterrâneas no Sul da Península Ibérica. International Association of Hydrologists. APRH publ, Lisbon, Portugal, pp 159–169

Monteiro JP, Oliveira MM, Costa JP (2007b) Impact of the Replacement of Groundwater by Dam Waters in the Albufeira-Ribeira de Quarteira and Quarteira Coastal Aquifers. XXXV AIH Congr. Groundw. Ecosyst. Lisbon, Portugal, pp 489–490

Monteiro JP, Ribeiro L, Martins J (2007c) Modelação Matemática do Sistema Aquífero Querença-Silves. Relatório Final. Validação e Análise de Cenários Relatório Técnico. Lisbon, Portugal

Monteiro JP, Santos J, Martins R (2002) Evaluation of the Impacts Associated to Changes in Exploration Regimes of Aquifers in the Central Algarve Using Numerical Models. III Iber. Congr. Water Manag. Plan. Sevilha, pp 717–724

Monteiro JP, Vieira J, Nunes L, Younes F (2006) Inverse Calibration of a Regional Flow Model for the Querenca-Silves Aquifer System. Int. Congr. Integr. Water Resour. Manag. Challenges Sustain. Dev. Marrakech, p 44

Moore WS (2010) The Effect of Submarine Groundwater Discharge on the Ocean. Ann Rev Mar Sci 2:59–88. doi: 10.1146/annurev-marine-120308-081019

Neuman SP (2005) Longitudinal dispersivity data and implications for scaling behavior. Ground Water 44:139–40; discussion 140–1. doi: 10.1111/j.1745-6584.2006.00166.x

Neves MC, Costa L, Monteiro JP (2016) Climatic and geologic controls on the piezometry of the Querença-Silves karst aquifer, Algarve (Portugal). Hydrogeol J 24:1015–1028. doi: 10.1007/s10040-015-1359-6

Newton A, Icely JD, Falcao M, et al (2003) Evaluation of eutrophication in the Ria Formosa coastal lagoon, Portugal. Cont Shelf Res 23:1945–1961. doi: 10.1016/j.csr.2003.06.008

Nicolau R (2002) Modelação e mapeamento da distribuição espacial da precipitação – Uma aplicação a Portugal Continental (Modeling and mapping of the spatial distribution of rainfall). Universidade Nova de Lisboa

Nocchi M, Salleolini M (2013) A 3D density-dependent model for assessment and optimization of water management policy in a coastal carbonate aquifer exploited for water supply and fish farming. J Hydrol 492:200–218. doi: 10.1016/j.jhydrol.2013.03.048

Nunes G, Monteiro JP, Martins J (2006) Quantificação do Consumo de Água Subterrânea na Agricultura por Métodos Indirectos – Detecção Remota (Indirect Methods for Quantifying Agricultural Groundwater Use - Remote Detection). In: ESIG (ed) Proc. IX Encontro Util. Informação Geográfica. Oeiras, Portugal, p 15

Oliveira MM (2006) Recarga de Águas Subterraneas - Metodos de Avaliaçao, 1st edn. Laboratório Nacional de Engenharia Civil, Lisbon, Portugal

Oliveira MM (2004) Recarga de Águas Subterraneas - Metodos de Avaliaçao. Universidade de Lisboa

Oliveira MM, Oliveira L, Ferreira JPL (2008) Estimativa da recarga natural no sistema aquífero de Querença-Silves (Algarve) pela aplicação do modelo BALSEQ_MOD (Estimation of natural recharge in the Querença-Silves aquifer system (Algarve)). Proc. 9.º Congr. da Água. Cascais, Portugal, p 15

Ouazar D, Cheng AHD (eds) (2003) Coastal Aquifer Management-Monitoring, Modeling, and Case Studies. Lewis Publisher, Boca Raton, FL

Oude Essink G (2001a) Saltwater Intrusion in 3D LargebScale Aquifers : A Dutch Case. 26:337–344.

Oude Essink G, Boekelman RH (1996) Problems with large-scale modelling of salt water intrusion in 3D.

Oude Essink GH. (2001b) Improving fresh groundwater supply—problems and solutions. Ocean Coast Manag 44:429–449. doi: 10.1016/S0964-5691(01)00057-6

Oude Essink GHP, van Baaren ES, de Louw PGB (2010) Effects of climate change on coastal groundwater systems: A modeling study in the Netherlands. Water Resour Res 46:n/a–n/a. doi: 10.1029/2009WR008719

Papadopoulou MP, Varouchakis EA, Karatzas GP (2010) Terrain Discontinuity Effects in the Regional Flow of a Complex Karstified Aquifer. 319–328. doi: 10.1007/s10666-009-9207-5

Payne DF (2010) Effects of climate change on saltwater intrusion at Hilton Head Island, SC. U.S.A. 21st Salt Water Intrusion Meet 293–296.

Peralta R, Timani B, Das R (2010) Optimizing Safe Yield Policy Implementation. Water Resour Manag 25:483–508. doi: 10.1007/s11269-010-9710-0

Pinder GF, Gray WG (2008) Essentials of Multiphase Flow and Transport in Porous Media. doi: 10.1002/9780470380802

Post VE a, Groen J, Kooi H, et al (2013) Offshore fresh groundwater reserves as a global phenomenon. Nature 504:71–8. doi: 10.1038/nature12858

Post VEA (2005) Fresh and saline groundwater interaction in coastal aquifers: Is our technology ready for the problems ahead? Hydrogeol J 13:120–123. doi: 10.1007/s10040-004-0417-2

Price RM, Swart PK, Fourqurean JW (2006) Coastal groundwater discharge – an additional source of phosphorus for the oligotrophic wetlands of the Everglades. Hydrobiologia 569:23–36. doi: 10.1007/s10750-006-0120-5

Rasmussen P, Sonnenborg TO, Goncear G, Hinsby K (2012) Assessing impacts of climate change, sea level rise, and drainage canals on saltwater intrusion to coastal aquifer. Hydrol Earth Syst Sci Discuss 9:7969–8026. doi: 10.5194/hessd-9-7969-2012

RBMP (2012) Plano de Gestão das Bacias Hidrograficas que Integram a Região Hidrográfica das Ribeiras do Algarve (RH8) (River Basin Management Plan for the Hidrografic Regin of the Algarve Streams(RH8)). Faro, Portugal

RBMP (1999) Plano de Bacia Hidrográfica das Ribeiras do Algarve, Agricultura e Agropecuária. Lisbon, Portugal

Reilly TE (2001) System and Boundary Conceptualization in Ground-Water Flow Simulation Techniques of Water-Resources Investigations of the United States Geological Survey. U.S. GEOLOGICAL SURVEY, Reston, Virginia

Reis E (2007) Contribuição para o Cálculo do Balanço Hídrico dos Principais Sistemas Aquíferos do Algarve.

Reis E, Gago C (2013) Pano Específico de Gestão da Água(PEGA) na Área Crítica do Algarve-Contributos para a sua Elaboração. 9º Semin. sobre Águas Subterrâneas APRH. Associação Portuguesa dos Recursos Hídricos (APRH), Lisbon, Portugal, pp 57–60

Rejani R, Jha MK, Panda SN (2008) Simulation-Optimization Modelling for Sustainable Groundwater Management in a Coastal Basin of Orissa, India. Water Resour Manag 23:235–263. doi: 10.1007/s11269-008-9273-5

Rocha C, Veiga-Pires C, Scholten J, et al (2015) Assessing land–ocean connectivity via Submarine Groundwater Discharge (SGD) in the Ria Formosa Lagoon (Portugal): combining radon measurements and stable isotope hydrology. Hydrol Earth Syst Sci Discuss 12:12433–12482. doi: 10.5194/hessd-12-12433-2015

Roseiro CM dos SD (2009) Recarga artificial de aquíferos:aplicação ao sistema aquífero da Campina de Faro. Universidade de Lisboa

Roumasset J a., Wada C a. (2010) Optimal and Sustainable Groundwater Extraction. Sustainability 2:2676–2685. doi: 10.3390/su2082676

Rozell DJ, Wong T (2010) Effects of climate change on groundwater resources at Shelter Island, New York State, USA. Hydrogeol J 18:1657–1665. doi: 10.1007/s10040-010-0615-z

Salvador N, Monteiro JP, Hugman R, et al (2012) Quantifying and modelling the contribution of streams that recharge the Querença-Silves aquifer in the south of Portugal. Nat Hazards Earth Syst Sci 12:3217–3227. doi: 10.5194/nhess-12-3217-2012

Santos FD, Miranda P (2006) Alterações climáticas em Portugal. Cenários, Impactos e Medidas de Adaptação (Climate change in Portugal. Scenarios, Impacts and Adaptation Measures) – Project SIAM II, 1ª edn. Gradiva, Lisbon, Portugal

Scanlon BR, Mace RE, Barrett ME, Smith B (2003) Can we simulate regional groundwater flow in a karst system using equivalent porous media models ? Case study , Barton Springs. 276:137–158. doi: 10.1016/S0022-1694(03)00064-7

Sedki A, Ouazar D (2011) Simulation-Optimization Modeling for Sustainable Groundwater Development: A Moroccan Coastal Aquifer Case Study. Water Resour Manag 25:2855–2875. doi: 10.1007/s11269-011-9843-9

Shiau J-T, Wu F-C (2007) Pareto-optimal solutions for environmental flow schemes incorporating the intra-annual and interannual variability of the natural flow regime. Water Resour Res 43:W06433. doi: 10.1029/2006WR005523

Silva AMV da, Vieira da Silva A, Portugal e Leitão de Freitas A (1986) Modelo de fluxo subterrâneo e salinização dos aquíferos costeiros entre Faro e Fuseta (Model of flow and salinization of the coastal aquifers between Faro and Fuseta). Comun dos Serviços Geológicos Port 72:71–87.

Silva ACF, Tavares P, Shapouri M, et al (2012) Estuarine biodiversity as an indicator of groundwater discharge. Estuar Coast Shelf Sci 97:38–43. doi: 10.1016/j.ecss.2011.11.006

Silva ML (1988) Hidrogeologia do Miocénico do Algarve [Hydrogeology of the Miocene of the Algarve]. Universidade de Lisboa

Simmons C, T. Bauer-Gottwein, P. Graf, et al (2010) Groundwater Modelling in Arid and Semi-Arid Areas, 1st edn. Groundw Model Arid Semi-Arid Areas. doi: 10.1017/CBO9780511760280

Simmons CT (2005) Variable density groundwater flow: From current challenges to future possibilities. Hydrogeol J 13:116–119. doi: 10.1007/s10040-004-0408-3

Sophocleous M (2000) From safe yield to sustainable development of water resources—the Kansas experience. J Hydrol 235:27–43. doi: 10.1016/S0022-1694(00)00263-8

Sophocleous M (1997) MANAGING WATER RESOURCES SYSTEMS: WHY “SAFE YIELD” IS NOT SUSTAINABLE. Ground Water 35:561–561. doi: 10.1111/j.1745-6584.1997.tb00116.x

Sophocleous M (2002) Interactions between groundwater and surface water: the state of the science. Hydrogeol J 10:52–67. doi: 10.1007/s10040-001-0170-8

Sousa FM, Carrara G, Fernandes J, et al (2014) Descargas de Águas Subterrâneas na região dos Olhos de Água , Algarve – alguns resultados das campanhas CTD Submarine Groundwater Discharges at Olhos de Água area , Algarve – some results of the CTD surveys. 8a Assem. Luso Esp. Geod. e Geofis. Évora, Portugal, pp 503–507

Souza WR, Voss CI (1987) Analysis of an anisotropic coastal aquifer system using variable-density flow and solute transport simulation. J Hydrol 92:17–41. doi: 10.1016/0022-1694(87)90087-4

Stigter T, Bento S, Varanda MP, et al (2013a) Combined assessment of climate change and socio-economic development as drivers of freshwater availability in the South of Portugal. TWAM2013 Int. Conf. Work.

Stigter T, Dill A, Malta E, Santos R (2013b) Nutrient sources for green macroalgae in the Ria Formosa lagoon - assessing the role of groundwater. Groundw. Ecosyst. CRC Press, pp 153–167

Stigter T, Dill AC, Malta E, Santos R (2007) Nutrient sources for green macroalgae in the Ria Formosa lagoon – assessing the role of groundwater. In: Ribeiro L, Chambel A, Condesso de Melo MT (eds) Hydrogeol. - Groundw. Ecosyst. Lisbon, Portugal, pp 153–168

Stigter T, Mazimpaka C, Zhou Y (2015) Modelling nitrate transport towards a coastal lagoon under the influence of aquifer properties, contaminating activities , restoration poilices and climate change. Aqua 2015 - 42nd IAH Congr. International Association of Hydrogeologists (IAH), Rome, Italy, p 1

Stigter T, Monteiro J, Nunes L, et al (2010) Regional spatial-temporal assessment of groundwater exploitation sustainability in the south of Portugal. IAH B. Ser. (IAH Sel. Pap. International Association of Hydrologists (IAH), p 10

Stigter T, Ribeiro L, Samper J, et al (2011a) Assessing and Managing the Impact of Climate Change on Coastal Groundwater Resources and Dependent Ecosystems. Final Report, CIRCLE-Med Project.

Stigter TY (2005) Integrated Analysis of Hydrogeochemistry and Assessment of Groundwater Contamination Induced by Agricultural Practices. Instituto Superior Técnico

Stigter TY, Carvalho Dill a. MM, Ribeiro L (2011b) Major issues regarding the efficiency of monitoring programs for nitrate contaminated groundwater. Environ Sci Technol 45:8674–8682. doi: 10.1021/es201798g

Stigter TY, Monteiro JP, Nunes LM, et al (2009) Screening of sustainable groundwater sources for integration into a regional drought-prone water supply system. Hydrol Earth Syst Sci Discuss 6:85–120. doi: 10.5194/hessd-6-85-2009

Stigter TY, Nunes JP, Pisani B, et al (2014) Comparative assessment of climate change and its impacts on three coastal aquifers in the Mediterranean. Reg Environ Chang 14:41–56. doi: 10.1007/s10113-012-0377-3

Stigter TY, Van Ooijen SPJ, Post VE a, et al (1998) A hydrogeological and hydrochemical explanation of the groundwater composition under irrigated land in a Mediterranean environment, Algarve, Portugal. J Hydrol 208:262–279. doi: 10.1016/S0022-1694(98)00168-1

Sulzbacher H, Wiederhold H, Siemon B, et al (2012) Numerical modelling of climate change impacts on freshwater lenses on the North Sea Island of Borkum using hydrological and geophysical methods. Hydrol Earth Syst Sci 16:3621–3643. doi: 10.5194/hess-16-3621-2012

Taniguchi M, Burnett WC, Cable JE, Turner J V. (2002) Investigation of submarine

groundwater discharge. Hydrol Process 16:2115–2129. doi: 10.1002/hyp.1145

Taylor RG, Scanlon B, Döll P, et al (2012) Ground water and climate change. Nat Clim Chang 3:322–329. doi: 10.1038/nclimate1744

Terrinha P, Rocha R, J. Rey, M. Cachão, D. Moura, C. Roque, L. Martins, V. Valadares, J. Cabral, M. R. Azevedo, L. Barbero, E. Clavijo(10), R. P. Dias(10), J. Gafeira(1, 16), H. Matias(11), L. Matias(17), J. Madeira(4, 2), C. Marques da Silva(4, 5), J. Munhá(4, 5), L. Rebelo(KB (2010) A BACIA DO ALGARVE: ESTRATIGRAFIA, PALEOGEOGRAFIA E TECTÓNICA.

Theis C V (1940) The source of water derived from wells: essential factors controlling the response of an aquifer to development. Civ Eng 10:277–280.

Van Camp M, Radfar M, Walraevens K (2010) Assessment of groundwater storage depletion by overexploitation using simple indicators in an irrigated closed aquifer basin in Iran. Agric Water Manag 97:1876–1886. doi: 10.1016/j.agwat.2010.02.006

van der Linden P, Mitchell JFB (2009) ENSEMBLES: Climate Change and its Impacts: Summary of research and results from the ENSEMBLES project. Met Office Hadley Centre, FitzRoy Road, Exeter EX1 3PB, UK

van Ooijen B, Post V, Stigter T (1996) Hydrogeology and hydrochemistry of groundwater in the Campina de Faro, Portugal. Vrije Universiteit, Amsterdam

Viegas J (2015) Modelação do Balanço Hídrico do Sistema Aquífero da Campina de Faro Em Diferentes Cenários Climáticos e de Exploração de Recursos. Universidade do Algarve

Vieira J, Cunha MC, Nunes L, et al (2011) Optimization of the Operation of Large-Scale Multisource Water-Supply Systems. J Water Resour Plan Manag 137:150–161. doi: 10.1061/(ASCE)WR.1943-5452.0000102

Vieira J, Monteiro JP (2003) Atribuição de Propriedades a Redes Não Estruturadas de Elementos Finitos Triangulares (Aplicação ao Cálculo da Recarga de Sistemas Aquíferos do Algarve). In: L R, Peixinho de Cristo F (eds) As Águas Subterrâneas no Sul da Península Ibérica. International Association of Hydrologists. APRH publ, pp 183–192

Wang HF, Anderson MP (1995) Introduction to Groundwater Modeling: Finite Difference and Finite Element Methods. Academic Press

Watson TA, Werner AD, Simmons CT (2010) Transience of seawater intrusion in response to sea level rise. Water Resour Res 46:W12533. doi: 10.1029/2010WR009564

Werner AD, Alcoe DW, Ordens CM, et al (2011) Current Practice and Future Challenges in Coastal Aquifer Management: Flux-Based and Trigger-Level Approaches with Application to an Australian Case Study. Water Resour Manag 25:1831–1853. doi: 10.1007/s11269-011-9777-2

Werner AD, Bakker M, Post VE a., et al (2012) Seawater intrusion processes, investigation and management: Recent advances and future challenges. Adv Water Resour. doi: 10.1016/j.advwatres.2012.03.004

Werner AD, Bakker M, Post VEA, et al (2013) Seawater intrusion processes, investigation and management: Recent advances and future challenges. Adv Water Resour 51:3–26. doi: 10.1016/j.advwatres.2012.03.004

Werner AD, Simmons CT (2009) Impact of sea-level rise on sea water intrusion in coastal

aquifers. Ground Water 47:197–204. doi: 10.1111/j.1745-6584.2008.00535.x

Winter TC, Harvey JW, Franke OL, Alley WM (1998) Ground Water Surface Water and A Single Resource. Denver, Colorado

Yin D, Shu L, Chen X, et al (2010) Assessment of Sustainable Yield of Karst Water in Huaibei, China. Water Resour Manag 25:287–300. doi: 10.1007/s11269-010-9699-4

Zhang Q, Volker RE, Lockington D a (2001) Influence of seaward boundary condition on contaminant transport in unconfined coastal aquifers. J Contam Hydrol 49:201–15.

Zhang Q, Volker RE, Lockington D a. (2004) Numerical investigation of seawater intrusion at Gooburrum, Bundaberg, Queensland, Australia. Hydrogeol J 12:674–687. doi: 10.1007/s10040-004-0333-5

Zhou Y (2009) A critical review of groundwater budget myth, safe yield and sustainability. J Hydrol 370:207–213. doi: 10.1016/j.jhydrol.2009.03.009